ISIM & ISWIM 2024

26-28 June 2024

Bucharest, Romania

www.isimconference.eu

NATIONAL UNIVERSITY OF SCIENCE AND TECHNOLOGY POLITEHNICA BUCHAREST
Center for Research and Training in Innovative Techniques of Applied Mathematics in Engineering "*Traian Lalescu*" (CiTi)
&
Military Technical Academy "Ferdinand I"

BOOK OF ABSTRACTS ISIM & ISWIM

International Symposium & International Student Workshop on Interdisciplinary Mathematics in the CiTi areas

Volume III

ISSN-L 2821 – 8779

2024
BUCHAREST, ROMANIA

ISIM & ISWIM 2024

The University POLITEHNICA of Bucharest, Center for Research and Training in Innovative Techniques of Applied Mathematics in Engineering "*Traian Lalescu*" (CiTi) in collaboration with he Military Technical Academy "Ferdinand I". are honored to invite you to participate in the 3rd Edition of the **International Symposium & International Student Workshop on Interdisciplinary Mathematics in the CiTi areas (ISIM & ISWIM)** that will be held at University Politehnica of Bucharest, Romania, between **26th** and **28th** of **June 2024**.

The 3rd edition of this international event has the support of the Romanian Mathematical Society and is organised in partnership with the Military Technical Academy "Ferdinand I".

The scope of the Symposium includes but is not limited to original research works and ideas related to CiTi interdisciplinary areas and Applications: **Fractional Calculus, Wavelet Analysis, Evolutionary Algorithms, Data Analysis and Information Security, Game Theory - including Quantum, Partial and Ordinary Differential Equations, Mathematical Statistics, Graph Theory.**

In order to participate, please access our website and complete your registration (www.isimconference.eu).

We have invited **Keynote Speakers** that will most definitely attract your attention:

- **Mostafa ADIMY**, INRIA, Lyon, France
- **Paul BOGDAN**, University of Southern California, USA
- **Dan CIMPEAN**, Romanian National Cyber Security Directorate
- **Radu GOLOGAN**, University POLITEHNICA Bucharest, Romania
- **Rob HAELTERMAN**, Royal Military Academy, Brussels, Belgium
- **Marius LEORDEANU**, University POLITEHNICA Bucharest, Romania
- **Marina MARCHISIO**, University of Turin, Italy
- **Andrei NEGUT**, Ecole Normale Polytechnique de Lausanne, France
- **Carla PINTO**, Polytechnic University of Porto, Portugal
- **Rathinasamy SAKTHIVEL**, Bharathiar University, India

Symposium Contact

E-mail: office@isimconference.eu

Website: https://isimconference.eu

Antonela Toma

University POLITEHNICA of Bucharest, Romania

Cristian-Emil Moldoveanu

Military Technical Academy "Ferdinand I"

BOUNDARY VALUE PROBLEMS FOR FRACTIONAL DIFFERENTIAL INCLUSIONS WITH Q-CAPUTO TYPE DERIVATIVE

Abdelaziz OUALID[1], Samira HAMANI[2]

[1,2]Abdelhamid Ibn Badis University Mostaganem, Department of Mathematics and Computer Science, ACSY Team-Laboratory of Pure and Applied Mathematics,
Faculty SEI-BP 227/118 Mostaganem 27000, Algeria.

Corresponding author email: abdelaziz.oualid.etu@univ-mosta.dz [1]

samira.hamani@univ-mosta.dz [2]

Abstract

In this manuscript, we discuss the existence of solutions for a boundary value problem (BVP) involving fractional differential inclusions with a q-difference derivative. We consider two cases: one where the right-hand side is convex-valued and the other where it is nonconvex-valued. The first result relies on the nonlinear alternative of the Leray Schauder type, while the second is based on a fixed point theorem for contraction multivalued maps due to Covitz and Nadler. These findings extend some previous results in the literature to the multivalued case, contributing to this emerging field.

Key words*: fractional differential inclusion; q-difference derivative; fixed point theorem; convex and non-convex multivalued maps.*

1. INTRODUCTION

The Fractional calculus has evolved into an important and interesting field of research in view of its numerous applications in technical and applied sciences. The mathematical modeling of many real world phenomena based on fractional-order operators is regarded as better and improved than the one depending on integer-order operators. In particular, fractional calculus has played a significant role in the recent development of special functions and integral transforms, signal processing, control theory, bioengineering and biomedical, viscoelasticity, finance, stochastic processes, wave and diffusion phenomena, plasma physics, social sciences, etc. For further details and applications.

The history of quantum calculus(QC) dates back to the work of the British mathematician Frank Hilton Jackson. In 1910, he gave a new definition of the derivative, by which the basic principles of quantum calculus. Jackson removed the concept of limit from the definition of the derivative and introduced two types of operators, namely q-derivative and h-derivative. Of course, q-derivative's growth was higher than h-derivative and it didn't take long for it to enter the field of Fractional Calculus. Fractional q-derivative has both the a dvantages of Fractional Calculus and due to the discreteness of the space, it provides the possibility of using the computer in solving and simulating complex equations. For the same reason, in the last decade, q-derivative has received a lot of attention from researchers and many articles have been published in this field. On the other hand, Set-Valued mappings, namely Multifunction, have interesting features whose properties have been investigated from different aspects and recently used in modeling due to their ability to interpret physical phenomena with shock.

The aim of our paper is to present existence results for Boundary value problem, when the right hand side is convex as well as nonconvex valued. The first result relies on the nonlinear alternative of Leray-Schauder type. In the second result, we shall use the fixed point theorem for contraction multivalued maps due to Covitz and Nadler.

2. CONTENT

This paper deals woth the existence of solution for boundary value problems (BVP for short), for fractional differential inclusions with q-Caputo type derivative. We consider the boundary value problem

.

$$\mathrm{D}_{\mathrm{q}}^{\alpha} y(t) \in F\big(t, y(t)\big), \quad \text{for almost all } \mathrm{t} \in \mathrm{J} = [0, \mathrm{T}],\ 0 < \alpha \leq 1 \quad (1.1)$$

$$y(T) + y(0) = b \int_0^{\mathrm{T}} \mathrm{y(s)d_q s}, \qquad \mathrm{bT} \neq 2 \quad (1.2)$$

Where $\mathrm{T} > 0$, $q \in [0,1]$ and $\mathrm{D}_{\mathrm{q}}^{\alpha}$ is the Caputo fractional q-Difference derivative, $\mathrm{F} : \mathrm{J} \times \mathfrak{R} \to \wp(\mathfrak{R})$ is a multivalued map, $\wp(\mathfrak{R})$ is the family of all nonamply subsets of $\mathfrak{R}$ and $b \in \mathfrak{R}$.

3. CONCLUSIONS

In this study, we have explored the existence of solutions for boundary value problems (BVPs) involving differential inclusions with q-Caputo derivatives, addressing both convex and nonconvex cases. By leveraging the nonlinear alternative of the Leray-Schauder type, we established the existence of solutions when the right-hand side is convex-valued. Additionally, using the fixed point theorem for contraction multivalued maps due to Covitz and Nadler, we extended our analysis to cases where the right-hand side is nonconvex-valued.

4. REFERENCES

[1] N. Guerraiche, S. Hamani and J.Henderson, Boundary value problems for Differential Inclusions with Integral and Anti-periodie Conditions, Communication on Applied Nonlinear Analyses 23(2016), 3,33-46

MENTAL CONDITIONS CLASSIFICATION USING SOCIAL MEDIA DATA

Alexandra-Codruța NEAGU[1], Stelian SPÎNU[2]

[1]Military Equipment and Technologies Research Agency, Bucharest, Romania
Military Technical Academy "Ferdinand I", District 5, Bucharest, Romania
[2]Military Technical Academy "Ferdinand I", District 5, Bucharest, Romania

Corresponding author email: alexandraneagu35@yahoo.com, aneagu@acttm.ro

Abstract

The study aims to conduct a detailed study on diverse artificial intelligence algorithms, especially Random Forest, Long Short Term Memory and Convolutional Neural Network using different processing methods as TF-IDF, Word Tokenization and GloVe embeddings, and training techniques such as data augmentation, class weights or regularization values. The algorithms are processing a binary classification followed by a multi-class classification in the same dataset. The data consists of Reddit posts, each label being part of a subgroup in the social media platform, from mental health spectrum as anxiety, depression or bpd and from every-day subjects. The posts are being written by individuals with unreported conditions or undergoing specific treatment. We started from the benchmark score of 63% to 73% for the multi-class classification and a final score of 96% for binary-classification.

Key words*: text classification; deep learning; natural language processing; mental health; machine learning; social media*

1. INTRODUCTION

The combination of mental health domain and artificial intelligence has garnered a significant interest in the research area. The new generations started to prioritize the mental health conditions, as a result of the numerous people associated with diverse affections in this field. The use of artificial intelligence in case of detection and prevention could improve the long run of individuals that struggles.

This study presents a comprehensive outline from input data to the identification of a possible mental health problems. Data, drawn from Reddit, help us to create two types of classification and do a vast comparations between the possible algorithms,

2. CONTENT

2.1. Data

The used data was collected from a study about the impact of COVID-19 on mental health in a modified version for the desired classification. The dataset was cleaned to ensure the proper quality and consistency of the data, as removing blank lines, URLs, punctuation or stop words. To ensure a better understanding of the data, steaming and lemmatization techniques were applied, and English correction of the words.

The dataset was stratified into two distinct subsets, one for the binary classification, were each data in the fields of mental health was labelled as "mental" and the ones from every day subjects were labelled as "non-mental", with a distribution of 36% for "mental" class. The second subset was built using the 13 classes, corresponding to each subreddit channel, in the field of mental health, with an unbalanced distribution, from 2% to 32%.

For the data understanding, the study followed a word frequency analysis for each class. Before the machine learning process, data was transformed in number format using TF-IDF, Tokenization or using GloVe embeddings.

2.2. Approach

The study follows two types of classification, the binary one, used for detecting the potential presence of mental illness and a multi-class classification for choosing the respective problem. The flux of the data is going from social media post into the binary model and in case of positive result about existence of a mental health

conditions, the text would go into the multi-class classification. The final results being one of the thirteen classes, corresponding to a condition from dataset or class "non-mental".
The first try for the binary model is implemented using LSTM architecture with a sentence size of 70 words and the embedding length of 300. The final accuracy was 96%.
For multi-class classification, the concentration was on F1-Score, due to the inconsistency in the number of data for each class, as a very unbalanced dataset. The used baseline model was **Random Forest** using TF-IDF with a final result of 68%.
The next experiment was with a **CNN** architecture, considering the data as a 1D matrix. For data pre-processing, using a simple Tokenization of the words came with a score of 63%, and with the combination of Tokenization and GloVe embeddings, a score of 73%. Despite the attempt to manage the unbalanced dataset, using class weights, the score improved too little or even decreased.
Using the **LSTM** architecture, the final model used two layers of BidirectionalLSTM, with SpatialDropout, configured with 70 words input and an embedding matrix of 300. Using the simple Tokenization, the obtained score was 72%, and 70% combining Tokenization with GloVe embeddings. Experimenting with a number of 300 words as input, in the case of using GloVe embeddings the final score was 73%, demonstrating the power of sentence length in natural language processing. For maximizing the performance, the model was trained using the class weights, without a noticeable improvement. Data augmentation was another method to increase the classification score, using character replacement or synonym replacement. The F1-Score using this was lower, even if the Recall increased. The best model used a combination of Tokenization, GloVe embeddings and the 300 word as input with a F1-Score of 73%.

2.3. Results

In the case of multi-class classification, the best model used a combination of Tokenization, GloVe embeddings and the 300 word as input with a F1-Score of 73%.

Model	Pre-process technique	Accuracy	Precision	Recall	F1-Score
CNN	Tokenization	64%	67%	60%	63%
Random Forest	TF-IDF	68%	82%	61%	68%
LSTM	Tokenization	70%	77%	67%	71%
CNN	Tokenization + GloVe embeddings	70%	76%	69%	72%
LSTM	Tokenization + GloVe embeddings	72%	78%	73%	73%

Table 1 - multi class classification results

Despite the performance, all models faced a common challenge to predict the "depression" and "suicidewatch" class, as the mental health conditions are usually corelated, the idea of suicide often come with depression, leading to an overlapping in classification process.
The model reveals variation in performance across different classes, such as "adhd", "EDAnonymous" and "ptsd" that demonstrate higher scores, while "depression", "lonely" and "suicidewatch" show lower scores. This is due to the similarity between different conditions, that complicates the process of learning and predict.

	precision	recall	f1-score	support
EDAnonymous	0.87	0.85	0.86	4373
addiction	0.81	0.79	0.80	2292
adhd	0.85	0.87	0.86	13689
autism	0.84	0.78	0.81	2661
bipolarreddit	0.75	0.44	0.56	1734
bpd	0.82	0.60	0.69	7288
depression	0.64	0.77	0.70	35199
healthanxiety	0.87	0.82	0.84	2594
lonely	0.61	0.58	0.60	7090
ptsd	0.89	0.64	0.75	2593
schizophrenia	0.79	0.60	0.68	2614
socialanxiety	0.75	0.75	0.75	6899
suicidewatch	0.69	0.58	0.63	19848
accuracy			0.72	108874
macro avg	0.78	0.70	0.73	108874
weighted avg	0.72	0.72	0.71	108874

Figure 1 - classification raport LSTM

3. CONCLUSIONS

The study introduces two classification problems using a dataset that was not used in this type of study, where more types of artificial intelligence algorithms were used, leading to a final score of 73% using a LSTM neural network model. The results showed the expected conclusions between the classes, as the real-life correlation between different conditions. The unbalanced dataset was a problem in classification, that cause the using of data augmentation, class weights or regularization.

POSITIVE SOLUTIONS TO SEMILINEAR DIRICHLET PROBLEMS WITH GENERAL BOUNDARY DATA

Lucian BEZNEA[1,2], Alexandra TEODOR[1,3]

[1]Simion Stoilow Institute of Mathematics of the Romanian Academy, P. O. Box 1-764, 014700 Bucharest, Romania

[2]POLITEHNICA Bucharest, CAMPUS Institute, Bucharest, Romania
[3]POLITEHNICA Bucharest, Bucharest, Romania

Corresponding author email: alexandravictoriateodor@gmail.com

Abstract *We give a probabilistic representation of the solution to a semilinear elliptic Dirichlet problem with general (not necessarily continuous) boundary data. The boundary behaviour of the solution is in the sense of the controlled convergence initiated by A. Cornea. Uniqueness results for the solution are also provided.*

Key words*: Semilinear Dirichlet problem, Boundary behaviour, Controlled convergence.*

Bibliography

[1] L. Beznea, A. Teodor: Positive solutions to semilinear Dirichlet problems with general boundary data, Analysis and Mathematical Physics 14 (2024), 39

GAME OF GREEN: STRATEGIES FOR SUSTAINABILITY IN THE BATTLE BETWEEN ELECTRIC AND DIESEL CARS

Alexandra- Maria BORȘ[1], Andrei- Robert COMAN[2], Simona-Mihaela BIBIC[3]
[1,2,3]National University of Science and Technology Politehnica Bucharest, 313 Splaiul Independentei, District 6, Bucharest, Romania
[1,2]Faculty of Applied Sciences
[3]Center for Research and Training in Innovative Techniques of Applied Mathematics in Engineering, 'Traian Lalescu' (CiTi), Bucharest, Romania
Corresponding author email: alexandra.bors@stud.fsa.upb.ro, andrei_robert.coman@stud.fsa.upb.ro,

Abstract
This research paper explores the impact of human decisions on the environment, focusing on the choice between electric and diesel vehicles through game theory. Game theory helps analyse complex decisions in the automotive sector, involving various stakeholders such as consumers, manufacturers, policymakers, and environmental advocates. It examines the pros and cons of electric versus diesel cars, independent of European legislation, and considers factors like governmental policies, consumer preferences, and industry dynamics. Key to this analysis is the concept of strategic interdependence, where the choices of one group affect others, influencing factors like cost, convenience, and environmental impact. This study examines the significant sustainability and climate change challenges in transportation, exploring how strategic interactions among stakeholders influence the sector's future. It highlights the role of policymakers in shaping the game against nature by promoting sustainable choices and imposing penalties for environmentally damaging practices. The outcome of this strategic game impacts the broader goals of reducing emissions and transitioning to cleaner energy, considering the obstacles facing electric vehicles and the ongoing prevalence of diesel vehicles.

Key words*: Game theory; games against nature; sustainability; Electric vs Diesel cars; solutions; climate change; CO_2 emissions.*

1. INTRODUCTION

Carbon dioxide emissions are the primary driver of global climate change, and our planet is now warming faster than at any point in recorded history. Through the application of game theory (GT), the aim is to elucidate the strategic considerations driving the transition towards sustainable transportation solutions. By analysing the incentives, trade-offs, and potential outcomes for electric and diesel vehicles, it offers insights into the complex interplay between economic, technological, and environmental factors shaping the future of mobility. Ultimately, informed decision-making informed by game theory can pave the way for a more sustainable and resilient transportation system, contributing to the collective effort to address the challenges of climate change and secure a brighter future for generations to come.

2. CONTENT

2.1. Impact of human decisions

Human activities, particularly the burning of fossil fuels and use of diesel vehicles, significantly impact the environment and contribute to global warming. Health-wise, Diesel emissions can cause serious respiratory and cardiovascular problems, affecting especially the elderly and children. Additionally, these emissions contribute to ground-level ozone and acid rain, further harming ecosystems and water sources. What constitutes a good or bad decision? This research delves into the concept of 'games against nature,' where human choices lead to environmental degradation and climate change, often without a complete understanding of the consequences.

2.2. Game Theory perspectives

GT studies the interactions between players, based on strategies, and provides an analytical framework illustrating how the adoption of cleaner technologies significantly influences the reduction of dependency on fossil fuels. This paper seeks to analyze the most optimal strategies that should be adopted to minimize the negative effects of diesel vehicles in the shortest possible time and to accelerate the adoption of electric vehicles, thus contributing to the fight against climate change.
Each game is composed of three essential parts:

- **A.** The players
- **B.** The strategies under which the game is conducted
- **C.** The benefits or utilities.

2.3. Mathematical Model

In addressing the issue described, we will use the framework of "games against nature" from game theory. This model treats the environment as a non-strategic player in a two-person game, whose outcomes are determined by probability. The human player chooses strategies without prior knowledge of the potential benefits or losses, effectively navigating decisions in an environment with unpredictable responses. Thus, the matrix of the described game is:

Nature (N) / Player (H)	De	In
E	u(E,De)	u(E,In)
D	u(D,De)	u(D,In)

Table 1. Game Matrix

where u is a function that depends on the player's strategy and the state of nature, representing their benefit or utility. In our analysis, we'll consider the global population (H) as the player with two strategic options:

a. Purchasing an electric car (E) – a sustainable choice.
b. Buying a diesel car (D) – an unsustainable choice.

The response from nature (N), influenced by these choices, will manifest as either:

a. A decrease (De) in global CO2 levels, signifying an improvement in environmental quality.
b. An increase (In) in CO2 levels, indicating accelerated environmental degradation.

The following figure illustrates the flow of our decision-making process, applying GT principles in evaluating strategies.

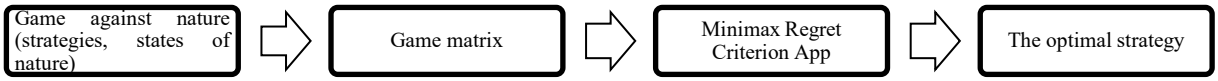

Fig.1. Strategic Decision Model

3. CONCLUSIONS

This article encourages society to quickly adopt electric vehicles to mitigate climate and environmental changes. Additionally, the adoption of electric vehicles not only lowers emissions but also benefits other crucial areas like the economy and society, fostering independence from fossil fuels and enhancing public health. Our research shows that individual choices to switch to electric vehicles significantly impact broad environmental goals. A promising area for future research is the battery production process for EVs, especially with the goal of reducing the pollution associated with this process.

Applications of complex numbers in counting problems

by Alexandru Baltărigă*

June 2024

Abstract

In the following, we will illustrate how ***complex numbers*** can be used to solve a range of counting problems. This methodology is extremely useful for tackling olympiad problems both at the 10th-grade level and in international competitions. Furthermore, we consider the use of ***complex numbers*** with ***polynomials***, this provides our students with a fresh perspective. The difficulty of the exercises presented increases gradually to allow for a more natural progression through the material.

Table of Contents

*International Informatics High School of Bucharest

1. Applications of our proposed method.

The primary application of ***complex numbers*** is to demonstrate certain combinatorial identities. We will also make use of Newton's binomial theorem.

Theorem 1.1. *The binomial theorem:* $(x+y)^n = C_n^0x^ny^0+C_n^1x^{n-1}y^1+C_n^2x^{n-2}y^2+\cdots+C_n^nx^0y^n$

Exercise 1.2. Let $n \in \mathbb{N}, n \geq 3$. Find: $S = C_n^0 + C_n^3 + C_n^6 + \cdots + C_n^{\lfloor \frac{n}{3} \rfloor}$

Proof: Let: $\varepsilon = \cos(\frac{2\pi}{3}) + i\sin(\frac{2\pi}{3})$, $\varepsilon^2 = 1$, $\varepsilon^2 + \varepsilon + 1 = 0$. By applying Theorem 1.1 we find:

$$\begin{aligned}(1+1)^n &= C_n^0 + C_n^1 \quad + C_n^2 \quad + \cdots + C_n^n \\ (1+\varepsilon)^n &= C_n^0 + C_n^1\cdot\varepsilon + C_n^2\cdot\varepsilon^2 + \cdots + C_n^n\cdot\varepsilon^n \\ (1+\varepsilon^2)^n &= C_n^0 + C_n^1\cdot\varepsilon^2 + C_n^2\cdot(\varepsilon^2)^2 + \cdots + C_n^n\cdot(\varepsilon^2)^n\end{aligned}$$

Sum up these 3 relations and you get: $2^n+(1+\varepsilon)^n+(1+\varepsilon^2)^n = 3\cdot(C_n^0+C_n^3+C_n^6+\cdots+C_n^{\lfloor \frac{n}{3} \rfloor})$

Therefore:

$$\begin{aligned}C_n^0 + C_n^3 + C_n^6 + \cdots + C_n^{\lfloor \frac{n}{3} \rfloor} &= \frac{2^n + (1+\varepsilon)^n + (1+\varepsilon^2)^n}{3} = \frac{2^n + (-\varepsilon^2)^n + (-\varepsilon)^n}{3} \\ &= \frac{2^n + (-1)^n(\varepsilon+\varepsilon^2)}{3} = \frac{2^n + (-1)^{n+1}}{3}\end{aligned} \tag{1.1}$$

Answer: $S = C_n^0 + C_n^3 + C_n^6 + \cdots + C_n^{\lfloor \frac{n}{3} \rfloor} = \frac{2^n+(-1)^{n+1}}{3}$ ■

Proposition 1.3. *Let p be a* **prime number**, $p \geq 2$, *and $f \in \mathbb{Q}[x]$, $f(x) = 1 + x + x^2 + \cdots + + x^{p-1}$. Then f is irreducible over the domain of rational numbers.*

Observation 1.4. *f is called the p-th* **cyclotomic polynomial**. *This observation is useful in proving the following lemma:*

Lemma 1.5. *Let p be a* **prime number**, $p \geq 2$, *and* $\varepsilon = \cos(\frac{2\pi}{p}) + i\sin(\frac{2\pi}{p})$.
If $a_0, a_1, \cdots, a_{p-1} \in \mathbb{Q}$ s.a. $a_0 + a_1\cdot\varepsilon + \cdots + a_{p-1}\cdot\varepsilon^{p-1} = 0$ then $a_0 = a_1 = \cdots = a_{p-1}$.

Exercise 1.6. **(Bay Area Math Circle, 1999)** Consider a *rectangle* with natural dimensions that can be covered with smaller *rectangles* of sizes $1 \times m$ or $n \times 1$. Then, prove it's possible to cover it is by using only one of the presented *rectangle* variants ($1 \times m$ or $n \times 1$).

Exercise 1.7. How many natural numbers with n digits from the *set* {2, 3, 7, 9} can be *divided* by 3?

Exercise 1.8. **(IMO, 1995)** For a finite *set* of real numbers A, we note $m(A)$ the sum of the *set*'s elements, and $|A|$ the *set*'s cardinal. Let p be a ***prime number***, and $A = \{1, 2, \cdots, 2p\}$.
Calculate the number of *subsets* $B \subset A$ with $|B| = p$ and $p \mid m(B)$.

Exercise 1.9. **(High-School Mathematics, 1994/1 Qihong Xie)** Calculate the number of *subsets* of the *set* $\{1, 2, \cdots, 2000\}$ whose elements' sum is *divisible* by 5.

2. Proving that lemma!

Next, we will prove a lemma that involves concepts of irreducibility of ***polynomials***. It is necessary to be familiar with the Eisenstein irreducibility criterion or the concept of ***cyclotomic polynomials***. Since these results are easily accessible, we will omit their demonstration.

Restatement of Lemma 1.5. Let p be a ***prime number***, $p \geq 2$, and $\varepsilon = \cos(\frac{2\pi}{p}) + i\sin(\frac{2\pi}{p})$.
If $a_0, a_1, \cdots, a_{p-1} \in \mathbb{Q}$ s.a. $a_0 + a_1 \cdot \varepsilon + \cdots + a_{p-1} \cdot \varepsilon^{p-1} = 0$ then $a_0 = a_1 = \cdots = a_{p-1}$.

Proof: Consider $f, g \in \mathbb{Q}[x]$,

$$\begin{aligned} f(x) &= 1 + x \quad + \cdots + x^{p-1} \\ g(x) &= a_0 + a_1 x + \cdots + a_p x^{p-1} \end{aligned}$$

Because f is irreducible over the domain of rational numbers and $f(\varepsilon) = 0 \Rightarrow$

$$\Rightarrow f(x) \,|\, g(x)$$

However, $\deg(f(x)) = \deg(g(x))$. It follows that $\exists\, c \in \mathbb{Q}$ s.a. $g(x) = c \cdot f(x)$. Identifying the coefficients we deduce that:

$$a_0 = a_1 = \cdots = a_{p-1} = c$$

■

Remember this lemma! This lemma will play a central role in the following solutions.

3. Solutions, and some more exercises.

Restatement of Exercise 1.6. **(Bay Area Math Circle, 1999)** Consider a *rectangle* with natural dimensions that can be covered with smaller *rectangles* of sizes $1 \times m$ or $n \times 1$. Then, prove it's possible to cover it is by using only one of the presented *rectangle* variants ($1 \times m$ or $n \times 1$).

Proof: Let a, b be the *rectangle*'s dimensions; $a, b \in \mathbb{N}$

We slice up the *rectangle* into 1×1 *squares*, and we note them like so:

$$\begin{matrix} (1,1) & (1,2) & \cdots & (1,b) \\ \vdots & \vdots & \ddots & \vdots \\ (a,1) & \cdots & \cdots & (a,b) \end{matrix}$$

If we associate the *square* (i, j) with the *complex number* $\varepsilon_1^i \cdot \varepsilon_2^j$ where:

$$\varepsilon_1 = \cos(\frac{2\pi}{n}) + i\sin(\frac{2\pi}{n}), \quad \varepsilon_2 = \cos(\frac{2\pi}{m}) + i\sin(\frac{2\pi}{m})$$

We notice that in every $1 \times m$ or $n \times 1$ *rectangle*, the sum of the corresponding *complex numbers* is 0, therefore the sum of all the *rectangles* is equal to 0

$$0 = \sum_{i=1}^{a}\sum_{j=1}^{b} \varepsilon_1^i \cdot \varepsilon_2^j = (\sum_{i=1}^{a} \varepsilon_1^i)(\sum_{j=1}^{b} \varepsilon_2^j) \tag{3.1}$$

One of the sums will be equal to $0 \Rightarrow n \mid a$ or $m \mid b$ ■

Exercise 3.1. Is it possible to cover a 13×13 *square* with 1×4 and 4×1 *rectangles* such that only the center cell of the *square* isn't filled?

Proof: We make the assumption that such a pavement can be realized.

By associating the cell (k, j) the *complex number* i^{k+2j}, notice that the sum of the corresponding numbers in any 1×4 or 4×1 *rectangle* is equal to 0. Therefore the sum of all the *rectangles* is equal to 0. This would mean that:

$$i^{21} = (i + i^2 + \cdots + i^{13})(i^2 + i^4 + \cdots + i^{26}) = i \cdot \frac{i^{13} - 1}{i - 1} i^2 \cdot \frac{i^{26} - 1}{i^2 - 1} = i^3$$ ■

which is **false**.

Restatement of Exercise 1.7. How many natural numbers with n digits from the *set* {2, 3, 7, 9} can be *divided* by 3?

Proof: Let x_n, y_n, z_n be the numbers of numbers with n digits in the given *set* that are congruent with 0, 1, and 2 modulo 3. We want to find x_n.

Let $\varepsilon = \cos(\frac{2\pi}{3}) + i\sin(\frac{2\pi}{3})$. We know that the remainder of the *division* of a number by 3 is the same as the remainder of the *division* of the sum of its digits by 3, so:

$$\begin{aligned} x_n + y_n \ + z_n &= 4^n \\ x_n + \varepsilon y_n + \varepsilon^2 z_n &= \sum_{j_1+j_2+j_3+j_4=n} \varepsilon^{2j_1+3j_2+7j_3+9j_4} = (\varepsilon^2+\varepsilon^3+\varepsilon^7+\varepsilon^9)^n \end{aligned}$$

Therefore:

$$\begin{gathered} x_n - 1 + \varepsilon y_n + \varepsilon^2 z_n = 0 \Rightarrow x_n - 1 = y_n = z_n = k \Rightarrow \\ \Rightarrow 4^n - 1 = 3k \Rightarrow k = \frac{4^n-1}{3} \Rightarrow x_n = \frac{4^n+2}{3} \end{gathered}$$

So the answer is:

$$x_n = \frac{4^n+2}{3} \tag{3.2}$$

■

Exercise 3.2. Let n be a ***prime number***, and $a_1, \cdots, a_m \in \mathbb{N}^+$. Consider $f(k)$ the number of m-tuples $(c_1, \cdots, c_m)$ of numbers c_i, $1 \le c_i \le a_i$, that satisfy the relation:

$$\sum_{i=1}^{m} c_i \equiv k \,(mod\, n)$$

Then prove: $f(0) = f(1) = \cdots = f(n-1) \Leftrightarrow n \mid a_j$ for a certain value of $j \in \{1, 2, \cdots, m\}$

Proof: Let $\varepsilon = \cos(\frac{2\pi}{n}) + i\sin(\frac{2\pi}{n})$. Then we have the following relations:

$$\prod_{i=1}^{m}(x + x^2 + \cdots + x^{a_i}) = \sum_{1\le c_i\le a_i} x^{c_1+\cdots+c_m} \text{ and} \tag{3.3}$$

$$f(0) + f(1)\cdot\varepsilon + \cdots + f(n-1)\cdot\varepsilon^{n-1} = \sum_{1\le c_i\le a_i} \varepsilon^{c_1+\cdots+c_m} = \prod_{i=1}^{m}(\varepsilon + \varepsilon^2 + \cdots + \varepsilon^{a_i}) \tag{3.4}$$

And we find that:

$$f(0) = f(1) = \cdots = f(n-1) \Leftrightarrow f(0) + f(1)\cdot\varepsilon + \cdots + f(n-1)\cdot\varepsilon^{n-1} = 0 \Leftrightarrow$$

$$\Leftrightarrow \prod_{i=1}^{m}(\varepsilon + \varepsilon^2 + \cdots + \varepsilon^{a_i}) = 0 \Leftrightarrow \ \varepsilon + \cdots + \varepsilon^{a_j} = 0 \text{ for a certain value of } j \Leftrightarrow n \mid a_j$$

■

Restatement of Exercise 1.8. **(IMO, 1995)** For a finite *set* of real number A, we note $m(A)$ the sum of the *set*'s elements, and $|A|$ the *set*'s cardinal. Let p be a ***prime number***, and $A = \{1, 2, \cdots, 2p\}$.

Calculate the number of *subsets* $B \subset A$ with $|B| = p$ and $p \mid m(B)$.

Proof: $p = 2$ can be verified directly. Let $\varepsilon = \cos(\frac{2\pi}{p}) + i\sin(\frac{2\pi}{p})$.

We note with x_j the number of *subsets* $B \subset A$ with $|B| = p$ and $m(B) \equiv j \,(mod\, p)$. Then:

$$\sum_{j=0}^{p-1} x_j \varepsilon^j = \sum_{B\subset A, |B|=p} \varepsilon^{m(B)} = \sum_{1\le c_1 \le \cdots \le c_p \le 2p} \varepsilon^{c_1+c_2+\cdots+c_p} \tag{3.5}$$

The last number is a coefficient of x^p from the product $(x+\varepsilon)(x+\varepsilon^2)\cdots(x+\varepsilon^{2p})$. And because $x^p - 1 = (x-1)(x-\varepsilon)\cdots(x+\varepsilon^{p-1})$ we derive that:

$$(x+\varepsilon)(x+\varepsilon^2)\cdots(x+\varepsilon^{2p}) = (x^p+1)^2 \Rightarrow \text{ The coefficient of } x^p \text{ is } 2.$$

Therefore:

$$\sum_{j=0}^{p-1} x_j \varepsilon^j = 2 \Rightarrow x_0 - 2 + x_1\varepsilon + \cdots + x_{p-1}\varepsilon^{p-1} = 0 \Rightarrow x_0 - 2 = x_1 = \cdots = x_{p-1} = k \Rightarrow$$

$$\Rightarrow pk = x_0 + \cdots + x_{p-1} - 2 = C_{2p}^p - 2 \Rightarrow k = \frac{C_{2p}^p - 2}{p} \Rightarrow x_0 = 2 + \frac{C_{2p}^p - 2}{p}$$

So the answer is:

$$x_0 = 2 + \frac{C_{2p}^p - 2}{p} \tag{3.6}$$

■

Exercise 3.3. Prove that the number N is not *divisible* by 5 for any $n \in \mathbb{N}$, where N is

$$N = \sum_{k=0}^{n} (C_{2n+1}^{2k+1} \cdot 2^{3k})$$

Proof: It is sufficient to prove that S_n is not *divisible* by 5:

$$S_n = \sum_{k=0}^{n} (C_{2n+1}^{2k+1} \cdot (-2)^k)$$

But if we look at $(1+i\sqrt{2})^{2n+1} = R_n + i\sqrt{2}S_n$ where R_n is:

$$R_n = \sum_{k=0}^{n} (C_{2n+1}^{2k} \cdot (-2)^k)$$

Transitioning to modules, we find: $3^{2n+1} = R_n^2 + 2S_n^2$
If $S_n \equiv 0 \,(mod\, 5)$ then

$$(R_n^2 - 3^{2n+1}) \equiv 0 \,(mod\, 5) \tag{3.7}$$

$$3^{2n+1} = 3 \cdot 9^n \equiv \pm 3 \,(mod\, 5) \tag{3.8}$$

From Eq. (3.7) and Eq. (3.8) $\Rightarrow R_n^2 \equiv \pm 3 \,(mod\, 5)$ which is a contradiction $\perp$ ■

Restatement of Exercise 1.9. **(High-School Mathematics, 1994/1 Qihong Xie)**
Calculate the number of *subsets* of the *set* $\{1, 2, \cdots, 2000\}$ whose elements' sum is *divisible* by 5.

Proof: Consider the ***polynomial***: $f(x) = (1+x)(1+x^2)\cdots(1+x^{2000})$

There exists a bijection between the *set* of m-tuples $\{a_1, \cdots, a_m\}$ and the *set* of elements $x^{a_1} \cdot x^{a_2} \cdots x^{a_m}$. So we turn our attention toward the sum of the coefficients of elements that take the form x^{5k} in the expansion of f. Let $S \equiv$ the sum of the coefficients.

Let $\varepsilon = \cos(\frac{2\pi}{5}) + i\sin(\frac{2\pi}{5})$.

$$\varepsilon^5 = 1 \text{ and } 1 + \varepsilon + \cdots + \varepsilon^4 = 0$$

Then the sum S:

$$S = \frac{\sum_{j=1}^{5} f(\varepsilon^j)}{5}$$

$$\varepsilon, \varepsilon^2, \varepsilon^3, \varepsilon^4, \varepsilon^5 \text{ are the roots of } g(x) = x^5 - 1 = (x-\varepsilon)\cdots(x-\varepsilon^5)$$

Then: $g(-1) = -2 = (-1-\varepsilon)(-1-\varepsilon^2)\cdots(-1-\varepsilon^5) \Rightarrow (1+\varepsilon)\cdots(1+\varepsilon^5) = 2$ and

$$f(\varepsilon) = 2^{400}.$$

Similarly, we find $f(\varepsilon^j) = 2^j$ for $j = 2, 3, 4$
Therefore $f(\varepsilon^5) = f(1) = 2^{2000}$

Thus, we arrive at the answer $S = \frac{4\cdot 2^{400} + 2^{2000}}{5} = \frac{2^{402} + 2^{2000}}{5}$ ■

Alphabetic Index of some key terms

4. Bibliography

In the composition of this material we made use of the following books and articles, we highly recommend the reader to turn toward them for a deeper understanding:

- [AD10] - A great problem book that covers Algebra, Geometry/Trigonometry, Number Theory and Combinatorics. In this volume they present innumerable beautiful results, intriguing problems, and ingenious solutions. A must for the bookshelves of both aspiring and seasoned mathematicians.
- [Dum06a] or [Dum06b] - A well organized textbook that covers Algebra 1 for mathematics and computer science students alike, whose consistency never fails to prove useful.

Additionally, some exercises and solutions were inspired by the website [24], it contains highly valuable resources and materials, so take a look at it when you can.

References

[24] *Art of Problem Solving*. `https://artofproblemsolving.com`. Accessed: 2024-06-05. 2024.

[AD10] T. Andreescu and G. Dospinescu. *Problems from the Book*. 2nd. XYZ Press, 2010.

[Dum06a] T. Dumitrescu. *Algebra 1*. Editura Universității, 2006.

[Dum06b] T. Dumitrescu. *Algebra: pentru studenții facultăților de matematică și informatică din anul 1*. Editura Universității, 2006.

AUTOMATIC DETECTION OF OBJECTS CROMATIC COMPONENTS IN IMAGES

Alexandru-Marian GALEA[1], Bogdan SEBACHER[1] , Silvia MARZAVAN[1]

[1]Military Technical Academy "Ferdinand I" of Bucharest, 39-49 George Coşbuc, District 5, Bucharest, Romania

Corresponding author email: alexandru.galea2000@gmail.com

Abstract

The analysis and identification of chromatic components in digital imagery have broad applications in fields such as computer vision, image processing, and artificial intelligence. This paper presents an innovative approach for the automatic detection of chromatic components in objects within images. Despite the critical importance of accurate color detection for specific objects, the field remains relatively underdeveloped, with limited robust solutions available. Various factors, including lighting conditions, object textures, and environmental influences, complicate the accurate identification of colors. This study leverages advanced solutions such as YOLOv8-seg for COCO object segmentation and FastSAM for detailed parts segmentation, combined with mathematical approaches for body proportion analysis and Color Thief for color palette extraction. These integrated techniques enable precise identification and analysis of the color properties of individual objects.

Keywords*: Chromatic component detection; color analysis; object segmentation; YOLOv8-seg; FastSAM; Color Thief.*

1. INTRODUCTION

This study focuses on refining color extraction techniques to ensure that captured colors closely align with human visual perception. The aim is to develop a robust methodology that can be extended to various object categories ensuring versatility and reliability. One intriguing application is in the automotive sector, where the windscreen significantly influences the overall color palette of a vehicle. Another challenging application involves extracting colors from people's clothing, which presents unique difficulties due to the diversity of styles (length) and colors. To achieve the overall purpose advanced segmentation networks are utilized. YOLOv8-seg is employed for object categorization, providing precise identification of the object of interest. For vehicles, FastSAM is used to isolate the hood, ensuring that the large reflective surface of the windscreen does not skew the color extraction process. For people, mathematical human body proportions are applied to accurately identify and segment the clothing. Following the segmentation, the Color Thief algorithm is used to extract the representative colors accurately.

2. CONTENT

Ultralytics models, specifically YOLOv8-seg and FastSAM, were selected for their versatility, efficiency in object segmentation, and comprehensive documentation. YOLOv8-seg is a state-of-the-art image segmentation model that builds upon the success of previous YOLO versions, offering enhanced speed, accuracy, and flexibility. Pretrained models for YOLOv8-seg support the COCO (Common Objects in Context) dataset, a widely used benchmark for object detection, segmentation, and captioning tasks in computer vision. The COCO dataset includes 80 labeled classes, covering a broad range of objects. Following tests in different scenarios, the small pretrained segmentation model, YOLOv8s-seg, was chosen for its performance. YOLOv8-seg was employed specifically for silhouette extraction across multiple categories, with a focus on people and vehicles. The application of the pre-trained model yielded accurate results, providing precise masks and a wide range of detections with rapid processing times.

To further enhance the accuracy of color extraction, an improved separation in the obtained masks was desired. For the vehicle category, this led to the utilization of a new deep-learning model from

Ultralytics: FastSAM (Fast Segment Anything Model). FastSAM is a more efficient variant of the Segment Anything Model (SAM), a computationally heavy Transformer model. FastSAM achieves comparable performance to SAM but with significantly reduced computational resource requirements, enabling real-time application. FastSAM decouples the segmentation task into two sequential stages: all-instance segmentation and prompt-guided selection. The focus was on the first stage, which is based on YOLOv8-seg, to produce segmentation masks for all instances in an image, although the results are unlabeled. By applying this network on top of the initial YOLOv8-seg vehicle masks, it was possible to extract specific parts, such as the hood, by sorting the obtained masks based on the occupied area.

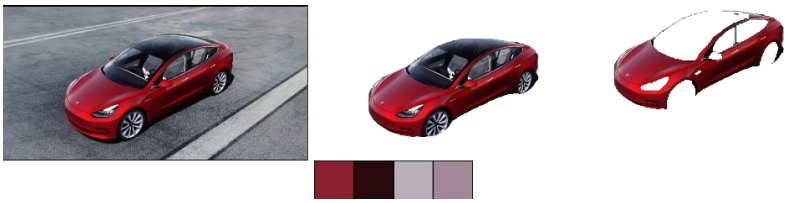

Figure 1: The visual steps in the process of vehicle color extraction

In the case of people, due to the lack of consistency of the previously found models in clothing extraction across different scenarios, a mathematical approach was adopted to separate the top from the bottom using human body proportions. Several calibrations were made to this method to enhance the generalization of the solution, ensuring more reliable and accurate segmentation.
After obtaining the most representative mask for the proposed task, the next step was color extraction. For this, Fast Color Thief was used, a Python module based on the ColorThief library, but faster and more efficient. It employs a modified version of the Median Cut Quantization algorithm optimized for speed, which facilitates the efficient extraction of dominant colors.
This combination of modules proved to be efficient in the task of color extraction for the desired categories, both in results and processing time.

Figure 2: The visual steps in the process of people color extraction

In a recent update to the research of people mask extraction tasks, the use of Segformer B2, which was specifically optimized for clothes segmentation, was noted as interesting. Better results are obtained with the semantic-based segmentation model. Although it requires more processing time, it can handle up to 18 categories and has shown promise for accuracy in a range of scenarios and sizes and it also benefits from integration support on the Hugging Face platform. To determine whether it can be integrated into the workflow, more testing and calibration will be done in this direction in the future.

3. CONCLUSIONS

This study has made progress in enhancing color extraction techniques within the framework of human vision by utilizing advanced segmentation networks like YOLOv8-seg and FastSAM. These networks have shown improvements in object classification and segmentation accuracy, especially in challenging scenarios like vehicle design and clothing styles. The integration of mathematical human body proportions for clothing segmentation and the use of Fast Color Thief for efficient color extraction have further optimized the process. Future research will aim to explore newer segmentation models, such as Segformer B2, to continue refining and expanding these techniques.

A STUDY OF THE REGIME TRANSITION TO TURBULENT FLOW IN BUBBLE COLUMN

Alexia Mirela DRAGAN[1,2], Marian Nicolae POȘOIU[1,2], Elena Corina CIPU[2,3], Cosmin Danuț BARBU[3]

[1]National University of Science and Technology Politehnica of Bucharest (UNSTPB), Power Engineering Faculty,
[2]Centre for Research and Training in Innovative Techniques of Applied Mathematics in Engineering "Traian Lalescu" (CiTi), Bucharest, Romania
[3]Applied Mathematics, Faculty of Applied Sciences

Corresponding author email: corina.cipu@upb.ro

Abstract

The processes in the bubble column are studied. The transition to turbulent flow is marked by increased bubble coalescence and breakup. This transition is influenced by the interplay of buoyancy, viscous, and inertial forces. Understanding this transition is essential for optimizing the design and operation of bubble columns to achieve efficient mixing, mass transfer, and reaction rates. The homogeneous-to-heterogeneous flow regime transition point dependence on gas and liquid properties was investigated. The transition gas holdup was empirically correlated as a function of the gas density, surface tension, and liquid viscosity, employing dimensional constants. The macroscopic phenomena that influence the performance of the bubble column were considered for the design and operation of bubble columns with specific orifice configurations to achieve desired flow regimes. By pursuing these research directions, a comprehensive understanding of orifice-induced turbulent flow and its effect on regime transition in bubble columns can be achieved, leading to improved design and operation of these systems in various industrial applications.

Key words*: mathematical modelling; regime transition; turbulent flow; numerical simulation; gas holdup*

1. INTRODUCTION

The performance of a bubble column is influenced by various microscopic phenomena [1-3]. Many investigators have tried to interpret and model the hydrodynamic phenomena using theoretical analysis and experimental results. However, most models have been limited to a low gas flow rate range [4-5]. The bubble formation process is affected by complicated interactions between bubbles and bulk liquid. Therefore, a reliable bubble formation model should be incorporated into the initial bubble size distribution.

2. CONTENT

Theoretical analysis of bubbling regimes transformation

A bubble column was used to study bubble formation from a submerged orifice. A single pore tube had its size adjusted with different drills, analysed with a high-resolution camera and software. Temperature effects were minimized using a three-wave lamp. A bubble column with various sparger designs was utilized to measure gas hold-up. Gas velocity was adjusted using mass flow controllers, with tap water as the liquid phase. The corresponding gas hold-up was calculated by:

$$\varepsilon_G(u_G) = \frac{\Delta P_0 - \Delta P_b(u_G)}{(\rho_L - \rho_G) g \Delta h} = 1 - \frac{\Delta P_b(u_G)}{\Delta P_0}, \text{ if } \rho_L >> \rho_G \quad (1)$$

The pressure signal was valid, and the drift flux method was used to identify gas velocity.

Various forces impact bubble shape and velocity during nucleation, growth, and detachment, including inertial, surface tension, gravitational, buoyancy, gas momentum transfer, and drag forces. The wake of bubbles, gas flow rate, and channelling also influence detachment, with different orifice sizes and flow rates affecting bubble size distribution. Important nondimensional numbers, such as

Bond number (Bo= $\frac{\rho_L g R_0^2}{\sigma}$ (2)) and Capillary number, differentiate the main forces acting on bubble formation.

Experimental set-up and bubble formation process

The bench-scaled cylindrical bubble column with various sparger designes could be used to measure gas hold-up, as in [1]. Statistical approaches to studying bubble dynamics in bubble columns:

- Spargers with different orifice diameters were used, changing the orifice number to maintain a constant free area.
- The effect on the sparger design on the gas hold-up and regime transition was obvious even though the column was high enough.

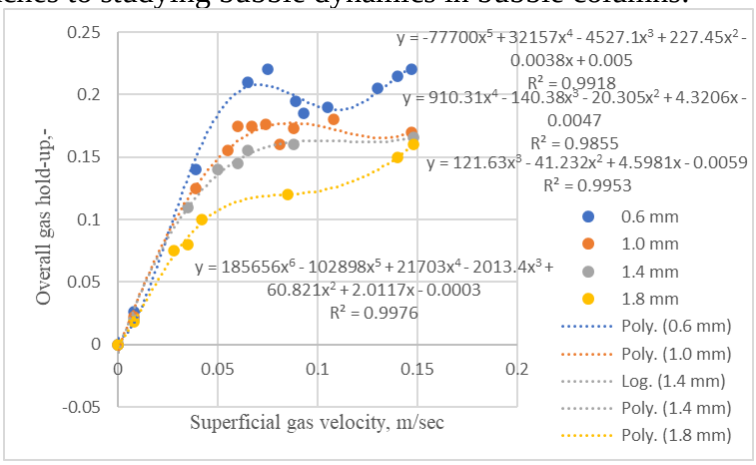

Figure 1

- A remarkable difference between the orifice and column induced transitions is observed in the transition of gas velocity variation with the column high.
- This column induced transition could be also characterized by the gradual change showing a maximum gas hold-up while the orifice induced transition was a sudden event with no maximum point.

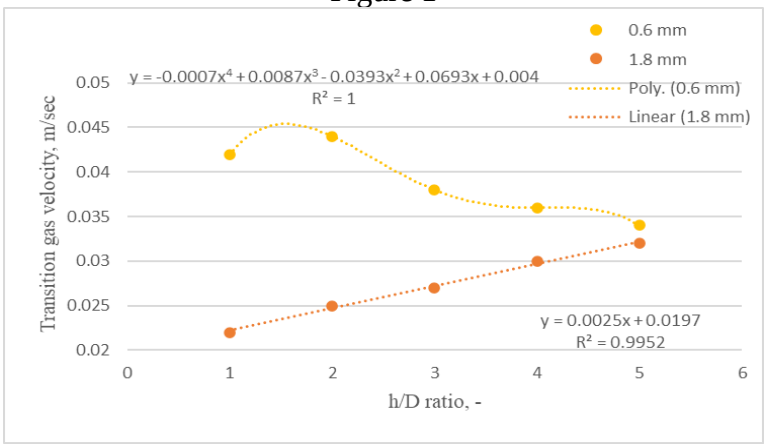

Figure 3

3. CONCLUSIONS

The bubble formation process in an air/water system is influenced by events such as the wake effect, channelling, and fluid turbulence. The detachment period of bubbles is strongly linked to these events, with an increase in gas flow rate leading to different modes of bubbling. Above a certain gas flow rate, a distinct transition is observed between orifice-induced and column-induced behaviours, each governed by specific factors and leading to different bubble generation patterns.

R E F E R E N C E S

[1]. Young Gul Hur et al.: Origin of regime transition to turbulent flow in bubble column: Orificeand column-induced transitions; International Journal of Multiphase Flow 50; 89-9; (2013)
[2]. Marek C. Ruzicka, Sandra Orvalho; Unsteady behaviour of bubble column in homogeneous flow regime: Startup and shutdown; Chemical Engineering Science 277; 118806; (2023)
[3]. Valois Parisien et al.: Bubble swarm characteristics in a bubble column under high gas holdup conditions; Chemical Engineering Science 15; 8 (2017)
[4]. Jun Young Kim et al.: Gas holdup and hydrodynamic flow regime transition in bubble columns; Journal of Industrial and Engineering Chemistry 56; 450-46; (2017)
[5]. Giorgio Besagni et al.: The effect of aspect ratio in counter-current gas-liquid bubble columns: Experimental results and gas holdup correlations; International Journal of Multiphase Flow 94; 53-78; (2017)

REMARKS ON THE STANLEY DEPTH AND HILBERT DEPTH OF MONOMIAL IDEALS WITH LINEAR QUOTIENTS

Andreea Ioana BORDIANU[1] and Mircea CIMPOEAȘ[1]

[1]National University of Science and Technology Politehnica Bucharest,
313 Splaiul Independentei, District 6, Bucharest, Romania

Corresponding author email: andreea.bordianu@stud.fsa.upb.ro

Abstract

We prove that if I is a monomial ideal with linear quotients in a ring of polynomials S in n indeterminates and depth(S/I) = n − 2, then sdepth(S/I) = n − 2 and, if I is squarefree, hdepth(S/I) = n – 2.

Key words*: Depth, Stanley depth, Hilbert depth, Monomial ideal, Linear quotients*

1. INTRODUCTION

Let $S = K[x_1, \dots, x_n]$ be a standard graded polynomial ring over a field KFor a finitely generated graded S-module M, the Hilbert series of M is defined by

$$H_M(t) = \sum_{j \geq 0} \dim_K(M_j)\, t^j$$

The Hilbert depth is $hdepth(M) = max\{r : (1-t)^r H_M(t) \text{ is positive}\}$.

Let $I \subset J \subset S$ be some monomial ideals. A Stanley decomposition of J/I is a decomposition

$$\mathcal{D}: J/I = \bigoplus_{i=1}^{r} u_i K[Z_i],$$

where u_i are monomials and $Z_i \subset \{x_1, \dots, x_n\}$ for all i. The Stanley depth of $\mathcal{D}$ is the minimal cardinality of some Z_i. The Stanley depth of J/I is

$$sdepth(J/I) = max\{sdepth(\mathcal{D}) : \mathcal{D} \text{ a Stanley decomposition of } J/I\}.$$

It is well known that hdepth(J/I) gives upper bounds for both depth(J/I) and sdepth(J/I).

Let $I \subset S$ be a monomial ideal and let G(I) be the set of minimal monomial generators of I. We say that I has linear quotients, if there exists a linear order $u_1 \leq u_2 \leq \cdots \leq u_m$ on G(I) such that the ideal $(u_1, \dots, u_{j-1}) : u_j$ is generated by a subset of variables for all $2 \leq j \leq m$.
Let $Z_1 = \{x_1, \dots, x_n\}$ and $Z_j = \{x_i : x_i \notin (I_{j-1} : u_j)\}$ for $2 \leq j \leq m$. With the above notations, we have the Stanley decomposition:

$$I = u_1 K[Z_1] \oplus u_2 K[Z_2] \oplus \cdots \oplus u_m K[Z_m]. \quad (1)$$

In particular, this shows that sdepth(I)≥depth(I).

On the other hand, the computation of sdepth(S/I) and hdepth(S/I) are very difficult. The aim of our paper is to tackle the first (not trivial) case, that is, when depth(S/I)=n-2. We show that, in this case, sdepth(S/I)=n-2 and, if I is squarefree, then hdepth(S/I)=n-2 also.

The presentation is based on the paper [1].

2. CONTENT

The main results of our paper are the following:

Theorem 1. Let $I \subset S$ be a monomial ideal with linear quotients and depth(S/I)=n-2.
Then sdepth(S/I)=n-2.

Theorem 2. Let $I \subset S$ be a squarefree monomial ideal with linear quotients and depth(S/I)=n-2.
Then hdepth(S/I)=n-2.

We mention that the proof of Theorem 1, rely on the following Lemma:

Lemma: Let $I \subset S$ be a monomial ideal with linear quotients and depth(S/I)=n-2, where n>2. Then there exists a variable x_i and a minimal monomial generator u such that $(I, x_i) = (u, x_i)$. Moreover, u can be chosen to be the last generator in the linear order of I.

Also, the proof of Theorem 2 is based on the expression of the Hilbert series of S/I which can be deduced from the decomposition (1).

3. CONCLUSIONS

We proved that any monomial ideal I with linear quotients with depth(S/I)=n-2 has sdepth(S/I)=n-2. Also, if I is squarefree with depth(S/I)=n-2 then hdepth(S/I)=n-2.

Bibliography

[1] A. Bordianu, M. Cimpoeas, *Remarks on the Stanley depth and Hilbert depth of monomial ideals with linear quotients*, to appear in Rocky Mountain Journal of Mathematics (2024).

SIMULATION MODELS FOR STRATEGIC DECISION MAKING:

GAMES - MILITARY VS CIVIL

Sorana-Eliza BĂLTĂREȚU[1,2], Robert-Mihai PIVODĂ[1,2], Antonela TOMA[1,2], Mihai REBENCIUC[1,2]

[1]University Politehnica of Bucharest, 313 Splaiul Independenței, District 6, Bucharest, Romania

[2]Center of Research and Training in Innovative Techniques of Applied Mathematics in Engineering ”Traian Lalescu”

Corresponding author email: sorana.baltaretu@stud.etti.upb.ro, robert_mihai.pivoda@stud.etti.upb.ro, antonela.toma@upb.ro, mihai.rebenciuc@upb.ro

Abstract

In control theory, differential games extend the concept by involving multiple controls, each managed by different players aiming to minimize their respective costs through optimal strategies. These games involve evolutionary processes described by dimensional systems of differential equations, with each player adjusting their control based on limited information about the opponent`s actions. The objective of each player is to optimize a payoff function, which typically includes a terminal payoff and an integral of costs over time, reflecting the continuous nature of the game. Differential games can be framed as zero-sum games, such as Blotto games and duels, where players` strategies and resource allocations directly impact each other`s outcomes, leading to a win-lose situation. Some important notions in military games are represented by analyses of specific military situations provided by Blotto games, exemplified by the strategic allocation of resources by two generals across multiple battlefronts, highlight the complexities and critical importance of effective resource distribution to achieve victory in military strategy.

Keywords*:* Control Theory, Differential Games, Payoff Functions, Zero-sum Games, Blotto Games

1. INTRODUCTION

In this paper, we aim to provide a clear overview of differential games, focusing on their main ideas and uses. We will explore how each player tries to maximize their payoff, which includes both a final reward and the total costs over time. This approach highlights the ongoing and dynamic nature of these games. We will also examine how differential games can be seen as zero-sum situations, like strategic allocation games and duels, where the choices of each player directly affect the outcomes for the others, creating a competitive environment.

2. CONTENT

2.1. Colonel Blotto Games

Blotto games are strategic scenarios where players independently and simultaneously allocate their resources across various battlegrounds. Success in each engagement is determined by the combination of these allocations. The overall outcome of the game depends on the strategic interactions among players, as each player's choices influence the final results. This makes Blotto games a differential game, where the outcome is not only influenced by individual strategies but also by how these strategies interact and compete across multiple fronts. Players must carefully

strategize their resource allocations, considering the potential moves of their opponents, to maximize their chances of success in each conflict and ultimately in the game.

Blotto Game Framework:

1. **Players and Resources:** There are two players: the attacker and the defender. Each player has a set amount of resources to allocate. In this example, the initial resources are denoted as A for the attacker and B for the defender.
2. **Targets/Battlefields:** Multiple targets are involved in either defense or attack. These targets are indexed by k.
3. **Allocation of Resources:** Each player decides how to distribute their resources across these targets. Let x_k represent the defender's allocation to target k , and y_k denote the attacker's allocation to the same target.
4. **Outcome Function:** The probability of success at each target depends on the resources allocated by both sides. The function $f_k(x,y) = \frac{y_k x^m}{y_k x^m + (1-y_k) y^m}$ determines the likelihood of the attacker capturing or destroying target k. This function incorporates the target's inherent defensibility (y_k) and the parameter m , which measures the influence of resource disparities on outcomes.
5. **Optimization and Strategy:** Both players strive to optimize their resource allocations to maximize their overall success. The defender aims to enhance the likelihood of successfully defending targets, while the attacker seeks to increase the chances of capturing or neutralizing them. Finding optimal strategies involves computing the best resource distribution based on the given characteristics and probabilities.

2.2. Differential games

Differential games in military strategy focus on dynamic resource allocation to achieve tactical superiority. Based on Lanchester's equations, which outline how opposing forces degrade each other's capabilities, these games extend to scenarios with diverse force compositions like infantry and artillery. Strategic decisions typically involve dividing resources in fixed ratios, but agile adversaries may exploit variable concentration tactics to sway the outcome during engagements. Research explores optimizing these allocation strategies within the framework of Lanchester's equations to enhance operational effectiveness in military contexts.

3. CONCLUSIONS

To conclude, the research aims to provide insights into differential games, highlighting their role in optimizing strategies through dynamic resource allocation. It demonstrates their zero-sum nature, as seen in Blotto games, and their critical applications in military contexts using Lanchester's equations to enhance tactical effectiveness.

4. REFERENCES

Barry O'Neil. "Game Theory Models of Peace and War". Yale University, Chapter 29

Shubik, M., and R. Weber (1979) ,Systems defense games, Colonel Blotto, command and control', Naval Research Logistics Quarterly, 28: 28 1-287.

Taylor, J. (1983) Lanchester Models of Combat. Alexandria, VA: Military Operations Research Society.

Taylor, J. (1978) ‚Differential-game examination of optimal time-sequential fire-support strategies', Naval Research Logistics Quarterly, 25: 323-355.

A FISHER-TYPE EVOLUTION EQUATION WITH APPLICATIONS IN IMAGE PROCESSING

Bogdan MAXIM[1]

[1]University of Craiova, 13 Alexandru Ioan Cuza Street, Craiova, Romania

Corresponding author email: maximdbogdan@gmail.com

Abstract. The aim of this paper is to present some applications of the Neumann Laplacian in image processing, along with the necessary mathematical background. We prove weak and strong versions of the maximum principle for weak solutions of elliptic and parabolic problems and apply them to a Fisher K.P.P.-type equation. The original contribution lies in the application of this equation in image processing, where various diffusion-like effects can be achieved. Additionally, a review of the basics of linear and nonlinear PDEs with Neumann boundary conditions is provided, along with updated bibliography and recent qualitative results. There are also some new theoretical results developed in this work.

Key words*: Neumann Laplacian, asymptotic behaviour, semilinear elliptic and parabolic problems, strong maximum principle, PDEs in image processing, weak formulation of PDEs.*

1. INTRODUCTION

The Fisher equation is primarily used in population dynamics models. However, due to its rich properties, such as global boundedness, it is also well-suited for applications in image processing.

In this research article, we will conduct a thorough study of the following semilinear evolution problem:

$$\begin{cases} \frac{\partial u}{\partial t} - d\Delta u = \alpha u(r(x) - p(x)u), \quad (t,x) \in (0,T) \times \Omega \\ \frac{\partial u}{\partial \nu} = 0, \qquad (t,x) \in (0,T) \times \partial\Omega \\ u(0,x) = u_0(x), \ x \in \Omega \end{cases} \tag{1}$$

The problem in set up in a domain $\Omega \subset \mathbb{R}^N$. Of particular interest will be the case when $N = 2$, especially considering its relevance to applications in image processing.

Simulating PDEs on images can provide valuable insights into how differential operators behave and their specific characteristics.

Engineers commonly refer to Neumann boundary conditions as natural conditions, whereas in image processing, they are termed reflective conditions and are suitable for applying PDEs to images. These conditions describe an isolated domain where there is no flux through the boundary. They are notable because, in formulating weak versions of PDEs, the space of test functions is not constrained by the boundary conditions, unlike in the case of Dirichlet conditions.

2. CONTENT

Section 1 begins by proving weak versions of the maximum principle for elliptic and parabolic PDEs, which will serve as the main results applied in this work. Complete proofs are provided since they may not be readily available in basic monographs on this subject.

In Section 2, we address linear heat equations with Neumann boundary conditions and lay the groundwork necessary for Section 3, where we study a semilinear para- bolic equation with a logistic term. We emphasize the importance of strong forms of the maximum principle, enabling analysis of our solutions in terms of the problem's parameters. Here, we utilize an elegant functional method involving the notion of almost interior points, introduced by J. Gluck and M. Weber.

Sections 4 and 5 are devoted to studying the steady-states of the parabolic problem. Subsequently, in Section 6, we present the main result of the paper: the uniform asymptotic stability of the only nontrivial steady state of our main problem.

Finally, we discuss how the gathered results can be applied to modify images and develop an algorithm implemented using Matlab R2023b, capable of transforming one picture into another using diffusion. Additionally, we explore the application of diffusion for two more puposes: causing an image to dissapear or gradually transforming it into a mathematical solution of (1).

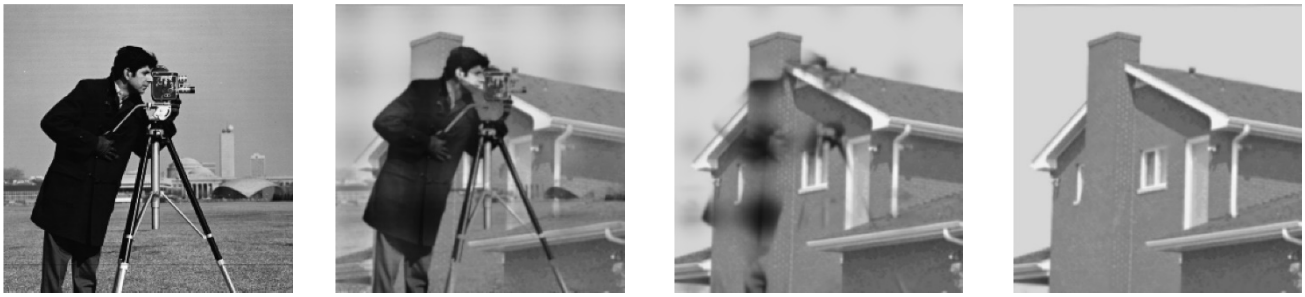

Figure 1: Transforming cameraman into house

There are some new results and many non-obvious details and tricks that fill the existent gaps in the proofs of some well-known results. The hypotheses in which we work mostly are very general: we use Lipschitz domains and weak solutions for PDEs.

3. CONCLUSIONS

Further investigations have to be made in order to improve the numerical algorithm. I also believe that the asymptotic stability holds in the case when Ω is not assumed to be convex.

A DIFFERENT APPROACH TO THE PROBLEMS GIVEN AT THE MATHEMATICS OLYMPIAD

Bogdan MAXIM[1]

[1]Costache Negruzzi National College, Strada Toma Cozma 4, Iași, Romania

Corresponding author email: maximdbogdan@gmail.com

Abstract. In this paper, I propose a practical approach to problems that might appear in mathematics olympiads. I will present several problems based on real-life situations, along with their solutions and comments. These problems are drawn from various branches of mathematics, including probability theory, differential and integral calculus, elementary geometry, game theory, and mathematical models in physics. At the end of the paper, I have included a list of challenging applied problems without solutions. This is intended as an invitation for students and teachers to engage with them, with the hope that we might one day encounter significant applied mathematics problems in school olympiads.

Key words*: applications of integral calculus; applications of differential calculus; game theory; practical geometry; probabilities and statistics; mathematical models in physics*

1. INTRODUCTION

In my opinion a big issue of the mathematical olympiad is the fact that applied problems seem to be prohibited and there is no attraction for the gifted pupils of this modern world to get involved in this type of purely abstract competition. I aim to show that applied mathematical problems can be part of the mathematical olympiad, at any level of difficulty.

2. CONTENT

Here are some of the statements of the problems I will present:

- **The grading of the wine barrel:** How can we grade a hose or a stick so that when we insert it into the bunghole of a wine barrel lying horizontally, we know exactly how many liters of wine are left in that barrel?

- **The release of the prisoners:** Say there are 100 prisoners, numbered 1 to 100. Slips of paper containing each of their numbers are randomly placed in 100 boxes in a sealed room. One at a time, each prisoner is allowed to enter the room and open any 50 of the 100 boxes, searching for their number. And afterwards, they must leave the room exactly as they found it, and they can't communicate in any way with the others prisoners. If all 100 prisoners find their own number during their turn in the room, they will all be freed. But, if even one of them fails to

find their number they will all be executed. The prisoners are allowed to strategize before any of them goes into the room.

a) What is the probability that all prisoners will be released if they do not adopt any strategy?
b) Prove that there exists a strategy that ensures all the prisoners are released with a probability greater than 30%.
c) Show that the same strategy can be used regardless of the number of prisoners, and the probability of all being released remains above 30% (they can open half of the boxes).
d) Prove that if the prisoners speak with a kind guard and he carefully exchange the numbers in two chosen boxes, then they can all be released with certainty.
e) If a malicious guard overhears their technique and arranges the boxes in a way that guarantees they will lose, can they do anything to maintain their chances of escaping at more than 30%?
f) Determine the limiting probability as the number of prisoners approaches infinity using the strategy described in part b).

Finally, here are some selected problems from the WORKSHEET OF APPLIED MATHEMATICS PROBLEMS given at the end of the paper:

- (STATISTICS) Having a set of points in the plane $P_1(x_1, y_1), P_2(x_2, y_2), \dots, P_n(x_n, y_n)$ prove that there is a unique line d (which will be an alternative of the best aproximation line) for which the sum: $\text{dist}(P_1, d)^2 + \text{dist}(P_2, d)^2 + \cdots \text{dist}(P_n, d)^2$ is minimized.
Maxim Bogdan

- (FINANCES) Demonstrate that a decreasing installment loan is always more advantageous (i.e., has a lower total cost) than a fixed installment loan, provided that the interest rate remains unchanged. *Maxim Bogdan*

- (GAME THEORY) There are 21 cards in a deck. You look at a card without touching it. The juggler shuffles the 21 cards and puts them into 3 columns, showing us where he places each card. He does this 3 times, and each time we only tell him which column our chosen card is in (without telling him which card it is). Each time, he places the column indicated by us in the middle (with one column of cards above and one below). Demonstrate that in the end, the 11-th card is the one we chose. *Maxim Bogdan*

- (CALCULUS) A lawn sprinkler waters the lawn from a height of $h \geq 0$ (in meters) with a launch speed of v m/s. Find the launch angle for which the water reaches the maximum distance from the launch point as a function of h and v. What is this maximum distance?

3. CONCLUSIONS

In conclusion, the beauty of applied mathematical problems should be promoted and not concealed from students.

GEOLOGICAL SOFT DATA INTEGRATION TO FACIES PROBABILITY FIELDS USING A REGULARIZED ELEMENT FREE GALERKIN METHOD

Roxana DOBRE[1], Bogdan SEBACHER[1], Silvia MARZAVAN[1]

[1]Military Technical Academy "Ferdinand I" of Bucharest, 39-49, BLV. George Coşbuc, Bucharest, Romania

Corresponding author email: bogdan.sebacher@mta.ro

Abstract

The exploration phase of a reservoir involves gathering geological information from various sources. Geophysical analysis using an inversion technique creates facies probability fields, while geologists studying the cores extracted from wells can identify the types of rocks (facies) found at those locations. However, these two pieces of information are uncertain and uncorrelated. This paper outlines a methodology that combines these two sources of information to update facies probability fields, integrating both core data and seismic information. The proposed method uses a regularized form of the element-free Galerkin, incorporating geological data observations in a probabilistic soft representation with a penalty term defined by the probability fields from seismic data. The method is tuned with multiple parameters, and its impact is analyzed.

Keywords: *Element-free Galerkin; Facies probability field; Geological soft data; Tikhonov regularization;*

1. INTRODUCTION

The reliable estimation of the distribution of facies in a reservoir it's important to effectively develop any field management planning of the reservoir. During the exploration phase of the reservoir, geologists, geophysicists, and other experts gather information about rock types from subsurface, their contacts, sizes, and orientations all of these from core observations, outcrop evaluations, and seismic data evaluation. One critical piece of information for geological simulation is the probability field of facies, which needs to be conditioned to facies observations from well locations. This paper outlines a method to condition the prior probability fields of facies to well-collected facies observations, merging information from a seismic inversion with well data. Here, the facies observations are considered in soft representation, which introduces uncertainty in the process of facies observation at the well locations. The proposed method involves a regularized form of the element-free Galerkin, incorporating the soft geological observations with a penalty term defined by the probability fields from seismic data. The method is tuned with multiple parameters, and its impact is analyzed. The experiments show the versability of the method in terms of its flexibility in weighting the influence of the two pieces of information, probability fields from seismic and soft geological data.

2. CONTENT

The methodology will be presented for a case with three facies types, denoted F1, F2, and F3 that occur in a hydrocarbon reservoir and have a certain spatial distribution (which is not relevant for this moment). From the seismic inversion come three facies probability fields, presented on the left side of Fig.1, and using the examination of cores extracted, the geologists consider that the occurrence of the facies types is characterized by the probabilities presented on the right side of Fig.1.

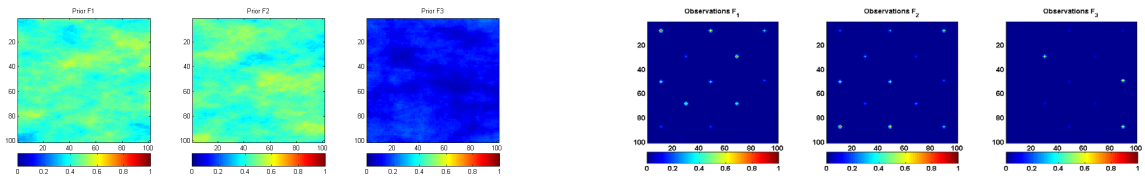

Figure 1. Facies probability fields from seismic (left side) and soft facies observatios (right side)

In Fig.1, at each location are three probabilities p_1, p_2, p_3 that sum up to 1, each expressing the confidence of the geologists in their occurrence in the entire grid-cell. To condition the probability fields to soft facies observations we use the element-free Galerkin method, with a Tikhonov regularization term, defining the cost function as in eq.1.

$$J\left(a^{(1)}, a^{(2)}, a^{(3)}\right) = \sum_i w_i \left(X_i^T a^{(1)} - obs^{(1)}(u_i)\right)^2 + \lambda_1 \left(X^T a^{(1)} - p^{(1)}(u)\right)^2 + \sum_i w_i \left(X_i^T a^{(2)} - obs^{(2)}(u_i)\right)^2 + \lambda_2 \left(X^T a^{(2)} - p^{(2)}(u)\right)^2 + \sum_i w_i \left(X_i^T a^{(3)} - obs^{(3)}(u_i)\right)^2 + \lambda_3 \left(X^T a^{(3)} - p^{(3)}(u)\right)^2 + \mu\left(X_i^T a^{(1)} + X_i^T a^{(2)} + X^T a^{(3)} - 1\right)^2 \quad (1)$$

For each unsampled location u of cartesian coordinates $u = (x, y)$, and for each facies type the updated probabilities are $p_1^{up}(u) = X^T a^{(1)}, p_2^{up}(u) = X^T a^{(2)}, p_3^{up}(u) = X^T a^{(3)}$, where the vectors $X^T = [1\ x\ y]^T$ and $X_i^T = [1\ x_i\ y_i]^T$ corresponds to all locations $u_i = (x_i, y_i)$ with facies observations (at the well locations, see Fig. 1 right side). The residuals are weighted with subunit values $w_i = W(||u - u_i||_B)$, calculated with a weight function of which values decreases as we move away from location u. The parameters $a^{(1)}, a^{(2)}, a^{(3)} \in R^3$ are the ones that minimize the cost function from eq.1. The solution is obtained analytically, but depending on the case one may use a pseudo-inverse instead of inverse when solving the linear system defined by setting the gradient equal to 0. The purpose of the final term $\mu\left(X_i^T a^{(1)} + X_i^T a^{(2)} + X^T a^{(3)} - 1\right)^2$ from the cost function is to ensure that all the updated probabilities $X^T a^{(1)}$, $X^T a^{(2)}$, $X^T a^{(3)}$ sum up to 1, so they can be considered real probabilities.

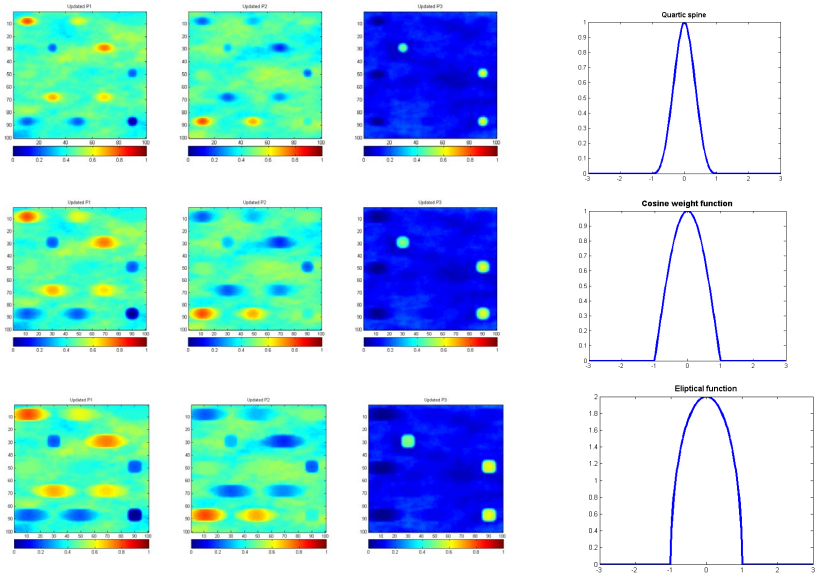

Figure 2. Updated facies probability fields with three weight functions

In Fig. 2 are presented three sets of facies probability fields constructed with the regularized EFG methodology presented before. The difference is made by the weight function used in the cost function from eq.1. The three functions presented on the right side of the figures are as follows, the quartic spline function, the cosine function, and the elliptic function. As observed examining the results, the weight function influences the estimation, so their choice should be done taking into account extra criteria and one could be the history matching result. However, this will be a subject of a future study. All the experiments from Fig. 2 used the same values for the Tikhonov parameters $\lambda_1 = \lambda_2 = \lambda_3 = \mu = 0.01$, and also the anisotropy was involved in the calculus of the B-distance $||u - u_i||_B$.

3. CONCLUSIONS

This paper presents a regularized version of the element-free Galerkin method used for conditioning the probability fields of rock types (facies) to soft facies observations. The results are probability fields for facies that consistently incorporate both sources of information and are input in any geological simulation model. The updated facies probability fields generated with the proposed regularized EFG method are the prior models in the assisted history matching process.

New Properties of Isogonal Cevians in a Triangle

By Petru Marian Braica,

Professor at *Mihai Eminescu National College*, Satu Mare

Summary

In this paper, we extend a classical property concerning the cyclicity of a quadrilateral with vertices at the projections of B and C onto two isogonal cevians originating from vertex A of an arbitrary triangle ABC. We will examine the intersections of the isogonal lines with circles in which sides AB and AC are chords subtending congruent, variable angles. The cyclic property is preserved, and the center of the obtained circumcircle is no longer the midpoint of side (BC), but is instead mobile on the perpendicular bisector of (BC). The proof of this result utilizes the concept of the radical axis of two circles and the radical center of three circles, notions that are included in the Olympiad curriculum, making this presentation suitable for the excellence group. This method of extending perpendicularity problems to those involving segments in circles subtending congruent angles can generate new, interesting results, such as the theorem presented in this paper. The difficulty of proving this result led to its selection in the prestigious 2023 "*Viitori Olimpici*" National Competition. Additionally, we will demonstrate the generation of the median and symmedian from vertex A as centers of circumcircles of quadrilaterals determined by the intersections of isogonal lines with perpendicular lines.

We will begin by presenting the source problem. We have chosen an obtuse angle for increased visibility of the diagram.

The Source Problem

Consider the triangle ABC with m(∠A) > 90°. Inside angle ∠BAC, consider the half-lines (AX and (AY such that ∠BAX ≡ ∠CAY (meaning the half-lines make the same angle with the sides of the triangle, or in other words, they are equally inclined to the sides, or isogonal). Let M be the midpoint of side BC, and let P and Q be the feet of the perpendiculars drawn from vertex C to the two half-lines (AX and (AY.

a) Prove that triangle MPQ is isosceles.

b) If we denote by R and S the feet of the perpendiculars drawn from point B to the half-lines (AX and (AY, can we affirm that points P, Q, R, S lie on the same circle?

(Petru Braica, *The National Camp Lyon-Someş*)

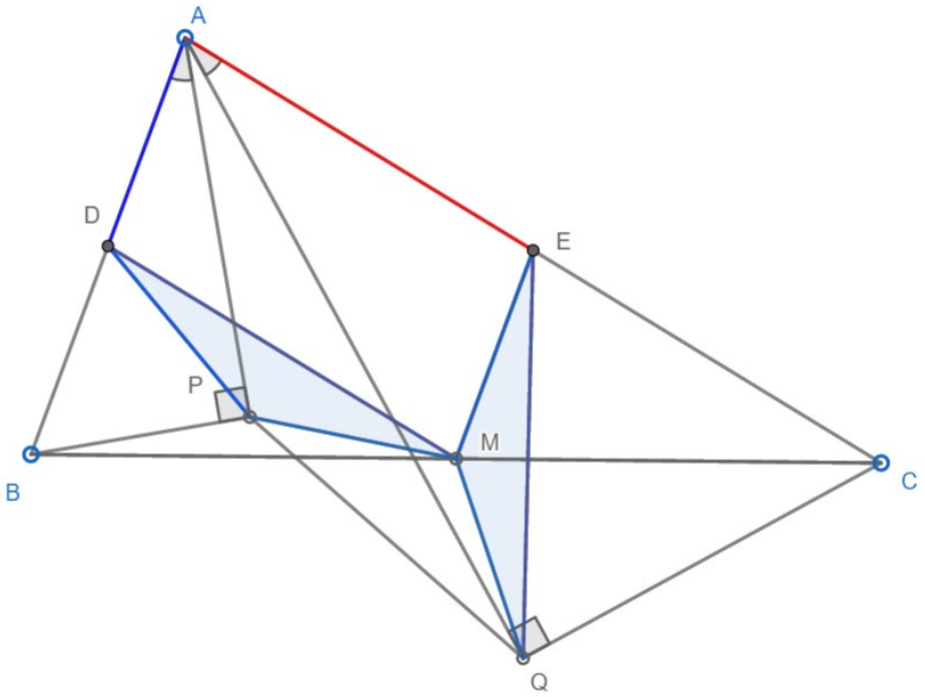
A
D
E
P
M
B
C
Q

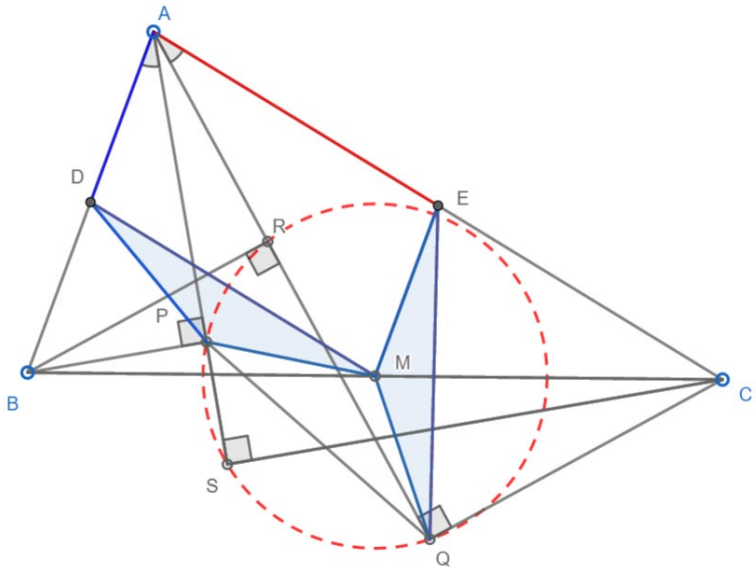
A
D
E
R
P
M
B
C
S
Q

Observations

1. The property that the projections of vertices B and C onto two isogonal cevians from vertex A are four concyclic points can also be observed when the angles are greater than the measure of angle ∠A. Thus, the half-lines will lie outside the triangle but will still be equally inclined to the sides of the triangle.

2. There is an alternative way to justify the conclusion of point b), namely through calculation. Thus, the lengths of segments MP and MQ can be determined by applying the Law of Cosines in the congruent triangles MPD and MQE. If we denote α as the measure of angle BAP, we obtain that the angle PDM measures the absolute value of the difference ∠A - 2α. Thus, the length of segment MP is given by the equality:

$$r = \sqrt{\frac{b^2 + c^2}{4} - \frac{bc}{2} \cdot \cos\ (\angle A - 2\alpha)}\,.$$

If we now consider the projections onto the isogonal lines with inclination A - α, and redo the calculation, we obtain the value:

$$r = \sqrt{\frac{b^2 + c^2}{4} - \frac{bc}{2} \cdot \cos\ (\angle A - 2(\angle A - \alpha))}\,.$$

or

$$r = \sqrt{\frac{b^2 + c^2}{4} - \frac{bc}{2} \cdot \cos\ (2\alpha - \angle A)}\,,$$

the distance which, in the parity of the cosine function, yields the same length as MP. Therefore, the metric form of the radius justifies the equality MP = MR. At the same time, we can pose the problem of the extreme length of the radius r.
It is immediately obtained that the extreme values of the radius of the circle with center at point M, which contains the projections of vertices B and C onto the isogonal lines, are:

$$r_{min} = |\, b - c \,| / 2$$

respectively

$$r_{max} = (\, b + c \,) / 2,$$

which occur for the angle $\alpha_{min} = \angle A / 2$ and $\alpha_{max} = (\pi + \angle A) / 2$.

3. Another more interesting generalization would be if we consider the points A, P, R, B and A, S, Q, C on circles where the sides of triangle ABC, (AB) and (AC), are subtended by congruent angles. The concyclicity of the points is preserved, however, the center of the circle is not necessarily the midpoint of side BC; it will be a point located on the perpendicular bisector of the side.

The main result of this paper

Regarding the last observation, we now formulate the main result as follows:

Theorem 1 (Petru Braica)

Consider triangle ABC with AB < AC and within which (AX and (AY are two interior half-lines of angle BAC, isogonal (meaning: ∠BAX ≡ ∠CAY). Let E and F be points exterior to the triangle, from which the sides (AB) and (AC) are seen under the same angle, in different half-planes determined by the line AB. The circumcircle of triangle ABE intersects the half-lines (AX and (AY at points M and P, respectively, and the circumcircle of triangle AFC intersects the half-lines (AX and (AY at points N and Q, respectively.

Prove that:

a) Points M, N, P, and Q are concyclic;
b) The center of the circumcircle of the quadrilateral with vertices M, N, P, and Q lies on the perpendicular bisector of segment (BC).

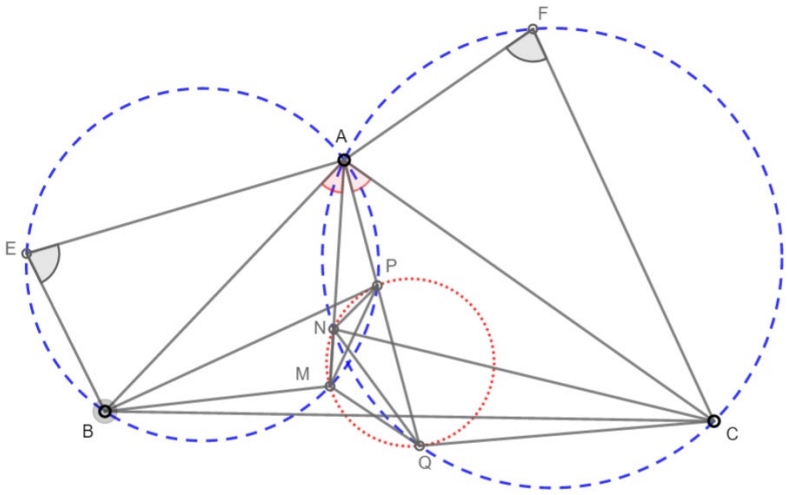

a) The quadrilateral APMB is inscribable, thus the angles ∠AMP and ∠ABP are congruent, as they subtend the chord (AP). The measure of these angles is 180° - m(∠BAP) - m(∠BPA). On the other hand, the measure of angle ∠NQA is equal to the measure of angle ∠NCA, which in turn equals 180° - m(∠NAC) - m(∠ANC). Since angle ∠ANC is the supplement of angle ∠AFC and angle ∠AMB is the supplement of angle ∠AEB, we deduce from the hypothesis of the problem, stating that ∠AEB is congruent to ∠AFC, that angles ∠ANC and ∠AMB are congruent. Additionally, from the isogonality of the half-lines (AM and (AQ, we deduce by the difference of congruent angles that angles ∠CAN and ∠BAP are congruent. Finally, we have that angles ∠NMP and ∠NQP are congruent, which is equivalent to the inscribability of the quadrilateral MNPQ. This justification is for the order of points M, N, P, Q as shown. For a different order, a similar demonstration of the concyclicity of points occurs.

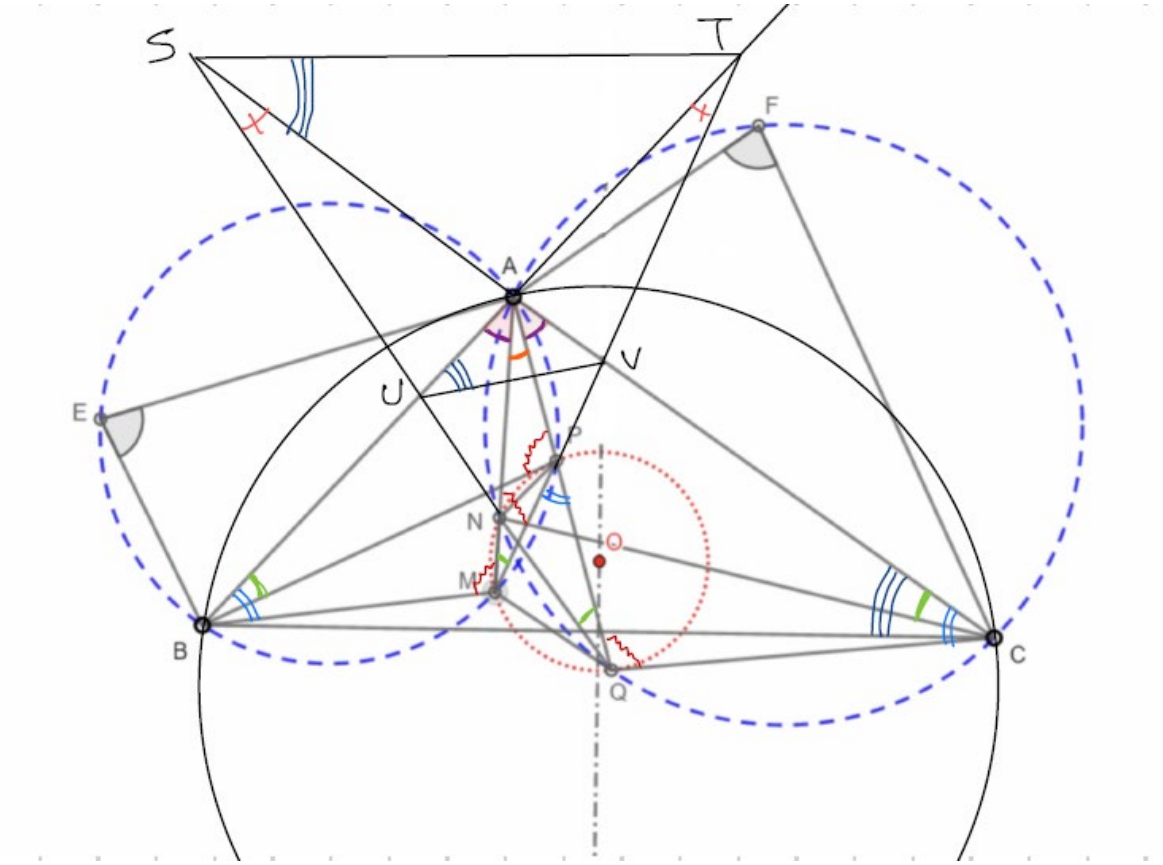
S
T
F
A
U
V
E
P
N
O
M
B
C
Q

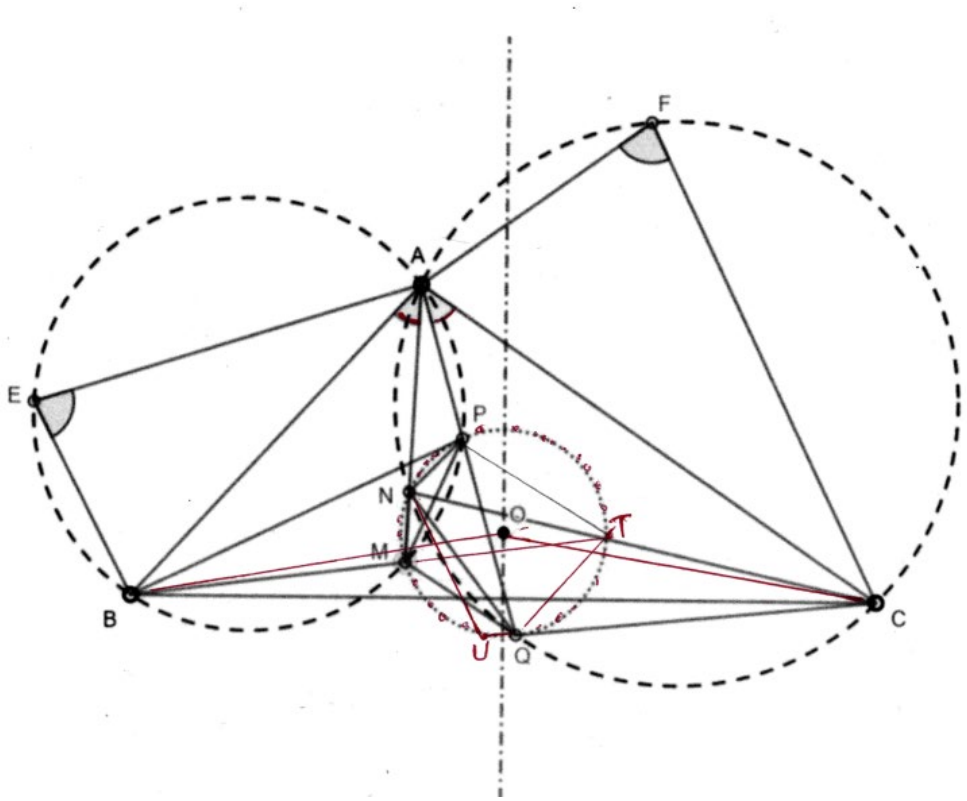

The next result refers to the concyclicity of the intersections of the altitudes from vertices B and C with two isogonal cevians drawn from vertex A, on a circle with a center that reconstructs the median from A of the triangle. A result from projective geometry, called the Brocard's theorem, will be needed for the second part of the demonstration.

Theorem 2 (David Anghel & Petru Braica)
Let ABC be any triangle, and let i_1, i_2 be two isogonal half-lines with origin at vertex A. The altitudes from B and C of triangle ABC intersect the two half-lines i_1 and i_2 at four points.

Show that these four points lie on a circle with the center located on the median from A of triangle ABC.

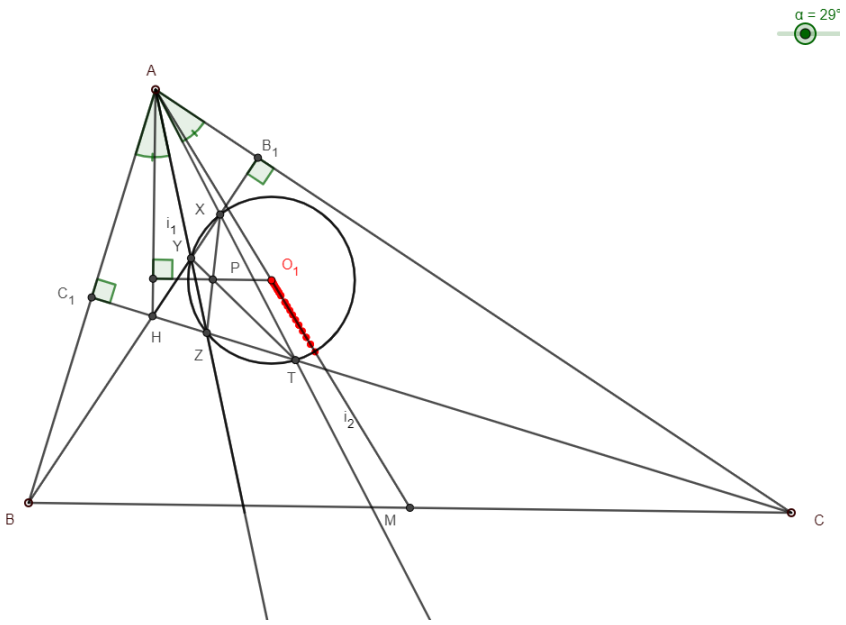

If we reverse the intersections in Theorem 2, we will obtain quadrilaterals inscribed in circles with centers on the median from vertex A of triangle ABC.

Theorem 3 (Petru Braica & David Anghel)

Sure, here is the formal and elegant translation of your mathematical text into English: Let $\triangle ABC$ be any given triangle, and let i_1 and i_2 be two isogonal lines originating from vertex A. The perpendicular drawn from vertex B to i_2 intersects i_1 at point X. The perpendicular from vertex B to i_1 intersects i_2 at point Y. The perpendicular drawn from vertex C to i_1 intersects i_2 at point Z, and the perpendicular from C to i_2 intersects i_1 at point T. Demonstrate that points X, Y, Z, and T lie on a circle with center O. Moreover, if S denotes the intersection of the tangents to the circumcircle of triangle ABC drawn at vertices B and C, then points A, O, and S are collinear.

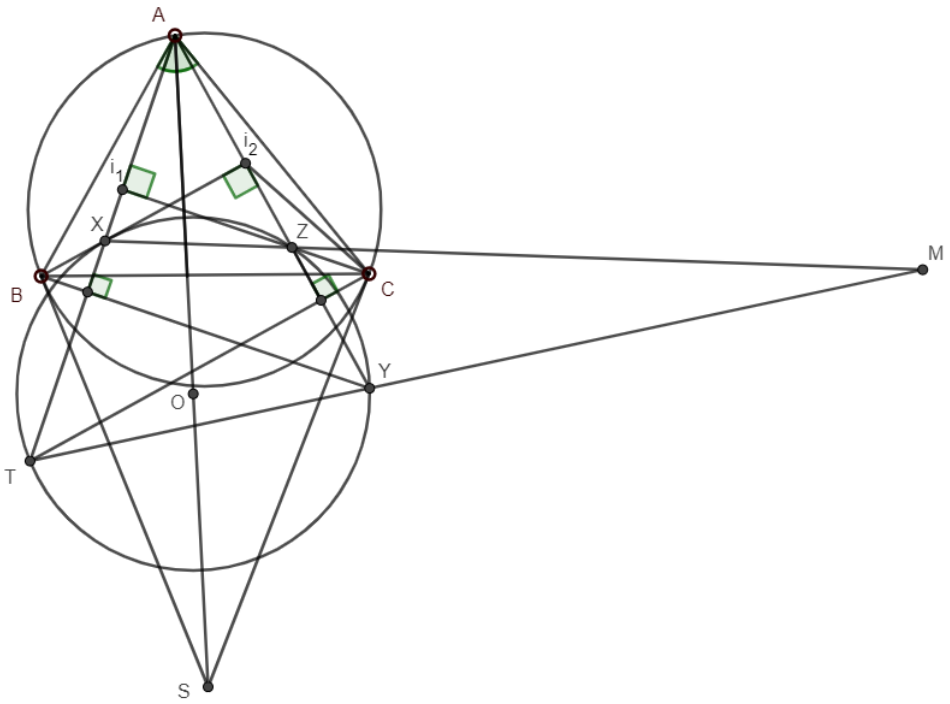

Final conclusions

The length of the radius of the circle with its center on the median of side BC can be deduced in terms of the lengths of the triangle's sides, the angle α, and the angle AEB, denoted as β for Theorem 1. The calculation could be the subject of a future paper.

Bibliography

[1] Brânzei, Colectiv (1974). "Bazele raționamentului geometric." Albatros Publishing House.

[2] "Viitori Olimpici" (n.d.). Competition. Retrieved from [https://www.viitoriolimpici.ro/].

Professor Dr. Petru Marian Braica

Email: pbraica@yahoo.com

Satu Mare 2024

ON SOME PROPERTIES OF SYLVESTER MATRIX RANK FUNCTIONS

Vasile POP[1], Constantin-Cosmin TODEA[2]

[1,2]Technical University of Cluj-Napoca, Department of Mathematics, Str G. Baritiu 25, Cluj-Napoca 40027, Romania

Corresponding author email: constantin.todea@math.utcluj.ro

Abstract

The aim of this short note is to obtain, using elementary methods, some properties of Sylvester matrix rank function. In the main result we show that the sum of Sylvester matrix rank functions of two matrix polynomials is the same as the sum of the Sylvester matrix rank function of the matrix obtained by applying greatest common divisor, with the Sylvester matrix rank function of the matrix obtained by applying lowest common multiple.

Key words*: field; matrix; rank; Sylvester.*

1. INTRODUCTION

Let k be a commutative ring and A be an associative unital k-algebra. A Sylvester matrix rank function rk is a function that assigns a non-negative real number to each matrix over A and satisfies some conditions. Historically, the first appearance of Sylvester matrix rank functions is given by Malcolmson [4], under the name of algebraic rank functions. The motivation of Malcolmson was to describe an alternative way of determining homomorphisms from associative unital rings to skew fields (division rings). For our first goal we will weaken the definition of Sylvester matrix rank function by removing some conditions. We will present *weak Sylvester matrix rank functions* in Section 2 and we continue with some probably well-known properties that are satisfied by Sylvester matrix rank functions (see [2], [3]) but, in order to obtain the proof, it is enough to consider weak Sylvester matrix rank functions. Let $k[X]$ be the algebra of polynomials with coefficients in k (which for the main result is a field) and f,g be two polynomials in $k[X]$. For shortness, we will denote by d the greatest common divisor (f,g) and by m we denote the lowest common multiple $[f,g]$ of the polynomials.

2. CONTENT

We give now the announced main result of this paper about the relation between the weak Sylvester matrix rank functions of two matrix polynomials and the weak Sylvester matrix rank functions of the matrix obtained by applying d, respectively m.

Theorem: Let A be a k-algebra and rk be a weak Sylvester matrix rank function on A. Let $f,g \in k[X]$ with d and m as above and assume that k is a field. Then for any positive integer n and any matrix $M \in (A)$ the following relation holds

$$(f(M)) + (g(M)) = (d(M)) + (m(M)).$$

The proof of this result is given in Section 3 using some properties of weak Sylvester matrix functions which we obtain in Section 2.

3. CONCLUSIONS

Obviously, if we take $A:=k$ as a k-algebra then the usual *rank of matrices* is a (weak) Sylvester matrix rank function on k. In this case, the above Theorem was proved by the first author and, as consequences he obtained a multitude of other results that are more or less known, see [6]. Note that we cannot use any of the new three proofs obtained by Pop and Negrescu in [5] for the above

Theorem. There is now a characterization, given by the first author, of the rank of matrices, using a functional inequation, see [1] page 321.

4. REFERENCES

[1]. *Gazeta Matematica*, Seria A, Vol. XXVI (CV), No. 4, 2008.
[2]. Jose Hermida-Alonso, On linear algebra over commutative rings, *Handbook of algebra*, 3:3-61, 2003.
[3]. Andrei Jaikin-Zapirain and Diego Lopez-Alvarez, On the space of Sylvester matrix rank functions, *arXiv:2012.15844 [math.RA]*, 2020.
[4]. Peter Malcolmson, Determining homomophisms to skew fields, *Journal of Algebra*, 64:399-413, 1980.
[5]. Alexandru Negrescu and Vasile Pop, Three New Proofs of the Theorem *rank f(M) + g(M) = rank(f,g)(M) +rank [f,g](M), Mathematics*, Vol. 12 (3):360, 2024.
[6]. Vasile Pop, Relations between ranks of matrix polynomials, *Journal of Algebra, Number Theory: Advances and Applications*, 24(1):35--41, 2021.

EXPLORING EXERGY MODELS: INVESTIGATING CONNECTIONS WITH NEGENTROPY AND HEAT TRANSFER FOR THERMODYNAMIC EFFICIENCY ANALYSIS

Ion CEBAN[1,2], Ștefan LUNCANU[1,3] , Andrei ZĂBREANU[1,3]
Elena Corina CIPU[1,4], Antonela TOMA[1,5]

[1]Centre for Research and Training in Innovative Techniques of Applied Mathematics in Engineering "Traian Lalescu" (CiTi), University Politehnica of Bucharest (UPB), 313 Splaiul Independentei, Romania
[2] Faculty of Energy Engineering, University Politehnica of Bucharest (UPB)
[3]Faculty of Applied Scinces, University Politehnica of Bucharest (UPB)
[4]Department of Applied Mathematics, Faculty of Applied Sciences, UPB
[5]Department of Mathematical Methods and Models, Faculty of Applied Sciences, UPB

Corresponding author email: corina.cipu@upb.ro

Abstract
This paper explores the intricate relationships between exergy models, negentropy, and heat transfer in the context of analysing thermodynamic efficiency. Exergy, representing the maximum useful work attainable from a system, serves as a crucial metric for assessing the quality of energy and the efficiency of energy conversion processes. By investigating the connections between exergy models, negentropy (the reverse of entropy), and heat transfer phenomena, we aim to enhance our understanding of thermodynamic systems' performance and efficiency. Through theoretical analysis and case studies, such as Carnot heat engine, reversible adiabatic expansion of an ideal gas and the model for the steady-state heat transfer process in a one-dimensional system, this study sheds light on the role of exergy in quantifying thermodynamic irreversibilities, the concept of negentropy as a measure of system order and organization, and the influence of heat transfer processes on overall system efficiency. Equations and resulting graphs are described in relation to the specified models. The present study contributes to the understanding and development of advanced methods for optimizing energy systems and increasing sustainability in engineering and other related fields.
Key words*: fractional calculus; wavelet analysis and applications; evolutionary algorithms and applications; data analysis and information security.*

1. INTRODUCTION

The growing awareness that the world's energy resources are limited has led many countries to re-examine their energy policies and take drastic measures to eliminate waste. It has also sparked the interest of the scientific community to take a closer look at energy conversion devices and develop new techniques for more efficient use of existing limited resources. The first law of thermodynamics refers to the *amount of energy* and states that energy cannot be created or destroyed. The second principle, however, deals with the *quality of energy*. More specifically, it is concerned with the loss of energy during a process, the generation of entropy, and the lost opportunities in working efficiently, leaving much room for improvement. The second law of thermodynamics has proven to be a very powerful tool in optimizing complex thermodynamic systems. In this paper, we examine the performance of engineering devices considering this principle. After an introduction of *fundamentals of thermodynamics* and definition of *exergy* which is the maximum useful work that could be obtained from the system at a given state in a specified environment, we discuss irreversibility (also called *exergy destruction or work loss*), which is the potential work wasted during a process due to irreversibilities.

2. CONTENT

Laws of Thermodynamics and equations are precised.

$dU = \delta Q - \delta L$ (1) Energy can't be created or destroyed, only transformed or transferred.	$\Delta S \geq 0$ (2) In any closed system, the total entropy (S), often viewed as a measure of disorder or randomness, can never decrease over time.	$\lim_{T \to 0\mathrm{K}} S = 0$ (3)

The second law of thermodynamics states that heat cannot be entirely converted to work, and therefore the work potential of internal energy must be less than the internal energy itself. But how much smaller? To answer this question, we need to check a closed system, in a steady state, in a specific state that undergoes a reversible process with respect to the state of the environment (that is, the final temperature and pressure of the system should be T_0 and respectively P_0). The exergy of a specified mass in a specified state is the useful work that can be produced as the mass undergoes a reversible process to the state of the environment:$\delta W_{\text{totalutil}} = -dU - P_0 dV + T_0 dS$. Noting that the kinetic and potential energies themselves are forms of exergy, the exergy of a closed system of mass m is $X = (U - U_0) + P_0(V - V_0) - T_0(S - S_0) + m\frac{v^2}{2} + mgz$. Relative to unit mass, *the exergy closed system* ϕ is: $\phi = (u - u_0) + P_0(\mathrm{v} - \mathrm{v}_0) - T_0(s - s_0) + \frac{v^2}{2} + gz$.

where u, v, s are the specific properties of the system at the initial state and u_0, v_0, $s_0$at the final state. The exergy change of a closed system during a process is

$$\Delta X = X_2 - X_1 = (U_2 - U_1) + P_0(V_2 - V_1) - T_0(S_2 - S_1) + m\frac{v_2^2 - v_1^2}{2} + mg(z_2 - z_1) \quad (5)$$

and for a unit of mass:

$$\Delta\phi = \phi_2 - \phi_1 = (u_2 - u_1) + P_0(\mathrm{v}_2 - \mathrm{v}_1) - T_0(s_2 - s_1) + \frac{v_2^2 - v_1^2}{2} + g(z_2 - z_1) \quad (6)$$

For a stationary regime and closed systems, the kinetic and potential energy terms vanish. The exergy of a closed system is either positive or zero.

Examples

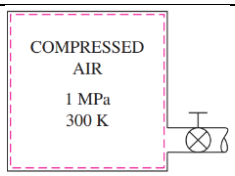

Fig. 1 The reservoir

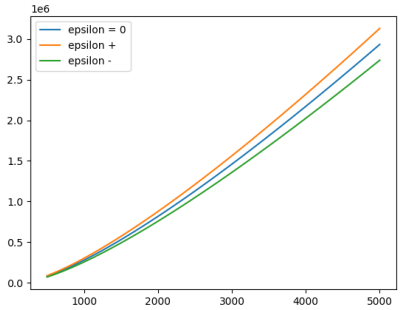

Fig2. Exergy of compressed air in a tank

The exergy content of compressed air in a rigid reservoir with volume V that contains air at pressure P_1 and temperature T_1 with P_0 și $T_0 = T_1$ environmental conditions is

$$\phi_1 = RT_0(ln\frac{P_1}{P_0} + \frac{P_0}{P_1} - 1)$$

An increase in air pressure in the tank leads to a significant increase in exergy. This suggests that air pressure has a significant impact on system efficiency and potential.

Higher reservoir pressure can provide more available energy and improve the performance of the system in which it is used. However, despite the potential benefits of increasing reservoir pressure, we are limited by the strength of the materials

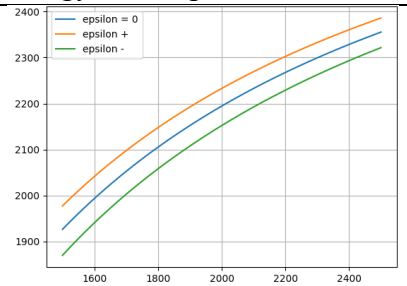

Fig.3 Exergy [Btu/s] vs furnace temperature

For a Carnot motor cycle, the work potential of the energy transferred from a heat source at temperature T is the maximum work that can be obtained from that energy in an environment at temperature T_0 and is equivalent to the work produced by a Carnot heat engine operating between source and environment.

$$X = \eta Q = (1 - \frac{T_0}{T})Q$$

3. CONCLUSIONS

Exergy can be used to compare different energy sources and energy conversion technologies in terms of their efficiency and sustainability. Similar to entropy in thermodynamics, exergy can provide insight into the direction in which processes and systems are heading, providing a measure of their degree of energy dissipation and, by implication, their ability to do useful work.

Configurations with n lines in general position

Cristi Săvescu

Romanian Mathematical Sciences Society

June 12, 2024

Abstract

The configurations of lines in general positions in the plane are quite wide and generic with regards to the regions and segments they generate, but have interesting common properties which can be researched. Unlike regular figures realm, these configurations generate uneven polygons, infinite regions and segments with various lengths, but still entangled in surprising relations. This article presents some properties of such configurations, well known results and various applications which reveal the potential of combinatorics results that can be achieved.

1 Introduction

First of all, we say that $n \geqslant 2$ lines in the plane are in general position $d_1, d_2, \ldots, d_n$ if there are no $i, j \in \{1, 2, \ldots, n\}$ such that $d_i \parallel d_j$ and if, for any three distinct indexes $i, j, k \in \{1, 2, \ldots, n\}$, we have $d_i \cap d_j \cap d_k = \varnothing$.

These lines cross eachother generating disjoint segments and semilines which we call *walls* within this article. These walls generate disjoint regions which partition the plane. Some of these regions are convex polygons whereas some of them are infinite regions.

2 Known results

Lema 1 *On each line of such configuration we can find n walls, two of which are infinite.*

From the configuration properties, we observe that each line is cut by the other $n - 1$ lines in n segments. Obviously, the two extremal ones will be infinte.

2 KNOWN RESULTS

Lema 2 *The number of finite regions is* $2n$.

Let $M = \{d_i \cap d_j | 1 \leqslant i < j \leqslant n\}$ be the set of all intersection points of two lines in the configuration. Obviously, set M contains $|M| = \binom{n}{2} = \frac{n(n-1)}{2}$ points. Let C be a circle with big enough ray such that it contains in its interior all points in M. Then, any infinite region is determined by two consecutive infinite walls (as followed clockwise with respect to C and an arc of C. Then, their number is $2n$. (This can be also proven by induction)

Lema 3 *Total number of regions is* $r_n = \frac{n(n+1)}{2} + 1$.

This can be proven inducting on $n \geqslant 2$. For $n = 2$ we have 4 (infinte) regions. When passing from n to $n+1$, the new line will cut in two each one of $n+1$ regions among existing ones, generating $n+1$ new regions.

Lema 4 *The regions can be colored each with one of two colors such that any two adjacent regions (sharing a wall) have different colors.*

We prove by inducting on $n \geqslant 2$ the following stronger result: For each $n \geqslant 2$ there exists such bicolor configuration, and n of the infinite regions (which represent, according to **lema 2**, half of the infinte regions) are white. For $n = 2$ it's obvious.

Let's consider a feasible configuration with n lines, and let d be one of them. Let C be positioned with one diameter on d and $M \in d$ a point far enough from C such that, we can consider a line d' disjoint of C with $M \in d'$, which intersect all other $n-1$ lines in the configuration. Let R be the black infinite section which contains M on one os it's walls (a black region exists because both cannot have the same color).

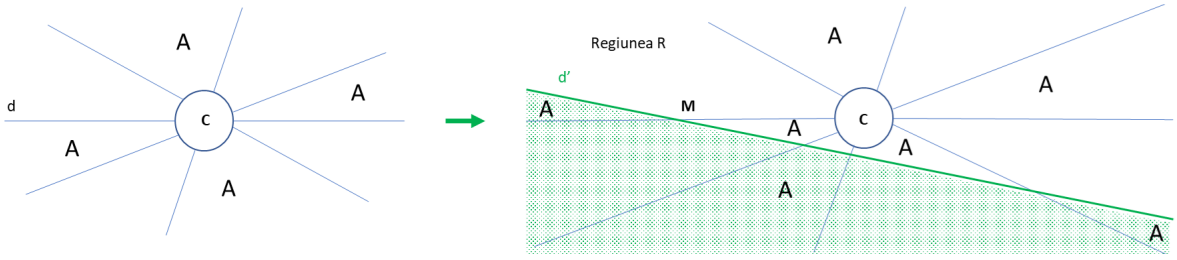

By alternatively coloring the new regions (by new region we mean a region appeared in the semiplane determined by d' not containing C), starting with the one cut from R, we see that we can achieve our goal.

Lema 5 *If F is the number of finite regions, L the number of finite walls and V the number of intersection points (cardinal of M), then $V + F - L = 1$.*

By lema 2 and lema 3, we have $F = \frac{n(n+1)}{2} + 1 - 2n = \frac{(n-1)(n-2)}{2}$. Then $V + F = \binom{n}{2} + \frac{(n-1)(n-2)}{2} = (n-1)^2$. By *lema* 1 we have $L = n(n-2)$, and the conclusion follows.

3 Regiuni finite nevecine cu număr egal de laturi

Ne propunem să stabilim o limită inferioară pentru numărul de regiuni finite cu acelaşi număr de laturi, oricare două nevecine.

Fie o marcare oarecare a poligoanelor, astfel încât oricare două poligoane marcate să nu aibă laturi în comun şi să avem marcate cel puţin jumătate dintre regiunile finite (posibil datorita bicolorării expuse la **Lema 4**). Din **Lema 1** deducem că numărul total de pereţi reprezentaţi de segmente finite este $n(n-2)$.

Numărăm segmentele care sunt laturi în cel puţin unul dintre poligoanele marcate. Dacă avem a_k poligoane cu k laturi, unde $k \geqslant 3$, atunci numărul segmentelor va fi $\sum_{k\geqslant 3} k \cdot a_k$. Fiecare segment este numărat cel mult o dată (datorită condiţiei de nevecinătate), deci avem $\sum_{k\geqslant 3} k \cdot a_k \leqslant n(n-2)$.

Numărul total a de poligoane este numărul total de regiuni finite, care este, conform **Lema 3**, egal cu $r_n = \frac{n(n+1)}{2} + 1$, din care scădem numărul de regiuni infinite, care este $2n$, totul împărţit la 2 (conform bicolorarării). Atunci $a \geqslant \frac{n(n-3)+2}{4}$.

Avem $n(n-2) \geqslant \sum_{k\geqslant 3} k \cdot a_k \geqslant 3a_3 + 4a_4 + 5a_5 + 6(a - a_3 - a_4 - a_5)$, deci $3a_3 + 2a_4 + a_5 \geqslant \frac{n^2 - 5n + 6}{2}$.

De aici, avem $\max\{a_3, a_4, a_5\} \geqslant \frac{n^2 - 5n + 6}{12}$.

4 O colorare a dreptelor

Dorim să colorăm cât mai multe dintre aceste drepte cu albastru, astfel încât orice regiune să aibă cel puţin un perete necolorat. Demonstrăm că numărul de drepte pe care le putem colora este $k \geqslant \sqrt{n/2}$. Fie K familia maximală de drepte pe care le putem colora cu albastru, respectând restricţiile date, şi fie $k = |K|$. Spunem că un punct de la intersecţia dreptelor

date este albastru dacă se află la intersecţia a două drepte albastre. Atunci avem $\binom{k}{2} = \frac{k(k-1)}{2}$ puncte albastre.

Fie d o dreaptă necolorată. Atunci, din modul de alegere a lui K, există o regiune finită ce are singură latură necolorată pe d, altfel toate aceste regiuni au încă câte o latură necolorată, deci d ar fi putut fi colorată. Această regiune, fiind finită, are cel puţin trei laturi, deci cel puţin două colorate. La intersecţia acestora se află un punct albastru. Atunci, putem asocia fiecărei drepte necolorate câte un punct albastru.

Orice punct aparţine însă la 4 regiuni (finite sau nu), deci la maxim 4 regiuni finite. Atunci, când numărăm punctele albastre asociate dreptelor necolorate, fiecare punct este numărat de cel mult 4 ori.

Numărul dreptelor necolorate este $n-k$, avem $n-k \leqslant 4 \cdot \frac{k(k-1)}{2} = 2k^2 - 2k$, deci $n \leqslant 2k^2$.

5 Circuit through the regions

Assume George plans to start from one region and perform several wall jumps (one at a time) to visit every region exactly once and return to his initial region. Let's find out the positive integers $n \geqslant 3$ for which there is such a configuration of n lines for which:

a) George cannot succeed;

b) George can succeed.

First of all, note that any region R_1 with only two walls (which both have to be infinite), if it has the neighbours R_0 and R_2, then George's path has to contain the subpath $R_0 - R_1 - R_2$. Otherwise, region R_1 cannot be reached (*).

a) We will show that, for every $n \geqslant 3$, there is a configuration of lines for which George cannot succeed. For $n = 3$ we see that the configuration is as in figure 1. As regions I, III and V have 2 walls each, from (*) we deduct that I–II–III–IV–V–VI–I has to be a subpath of George's path, so region VII cannot be visited.

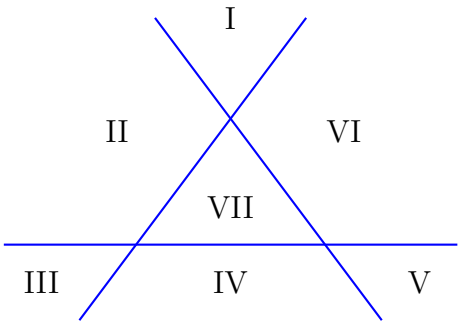

figure 1

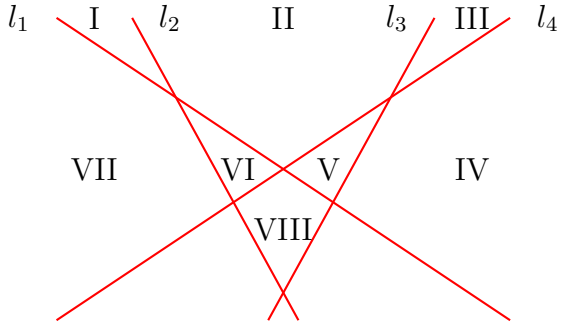

figure 2

For $n \geqslant 4$, we consider the configuration of 4 lines drafted in figure 2 and all additional lines slightly horizontal, beneath region VIII. As regions I and III have 2 walls each, from (*) we deduct that VII–I–II–III–IV should be a subpath of George's path, assume WLOG that in this direction. If George doesn't jump from IV to V, then V will have only one wall left (the one common with VIII) to be used for jumping in and out of it, contradiction. So George must continue his path through V and then to VIII. Similarly, if George hasn't jumped to VII from VI then VI will have only one wall left (the one common with VIII) to be used for jumping in and out of it, contradiction. So George jumped in VII from VI and thus, from VIII to VI. We see that George made already a cycle, so he cannot reach the remaining regions.

b) We see that the number of the regions is $R = \frac{n(n+1)}{2}+1$. This can be proven by induction on $n \geqslant 1$. Case $n = 1$ is trivial. For the induction step, each time a new line is added, we see it passes through $n+1$ previous regions and sections each in two regions, so $n+1$ additional regions appear. Therefore, the number of new regions is $\frac{n(n+1)}{2} + 1 + (n+1) = \frac{(n+1)(n+2)}{2} + 1$.

As George returns to the initial region (position), for each one of the given lines, he has to jump it an even number of times. Therefore, the number of jumps, which is R, has to be even, so n has to be 1 or 2 modulo 4. We will show that for $n = 4k+1$ and $n = 4k+2$, where $k \geqslant 1$ we can build a line configuration for which George succeeds.

Let $\mathscr{P}(k), k \geqslant 1$ be the follwoing proposition: *We can build a configuration of* $4k+1$ *lines for which George has a successfull full cyclic path and for which there is an extreme south horizontal line* l *(such that all intersection points are beyond* l*), which George jumps exactly two times, both times over one of his infinite walls. We call this kind of configuration* proper*, and let* l *be called the* base *of the configuration.*

For $k = 1$, the proof is given by figure 3.

5 CIRCUIT THROUGH THE REGIONS

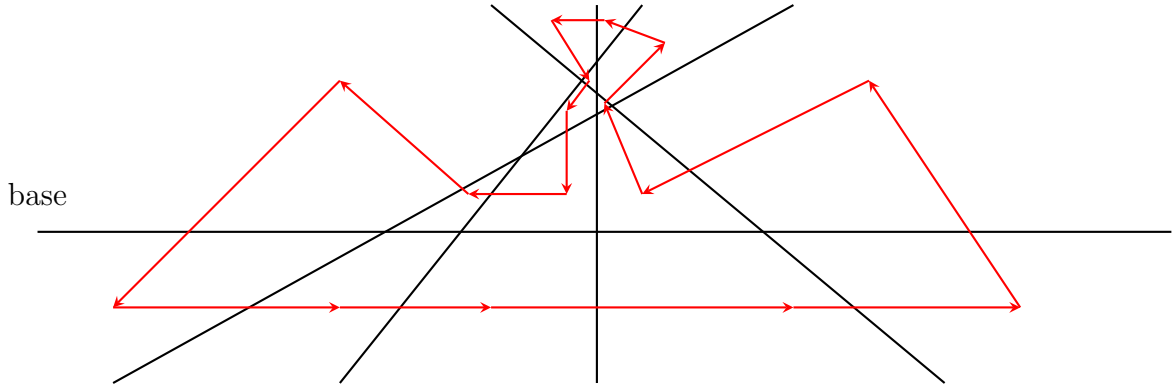

figure 3

Let's assume we found a configuration for $n = 4k + 1$:

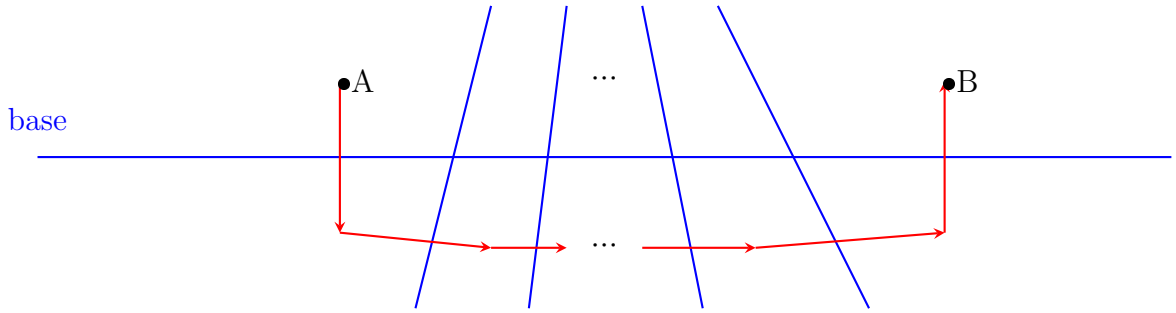

figure 4

We will show that it is possible to add four more lines, such that the path from A to B passes through all additional generated regions. This configuration is shown in figure 5.

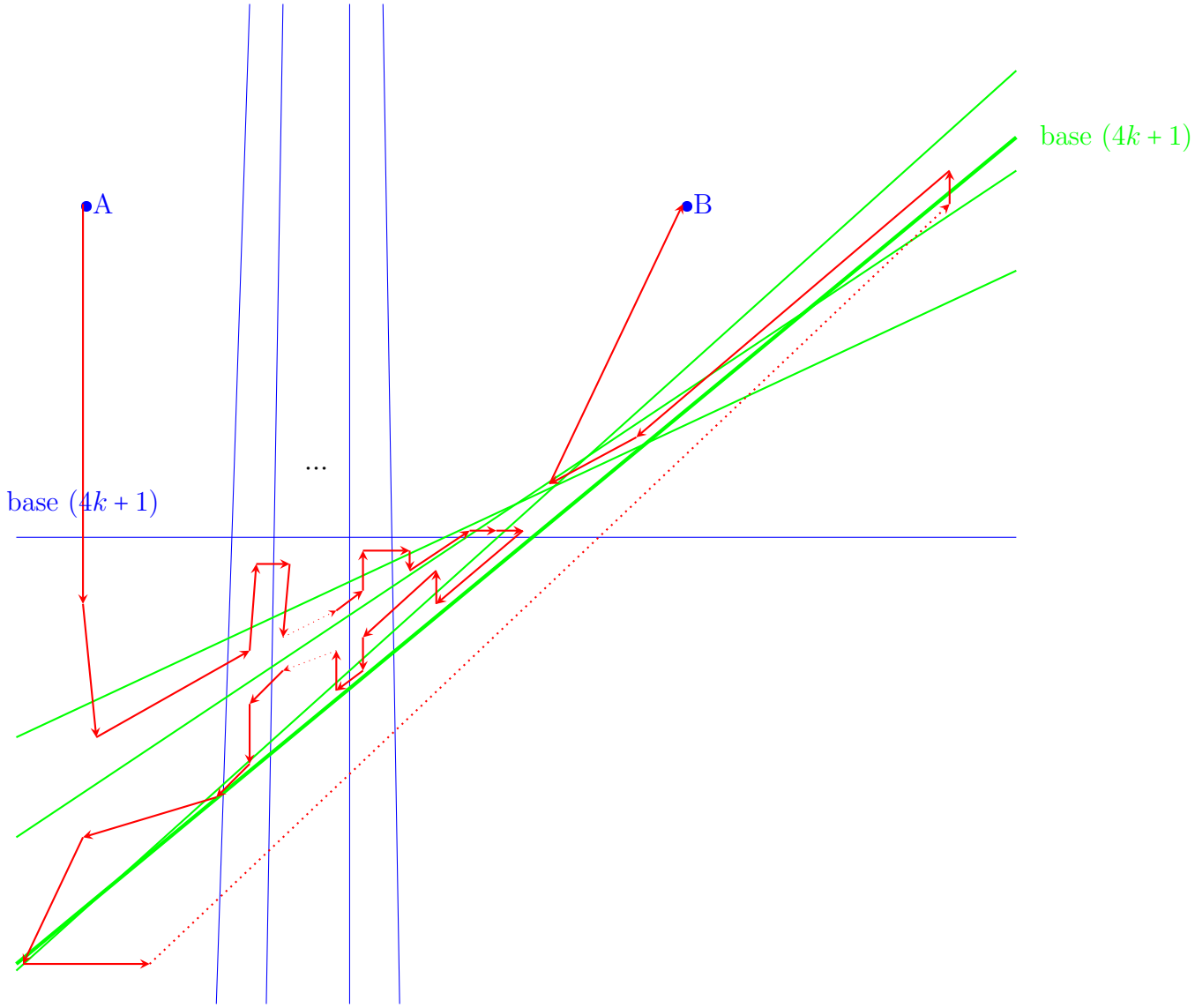

figure 5

So we have proven by induction on $k \geqslant 1$ that there is a proper configuration with $n = 4k+1$ lines. The last part is to show that starting from a proper configuration with $4k+1$ lines, we can build one with $4k+2$ lines. This is shown in figure 6.

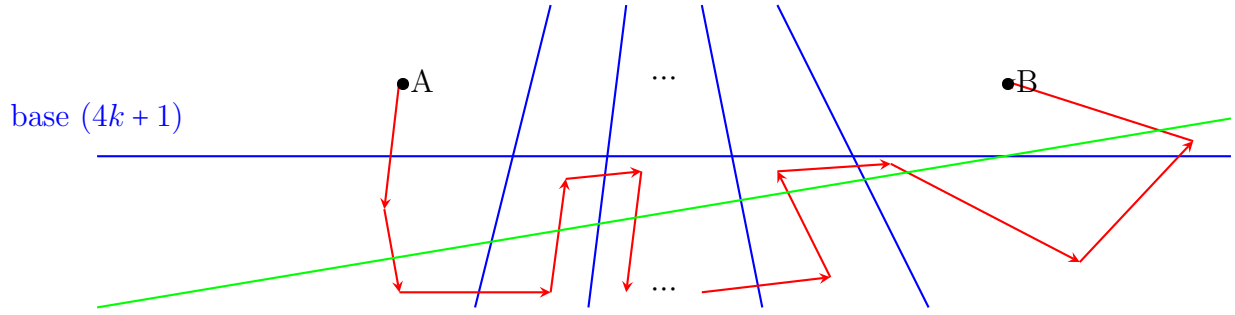

figure 6

Conclusions

These configurations, although they seem very rigid at first sight, can open various research horizons in studying the various properties of generated elements. I recommend for further study this very interesting lesson of Călin Popescu:

https://www.youtube.com/watch?v=tBxs-fojXNE

References

[1] C. Săvescu, *Problem 2*, **IMAR Test** : 14, December (2023)

[2] Austria, *Problem C5*, **IMO Shortlist** : (2014)

[3] C. Săvescu, *Problem 28477*, **Gazeta matematică** : December (2022)

DIGITAL MATHEMATICS APPLIED IN DEFENCE AND SECURITY EDUCATION

Cristian-Emil MOLDOVEANU[1], Alin-Constantin SAVA[1], Andrada-Livia CÎRNEANU[1], Linko NIKOLOV[2], Nikolaos KARADIMAS[3], Marina MARCHISIO CONTE[4], Enrico SPINELLO[5], Magdalena RYKALA[6]

[1] Military Technical Academy "Ferdinand I", 39-49 George Coşbuc Avenue, Bucharest, Romania [2] National Military University "Vasil Levski", 1 Karel Shkorpil, Shumen, Bulgaria
[3] Hellenic Army Academy, Leoforos Eyelpidon Avenue, Vari, Greece
[4] University of Turin, 8 Via Giuseppe Verdi, Turin, Italy
[5] Education and Training Command and School of Applied Military Studies, 22 Via Arsenale, Turin, Italy
[6] Military University of Technology, gen. Sylwestra Kaliskiego 2, Warsaw, Poland Corresponding author email: andrada.cirneanu@gmail.com

Abstract. *Using dedicated mathematical software with the appropriate skills, mathematics teachers and defence and security specialists can better explain and describe why some mathematical models and theorems are useful for real phenomena in the defence and security field. The connection between mathematics and its application in the defence and security field is strengthened through this article. Teaching and learning mathematics in a contemporary digital environment, which requires online learning, seems inadequate among young audiences. There are difficulties in presenting formulas, equations, theorems, etc. The result of the presented research is that the authors intend to increase interest in studying mathematics and provide more understandable mathematical problems and easy-to-imagine mathematical applications via the power of contemporary mathematical teaching digital tools.*

Keywords*: mathematical software; digital mathematics; defence and security education*

1. INTRODUCTION

The most important objectives of polytechnical universities are increasing students' interest in learning mathematics and increasing the internationalisation of mathematical-based subjects. The research's main objectives are to increase interest in mathematical science for defence and security education and improve the possibility of understanding mathematical theory with examples applied. The main expected results are better achievement of the mathematical tasks, problem resolutions, and analytical thinking gained by students. For those reasons, digitally applied mathematical teaching competencies are required, and students' capabilities to work on mathematical problems in a software environment are needed.

2. CONTENT

The main steps of the scientific research methodology are to identify the areas of mathematics used in defence and security education, select the main directions of defence and security education based on mathematical models, and propose a scenario-based methodology for teaching mathematics using examples for real-life phenomena. A hybrid approach between the traditional method of teaching mathematics and the modern method based on digital technology is considered an optimal solution. This article uses the *partial differential equation* (PDE) as an example of the area of mathematics being included within a scenario such as *the turbulent flow of an aircraft's wake.* The mathematical model consists of the Navier-Stokes equations [1]:

$$\frac{\partial u}{\partial x}+\frac{\partial v}{\partial y}+\frac{\partial w}{\partial z}=0\,, \tag{1}$$

$$\frac{\partial u}{\partial t}+u\frac{\partial u}{\partial x}+v\frac{\partial u}{\partial y}+w\frac{\partial u}{\partial z}=-\frac{\partial p}{\partial x}+\frac{\mu}{\rho}\left(\frac{\partial^2 u}{\partial x^2}+\frac{\partial^2 u}{\partial y^2}+\frac{\partial^2 u}{\partial z^2}\right), \tag{2}$$

$$\frac{\partial v}{\partial t}+u\frac{\partial v}{\partial x}+v\frac{\partial v}{\partial y}+w\frac{\partial v}{\partial z}=-\frac{\partial p}{\partial y}+\frac{\mu}{\rho}\left(\frac{\partial^2 v}{\partial x^2}+\frac{\partial^2 v}{\partial y^2}+\frac{\partial^2 v}{\partial z^2}\right), \tag{3}$$

$$\frac{\partial w}{\partial t}+u\frac{\partial w}{\partial x}+v\frac{\partial w}{\partial y}+w\frac{\partial w}{\partial z}=-\frac{\partial p}{\partial z}+\frac{\mu}{\rho}\left(\frac{\partial^2 w}{\partial x^2}+\frac{\partial^2 w}{\partial y^2}+\frac{\partial^2 w}{\partial z^2}\right), \tag{4}$$

where u, v, w and p are the velocity components, and the air pressure, and μ and ρ are the viscosity and the density of the air [1].

The most important issue related to the plane wake phenomenon is the risk of air incidents due to another aircraft's entry into the wake area of influence [2]. This problem arises especially in the take-off and landing phases when the planes are forced to follow closely with a relatively high frequency. Generally, the wake turbulence of a flying aircraft consists of a pair of longitudinal vortices, which prove to be quite stable and can persist for a long time in the atmosphere (Figure 1).

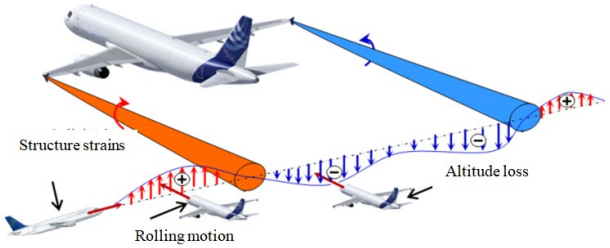

Figure 1 The effect of wake on an aircraft

According to Figure 2, a downward trajectory is obtained by numerically simulating in ANSYS FLUENT [3] the evolution of a pair of counter-rotating longitudinal vortices in the presence of the ground.

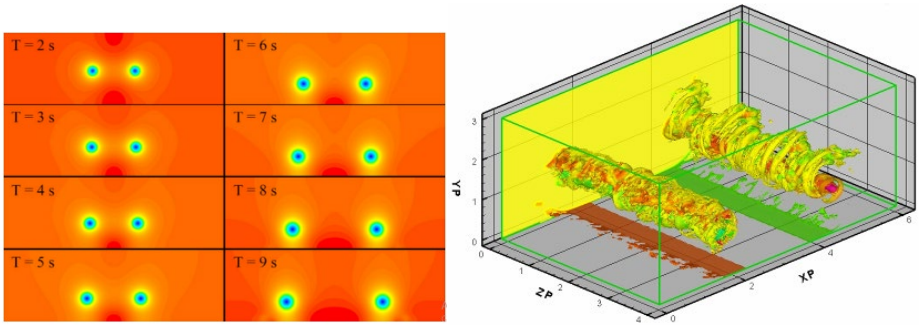

Figure 2 The downward trajectory of the longitudinal counter-rotating vortices in the presence of the ground

3. CONCLUSIONS

Digital tools can be used to learn mathematics in different scenarios. The applied research described in this paper aims to optimise teaching and learning mathematics in higher education within the defence and security fields by using problematisation as the main didactic method and as a teaching procedure within other teaching methods. Students will better understand the mathematical models when they visualise the simulation of real-world phenomena.

REFERENCES

1. Moldoveanu C.E., Giovannini A., Boisson H.C., *Turbulence receptivity of longitudinal vortex-dominated flows*, Lecture Notes in Computational Science and Engineering, Vol. 69, Springer Verlag, Berlin, pp. 227 – 236 (10 pag.), ISBN: 978-3-642-00604-3, 2009.

2. Leweke T.,Far-Wake. *Fundamental Research on Aircraft Wake Phenomena*. Publishable Final Activity Report, Marseille, France, 2008.

3. Mohammad Shaffri B. Mat Sabri, *CFD Simulation of 81 mm Mortar Ammunition using ANSYS FLUENT 13.0*, National Defence University of Malaysia, 2020.

ON SOME GENERALISATIONS OF THE GOLDEN PROPORTION

Cristina - Elena HREŢCANU[1]

[1]Ştefan cel Mare University of Suceava, str. Universitatii, no. 13, Suceava, Romania

Corresponding author criselenab@yahoo.com

Abstract

The purpose of the present paper is to present some generalizations of the golden proportion and to illustrate some relationships between the generalized golden proportions and some generalizations of the Fibonacci or Lucas sequences. The concept of the golden proportions extends several new mathematical constants, which can be useful in finding new applications into geometry.

Key words*: Golden Proportion, Fibonacci Numbers, Lucas Numbers, Generalized Golden Proportion.*

1. INTRODUCTION

The *golden proportion* (also called as the *golden ratio* or *golden mean*) is a ratio found in fundamental forms: plants, flowers, shells, planets, galaxies and so on.
In the *Elements*, Euclid of Alexandria (365 BC - 300 BC), defines a proportion derived from a division of a line into what he calls its "extreme and mean ratio. Euclid 's definition states: *"A straight line is said to have been cut in extreme and mean ratio when, as the whole line is to the greater segment, so is the greater to the lesser*" ([7]).
Statistical experiments have shown that people involuntarily give reference to proportions that approximate to the golden section. Throughout the history of art and architecture, traditional artists adopted the golden ratio as sacred measure and aesthetic proportion in order to embody the spirit in the matter.
The great Egyptian Pyramids of Giza (constructed in roughly 2600 BC) has the dimensions of its height and base being the golden ratio ([8]).
The golden proportion is also present in nature, through the appearance of the Fibonacci numbers. These numbers occur in most flowers, as the number of petals such as 3, 8, 13, 21, 34, 55, or 89. Also, these numbers appear in sunflowers, as the number of spirals in the head of the sunflower going clockwise and the number going anti-clockwise are two consecutive Fibonacci numbers ([9]).

2. GOLDEN RATIO AND ITS APPLICATIONS IN GEOMETRY

The golden ratio is the positive solution of the equation $x^2 = x + 1$. The golden ratio (noted by φ) turns up frequently in geometry, particularly in figures with pentagonal symmetry. The golden ratio partitions a line segment into a major and a minor subsegment in such a way that the ratio of the whole and the major equals the ratio of the major and the minor.
One of the *"horizontal"* generalizations of the golden ratio is given as one of the solutions of the equation $x^2 = ax + b$, where are a and b real numbers (or, more generally, complex numbers).
If a and b are positive integer numbers, then the positive solution of this equation is named metallic number, introduced by Vera W. de Spinadel in (*Spinadel,* 2002). Moreover, these numbers have the form $\sigma_{a,b} = \frac{a+\sqrt{a^2+4b}}{2}$ and are named "*metallic means family*" (MMF). Metallic means family contains some generalizations of the golden proportion, such as: the silver mean (for $a = 2$ and $b = 1$), the

bronze mean (, for $a = 1$ and $b = 2$), the Copper Mean (for $a = 1$ and $b = 3$) and many others (Spinadel, 1999).

Another generalization can be viewed as a *"vertical"* generalizations of the golden proportion, given by the solutions of the equation $x^m - x - 1 = 0$ (*Stakhov*, 1989).

Moreover, we can consider the equations of the form $x^{m+1} - x^m - 1 = 0$, for any positive integer numbers m, and its positive roots are called the g*eneralized golden m-proportion*. The problem of the line division in extreme and middle ratio that came to us from the Euclidean Elements allows the following generalization (*Stakhov*, 2007): let us give the integer non-negative number $m \in \{1,2,3, \dots\}$ and divide the line AB by the point C in the following ratio $\left(\frac{AB}{BC}\right)^m = \frac{BC}{AC}$. If we denote $\frac{AB}{BC} = x$ then, from AB = AC + CB, the following algebraic equation follows: $x^{m+1} - x^m - 1 = 0$.

Modern science widely applies to the Fibonacci *{F(n)}* and Lucas *{L(n)}* sequences, respectively, which result from application of the following recurrence relations (*Kilic,* 2009): $F(n) = F(n-1) + F(n-2)$, with $F(0) = 0$, $F(1) = 1$ and $L(n) = L(n-1) + L(n-2)$, with $L(0) = 2$, $L(1) = 1$, for any integer number *n > 1*.

There are some remarkable connections between golden proportions and Fibonacci numbers, given by (*Kilic,* 2009):

$$\lim_{n\to\infty} \frac{F(n+1)}{F(n)} = \phi, \quad \lim_{n\to\infty} \frac{F(n+2)}{F(n)} = \phi^2, \dots, \lim_{n\to\infty} \frac{F(n+k)}{F(n)} = \phi^k$$

They are expressed by the Binet's formulas, (*Kilic,* 2009): $F(n) = \frac{\phi^n - (-1)^n \cdot \phi^{-n}}{\sqrt{5}}$ and $L(n) = \phi^n + (-1)^n \cdot \phi^{-n}$. The Fibonacci sequences may be generalized by:

$$G(n+1) = aG(n) + bG(n-1),$$

where *a* and *b* are positive integer numbers and *G*(0)=*G*(1)=1, named *"generalized secondary Fibonacci sequence"*. Moreover, we remark that $\frac{G(n+1)}{G(n)} = a + \frac{b}{\frac{G(n)}{G(n-1)}}$. If the limit $\lim_{n\to\infty} \frac{G(n+1)}{G(n)} = x$ exists, we obtain $x = a + \frac{b}{x} \Leftrightarrow x^2 - ax - b = 0$.

Research on the general properties of the Golden structure (a polynomial structure with the structure polynomial $P(X)=X^2-X-I$, where *I* is the identity*)* is carried out by Crasmareanu and Hretcanu in (*Crasmareanu*, 2009), where the authors studied some applications of the golden proportion in differential geometry. Moreover, they introduced the notion of a „*complex golden ratio*", given by the complex number $\phi_c = \frac{1+i\sqrt{5}}{2}$ and they found some applications of these numbers in differential geometry.

Another complex golden ratio is given in [10], as a solution $\phi_i = \frac{1+i\sqrt{3}}{2}$ of the equation $x^2 = x - 1$, and it is named „*imaginary golden ratio"*.

3. REFERENCES

1. Crasmareanu M., Hretcanu C.E, *Golden differential geometry*, Chaos Solitons & Fractals 38(5) (2009), 1229-1238.
2. E. Kilic and A.P. Stakhov, *On the Fibonacci and Lucas p-numbers, their sums, families of bipartite graphs and permanents of certain matrices*, Chaos, Solitons & Fractals, Vol. 40, issue 5, (2009), 2210-2221;
3. A.P. Stakhov, *The generalized golden proportions, a new theory of real numbers, and ternary mirror-symmetrical arithmetic*, Chaos, Solitons & Fractals 33 (2007), 315–334;
4. Stakhov, A. P., *The Golden section in the measurement theory*, Computers Math. Applic., 17 (1989), 613-638.
5. V.W. de Spinadel, *The metallic means family and forbidden symmetries*, Int. Math. J., 2 no. 3, (2002), 279—288.
6. V.W. Spinadel*, The family of metallic means*. Vis Math;1(3), 1999.
7. https://academic.sun.ac.za/mathed/shoma/MATUNIT24_08.htm
8. https://en.wikipedia.org/wiki/Great_Pyramid_of_Giza
9. https://www.mathnasium.com/blog/14-interesting-examples-of-the-golden-ratio-in-nature
10. https://math.stackexchange.com/questions/1851698/imaginary-golden-ratio

Regarding a Theorem of Alexandru Lupaş

Dan-Ștefan Marinescu[1], Mihnea-Ionuț Marinescu[2]
[1] "Iancu de Hunedoara" National College, Hunedoara, Romania
[2] Babeș-Bolyai University, Cluj-Napoca, Romania
Corresponding author email: marinescuds@gmail.com

Keywords: approximation theory, inequalities, numerical analysis

1 INTRODUCTION

In 1974, A. Lupaş, a great Professor and a brilliant Mathematician, published a notable result in [4], which in a particular form has the following statement:

Theorem. (A. Lupaş) Let $x_1, x_2, \ldots, x_n$ be real numbers, not all equal, from the interval I of the real axis, and let $p_1, p_2, \ldots, p_n$ be positive numbers with a sum of 1, where $n \in \mathbb{N}^*$ and $f : I \to \mathbb{R}$ is a continuous function. Then there exist two distinct numbers c_1, c_2 in the interval

$$\left[\min_{1\le i\le n} x_i, \max_{1\le i\le n} x_i\right]$$

such that:

$$\sum_{i=1}^{n} p_i f(x_i) - f\left(\sum_{i=1}^{n} p_i x_i\right) = \left(\sum_{i=1}^{n} p_i x_i^2 - \left(\sum_{i=1}^{n} p_i x_i\right)^2\right) \frac{2\left[f(c_1) + f(c_2) - 2f\left(\frac{c_1+c_2}{2}\right)\right]}{(c_1 - c_2)^2}$$

Lupaş's result garnered significant interest from mathematicians specializing in Approximation Theory and Inequalities.

In 1998 and 1999, A. McD. Mercer rediscovered this theorem under more stringent conditions in [5] and [6], subsequently generalizing the results under additional constraints.

In this article, we aim to present and refine Mercer's 1999 findings, offer a new proof, propose an alternative formulation of the aforementioned theorem, and underscore the significance of Lupaş's theorem in the realm of inequalities.

2 CONTENT

In the following, I is a non-degenerate interval of the real axis, n a natural number, $n \geq 2$, $x_1, x_2, \ldots, x_n$ from I not all equal, $p_1, \ldots, p_n$ positive numbers with sum 1, J is the closed interval determined by $\min_{1\leq i\leq n} x_i$, $\max_{1\leq i\leq n} x_i$ and $\bar{x} = \sum_{i=1}^{n} p_i x_i$.

The following result holds:

.

Proposition 2.1. With the above specifications, if $f, g : I \to \mathbb{R}$ are functions that are twice differentiable on J, $g''(x) \neq 0$ for any x in the interior of J, then:

(i) $\sum_{i=1}^{n} p_i g(x_i) - g(\bar{x}) \neq 0$;

(ii) there exists c in the interior of J such that

$$\frac{\sum_{i=1}^{n} p_i f(x_i) - f(\bar{x})}{\sum_{i=1}^{n} p_i g(x_i) - g(\bar{x})} = \frac{f''(c)}{g''(c)}.$$

Proof. Let $F, G : [0,1] \to \mathbb{R}$ be the functions defined by

$$F(t) = \sum_{i=1}^{n} p_i f(tx_i + (1-t)\bar{x}),$$

$$G(t) = \sum_{i=1}^{n} p_i g(tx_i + (1-t)\bar{x}) \quad \text{for any} \quad t \in [0,1].$$

We observe that F and G are twice differentiable and we have the equalities

$$F'(t) = \sum_{i=1}^{n} p_i (x_i - \bar{x}) f'(tx_i + (1-t)\bar{x}),$$

$$F''(t) = \sum_{i=1}^{n} p_i (x_i - \bar{x})^2 f''(tx_i + (1-t)\bar{x}), \quad \forall t \in [0,1] \quad \text{and analogously for} \quad G.$$

In addition,

$$F'(0) = G'(0) = 0 \quad (F'(0) = \sum_{i=1}^{n} p_i (x_i - \bar{x}) \cdot f'(\bar{x}) = f'(\bar{x}) \cdot \sum_{i=1}^{n} (p_i x_i - p_i \bar{x}) =$$

$$f'(\bar{x})(\bar{x} - \bar{x}) = 0) \quad \text{and} \quad \sum_{i=1}^{n} p_i f(x_i) - f(\bar{x}) = F(1) - F(0), \quad \sum_{i=1}^{n} p_i g(x_i) - g(\bar{x}) = G(1) - G(0).$$

(i) If $\sum_{i=1}^{n} p_i g(x_i) - g(\bar{x}) = 0$, then with the observations above we have $G(1) = G(0)$ and since G satisfies the conditions of Rolle's theorem there exists $t_0 \in (0,1)$ such that $G'(t_0) = 0$. However, $G'(0) = 0$ and then with the same result there exists $t_1 \in (0, t_0)$ such that $G''(t_1) = 0$,that is $\sum_{i=1}^{n} p_i(x_i - \bar{x})^2 g''(t_1 x_i + (1-t_1)\bar{x}) = 0$ which is false because $g'' > 0$ or $g'' < 0$, as a consequence of the fact that the function g'' has the property of Darboux.

(ii) Let $H : [0,1] \to \mathbb{R}$ be the function defined using an idea often used in the proof of the mean value theorems, $H(t) = [G(1) - G(0)][F(t) - F(0)] - [F(1) - F(0)][G(t) - G(0)]$ for any $t \in [0,1]$.

Clearly, H is at least twice differentiable on $[0,1]$ and $H(0) = H(1) = 0$. Thus, $H'(0) = [G(1) - G(0)] \cdot F'(0) - [F(1) - F(0)] \cdot G'(0) = 0$. Then, by applying Rolle's theorem twice, there exists $s \in (0,1)$ such that $H''(s) = 0$, that is,

$$[G(1)-G(0)]\cdot\sum_{i=1}^{n} p_i(x_i-\bar{x})^2 f''(s\cdot x_i+(1-s)\bar{x}) = [F(1)-F(0)]\cdot\sum_{i=1}^{n} p_i(x_i-\bar{x})^2 g''(s\cdot x_i+(1-s)\bar{x}) \quad (1)$$

With the properties of g'', (i) and the notations $c_i = sx_i + (1-s)\bar{x}, w_i = \frac{p_i(x_i-\bar{x})^2 g''(c_i)}{\sum_{k=1}^{n} p_k(x_k-\bar{x})^2 g''(c_k)}$

for any $i \in \{1, \ldots, n\}$ equality (1) implies

$$\frac{F(1) - F(0)}{G(1) - G(0)} = \sum_{i=1}^{n} \frac{p_i(x_i - \bar{x})^2 g''(c_i)}{\sum_{k=1}^{n} p_k(x_k - \bar{x})^2 g''(c_k)} \cdot \frac{f''(c_i)}{g''(c_i)} = \sum_{i=1}^{n} w_i \cdot \frac{f''(c_i)}{g''(c_i)}.$$

Since $\sum_{i=1}^{n} w_i = 1, w_i \geq 0$ for any $i \in \{1, \ldots, n\}$, $\frac{f''}{g''}$ has Darboux's Property, from Jarnik's theorem we deduce that there exists an s between $\min_{1 \leq i \leq n} c_i$ and $\max_{1 \leq i \leq n} c_i$,

i.e., in the interior of the interval J such that

$$\frac{f''(c)}{g''(c)} = \sum_{i=1}^{n} w_i \cdot \frac{f''(c_i)}{g''(c_i)}$$

and then the conclusion follows.

Corollary 2.2. Under the conditions of Lupas's Theorem, if f is twice differentiable on I, there exists c in the interior of I such that

$$\sum_{i=1}^{n} p_i f(x_i) - f(\bar{x}) = \left[\sum_{i=1}^{n} p_i x_i^2 - \left(\sum_{i=1}^{n} p_i x_i\right)^2\right] \cdot \frac{f''(c)}{2}.$$

Proof. Let $c_1, c_2 \in I$ that verify the Lupas Theorem, then by applying Proposition 2.1 for $c_1, c_2, p_1 = p_2 = \frac{1}{2}$ and the functions f and $g : I \to \mathbb{R}$

defined by $g(x) = x^2$, we deduce that there exists c between c_1 and c_2 such that:

$$\frac{2\left[f(c_1)+f(c_2)-2f\left(\frac{c_1+c_2}{2}\right)\right]}{(c_1-c_2)^2} = \frac{f''(c)}{2}$$

and the conclusion follows immediately.

3 Applications

Before proceeding to applications, we notice that given the specifications at the beginning of section 2, the following hold:

$$\sum_{i=1}^{n} p_i x_i^2 - \bar{x}^2 = \sum_{i=1}^{n} p_i (x_i - \bar{x})^2 = \sum_{1\le i<j\le n} p_i p_j (x_i - \bar{x})^2$$

The proof of this equality is done using the Lagrange-Leibniz equality. For any $x \in \mathbb{R}$,

$$(x-\bar{x})^2 = \sum_{i=1}^{n} p_i (x_i - \bar{x})^2 - \sum_{1\le i<j\le n} p_i p_j (x_i - x_j)^2$$

and then x is replaced with 0 and $\bar{x}$.

.

Application 3.1. (*"Formula" for the ratio between AM and GM*) Let $n \in \mathbb{N}^*, x_1, \ldots, x_n \in (0,\infty)$ not all equal,

$$A_n = \frac{x_1 + \cdots + x_n}{n}, \quad G_n = \sqrt[n]{x_1 \cdots x_n},$$

then there exists $c \in (\min_{1\le i\le n} x_i, \max_{1\le i\le n} x_i)$ such that

$$\ln \frac{A_n}{G_n} = \left[\frac{x_1^2 + \cdots + x_n^2}{n} - \left(\frac{x_1 + \cdots + x_n}{n}\right)^2\right] \frac{1}{2c^2} = \frac{(x_1-\bar{x})^2 + \cdots + (x_n-\bar{x})^2}{n} \cdot \frac{1}{2c^2}.$$

Proof. Apply **Corollary 2.2** on $I = (0,\infty)$ with the function $f = -\ln$ (natural logarithm) and the equality from the beginning of the paragraph.

Remark. With **Application 3.1**, the inequality of means enters the "realm" of inequalities that come from equalities, namely Cauchy-Schwarz, Chebyshev, etc., but there are also other such formulas.

Consequence 3.1. Under the conditions of **Application 3.1**, we have:

(i) $A_n \ge G_n$;

(ii) The inequality $A_n \ge G_n$ is equivalent to $Q_n \ge A_n$ (Q_n is the quadratic mean). (Two inequalities are called equivalent if each can be deduced only with the help of the other inequality, see [1]).

Proof.

(i) If all are equal, we have equality; otherwise, from the second equality we have: $\ln \frac{A_n}{G_n} > 0$, from which $A_n > G_n$. With this, we have established the case of equality.

(ii) This follows from the first equality in **Application 3.1**.

.

Application 3.2. ("Formula" for Radon's inequality)

If $n \in \mathbb{N}^*, a_1, \ldots, a_n \geq 0, b_1, \ldots, b_n > 0$ and the numbers $\frac{a_i}{b_i}$ are not all equal, $p > 0$ then there exists c between $\min_{1 \leq i \leq n} \frac{a_i}{b_i}$ and $\max_{1 \leq i \leq n} \frac{a_i}{b_i}$ such that

$$\sum_{i=1}^{n} \frac{a_i^{p+1}}{b_i^p} - \frac{(a_1 + \cdots + a_n)^{p+1}}{(b_1 + \cdots + b_n)^p} = \left[\sum_{i=1}^{n} \frac{a_i^2}{b_i} - \frac{(a_1 + \cdots + a_n)^2}{b_1 + \cdots + b_n} \right] \cdot \frac{p(p+1) \cdot c^{p-1}}{2}.$$

Proof. We apply Corollary 2.2 on $I = [0, \infty)$ to the function $f : [0, \infty) \to \mathbb{R}$ defined by $f(x) = x^p$, $x_i = \frac{a_i}{b_i}$, $p_i = \frac{b_i}{b_1 + \cdots + b_n}$ for any $i \in \{1, \ldots, n\}$.

.

Consequence 3.2. Under the conditions of **Application 3.2** we have:

(i)
$$\sum_{i=1}^{n} \frac{a_i^{p+1}}{b_i^p} \geq \frac{(a_1 + \cdots + a_n)^{p+1}}{(b_1 + \cdots + b_n)^p},$$

and the equality holds if and only if

$$\frac{a_1}{b_1} = \cdots = \frac{a_n}{b_n}.$$

(Radon's Inequality)

(ii) Radon's Inequality is equivalent to Bergström's Inequality.

$$\left(\sum_{i=1}^{n} \frac{a_i^2}{b_i} \right) \geq \frac{(a_1 + \cdots + a_n)^2}{b_1 + \cdots + b_n}.$$

Proof is immediate.

.

Application 3.3. ("Formula" for Shannon's inequality)

If $n \in \mathbb{N}^*, a_1, \ldots, a_n, b_1, \ldots, b_n$ are from $(0, \infty)$ such that the numbers $\frac{a_i}{b_i}$ are not all equal, then there exists a c between $\min_{1 \leq i \leq n} \frac{a_i}{b_i}$ and $\max_{1 \leq i \leq n} \frac{a_i}{b_i}$ such that:

$$(a_1 + \cdots + a_n) \ln \frac{a_1 + \cdots + a_n}{b_1 + \cdots + b_n} - \sum_{i=1}^{n} a_i \ln \frac{a_i}{b_i} = \left[\frac{b_1^2}{a_1} + \cdots + \frac{b_n^2}{a_n} - \frac{(b_1 + \cdots + b_n)^2}{a_1 + \cdots + a_n} \right] \cdot \frac{1}{-2c^2}.$$

Proof. Let $I = (0, \infty)$, $f = \ln$, $x_i = \frac{b_i}{a_i}$, $p_i = \frac{a_i}{\sum_{i=1}^{n} a_i}$, $\forall i \in \{1, \ldots, n\}$.

From **Corollary 2.2** we deduce the conclusion.

Consequence 3.3. Under the conditions of **Application 3.3** we have:

(i) $a_1 \ln \frac{a_1}{b_1} + \cdots + a_n \ln \frac{a_n}{b_n} \geq (a_1 + \cdots + a_n) \ln \frac{a_1 + \cdots + a_n}{b_1 + \cdots + b_n}$, with equality if and only if $\frac{a_1}{b_1} = \cdots = \frac{a_n}{b_n}$. (Shannon's Inequality)

(ii) Shannon's Inequality is equivalent to Bergström's Inequality:

$$\left(\sum_{i=1}^{n} \frac{a_i^2}{b_i} \right) \geq \frac{(a_1 + \cdots + a_n)^2}{b_1 + \cdots + b_n}.$$

Proof. Application 3.3 is applied.

.

Application 3.4. Let $I \subseteq \mathbb{R}$ be an interval and $f : I \to \mathbb{R}$ a continuous function. f is convex if and only if f is semi-convex. That is

$$f(tx + (1-t)y) \leq tf(x) + (1-t)f(y), \quad \forall x, y \in I \text{ and } \forall t \in [0,1]$$

is equivalent to

$$f\left(\frac{x+y}{2} \right) \leq \frac{f(x) + f(y)}{2}. \quad \forall x, y \in I$$

.

Proof. From the convexity of f, it immediately follows that f is semi-convex, and thus the necessity is proven.

Sufficiency. Let us assume that $x \neq y$ and $t \in (0,1)$, and consider Lupas' theorem with $n = 2$, $x_1 = x$, $x_2 = y$, $p_1 = t$, $p_2 = 1 - t$. Then there exist two distinct numbers c_1, c_2 between x and y such that

$$tf(x) + (1-t)f(y) - f(tx + (1-t)y) =$$

$$= [tx^2 + (1-t)y^2 - (tx + (1-t)y)^2] \cdot \frac{2\left[f(c_1) + f(c_2) - 2f\left(\frac{c_1+c_2}{2}\right)\right]}{(c_1 - c_2)^2}$$

$= t(1-t)(x-y)^2 \cdot \frac{2\left[f(c_1) + f(c_2) - 2f\left(\frac{c_1+c_2}{2}\right)\right]}{(c_1 - c_2)^2}$. With this equality, the sufficiency is proven.

In conclusion, we propose to establish the equivalence between the Cauchy-Schwarz inequality and the Hölder-Rogers inequality.

.

Application 3.5. (*"Formula" for Hölder-Rogers inequality*)

Let $n \in \mathbb{N}^*, a_1, \ldots, a_n > 0, b_1, \ldots, b_n > 0, p, q > 0$ with $\frac{1}{p} + \frac{1}{q} = 1$ such that not all numbers $\frac{b_i}{a_i^{p-1}}, i \in \{1, \ldots, n\}$ are equal, then there exists $c \in \left(\min_{1 \leq i \leq n} \frac{b_i}{a_i^{p-1}}, \max_{1 \leq i \leq n} \frac{b_i}{a_i^{p-1}} \right)$ such that

$$\left(\sum_{i=1}^{n} a_i^p \right)^{\frac{q}{p}} \left(\sum_{i=1}^{n} b_i^q \right) - \left(\sum_{i=1}^{n} a_i b_i \right)^q = \left(\sum_{i=1}^{n} a_i^p \right)^{q-2} \left(\left(\sum_{i=1}^{n} a_i^p \right) \left(\sum_{i=1}^{n} a_i^{2-p} b_i^2 \right) - \left(\sum_{i=1}^{n} a_i b_i \right)^2 \right) \frac{q(q-1)}{2} c^{q-}$$

Proof. Consider Corollary 2.1 $I = (0, \infty), f : I \to \mathbb{R}, f(x) = x^q$,

$\forall x \geq 0, p_i = \frac{a_i^p}{\sum\limits_{i=1}^{n} a_i}, x_i = \frac{b_i}{a_i^{p-1}}, \forall i \in \{1, \ldots, n\}$ and thus we have

$$p, q > 1, \quad q(p-1) = p, \quad q - 1 = \frac{q}{p}.$$

Corollary 3.4. Under the conditions of Application 3.4, we have:

(i)
$$\sum_{i=1}^{n} a_i b_i \leq \left(\sum_{i=1}^{n} a_i^p\right)^{\frac{1}{p}} \left(\sum_{i=1}^{n} b_i^q\right)^{\frac{1}{q}}$$
(Hölder-Rogers inequality).

(ii) The Hölder-Rogers inequality is equivalent to the Cauchy-Schwarz inequality.

.

Proof.

(i) From the equality of Application 3.4 and the positivity of the right term in Corollary 2.2, if $f'' \geq 0$, we deduce that Hölder-Rogers holds. With equality occurring only if
$$\frac{b_1}{a_1^{p-1}} = \cdots = \frac{b_n}{a_n^{p-1}} \Longleftrightarrow \frac{b_1^q}{a_1^p} = \cdots = \frac{b_n^q}{a_n^p}$$
Clearly, the inequality is valid if $a_1, a_2, \ldots, a_n \geq 0$. Strictly "positivizing" with $\epsilon > 0$ and then taking the limit, we obtain the above statement. Therefore, Hölder-Rogers implies Cauchy-Schwarz. We only need to take $p = q = 2$.

From Cauchy-Schwarz we have
$$\left(\sum_{i=1}^{n} a_i^p\right)\left(\sum_{i=1}^{n} a_i^{2-p} b_i^q\right) = \left[\sum_{i=1}^{n} \left(a_i^{\frac{p}{2}}\right)\right]\left[\sum_{i=1}^{n} \left(a_i^{1-\frac{p}{2}} b_i\right)^2\right] \geq \left(\sum_{i=1}^{n} a_i b_i\right)^2$$
and then, with the equality from Application 3.4, we have
$$\left(\sum_{i=1}^{n} a_i b_i\right)^q \leq \left(\sum_{i=1}^{n} a_i^p\right)^{\frac{2}{p}} \left(\sum_{i=1}^{n} b_i^q\right), \text{ that is, } \sum_{i=1}^{n} a_i b_i \leq \left(\sum_{i=1}^{n} a_i^p\right)^{\frac{1}{p}} \left(\sum_{i=1}^{n} b_i^q\right)^{\frac{1}{q}}.$$

We leave it to the reader to discover new applications of Lupas' Theorem, Proposition 2.1 and Corollary 2.2.

4 CONCLUSIONS

In this article, we aim to provide a significant contribution to the development and understanding of this theorem, demonstrating and illustrating its impact and relevance in the field of Approximation Theory and mathematical inequalities. Specifically, we present and improve Mercer's result from 1999, provide a new demonstration of it, and obtain another form of the theorem.

References

1. P.S. Bullen, *Equivalent inequality*, arXiv: 0809.0641, September 2008.
2. J. Bustamante, *Bernstein Operators and Their Properties*, Birkhäuser, 2017.
3. I. Garvea, M. Ivan, *Sur une inégalité de Levinson-Popoviciu*, J. of Numerical Anal and Approximation Theory, Vol. 11, No. 1-2 (1982), 75-79.
4. A. Lupaş, *Teoreme de Medie pentru Transformări liniare şi pozitive*, Rev. de Analiză Numerică şi Teoria Aproximării, Vol. 3 Fasc. 2, 1974, pp. 121-140.
5. A. McD. Mercer, *An "Error Term" for the Ky Fan Inequality*, Journal of Math. Analysis Appl., 220, 774-777 (1998).
6. A. McD. Mercer, *Some New Inequalities Involving Elementary Mean Values*, Journal of Math. Analysis Appl. 229, 667-681 (1999).

IMPLEMENTATION OF AN EFFICIENT SUPERVISION SYSTEM FOR LORA GATEWAYS IN FARM ENVIRONMENTS

Douae DEN GUIR[1,2], Latifa BOUTAT-BADDAS[1]

[1]Université de Lorraine, IUT de Longwy, 186, Rue de Lorraine,
54400 Cosnes et Romain, France
[2]Maraissa Groupe Azura, Route de Tiznit km39 Tin Mansour Province Chtouka Ait Baha,
Agadir, Morocco

Corresponding author email: douae.den-guir4@etu.univ-lorraine.fr
Corresponding author email: latifa.baddas@univ-lorraine.fr

Abstract: *This project outlines the design and implementation of a comprehensive supervision system for LoRa gateways in farm environments using Raspberry Pi, Node Exporter, Prometheus, Grafana, and Alertmanager. It explores the feasibility of utilizing these technologies to create an efficient and reliable monitoring and alerting system. Data related to server resources like RAM, disk space, and CPU utilization is collected from the LoRa and visualized in Grafana dashboards for monitoring. An alerting mechanism using Alertmanager sends email alerts to administrators in case of anomalies or issues. This project works to ensure robust and reliable monitoring of LoRa gateways for optimal performance and maintenance.*

Key words*: LoRa, Raspberry Pi, Node Exporter, Prometheus, Grafana, Alertmanager, Supervision System, metrics, Monitoring, IoT.*

1. INTRODUCTION:

In recent years, the Internet of Things (IoT) has been a trending field for research and development. The future of IoT has the potential to be limitless. By 2025, it is estimated that there will be more than 21 billion IoT devices.
Azura, a leading agriculture company, runs over 50 farms with sensors collecting vital data essential for optimizing agricultural processes. Using LoRa, this data goes to gateways across farms. Our project ensures these gateways work smoothly, crucial for collecting and analyzing data. We monitor server resources and gateway connectivity to ensure Azura's IoT system runs smoothly.

2. PROJECT OBJECTIVES:

The ultimate objective of the project is to develop a visually intuitive dashboard on Grafana, displaying various measurements related to server resources and the status of gateways – indicating whether they are connected or not. This dashboard will be prominently displayed on a large screen, allowing data analysts within the company easy access for analysis. Additionally, the project aims to implement an alert system, ensuring timely notifications of any anomalies or critical events by email.

3. PROJECT DESCRIPTION:

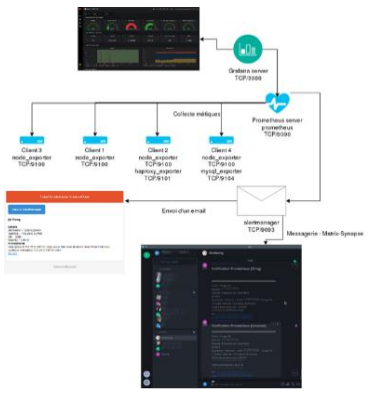

Figure 1: The idea of the project

The figure above illustrates the core concepts and tools utilized in the project. Each gateway is essentially a Raspberry Pi, serving as a compact computer.

At the core of this setup is the Prometheus server, hosted on a Raspberry Pi in the office network. Prometheus serves as an open-source metrics database and monitoring system, accessible via HTTP at the Raspberry Pi's IP address followed by port 9090. (http://IP_address_raspberry_server:9090/)
In the farms, Raspberry Pi devices serve as clients, with Node Exporter installed on each. Node Exporter is a Prometheus exporter designed to collect and export server and OS-level metrics, including RAM usage, disk space, and CPU utilization. These metrics are then scraped by Prometheus from each client on port 9100 and stored in its time-series database.
Remark: All Raspberry Pis are interconnected within the same network to facilitate easy access via SSH and configuration of the installed tools such as Prometheus, Node Exporter, and Grafana using their respective IP addresses.
To visualize and analyze this data effectively, Grafana comes into play. Grafana, another open-source tool, allows querying, visualization, alerting, and exploration of metrics, logs, and traces. Installed on the Raspberry Pi server, Grafana provides a user-friendly interface accessible via HTTP at the Raspberry Pi's IP address followed by port 3000. (http://IP_address_raspberry_server:3000/)
Furthermore, on the Raspberry Pi server, AlertManager was installed and configured to send email notifications to a specified email address in the event of client disconnection.
Here, dashboards are created to provide a comprehensive overview of the IoT infrastructure's performance and status.

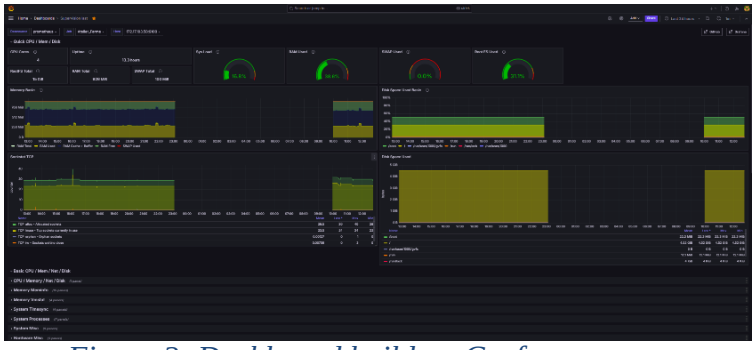

Figure 2: Dashboard build on Grafana

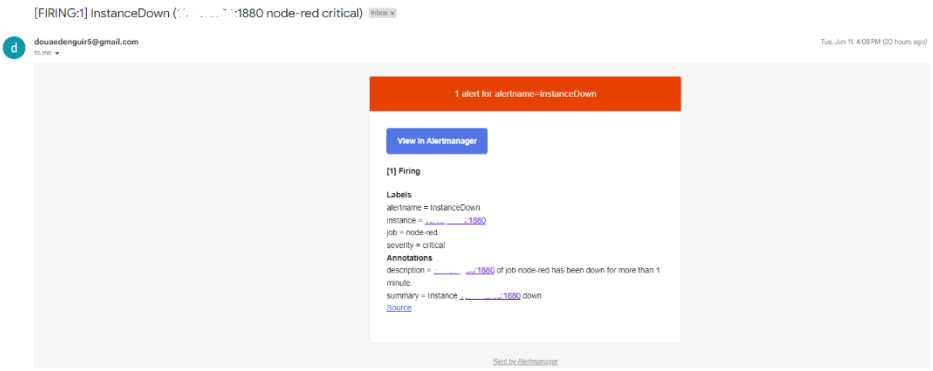

Figure 3: Alert: Gateway 'TGPT' Disconnected - Email Notification from AlertManager

4. CONCLUSION:

To conclude, this project is highly beneficial for data analysts, farmers, and the company as a whole. By analyzing the collected metrics, we can ensure successful agricultural production and achieve high-quality yields on time. One of the advantage of IoT projects like this one is their ease of development and modification. By simply installing and configuring various tools such as data collectors and monitoring platforms on Raspberry Pi, the system can be enhanced. Currently, I'm exploring how to configure Node-RED to collect metrics, store them in Prometheus, and visualize them in Grafana.

Acknowledgments :
We would like to express our sincere gratitude to Company « MARAISSA GROUPE AZURA » for their invaluable support throughout the duration of this project. The resources,and insights provided were crucial in facilitating our research endeavors.

OLYMPIAD PROBLEMS SOLVED USING MASON-STOTHERS THEOREM

Dumitrescu Dan-Ștefan
International Informatics High School,9 Balta Albina, District 3, Bucharest, Romania
dlrici234@gmail.com

Abstract: ***The purpose of this work is to highlight some key topics related to an important chapter in mathematics: Polynomials. This chapter is part of the high school curriculum in Romania and includes many challenging and interesting problems that have appeared over the years in various national and international competitions. In this work, I aim to address certain difficult problems that can be solved using advanced methods. The problems are based on two recent results: the Mason-Stothers theorem (1981) and a version of Fermat's Last Theorem for polynomials. There are a lot of difficult problems given in many competition which can be solved with these advanced methods which can show the beauty of this chapter and importance of it.***

Key words: Polynomials, Mason-Stothers, competition, Olympiads, Fermat's Last theorem on polynomials.

1. Introduction

The purpose of this article is to present the Mason-Stothers theorem and some of its very interesting and challenging applications, which admit clear and sophisticated solutions through its use. I will begin by stating the Mason-Stothers theorem and then illustrate results such as Fermat's Last Theorem for polynomials and problems given at international competitions. Through these demonstrations, I will show how a powerful result provides a significant advantage in competitions for tackling difficult problems and offers students the opportunity to devise sophisticated solutions.

(Theorem of Mason Stothers)

Let $P(x)$, $Q(x)$, $R(x)$ *polynomials primes between them such that*

$$P(x) + Q(x) + R(x) = 0.$$

We have the relation

$$\max(deg(P), deg(Q), deg(R)) \leq n_0(PQR) - 1,$$

where $n_0(P)$ *is the number of distinct roots of* P.

2. Content

(Fermat's Last theorem on polynomials). *Let* P, Q *,si* R *polynomials primes between them, at least one of them nonconstant.* $P^n + Q^n = R^n$ *hasn't solutions for* $n \geq 3$.

Proof. We will apply Mason-Stothers theorem for polynomials P^n, Q^n and $-R^n$. Also we will use the fact that $n_0(P^n) = n_0(P)$. □

(Davemport) Let f and g be 2 polinomyals which are primes,of degree at least 1. Prove that $deg(f^3 - g^2) \geq \frac{1}{2} deg(f) + 1$.

Proof. We will apply Mason-Stothers for $F = f^3$, $G = g^2$ and $H = F - G = f^3 - g^2$ □

(RMM 2018) Determine whether there exist non-constant polynomials $P(x)$ and $Q(x)$ with real coefficients satisfying

$$P(x)^{10} + P(x)^9 = Q(x)^{21} + Q(x)^{20}.$$

Proof. We can work with generalized form of this problem. Let $r, s \in N^*$ such that $r \geq 2$ and $s \geq 2r$, we will show that if $P^r + P^{r-1} = Q^s + Q^{s-1}$, then Q is constant. Let $m = deg(P)$ and $n = deg(Q)$. $mr = ns$ then $m \geq 2 \cdot n$. We will probe that $P(P+1)$ has at least $m+1$ distinct roots. We will apply Mason-Stothers for P, $-(P+1)$ and $R = 1$.

$$\max\{deg(P), deg(P+1), deg(1)\} \leq n_0(P(P+1)) - 1$$

$\max\{deg(P), deg(P+1), deg(1)\} = m$ then $n_0(P(P+1)) \geq m+1$ so $P(P+1)$ has at least $m+1$ distinct roots. But $m+1 \geq 2n+1$ from we obtain that Q takes value 0 or 1 at least of $n+1$ times, so Q is constant.

□

(SHL RMM 2018) Let m and n be integers greater than 2, and let A and B be non-constant polynomials with complex coefficients, at least one of which has a degree greater than 1.Prove that if the degree of the polynomial $A^m - B^n$ is less than $\min(m, n)$, then $A^m = B^n$.

Proof. $C = A^m - B^n$. We suppose $C \neq 0$ so $m \cdot deg(A) = n \cdot deg(B)$.

If $m = n$,then $deg(A) = deg(B)$ and $deg(A) \geq 2$. Apply Mason-Stothers for C, B^n, $-A^m$ we obtain $\max\{deg(A^m), deg(B^n), deg(C)\} \leq 2deg(A) + m - 2$.

So $(m-2) \cdot deg(A) \leq m-2 \Rightarrow deg(A) \leq 1$ which is a contradiction.

Case $m < n$ is treated analogously.

□

3. Conclusion

Over the years of working with students for math olympiads, I have observed a tendency among them to seek out powerful results that enable quick solutions to very difficult problems. Most of the time, achieving this goal is quite challenging, but there may be a set of problems that can be tackled using an advanced result.

In my opinion, the Mason-Stothers theorem is a powerful result that can be used to solve and approach very interesting, difficult problems with significant mathematical statements. If well understood by students, it can provide real help in solving various polynomial applications in a very elegant, clear, and concise manner.

References

[1] Recreatii Matematice 2/2009

[2] Victor V.Prasolov , Polynomials

[3] RMM 2018

[4] AOPS

MASTERING THE NEXT WAVE OF MALWARE: AN EDUCATIONAL FRAMEWORK FOR RANSOMWARE

ing. Eduard-Ștefan SANDU

National University of Science and Technology POLITEHNICA Bucharest, 313 Splaiul Independentei, Bucharest, Romania

Corresponding author e-mail: edy.eminem@yahoo.com

Abstract

Ransomware attacks take advantage of the growing popularity of on-line gaming by targeting private servers run by independent administrators, serving as vectors for cyber threats. This study examines the mechanisms and implications of ransomware dissemination through on-line gaming platforms. Techniques analyzed include embedding malicious code in game updates, manipulating server scripts, and exploiting vulnerabilities specific to custom game users. This research delves into the socio-technical landscape that facilitates such attacks, highlighting the interplay between user trust, administrative privileges, and the often-opaque nature of private server operations. This paper contributes to the field of cyber security by providing a new perspective on the vulnerabilities inherent in on-line gaming environments.

Key words*: ransomware, on-line games, private server, users.*

1. INTRODUCTION

The term "ransomware" refers to a category of malicious software that extorts a ransom from victims to release compromised data. The name originates from the fusion of "ransom" and "software." Typically, payment is demanded in cryptocurrencies such as Bitcoin, although there is no assurance that data will be restored upon payment. As ransomware evolves and the anonymity afforded by the internet creates numerous opportunities for exploitation, cyber attackers can exploit legal loopholes and evade detection and retribution. Consequently, ransomware has become an attractive and low-risk criminal enterprise. [1]

In the context of this paper, dynamic link libraries (DLLs) are essential due to their efficiency and reusability in executing shared code across various applications. This scenario examines an advanced threat actor embedding a ransomware payload into a DLL ostensibly used on a private server. The complexity arises from the actor's sophisticated understanding of both the target game's architectural dependencies and the social dynamics of its community. Employing advanced reverse engineering techniques, we will decompile a trusted DLL file and embed a ransomware payload designed to circumvent signature-based detection mechanisms typically employed by antivirus software. The distribution strategy exploits the inherent trust within gaming communities. By presenting a seemingly legitimate update or patch, we will employ digital social engineering tactics to propagate the compromised DLL file.

2. INVESTIGATING THE IMPACT OF THE RANSOMWARE ATTACK

The overall ransomware attack lifecycle, often referred to as the chain of destruction, delineates fundamental attack patterns that are consistent across different ransomware variants providing a comprehensive understanding of the typical steps involved in such a cyberattack.

The distribution stage encompasses a wide range of strategies aimed at propagating ransomware. Infection, the second stage, signifies the delivery mechanism through which the ransomware binary initiates its infection process and involves executing a sequence of tasks comprising various actions designed to compromise the target system, either fully or partially. The third stage, considered one of the most vital, involves communication with command and control servers. The file search step is a

pivotal stage in the attack chain, during which the malware identifies and selects files and extensions for encryption. Encryption, the fundamental operation in ransomware attacks, converts the victim's files into an unreadable or uneditable format, rendering them inaccessible until a decryption key is provided. Ransom, the final stage of the attack, entails the display of a ransom note on the victim's targeted machine.

3. TRAVERSING THE CYBER MAZE ON VECTORS AND ALGORITHMIC TRAJECTORIES

The injection technique is a cornerstone and extensively applied method in cybersecurity and exploitation. It involves a traditional approach enabling attackers to embed customized code into the memory space of a target process, typically to execute the attacker's directives. Commonly utilized for this technique are standard Windows commands. [2]

In an operating system, the execution of ransomware necessitates the loading of dynamic link libraries, which are essential for its functioning. These libraries play a vital role in facilitating various ransomware functionalities, such as establishing connections to command and control servers, key generation, file encryption, key destruction, and other tasks defined by the attacker. The coordinating of executing the malware binaries is managed by the operating system loader, responsible for mapping the memory addresses of the libraries utilized in the ransomware binary.

Private on-line gaming servers have garnered substantial popularity among gamers seeking distinctive gaming encounters. However, these servers, typically managed by individuals or small collectives, encounter notable cybersecurity hurdles, notably the looming threat of ransomware. DLL injection stands as a potent vector for ransomware infiltration, presenting considerable risks to the integrity of the gaming milieu and the security of end-user data.

4. CONCLUSIONS

In conclusion, the intricate interplay of technical intricacies, socio-economic ramifications, and mitigation imperatives emphasizes the necessity for continual academic inquiry and interdisciplinary cooperation in combating ransomware-driven cyberattacks directed at private on-line gaming servers. By employing academic rigor and fostering collaborative efforts, the gaming community can adeptly confront these varied challenges and enhance its resilience against the evolving threat landscape, thus preserving the integrity and security of digital gaming ecosystems.

5. REFERENCES

[1]. Eduard-Ștefan SANDU, “Prevention of widespread ransomware cyber-attacks through the SEAP platform”, The International Conference on Cybersecurity and Cybercrime, Online ISSN : 2393-0837, Print ISSN : 2393-0772, 2023.

[2]. Windows app development documentation, https://learn.microsoft.com/en-us/windows/apps/, accessed in June 2024.

CONTRIBUTIONS ON THE NON-LINEAR MODELLING OF THE IMMUNE SYSTEM ACTIVATION IN SECONDARY LYMPHOID ORGANS

Andra Cristiana MARIA-FULAȘU[1,2], Ruxandra Ioana CIPU[1,3]
Ștefan Cătălin PETRESCU[1,4], Elena Corina CIPU[1,5]

[1]Centre for Research and Training in Innovative Techniques of Applied Mathematics in Engineering "Traian Lalescu" (CiTi), University Politehnica of Bucharest, Romania
[2] Faculty of Applied Sciences, University Politehnica of Bucharest
[3] Faculty of Medical Engineering, University Politehnica of Bucharest
[4] Faculty of Engineering in Foreign Languages, University Politehnica of Bucharest
[5]Department of Applied Mathematics, Faculty of Applied Sciences, University Politehnica of Bucharest

Corresponding author email: andra.maria@stud.fsa.upb.ro

Abstract

The immune system is an important and vital defense network in the body, where lymph and lymph nodes have significant roles. Lymph, a transparent fluid containing leukocytes, flows through the lymphatic system to combat viruses and germs. Lymph nodes serve to filter and remove pathogens and aberrant cells from lymphatic fluid prior to its reentry into the circulatory system. Within lymph nodes, plasmacytoid dendritic cells and macrophages interact intricately: dendritic cells identify viral intruders and generate interferons, which stimulate other immune cells and hinder viral reproduction, while macrophages engulf pathogens and present their antigens to lymphocytes to trigger an immune response. This study conducts a thorough meta-analysis in order to gain a full understanding of the interactions between interferons, dendritic cells, and macrophages. A nonlinear model is employed, and the corresponding Cauchy problem is used to generate graphical representations of these interactions. This study combines the movement of lymph towards and into in lymph nodes, offering valuable understanding into the dynamics of immune responses. This research employs an interdisciplinary approach to provide new insights and highlight areas that require further inquiry in order to enhance our comprehension of and ability to combat hepatitis virus infections.

Key words*: immune system, non-linear model, lymph nodes, fluid mechanics, macrophages, interferons*

1. INTRODUCTION

This study provides valuable insights into the complex interaction between lymphatic flow and the immune system, specifically in the context of viral diseases like hepatitis, improve our understanding of the immune response by using mathematical models to analyze the movements of lymph, immune cells, and interferons. The results emphasize the intricate nature of lymphatic circulation and the crucial functions of macrophages, plasmacytoid dendritic cells (pDCs), and interferons in orchestrating a synchronized immune response against viral infections.

2. CONTENT

The aim of this study focuses on replicating the initial response of the immune system with a particular emphasis on the macrophages and the plasmacytoid dendritic cells. This early response is triggered by the antiviral interferon-α, whose quantities we want to monitor.

2.1. Mathematical Modelling

The way that infectious diseases spread across a population has always been a much-debated topic, since it can help in making the appropriate choices to eradicate a life-threatening epidemic. Mathematical modelling can help with identifying certain patterns of the development of a disease in a population, based on factors that interact with each other such as environment, properties of the virus, the rate of transfer, access to medical care etc., considering the most important of the above-mentioned aspects, aiming to see how heavy their impact is. Mathematical modelling can be divided

into two large categories: deterministic and probabilistic/stochastic. In this project we discuss and compare the non-linear model to the SIR and SEIRDH model.

2.2. Immunology and Numerical Analysis

The interplay between these three components is highly intricate. Macrophages, plasmacytoid dendritic cells (pDCs) and interferons work together in a coordinated manner to create a successful immune response. When macrophages come into contact with a virus, they release pro-inflammatory cytokines, which are messenger proteins and have a role in attracting and activating other immune cells, including pDCs. Plasmacytoid dendritic cells, recognized for their strong capacity to generate significant amounts of type I interferons, additionally intensify the antiviral condition by augmenting the function of both macrophages and other immune cells, underlined by the mathematical model.
Figure 1 illustrates the secretion of macrophages during the initial stage of infection, with a subsequent decrease in production due to their prompt immunological response.

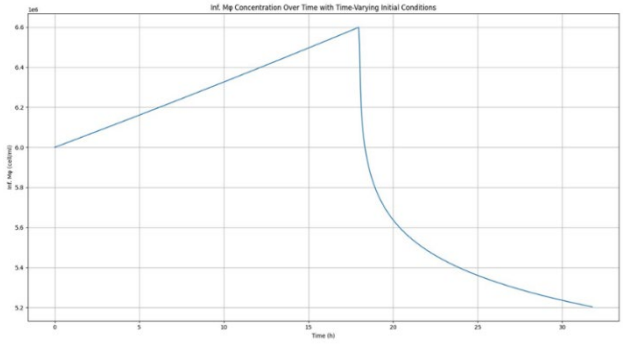

Fig. 1

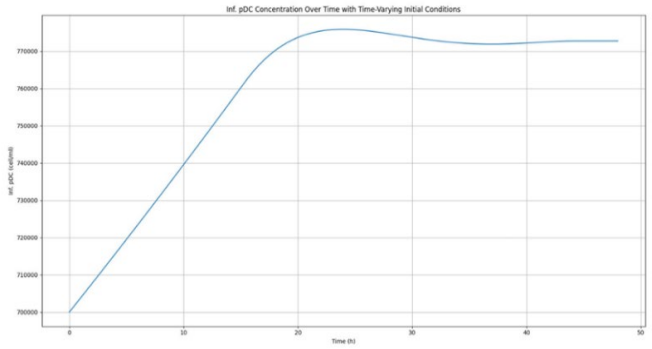

Fig.2

In Figure 2 we can observe a linear secretion pattern of plasmacytoid dendritic cells is illustrated in the following graph, with a significant increase in quantity during the initial 18 hours. The infected pDCs quantity stabilizes thereafter, which can be correlated to their primary function as ‘sensors’ for viruses and bacteria.

2.3. LYMPH - FLUID MECHANICS

To have a full picture of how the immune system reacts when it encounters a virus, taking into consideration the way lymph flows through the body and how it interacts with the ganglions is an important part of this study. This section proposes formalisms for understanding the dynamics of lymph flow. The structure of a lymph node is highly complex. Initially, we will adopt a significantly simplified geometry to get a clear and precise equation for the solution, even when there is a pulsating pressure gradient. To be more specific, the lymph node is a cylinder, and it is filled with an incompressible, uniform Newtonian fluid.

3. CONCLUSIONS

The research highlights the interaction of the most important immune cells with the dynamics of lymph flow, given the complex structure of lymph nodes, arteries, and capillaries. In conclusion, this discovery is crucial for advancing medical progress and enhancing the effectiveness of interferon therapies and the control of viral infections.

REFERENCES

[1]. Ali S, Mann-Nüttel R, Schulze A, Richter L, Alferink J, Scheu S. Sources of Type I Interferons in Infectious Immunity: Plasmacytoid Dendritic Cells Not Always in the Driver's 26 Seat. Front Immunol. 2019 Apr 12;10:778. doi: 10.3389/fimmu.2019.00778. PMID: 31031767; PMCID: PMC6473462.
[2]. Bui TM, Wiesolek HL, Sumagin R. ICAM-1: A master regulator of cellular responses in inflammation, injury resolution, and tumorigenesis. J Leukoc Biol. 2020 Sep;108(3):787-799. doi: 10.1002/JLB.2MR0220-549R. Epub 2020 Mar 17. PMID: 32182390; PMCID: PMC7977775.
[3]. Kretzschmar, M., Wallinga, J. (2009). Mathematical Models in Infectious Disease Epidemiology. In: Krämer, A., Kretzschmar, M., Krickeberg, K. (eds) Modern Infectious Disease Epidemiology. Statistics for Biology and Health. Springer, New York, NY. https://doi.org/10.1007/978-0-387-93835-6_12

Recurrent Sequences in Integral Calculus
Differential-fractional games and international relations

Andrei GHENOIU[1], Robert-Mihai PIVODĂ[2], Sorana-Eliza BĂLTĂREȚU[3] , Antonela TOMA[1,2], Mihai REBENCIUC[1,2]
Prof. EMILIA-CLAUDIA PREDA

[1]University Politehnica of Bucharest, 313 Splaiul Independentei, District 6, Bucharest, Romania
[2] National Bilingual College "George Cosbuc", Strada Olarie 48-52, District 2, Bucharest, Romania
Center of Research and Training in Innovative Techniques of Applied Mathematics in Engineering
"Traian Lalescu"
e-mail: claudia_emilia_preda@yahoo.com

Introduction:

We approach a topic often encountered in the problems proposed in the baccalaureate exam, namely recurrence relations in integral calculus, as well as the study of the convergence of sequences defined by such recurrences.

Content:

We begin the article with a problem given several times in the baccalaureate exam.

Problem 1.

For each non-zero natural number n, consider the number $I_n = \int_0^1 x^{n+1} e^x \, dx$

Show that $I_n + (\mathrm{n}+1) I_{n-1} = \mathrm{e}$, for any $\mathrm{n} \in \mathrm{N}$, with $\mathrm{n} \geq 2$.

Baccalaureate exam, July 2005, Mathematics–Informatics

Problem 2.

For each non-zero natural number n, consider the number $I_n = \int_1^e x(lnx)^n \, dx$

Show that $2I_{n+1} + (\mathrm{n}+1) I_n = \mathbf{e^2}$, for any $\mathrm{n} \in N^*$

Baccalaureate exam, 2014, reserve subject

Problem 3.

Consider the sequence $(I_n)_{n\geq 1}$, with $I_n = \int_0^1 (1-x^2)^n \, dx$, for any $\mathrm{n} \in N^*$.

Show that $(2\mathrm{n}+1) I_n = 2\mathrm{n} I_{n-1}$, for any $\mathrm{n} \in \mathrm{N}$, with $\mathrm{n} \geq 2$.

Baccalaureate exam, 2012, model

Problem 4.

Let the sequence $(I_n)_{n\geq 1}$, with $I_n = \int_0^1 (x-x^2)^n \, dx$ for any $\mathrm{n} \in N^*$

Differential-fractional games and international relations

a) Show that $I_n = \frac{n}{4n+2} I_{n-1}$ for any n ≥ 2.

Andrei GHENOIU[1], Robert-Mihai PIVODĂ[2], Sorana-Eliza BĂLTĂREȚU[3] , Antonela TOMA[1,2], Mihai REBENCIUC[1,2]

b) Study the convergence of the sequence $(I_n)_{n\geq 1}$, and, if convergent, calculate its limit.

[1]University Politehnica of Bucharest, 313 Splaiul Independentei, District 6, Bucharest, Romania
[2]Central of Research, 2019, mingle, Innovative Techniques of Applied Mathematics in Engineering "Traian Lalescu"

Problem 5.

Consider the function f: [1,2] → R, defined by f(x) = $x^2 - 3x + 2$, for any x ∈ [1,2]. Show that:

$$2(2n+1)\int_1^2 (f(x))^n\, dx + n\int_1^2 (f(x))^{n-1}\, dx = 0,$$

for any natural number n≥2.

Baccalaureate exam, June 2011

Problem 6.

Consider the sequence$(I_n)_{n\geq 1}$, defined by:

$$I_n = \int_0^{\frac{\pi}{4}} tan^{2n}t\, dx$$

for any natural number n. Show that:

a) $I_n + I_{n+1} = \frac{1}{2n+1}$
b) The sequence $(I_n)_{n\geq 1}$ converges to 0.

Conclusion

In conclusion, we hope that this article proves to be truly useful for tackling this type of problem and serves as a starting point for discovering new methods of approaching them.

Bibliography

Alexandru Negrescu, CAPES de Mathematiques, *Didactica Matematică*, nr. 1, 2014, pp. 28–32.

Dorin Vasile, Metode de calcul al unor limite de şiruri date prin integrale, *Didactica Matematică*, nr. 2, 2021, pp. 55–60.

Adrian Zanoschi, Gheorghe Iurea, Gabriel Popa, Petru Răducanu, Ioan Şerdean, *Bacalaū- reat 2024 M mate-info*, Editura Paralela 45, Pite şti, 2023.

Subiecte bacalaureat MECTS (https://www.pro-matematica.ro/).

Differential-fractional games and international relations

Andrei GHENOIU[1], Robert-Mihai PIVODĂ[2], Sorana-Eliza BĂLTĂREȚU[3] , Antonela TOMA[1,2], Mihai REBENCIUC[1,2]

GENERALIZATION OF SOME RECURRENCE RELATIONS FOR SEQUENCES

[1]University Politehnica of Bucharest, 313 Splaiul Independentei, District 6, Bucharest, Romania
[2]Center of Research and Training in Innovative Techniques of Applied Mathematics in Engineering
Magnolia Anda TILCA[1], Florin BOJOR[2] Traian Lalescu"

[1] "Vasile Goldiș" Western University of Arad, 94 B-dul Revoluției Arad, Romania
[2]"Gheorghe Șincai" National College, 25 Gheorghe Șincai, Baia Mare, Romania
Corresponding author email: f_bojor@yahoo.com

Abstract

In this paper we will modify the recurrence relations of some convergent sequences in the following way: we will replace some of the constants in the recurrence relation with sequence converging to this constant. Then we will study the convergence of the new sequence obtained. Making these changes, some of the obtained sequences will remain convergent while others will become divergent. Then for the obtained convergent sequences, we study the asymptotic evaluation.

***Key words**: convergence, recurrent sequence*

In [1.] D. Andrica and O. Bagdasar generalized the first-order linear recurrence relation as follows:

Let $(a_n)_{n\geq 0}$ and $(b_n)_{n\geq 0}$ be two sequences of real numbers satisfying the properties:

i. $a_n \neq 0$ *for all* $n \in \mathbb{N}$ *and* $\lim_{n\to\infty} a_n = a \in (-1,1)$

ii. $\lim_{n\to\infty} b_n = 0$.

Then the sequence $(x_n)_{n\geq 0}$ defined by $x_{n+1} = a_n x_n + b_n$, for all $n \in \mathbb{N}$ and $x_0 \in \mathbb{N}$ is convergent to 0.

In what follows, using recurrent sequence that have already become classical, we will obtain new sequences by replacing some constants with sequences converging to those constants.

D. Popa [2.], introduced the concept of *asymptotic evaluation* of convergent sequences, in this way:

If the sequence $(x_n)_{n\geq 0}$ converges to ℓ, we find a sequence $(y_n)_{n\geq 0}$ with property $\lim_{n\to\infty} y_n (x_n - \ell) \in \mathbb{N}^*$. The sequence $(y_n)_{n\geq 0}$ is called the asymptotic evaluation of order I.

For some of the new sequences, we study the asymptotic evaluation.

These sequences are:

a. $(x_n)_{n\geq 0}$ defined by $x_{n+1} = \sqrt{2 + x_n}$, for all $n \in \mathbb{N}$ and $x_0 \geq 0$. The sequence converge to 2 and the sequence $(2^n)_{n\geq 0}$ is the asymptotic evaluation of sequence (x_n).

b. $(x_n)_{n\geq 0}$ defined by $x_{n+1} = \frac{2x_n}{1 + x_n}$, for all $n \in \mathbb{N}$ and $x_0 > 0$. The sequence converge to 2 and the sequence $(2^n)_{n\geq 0}$ is the asymptotic evaluation of sequence (x_n).

Differential-fractional games and international relations

Andrei GHENOIU[1], Robert-Mihai PIVODĂ[1], Sorana-Eliza BĂLTĂREȚU[1], Antonela TOMA[1,2], Mihai REBENCIUC[1,2]

[1]University Politehnica of Bucharest, 313 Splaiul Independenței, District 6, Bucharest, Romania
[2]Center of Research and Training in Innovative Techniques of Applied Mathematics in Engineering "Traian Lalescu"

c. $(x_n)_{n\geq 0}$ defined by $x_{n+1} = \frac{x_n^2 + a^2}{2x_n}$, for all $n \in \mathbb{N}$, where $a > 0$ and $x_0 > 0$. The sequence converge to a and for $a \neq x_0$, the sequence $\left(\left(\frac{x_n + a}{x_n - a}\right)^n\right)_{n\geq 0}$ is the asymptotic evaluation of sequence (x_n).

d. $(x_n)_{n\geq 0}$ defined by $x_{n+1} = x_n^2 - x_n + 1$, for all $n \in \mathbb{N}$ and $x_0 \in (0,1)$. The sequence converge to 1 and the sequence $(n)_{n\geq 0}$ is the asymptotic evaluation of sequence (x_n).

2. CONTENT

2.1. Generalization of recurrence relations

The generalization of the recurrence relations can be done in several ways. For the sequences presented in the introduction, we will give a generalization considered representative by the authors and we study the convergence of the new sequences.

Lemma 2.1.1. Let $(a_n)_{n\geq 0}$ be a sequence with positive terms that converges to 2. We define the sequence $(x_n)_{n\geq 0}$ by $x_0 > 0$ and $x_{n+1} = \sqrt{x_n + a_n}$, for all $n \in \mathbb{N}$. Then the sequence $(x_n)_{n\geq 0}$ converges to 2.

Lemma 2.1.2. Let $(a_n)_{n\geq 0}$ be a sequence with positive terms that converges to 2. We define the sequence $(x_n)_{n\geq 1}$ by $x_{n+1} = \frac{a_n x_n}{x_n + 1}$, for all $n \geq 0$ and $x_0 > 0$. Then x_n converges to 1.

3. CONCLUSIONS

We further confine to the opinion expressed by Peter Olver in his celebrated work, which says that 1-jet spaces and their duals are appropriate fundamental ambient mathematical spaces used to model classical and quantum field theories. In such a physical and geometrical context, followed papers which are devoted to developing the *time-dependent covariant Hamilton geometry on dual 1-jet spaces* (in the sense of d−tensors, time-dependent semisprays of momenta, nonlinear connections, N-linear connections, d−torsions and d−curvatures), which is a natural dual jet extension of the Hamilton geometry on the cotangent bundle.

Differential-fractional games and international relations
NUMERICAL SIMULATION OF WATER INFILTRATION IN HETEROGENEOUS SOILS

Andrei GHENOIU[1], Robert-Mihai PIVODA[2], Sorana-Eliza BALTĂREȚU[3], Antonela TOMA[1,2], Mihai REBENCIUC[2]

[1]University Politehnica of Bucharest, 313 Splaiul Independenței, District 6, Bucharest, Romania
[2]Center of Research and Training in Innovative Techniques of Applied Mathematics in Engineering "Traian Lalescu"
[3] Ibn Zohr University, Faculty of Sciences, Agadir, Morocco

Corresponding author email: fouzia.shile@edu.uiz.ac.ma

Abstract

We aim to simulate water infiltration through heterogeneous soils using a meshless method based on Radial Basis Functions (RBF) with Picard iterations combined with the proper orthogonal decomposition. The groundwater flow is described by the h-form Richards equation. The heterogeneity is represented by the random behaviour of the saturated hydraulic conductivity. This later is treated as a lognormally distributed random field. In general, the results demonstrate that the proposed numerical method provides a remarkably accurate solution to infiltration problems in unsaturated heterogeneous soils.

***Key words**: heterogenous soils; meshless method; Picard iterations; Richards equation.*

1. INTRODUCTION

In recent years, the scientific community has devoted significant attention to numerical methods aimed at approximating the solution of flow equations that model flow in heterogeneous porous media. Several studies have been published on this topic. However, these methods encounter challenges in terms of computational feasibility. The objective of this work is to leverage the innovative characteristics of a meshless method that relies on radial basis functions to address the issues discussed in the literature.

2. CONTENT

Our proposal involves the utilization of the radial basis function method as an efficient computational technique. This approach has gained popularity owing to its advantages in solution approximation and reduced computational costs, eliminating the need for mesh generation. We use the Karhunen-Loève method for generating the uncertain saturated hydraulic conductivity. We perform numerical experiments for the solution of the governing Richards equation to prove the efficiency of the proposed approach.

3. CONCLUSIONS

Our results confirm the accuracy and efficiency of the proposed method for the simulation of water infiltration in heterogeneous soils.

Differential-fractional games and international relations
FRAUD DETECTION SYSTEM FOR ONLINE TRANSACTIONS

Andrei GHENOIU[1], Robert-Mihai PIVODA[2], Sorana-Eliza BALTĂREȚU[3], Antonela TOMA[1,2], Mihai REBENCIUC[1,2]

Georgiana CREȚU[1,2], Simona Mihaela BIBIC[1,3]

[1]University Politehnica of Bucharest, 313 Splaiul Independentei, District 6, Bucharest, Romania

[2]Center of Research and Training in Innovative Techniques of Applied Mathematics in Engineering National University of Science and Technology POLITEHNICA Bucharest, 313 Splaiul Independentei, District 6, Bucharest, Romania, „Traian Lalescu"

Faculty of Electrical Engineering

[3]Center for Research and Training in Innovative Techniques of Applied Mathematics in Engineering, 'Traian Lalescu' (CiTi), Bucharest, Romania

Corresponding author email: georgiana.cretu1106@stud.electro.upb.ro

Abstract

This paper presents a cutting-edge Fraud Detection System designed to address the growing challenges of online transaction fraud. It utilizes advanced mathematical analyses and statistical methodologies for real-time detection of fraudulent activities. Leveraging machine learning, the system swiftly identifies patterns and anomalies in transactional data, facilitating rapid fraud identification. By amalgamating these technologies, it provides a robust defence against online fraud, safeguarding transactions proactively. Additionally, the system's adaptability is further strengthened by the continuous refinement of detection capabilities through machine learning algorithms. These algorithms dynamically adjust to evolving data inputs, ensuring that the system remains agile and responsive to emerging fraud tactics. This iterative process not only enhances the system's adaptability but also guarantees its effectiveness in combating the ever-evolving landscape of fraudulent activities in online transactions.

Keywords*: Advanced Mathematical Analyses; Statistical Methodologies; Machine Learning; data analysis and information security.*

1. INTRODUCTION

The rapid increase in online transactions has brought with it a corresponding rise in online payment fraud. As e-commerce continues to expand, the need for robust fraud detection systems has become paramount. This paper introduces a sophisticated Fraud Detection System designed to counteract these fraudulent activities effectively. The system can detect fraudulent activities in real-time by
utilizing advanced mathematical analyses and statistical methodologies. Furthermore, the integration of machine learning allows the system to swiftly identify patterns and anomalies within transactional data.

2. CONTENT

2.1. System Architecture

The Fraud Detection System employs a multi-layered architecture that incorporates various analytical tools and algorithms. At its core, the system uses advanced statistical methods to establish baseline behavioural patterns. These methods include:

- Statistical Analysis: techniques such as regression analysis, clustering, and hypothesis testing are used to identify deviations from established norms.
- Mathematical Modelling: models are constructed to predict transaction outcomes based on historical data.

Differential-fractional games and international relations

Andrei GHENOIU[1], Robert-Mihai PIVODĂ[2], Sorana-Eliza BĂLTĂREȚU[3] , Antonela TOMA[1,2], Mihai REBENCIUC[1,2]

[1] University Politehnica of Bucharest, 313 Splaiul Independenței, District 6, Bucharest, Romania
[2] Center of Research and Training in Innovative Techniques of Applied Mathematics in Engineering "Traian Lalescu"

2.2. Machine Learning Integration

Machine learning plays a critical role in enhancing the system's detection capabilities. By training algorithms on vast datasets, the system learns to recognize the subtle signs of fraudulent behaviour. Key machine learning components include:

- Supervised Learning: algorithms are trained on labelled datasets where the outcomes (fraudulent or legitimate) are known. Common methods include decision trees, support vector machines, and neural networks
- Unsupervised Learning: these algorithms detect hidden patterns in data without prior labelling. Clustering techniques and anomaly detection algorithms fall under this category.

2.3. Real-Time Detection

Real-time detection is achieved through the continuous monitoring and analysis of transaction data. The system's ability to process data in real-time is critical for preventing fraud before it occurs. This is facilitated by:

- Data Stream Processing: utilizes frameworks like Apache Kafka and Apache Flink to handle and analyze streaming data.
- Adaptive Algorithms: machine learning algorithms that continuously learn and adapt to new data inputs, ensuring the system remains responsive to evolving fraud tactics.

2.4. System Adaptability and Iterative Improvement

The system's adaptability is a significant strength. As fraud tactics evolve, the machine learning algorithms adjust dynamically. This continuous learning process involves:

- Regular Updates: algorithms are regularly retrained with new data to capture the latest fraud patterns.
- Feedback Loops: outcomes of detected fraud cases are fed back into the system to improve future detection accuracy.

For the mathematical and statistical methodologies, the following equation represents a simplified fraud detection model:

$$P(Fraud) = \sigma(w \cdot x + b) \tag{1}$$

$$\sigma(z) = \frac{1}{1 + e^{-z}}, \tag{2}$$

where *P(Fraud)* represents the probability that a given transaction is fraudulent, σ is the sigmoid function, also known as the logistic function. It is used to map any real-valued number into the range [0, 1], making it suitable for probability estimation. Also, w represents the weight vector, x is the input feature vector of the transaction and b is the bias term.

3. CONCLUSIONS

The presented Fraud Detection System offers a robust solution to the challenges posed by online transaction fraud. By integrating advanced statistical methodologies with machine learning algorithms, the system can detect fraudulent activities in real-time. Its adaptability and continuous learning capabilities ensure that it remains effective against the ever-evolving landscape of online fraud. This approach not only protects transactions proactively but also enhances overall trust in online payment systems. Future developments will focus on further refining the machine learning models and exploring new data sources to enhance detection accuracy and speed.

Differential-fractional games and international relations

BURNOUT AND ACADEMIC PERFORMANCE: CAUSES, IMPACT AND MANAGEMENT STRATEGIES

Andrei GHENOIU[1], Robert-Mihai PIVODA[1], Sorana-Eliza BALTARETU[1], Antonela TOMA[1,2], Mihai BREBENOIU[1,2]

[1]University Politehnica of Bucharest, 313 Splaiul Independentei, District 6, Bucharest, Romania

[2]Center of Research and Training in Innovative Techniques of Applied Mathematics in Engineering ”Traian Lalescu”

Georgiana CRETU[1,2], Ana-Maria MARIN[1,2], Veronica CONSTANTIN[1,2], Simona Mihaela BIBIC[1,3]

[1]National University of Science and Technology POLITEHNICA Bucharest, 313 Splaiul Independentei, District 6, Bucharest, Romania,

[2]Faculty of Electrical Engineering

[3]Center for Research and Training in Innovative Techniques of Applied Mathematics in Engineering, ‘Traian Lalescu’ (CiTi), Bucharest, Romania

Corresponding author email: georgiana.cretu1106@stud.electro.upb.ro , vconstantin2704@stud.electro.upb.ro, ana_maria.marin1007@stud.electro.upb.ro

Abstract

Academia represents an intense and demanding environment where academic pressure and stress can lead to exhaustion and burnout among students and teaching staff. To address this issue, it is essential to develop mental health programs and policies that provide adequate support and resources for managing stress and preventing burnout. Implementing counselling and psychological support services, encouraging a balance between academic and personal life, and facilitating open communication and sharing experiences can significantly reduce the incidence of burnout within the institution.

Key words*:* burnout, academic pressure, mental health, counselling support, open communication

1. INTRODUCTION

The syndrome of emotional exhaustion, also known as burnout syndrome, is an alarming issue in the contemporary academic environment. Increased university demands, social pressures, and intense cognitive requirements contribute to depressive states and negative behaviors among students. This form of academic exhaustion can be likened to an engine depleting its resources over time and no longer functioning efficiently.

The problem of burnout among students is growing. In an era of fast pace and high academic demands, many students face stress and emotional exhaustion, affecting their mental health and academic performance. Intense cognitive demands and social pressures exacerbate this phenomenon.

According to the World Health Organization (WHO), burnout stems from chronic, unmanaged stress. The WHO describes symptoms as "exhaustion, mental distancing from work, negativism, and reduced professional efficacy." Although these symptoms can severely affect health and require medical assistance, burnout is not recognized by the WHO as a distinct medical condition or mental disorder.

2. CONTENT

2.1. Mathematical approaches

The Fast Fourier Transform is an essential mathematical tool in signal and system analysis. It transforms a signal from the time domain to the frequency domain, allowing for the analysis of the signal's frequency components. This is particularly useful in many applications, including the

Differential-fractional games and international relations

Andrei CHIENOIU[1], Robert-Mihai PIVODĂ[1,2], Sorina-Eliza BĂLTĂREȚU[3], Antonela TOMA[1,2], Mihai REBENCIUC[1,2]

[1] University Politehnica of Bucharest, 313 Splaiul Independenței, District 6, Bucharest, Romania
[2] Center of Research and Training in Innovative Techniques of Applied Mathematics in Engineering "Traian Lalescu"

development of a stress meter, a device that measures a person's stress level.Electrodermal activity (EDA) sensors measure skin conductance influenced by sweat gland activity. The signal yields skin conductance level (SCL) and skin conductance response (SCR). SCR is the peak-to-trough difference in a window, while SCL is the average conductance over time.Skin temperature variation over time can be analyzed using basic statistics or sophisticated methods like wavelet analysis to detect pattern changes.The Wavelet Analysis uses techniques such as Continuous Wavelet Transformation or Discrete Wavelet Transformation.

2.2. Stress quantification

Is the process of measuring and evaluating a person's stress levels using various methods and tools. This involves collecting and analyzing physiological and psychological data to provide a clear and accurate picture of the stress state.

PHYSIOLOGICAL	PSYCHOLOGICAL	DATA ANALYSIS
Electrodermal Activity (EDA): measures skin conductance, which changes with sweat gland activity influenced by the sympathetic nervous system.	*Questionnaires and Scales:* tools like the Perceived Stress Scale (PSS) or the State-Trait Anxiety Inventory (STAI) are used to assess subjective perceptions of stress.	*Statistical Analysis:* calculating mean, variance, and other statistical measures to interpret the data.
Heart Rate Variability (HRV): analyzes fluctuations in the time intervals between heartbeats, providing insights into the balance between the sympathetic and parasympathetic nervous systems.	*Structured Interviews:* interviews with specific questions about the events and feelings experienced by the person.	*Fourier Transform:* used to analyze the frequency components of physiological signals.
Respiratory Rate: measures the frequency and dept0h of breathing, which changes under stress.	*Cognitive Assessments:* tests and tasks designed to measure cognitive functions such as memory, attention, and executive function under stress.	*Wavelet Analysis:* a sophisticated technique for detecting pattern changes in temporal data, such as skin temperature variations.
Skin Temperature: Measures variations in skin temperature, which can be influenced by the stress response.	*Behavioral Observations:* systematic recording of behaviors that can indicate stress, such as fidgeting or facial expressions.	*Machine Learning*: algorithms to predict stress levels based on physiological and psychological data inputs.

Table 1. Measurement methods

3. CONCLUSIONS

Academic pressures significantly affect students, causing exhaustion that impacts their mental and physical health, personal relationships, sleep, and daily tasks. Increased awareness of stress management highlights the need for institutions to provide adequate support. Tools like a "stress meter" with HRV and EDA sensors can monitor stress in real time for personalized interventions by qualified medical staff.

To combat burnout, institutions should implement comprehensive mental health programs, including counseling and psychological support services, promote a balance between academic and personal life, and encourage open communication. This approach can reduce burnout and improve students' well-being and academic performance.

Differential-fractional games and international relations

Andrei GHENOIU[1], Robert-Mihai PIVODĂ[2], Sorana-Eliza BĂLTĂREȚU[3] , Antonela TOMA[1,2], Mihai REBENCIUC[1,2]

[1]University Politehnica of Bucharest, 313 Splaiul Independentei, District 6, Bucharest, Romania
[2]Center of Research and Training in Innovative Techniques of Applied Mathematics in Engineering ”Traian Lalescu”

1.INTRODUCTION

This research presents the differential games and together with the differential-fractional games are applied various fields.they have been studied in the past for their character of analysis of the situation in real time and finding an optimal solution.We will direct the interest toward military and economic applications in relations the first is that of the first two.

2.CONTENT

Differential games involve developing optimal strategies for dynamic systems with competing players, using differential equations to model the system's state. The process involves:

1.Formulating the Problem.

Define state variables (dependent on time) and control variables for each player, $x(t)$, where t is time.

Specify the control variables for each player, usually $u(t)$ for player 1 and $v(t)$ for player 2.

Establish the dynamics with differential equations:

$$\dot{x}(t) = f\big(x(t), u(t), v(t)\big)$$

Specify each player's payoff function.:

$$J_1 = \int_0^T L_1(x(t), u(t), v(t))dt$$

$$J_2 = \int_0^T L_2\big(x(t), u(t), v(t)\big)dt$$

2. Determining the Type of Game:

Zero-sum game: One player's gain equals the other's loss.

3. Finding the Hamiltonian:

Define Hamiltonian functions for each player, incorporating cost variables.. For player 1 we have:

$$H_1 = L_1(x, u, v) + \lambda_1^T f(x, u, v)$$

Differential-fractional games and international relations

Andrei GHENOIU[1], Robert-Mihai PIVODĂ[2], Sorana-Eliza BĂLTĂREȚU[3] , Antonela TOMA[1,2], Mihai REBENCIUC[1,2]

[1]University Politehnica of Bucharest, 313 Splaiul Independentei, District 6, Bucharest, Romania
[2] Center of Research and Training in Innovative Techniques of Applied Mathematics in Engineering ”Traian Lalescu”

4. Deriving Necessary Conditions:

Apply Pontryagin's Maximum Principle to find optimal control laws by maximizing the Hamiltonians.

$$\lambda_1(t) = -\frac{\partial H_1}{\partial x}, \lambda_2(t) = -\frac{\partial H_2}{\partial x}$$

Determine the optimal control laws by maximizing the Hamiltonians:

$$u^*(t) = \arg\ \max_u H_1, v^*(t) = \arg\ \max_v H_2$$

5. Solving the Two-Point Boundary Value Problem:

Solve the state and costate equations using numerical methods.

6. Verifying the Solution:

Ensure consistency and optimality, confirming the strategies meet initial conditions and maximize payoffs.

2.1. In the field of military strategy, differential games are used to shape conflicts where at least two parties have competing interests. the ultimate goal is to determine the best strategy in several respects, that is, the optimal strategy of each player to maximize their own profit and minimize that of their opponents a formal explanation of the steps to be taken to solve such a problem.

The first step is to identify the players who take part in the conflict and define the purpose for each of them. The next step is to identify the key variables that describe the state of the system and formulate the equations that describe how these variables change over time and the actions that take place control variables for each participant of the game, these variables aim to limit the players' actions so as not to experience certain errors during calculations. another step would be to create the cassig functions that quantify the results according to the status variables and the allegerilization that were taken an example of the won and lost lands.

With all these variables and well-defined systems of equations, solutions such as Nash balance, Pareto Optimality and evolutionary stable strategies will be used to analyze and predict the outcome.

2.2.in the economic field in the context of international relations we will present an example of application for a differential game with 2 people with the strategy pursuit-evasion.We have the following situation:

In two countries, in crisis, they try to become diplomatic and economic. One example is that one country tries to put pressure on another through various sanctions and the other tries to resist or find a way to avoid pressure.

We will continue to write the dynamic system that describes the state equations for each player:

$$\dot{x} = \begin{bmatrix} \dot{x}_P \\ \dot{x}_E \end{bmatrix} = \begin{bmatrix} f_P(x_p, u_p, t) \\ f_E(x_E, u_E, t) \end{bmatrix}$$

Differential-fractional games and international relations

Andrei GHENOIU[1], Robert-Mihai PIVODĂ[2], Sorana-Eliza BĂLTĂREȚU[3], Antonela TOMA[1,2], Mihai REBENCIUC[1,2]

[1]University Politehnica of Bucharest, 313 Splaiul Independentei, District 6, Bucharest, Romania
[2]Center of Research and Training in Innovative Techniques of Applied Mathematics in Engineering
"Traian Lalescu"

având condiția inițială $x(t_0) = x_0, t_0 \leq t \leq t_f, t_0 = 0$ și $u_P(\cdot)$ reprezentând urmăritorul iar $u_E(\cdot)$ the evader.

We add the catch function that determines the condition that the country to which the sanctions are applied is obliged to pay them:$l(x(t_f), t_f) = 0$ At the end of the game.

The cost function is $J = \emptyset(x(t_f), t_f) + \int_{t_0}^{t_f} L(x, u_p, u_E)dt$ for the purpose of the game find the optimal control represented by a foru_P and b foru_E so that$J(a, u_E) \leq J(a, b) \leq J(u_P, b)$ .the next one has the purpose of shrinking this function in contrast to the purpose of evader.so that the control rules can be manifested as finctions of the initial state variables will be introduced two open-loop feedback strategies:K_P siK_E.

L is the cost of integration.

$u_P(t) = K_P(x_P(0), t)$ that is,$u_E(t) = K_E(x_E(0), t)$ with the value of the game being defined as the result of the objective function when the optimal strategies were developed:

$$V = \min_{c} \max_{d} J = \max_{d} \min_{c} J = J(a, b)$$

also, $K_P and\ K_E\ dupa\ parcurgerea\ strategiilor\ optime\ se\ noteaza\ cu\ c\ respectiv\ d.$

The necessary conditions for open-loop representation of the saddle point solution:

$$H \equiv \lambda^T f + L$$

cost vector$\lambda = \begin{bmatrix} \lambda_P \\ \lambda_E \end{bmatrix}$, derivative vector:$f = \begin{bmatrix} f_P \\ f_E \end{bmatrix}$, stopping condition: $\Phi \equiv \emptyset + v^T l$

Where v represents the Lagrange multiplier for stopping constraint.

The equation that will contain the cost is$\dot{\lambda} = -H_x = -[\frac{\partial f}{\partial x}]^T \lambda$ having the condition of capture or the final cost $\lambda^T(t_f) = \frac{\partial \emptyset(x(t_f), t_f)}{\partial x}$.

The add-point solution must meet the following conditions:

$$u_P = arg \min_{u_P} H = arg \min_{u_P} (\lambda_P^T f_P)$$

$$u_E = arg \max_{u_E} H = arg \max_{u_E} (\lambda_E^T f_E)$$

The following player tries to bring the other player to the terminal area where he can be captured. A barrier divides the state area into two zones: Capture zone and escape zone. If the country that is under pressure is in capture zones, it will no longer be able to oppose the other country's earrings and the other similarly, if the country that puts pressure reaches the evasion zone, it will never be able to achieve its goal.

2.3. Fractional differential games offer a substantial expansion of traditional differential games as they incorporate fractional calculus, encompassing derivatives and integrals of non-integer value. This broader approach allows for a more adaptable and precise representation of memory and hereditary characteristics in dynamic systems, establishing a more inclusive framework for comprehending and examining complex systems with unique physical attributes.

Implementation in differential game issues:

1. Formulating the Problem:

Define the state variables $x(t)$ and the control variables $u(t), v(t)$.

Establish the dynamics with fractional differential equations.

$$D_t^{\alpha} x(t) = f(x(t), u(t), v(t))$$

where D_t^{α} denotes the fractional derivative of order α.

2. Objective Functions:

The payoffs for each player:

$$J_1 = \int_0^T L_1(x(t), u(t), v(t))dt \, , J_2 = \int_0^T L_2(x(t), u(t), v(t))dt$$

3. Finding the Hamiltonian:

For fractional systems, the Hamiltonian functions for player 1 is:

$$H_1 = L_1(x, u, v) + \lambda_1^T D_t^{\alpha} x$$

4. Deriving Necessary Conditions:

- Use Pontryagin's Maximum Principle adapted for fractional systems.

2.4 military and economic

Military and economic connections are highlighted by the arms race between Western market economies and Eastern centrally planned economies, impacting military expenditures. Both blocs assume identical preferences,technologies, and populations, with Eastern variables marked by an asterisk.

In the Eastern economy, government controls consumption, labor, and production without taxes to maximize household utility. Total production equals consumption plus government spending, ensuring the marginal rate of substitution matches labor's productivity.

The "guns versus butter" dilemma illustrates the trade-off between defense spending and civilian consumption. In the Eastern bloc, more resources for weapons mean less for consumption, necessitating more work and less consumption. In the West, labor taxes reduce work incentives, lowering labor supply and consumption.

The study finds that for identical defense investments, Eastern households work and consume more than Western ones. The analysis links game theory to economic contexts by examining how economic policies influence strategic military decisions, highlighting the interplay between defense spending and economic welfare in different systems.

3.CONCLUSION

To conclude, differential games provide a robust framework for modeling strategic conflicts in various fields, from military strategies to international economic relations. By defining state and control variables and leveraging the Hamiltonian and Pontryagin's Maximum Principle, one can derive optimal strategies for competing players. The application of these methods, whether in traditional or fractional forms, reveals the intricate balance between objectives like resource allocation and strategic dominance.

ARITHMETIC PROGRESSIONS AND PERFECT POWERS

Gheorghe BOROICA[1] **, Gabriela BOROICA**[2]

[1]National College Gheorghe Șincai, 25 Gheorghe Șincai, Baia Mare, România

[2]National College Vasile Lucaciu, 2 Culturii, Baia Mare, România

Corresponding author email:ghitaboroica64@gmail.com, gabiboroica@yahoo.com

Abstract

This paper presents some theoretical aspects, both elementary and less elementary, related to certain arithmetic progressions, as well as problems that make the connection between these and perfect powers. In the paper, sufficient conditions are given for a sequence of numbers not to contain an infinite arithmetic progression. Additionally, the paper answers the question:what is the maximum number of terms of an arithmetic progression contained in the sequence of perfect squares of natural numbers. The well-known property:if an arithmetic progression of natural numbers contains a perfect square, then it contains an infinity of perfect squares, is complemented by a similar property for the terms of the Fibonacci sequence:If a non-constant arithmetic progression of natural numbers contains a term from this sequence, then it contains an infinity of such terms.

Key words*: arithmetic progressions , perfect powers, applications*

1.INTRODUCTION

The first part of the paper has an informative character and presents some significant results related to arithmetic progressions.Famous mathematicians such as Dirichlet, Van der Waerden, Ben Green, Terence Tao, etc., have formulated and proven interesting properties of some arithmetic progressions in problems of number theory or coloring. This part of the paper aims to be a basis for a study that the author intends to deepen in the future.

2. CONTENT

The starting point in this endeavor is the following problem:

Problem 2.1. Does the string $1^2, 2^2, 3^2, ..., n^2, ...$ contain an infinite arithmetic progression?

Not only is the answer negative, but it can be generalized through the following two problems:

Problem 2.2. If k is a positive integer, $k \geq 2$, then the string $1^k, 2^k, 3^k, ..., n^k, ...$ doesn't contain an infinite arithmetic progression.

Problem 2.3. If $f : (0, \infty) \to$ □ is a strictly increasing function and $f\left(\frac{x+y}{2}\right) < \frac{f(x)+f(y)}{2}, \forall x, y > 0, x \neq y$, then the string $(a_n)_{n\geq 1}, a_n = f(n)$ doesn't contain an infinite arithmetic progression.

Consider the following problem: How many perfect squares or perfect cubes or perfect powers can a finite arithmetic progression of natural numbers contain?A partial answer is given by :

Problem 2.4. Consider the infinite arithmetic progression $a, a+r, a+2r, \ldots$ with *a* and *r* as integers, $r \neq 0$. Then for every $k \in \mathbb{N}, k \geq 2$ the given progression doesn't contain a term that can be written as the root of *k-a* of an integer or contain an infinity of such terms.

It naturally led to another question: What is the maximum length of a finite arithmetic progression contained in the string of non-perfect squares? The answer is given in the following two problems:

Problem 2.5. There is an infinity of integers *x, y, z*, which are prime to each other so that x^2, y^2, z^2 are in an arithmetic progression.

Problem 2.6. There are no four distinct perfect roots in an arithmetic progression.

The paper also contains solved problems that fit into this topic and ends with a list of proposed problems.

3. CONCLUSIONS

A solid understanding of the theoretical foundations, along with familiarity with some non-standard results, broadens the horizon for tackling more challenging problems.

REFERENCES

[1] T. Andreescu, V. Crișan, *Mathematical Induction. A powerful and elegant method of proof,* 2017 XYZ Press, LLC.

[2] T.Andreescu, D. Andrica, *An introduction to the study of Diophantiene equations,* Ed. Gil, Zalău, 2002.

[3] Arthur Engel, *Mathematics problems-solving strategies,* Ed.Gil, Zalău,2006.

[4] L. Panaitopol, Al. Gica, *Arithmetic and number theory problems,* Ed.Gil, 2006.

[5] V. Pop, M.Pop, *Problem-solving strategies for combinatorial geometry,* Ed. Mega, Cluj-Napoca, 2015.

[6] I. Savu, *Preparatory problems for school olympiads, grades 9-12,* Ed.Art , 2006.

[7] M. Teleucă, V. Pop, D. Croitoru, *Elementary number theory problems for school competitions,* Ed. Mega, Cluj-Napoca, 2016.

[8] V. Pop, *Some non-elementary results about arithmetic progressions,* Journal Argument, No.15-2013.

COLLINEARITY AND CONCURRENCY IN SPACE

Ioan CIOBANAȘU[1], Mariana CIOBANAȘU[2]

[1]Școala Gimnazială Nr. 8 „Elena Rareș”, Botoșani, Romania
[2] Școala Gimnazială Nr. 11, Botoșani, Romania

Corresponding author email: ioan_ciobanasu@yahoo.com

Abstract
We present some methods for studying the collinearity of points and the concurrency of lines in space. We exemplify the approaches presented by solving some problems.

Keywords*: geometry, collinearity, concurrency.*

1. INTRODUCTION

Collinearity and concurrency problems are sometimes truths that are easy to intuit, but whose rigorous demonstration requires precise reasoning and a varied range of techniques, which suppose

mathematical culture and creativity. One can speak of their importance in the teaching of geometry at all levels, considering the various methods of approach and solution.
In space, collinearity and concurrency problems can be approached by methods specific to spatial geometry, but also by methods specific to planar geometry.
To prove collinearity we use the fact that if two planes have a common point, then all their common points are collinear.

2. CONTENT

We propose some problems that can be solved with students capable of performance.

Problem 1. Let A, B, C, and D be four distinct and non-coplanar points, $M \in (AB)$, $N \in (AC)$, $P \in (AD)$, and $MN \cap BC = \{E\}$, $MP \cap BD = \{F\}$, $NP \cap CD = \{G\}$. Prove that the points *E*, *F* and *G* are collinear.

Problem 2. In the cube *ABCDA'B'C'D'* the point *P* is the foot of the perpendicular from the point *A* on the plane (*A'B'C*), point Q is the foot of the perpendicular from the point B on AC and the point R is symmetric to point D with respect to the point C. Prove that the points *P*, *Q* and *R* are collinear.

Problem 3. Consider *ABCA'B'C'*, a regular triangular prism, with base side *AB* = 12 cm. Let *M* be the midpoint of the side [*BC*], $BC' \cap B'C = \{O\}$, $BN \perp AO$, $N \in AO$, such that $BN = 6\sqrt{2}$ cm.
a) Prove that $BC \perp AO$.
b) Determine the height of the prism and show that the points *A'*, *N* and *M* are collinear.

Mathematical Olympiad, Local Stage, Dâmbovița, 2018

Problem 4. Let *ABCDA'B'C'D'* be a rectangular parallelepiped. We denote by *M*, *N* and *P* the midpoints of the edges [*AB*], [*BC*], respectively [*BB'*]. Let $\{O\} = A'N \cap C'M$. Prove that the points *D*, *O* and *P* are collinear.

Mathematics Olympiad, County Stage, 2018

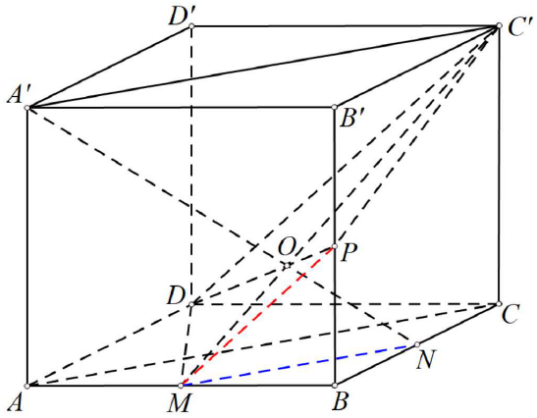

Problem 5. Let *ABCDA'B'C'D'* be a cube and the points $M \in (AB)$, $N \in (CC')$, $P \in (D'A')$, so that $AM = CN = D'P$. Prove that the center of gravity of the triangle *MNP* belongs to the segment [*B'D*].

Dan Brânzei, National Contest „Alexandru Myller", Iași, 2004

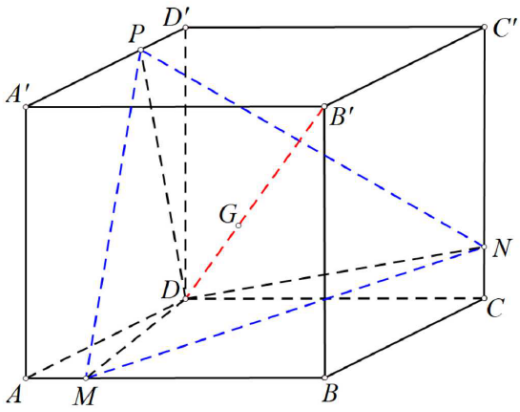

3. BIBLIOGRAPHY

[1] Artur Bălăucă, *Algebră. Geometrie. 1050 de probleme semnificative. Olimpiade, concursuri și centre de excelență. Clasa a VIII-a*, Editura Taida, Iași, 2019.

[2] Dan Brânzei, Sorin Ulmeanu, Vasile Gorgotă, Ioan Șerdean, *Matematica în concursurile școlare. Clasele V-VIII*, Editura Paralela 45, Pitești, 2001.

[3] Maranda Lință, Dorin Lință, Rozalia Marinescu, Dan Ștefan Marinescu, Mihai Monea, Steluța Monea, Marian Stroe, *Matematică de excelență. Clasa a VIII-a*, Editura Paralela 45, Pitești, 2014.

[4] Ion Vîrtopeanu, Alexandru Leonte, *Geometrie în spațiu pentru gimnaziu și liceu*, Editura Sibila, Craiova, 1994.

[5] Colecția *Gazeta Matematică* , Seria B.

[6] https://www.viitoriolimpici.ro/.

INNOVATIVE APPROACHES IN EDUCATION WITH AI-POWERED VIRTUAL ASSISTANTS

[1] David-Theodor IONIȚĂ, [2] Ioana Corina BOGDAN, [1] Horia Alexandru MODRAN

[1]Transilvania University of Brasov, Bulevardul Eroilor 29, Brașov 500036, Romania
[2]Transilvania University of Brasov & CITI, Bulevardul Eroilor 29, Brașov 500036, Romania

Corresponding author email: corina.bogdan@unitbv.ro

Abstract

In the computer age, virtual assistants have become a significant part of educational and professional environments. Through the proposed VA, it was focused on simplifying the learning process by providing analogies and examples of exercises for specific subjects. Moreover, the VA could generate personalized virtual profiles adapted to the user`s needs, depending on their pre-university or university education. In this context, two types of solutions are available: (1) the technical aspect, which offers academic support in subjects like mathematics, physics, and electrical engineering, alongside feedback and learning strategies tailored to enhance user performance and acquired information; (2) the social solution, which facilitates human-like interaction to reduce social anxiety and offers psychological support, guiding adolescents and young adults to seek specialized help for their mental health concerns. Our VA represents a pioneering approach integrating advanced technology with customized assistance to enrich users` academic and personal journeys and experiences.

Key words*: Artificial Intelligence, Virtual Assistant, Androids, Education.*

1. INTRODUCTION

In our day, artificial intelligence and virtual assistants play a key role in education and most work environments. Virtual assistants (VA) are developed to offer and monitor both educational and psychological support to students and any individual by helping during their learning process and adapting them to academic and personal challenges [1], [2]. In addition, VAs could be a step toward the development of a psychological profile adapted efficiently to the user's aptitudes and needs, ensuring a personalized, optimized, and effective interaction. Previous applications that are also available for students and any individual who are eager to develop their knowledge based on novel technologies are: Alexa, a VA designed and developed for smart homes; Siri, which is able to control Apple devices; Bixby, conceived to control through available functions Samsung devices; Cortana for Microsoft Windows; Woebot, which offers psychological support for companies and enterprises; or Replika, a chatbot used for counseling and psychological support [1]-[4].

2. MODEL OF THE VIRTUAL ASSISTANT AND SOLUTIONS

Virtual assistants are generally used for establishing interaction with students in order to improve their academic performance and professional development. The VA is capable of engaging students in digital interaction through vocal interaction. In this way, there is no need to write each message or question that the user wants to address to the VA. Moreover, the response is received through an audio signal and a text prompt. This artificially intelligent system could be integrated into a humanoid robot [5], [6], such as PKD, Eve, Sophia, Ameca, Alter3, or Jiajia, that can be trained to imitate human behavior during interaction. The model of the VA presents two types of solutions: a technical solution and a social one.

(1) Technical Solution: The VA offers assistance in understanding subjects from pre-university or university education as well as improving academic performance by generating explanations and exercises. The verification of knowledge is made through tests at the end of a lesson. As feedback, this one is based on results that provide a positive outlook on the situation, adapted to the user's

psychological profile, level, and academic preparation. Based on strategies and learning plans, the VA supports students to improve their information retention and offers suggestions and best practices.

(2) Social Solution: As previously mentioned, the main advantage of VA is that the user can speak directly with it, giving the impression of an interaction as close as possible to that with a teacher or human mentor. Its goal is to help adolescents or young people suffering from social anxiety or who are shyer find a useful solution that can offer them the opportunity to improve their academic performance. Subsequently, they can be guided towards seeking specialized help if needed.

In the current version of the VA, vocal communication between humans and the machine is possible for the purpose of asking trivial questions using the GPT-4 [7] engine to generate responses, which are also provided as audio output through the output devices. The process is described in Fig. 1, where it is given the example of the VA Interface with available selections (username, input and output devices, and AI voice), and Fig. 2, which describes steps on obtaining the final result, the response from the VA. The user question is processed (steps of listening, processing, correcting errors of misunderstanding, and finally the expected result).

Figure 1: VA Interface.

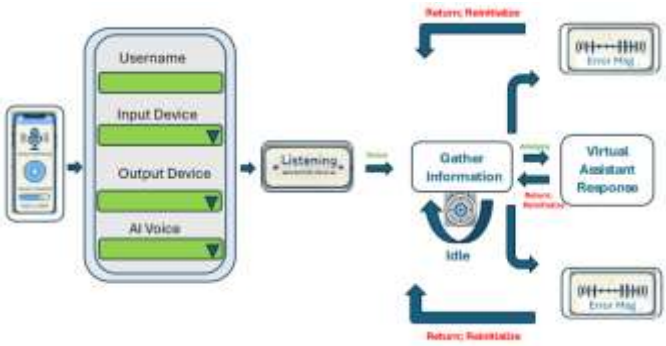

Figure 2: Steps in VA feedback process.

3. CONCLUSIONS

Through the integration of educational and psychological features, our VA establishes itself as a reliable ally for students as they navigate their paths of learning and personal growth. For accurate results, a convenient way is to follow the upgrade to the GPT-4o engine to generate responses with greater accuracy in a shorter time. Moreover, the creation of a new modern and visually appealing graphical interface by generating short and concise audio responses with detailed explanations including diagrams, equations, and syntaxes is crucial. Implementation of a text box that VA can read on the user's command In addition, access to a database specific to the field of cybersecurity and telecommunications specialization is an essential aspect..

BIBLIOGRAPHIC REFERECES

[1]. https://clickup.com/blog/ai-tools-for-virtual-assistants/#1-the-10-best-ai-virtual-assistants-to-use-in-2024.
[2]. P. N. R, Mina et al., Leveraging Education through Artificial Intelligence Virtual Assistance: A Case Study of Visually Impaired Learners. International Journal of Educational Innovation and Research, 2(1), 10–22, 2023.
[3]. M. Mariani et al., Artificial intelligence empowered conversational agents: A systematic literature review and research agenda, Journal of Business Research, Vol. 161, 2023, 113838, ISSN 0148-2963.
[4]. N. Loideain et al., From Alexa to Siri and the GDPR: The gendering of Virtual Personal Assistants and the role of Data Protection Impact Assessments, Computer Law & Security Review, Vol. 36, 2020, 105366, ISSN 0267-3649.
[5]. A. Habib et. al., Lerning Human-Like Facial Expressions for the Android, Phillip K. Dick, IEEE Int. CASE 2014, Taipei, Taiwan, 109/CoASE.2014.6899473.
[6]. I.C. Bogdan et al., Games theory involvement in the social robots facial expressions, U.P.B. Sci. Bull., Series C, Vol. 85, Iss. 1, 2023, ISSN 2286-3540.
[7]. https://openai.com/chatgpt/

Dimitrie Pompeiu's Theorem

Ioana Monica Mașca

Colegiul Național de Informatică "Grigore Moisil"

Calea București nr 75, Brașov

Ioana.masca@moisilbv.ro

Abstract: *In the first part we present four different proofs of the famous theorem of Dimitrie Pompeiu coming from the geometry of the triangle, a reciprocal of it, as well as an application of it, proposed in an admission exam.*

We also present other famous theorem than can be conssidered as a particular case of Pompeiu's theorem: the theorem of Shooten.

In the second part, we suggest some interesting relations which involve the triangle from Pompeiu's theorem: area, side lenghts, relationships between the sides of the triangle from theorem and the initial triangle.

We remind, as well, different lemmas, theorems and important known results that are used to prove the theorem and the relationships between the two triangles.

Key words: *side lengths of a triangle. circumscribed circle of a triangle, construction of a triangle, inequalities between the sides of a triangle, distance from a point to the sides of a triangle, maximum area.*

Throughout the paper, we will consider an equilateral triangle *ABC* and an arbitrary point *P* in the triangle's plane.

We know the following aspects:

Theorem (Pompeiu) [3] Let *ABC* be an equilateral triangle and *P* a point in the triangle's plane, that does not belong to the circumscribed circle of the triangle. Then, the distances from point *P* to the vertices of the triangle *PA, PB, PC* represent the side lenghts of a triangle (possibly degenerate).

We have four ways to prove this theorem: two using geometrical transformations - rotations and inversions [1], [6], [7] and two with complex numbers – using triangle's inequatity and the roots of the third order of the unit [3], [5].

A particular case in the theorem of Pompeiu when point *P* belongs to circumscribed circle of the triangle is theorem of Shooten. Even here we have two different ways to prove Shooten theorem: using the first theorem of Ptolemeu or using arcs and congruent angles [3].

Reciprocal theorem of Pompeiu tells us that if we can construct a triangle with the distances from a point *P* from the triangle's plane to the triangle's vertex, then the triangle is an equilateral one.

To prove the reciprocal theorem we use mathematical analysis methods [2], [4].

If point *P* belongs to the circumscribed circle of the triangle, then with *PA, PB* and *PC* we obtain a degenerate triangle and to prove this we use first theorem of Ptolemeu [3].

As an example of Pompey's theorem, we will present a problem proposed to be solved in an admisssion exam in a technical university, in 1988.

There are some interesting relationships which involve the triangle from Pompeiu's theorem:

- **Its area is maximum if the point *P* coincides with the center of the circumscriebed circle of the original triangle [1], [3];**
- **The sum of distances from point *P* to the sides of an equilateral triangle is always constant [1];**
- **The sum of distances from point *P* to the triangle's vertex is minum, if point *P* coincides to the centroid of the triangle [1];**
- **We can express the side lenghts of the original equilateral triangle from *PA, PB PC* and from the distances from *P* to the sides of the triangle [1], [5];**
- **We can express also the area of the triangle from Pompeiu's theorem depending on *d* and the length of the side of the triangle, if the point *P* is located at a distance *d* from the centroid of the triangle [5].**

References:

[1] C. Cocea, *200 de probleme de geometria triunghiului echilateral*, Editura Gh. Asachi, Iași, 1992.

[2] M. Ganga, *Matematică. Manual pentru clasa a XII-a,* Editura Mathpress, Ploiești, 2007.

[3] L. Nicolescu, W.G. Boskoff, *Probleme practice de geometrie*, Editura Tehnică, București, 1990.

[4] I. Petrică, E. Constantinescu, D. Petre, *Probleme de analiză matematică,* Editura Petrion, București, 1983

[5] F. Smarandache, *Probleme de geometrie și trigonometrie, compilate și rezolvate,* 2015, https://archive.org/details/ProblemeGeomTrig/

[6] https://math.fandom.com

[7] *Concursul Gazeta Matematică și ViitoriOlimpici.ro*, Ediția a XI-a, Etapa 7.

APPLIED MATHEMATICS IN MACHINE LEARNING

Iuliana-Petruța-Diana SANDU

National University of Science and Technology POLITEHNICA Bucharest, 313 Splaiul Independenței, District 6, Bucharest, Romania

iuliana.sandu@stud.fsa.upb.ro

Abstract

This paper explores the foundational role of mathematics in Artificial Intelligence (AI) and Machine Learning (ML). Mathematics, encompassing disciplines such as linear algebra, calculus, probability, and statistics, provides the essential framework for developing and optimizing intelligent systems. Practical examples are presented to illustrate the application of these mathematical concepts in AI and ML. Specifically, the paper discusses the use of gradient descent for optimizing loss functions and demonstrates the training of a neural network to solve the XOR problem, showcasing the transformative impact of mathematical approaches in these fields.
Key words: *artificial intelligence; machine learning; linear algebra; calculus; probability; statistics.*

1 Introduction

Artificial Intelligence (AI) and Machine Learning (ML) are revolutionary fields in contemporary technology, aiming to develop systems and algorithms that emulate and enhance human cognitive abilities. Mathematics provides the tools and frameworks necessary for designing algorithms, processing data, and making informed decisions. This paper delves into the mathematical foundations of AI and ML, exploring key concepts such as linear algebra, calculus, probability, and statistics, and demonstrating their practical applications.

1.1 Linear Algebra

Linear algebra is fundamental to many AI and ML algorithms. It involves the study of vectors, vector spaces, and linear transformations, essential for representing data and operations.

1.1.1 Vectors and Matrices

Vectors and matrices are used to represent data points and relationships between variables. For instance, in image processing, an image can be represented as a matrix where each element corresponds to a pixel's intensity.

1.1.2 Eigenvalues and Eigenvectors

Eigenvalues and eigenvectors provide insights into the properties of matrices and are used in algorithms such as principal component analysis (PCA) to reduce data dimensionality.

$$A\mathbf{v} = \lambda\mathbf{v} \tag{1}$$

where A is the matrix, $\mathbf{v}$ is the eigenvector, and λ is the eigenvalue.

1.2 **Calculus**

Calculus is crucial for modeling and optimizing functions in ML algorithms.

1.2.1 Derivatives and Gradients

Derivatives measure how a function changes as its input changes, while gradients are used in optimization algorithms like gradient descent to minimize error.

$$\theta = \theta - \eta \cdot \frac{dL}{d\theta} \tag{2}$$

where θ is the parameter vector, η is the learning rate, and $\frac{dL}{d\theta}$ is the gradient of the loss function.

1.3 **Probability and Statistics**

Probability and statistics are essential for modeling uncertainty and making inferences from data.

1.3.1 Probability Distributions

Probability distributions describe the likelihood of different outcomes, crucial for designing and interpreting ML models.

1.3.2 Statistical Inference

Statistical inference involves drawing conclusions from data using techniques like hypothesis testing and regression analysis.

2 Conclusions

As we conclude our exploration of mathematical approaches in AI and ML, it is evident that mathematics forms the foundation of these fields. From linear algebra and calculus to probability and statistics, these mathematical concepts provide the tools necessary for developing and optimizing machine learning algorithms. Looking forward, advances in mathematical research will continue to drive innovation in AI and ML, enabling the development of more sophisticated and powerful algorithms and expanding their application to various domains. As Richard Feynman aptly said, "Mathematics is like a game of puzzle in which you create your own rules and explore their consequences." With these mathematical tools in hand, the future of AI and ML is boundless, and the potential for innovation and discovery is limitless.

COMPARATIVE ANALYSIS BETWEEN ALPHA-BETA-GAMMA FILTER AND KALMAN FILTER. MATHEMATICAL APPROACHES.

Iulian-Nicolae PETRIIA[1,2], Antonela TOMA[1,3], Octavian POSTAVARU[1,3]

[1]National University of Science and Technology POLITEHNICA Bucharest, 313 Splaiul Independentei, District 6, Bucharest, Romania,
[2]Faculty of Electronics, Telecommunications and Information Technology, Bucharest
[3]Center for Research and Training in Innovative Techniques of Applied Mathematics in Engineering, 'Traian Lalescu' (CiTi), Bucharest, Romania

Corresponding author email: iulian.petriia@stud.etti.upb.ro

Abstract: *This paper investigates the impact of sensor limitations on drone stabilization and proposes a comparative study between two sensor fusion techniques: the alpha-beta-gamma filter and the Kalman filter. Inherent discrepancies exist between GPS and accelerometer data due to vastly different sampling frequencies. Low GPS update rates can lead to inaccurate position estimation, while high-frequency accelerometer data suffers from drift over time when integrated to obtain position. To address this challenge, the paper explores the application of an alpha-beta-gamma filter to fuse data from both sensors. This filter offers a computationally efficient approach to combine sensor measurements, potentially leading to a more precise and accurate estimation of the drone's position and velocity. Furthermore, the paper delves into the application of the Kalman filter, a widely used sensor fusion technique known for its robustness. By employing state extrapolation equations to model the dynamics of a drone, both filters are evaluated and compared. This interdisciplinary approach aims to identify the optimal sensor fusion technique for achieving robust drone stabilization, considering factors such as computational efficiency, accuracy, and filter complexity.*

Key words*: GPS, Sensor Fusion, Drone, Physical state estimation, Interdisciplinary Mathematical Modelling.*

1. INTRODUCTION

Building an autonomous drone model from scratch can often be difficult due to the multiple characteristics that must be taken into account, but another rather important aspect is that the drone must be able to know its position in space. Starting from this statement, this study tries to compare two models by analyzing both the similarities and the differences and manages to find the best theoretical model that can be successfully implemented in a UAV type drone.

2. CONTENT

The method to implement the α - β – γ filter describes the State Extrapolation Equations for position, velocity, and acceleration:

$$\hat{x}_{n+1,n} = \hat{x}_{n,n} + \hat{\dot{x}}_{n,n}\Delta t + \hat{\ddot{x}}_{n,n}\frac{\Delta t^2}{2} \quad (1)$$

$$\hat{\dot{x}}_{n,n} = \hat{x}_{n,n} + \hat{\ddot{x}}_{n,n}\Delta t \quad (2)$$

$$\hat{\ddot{x}}_{n+1,n} = \hat{\ddot{x}}_{n,n} \quad (3)$$

The next step is the State Update Equations for *position*, *velocity*, and *acceleration*:

$$\hat{x}_{n,n} = \hat{x}_{n,n-1} + \alpha * \left(z_n - \hat{x}_{n,n-1}\right) \quad (4)$$

$$\hat{\dot{x}}_{n,n} = \hat{\dot{x}}_{n,n-1} + \beta * \left(\frac{z_n - \hat{x}_{n,n-1}}{\Delta t}\right) \quad (5)$$

$$\hat{\ddot{x}}_{n,n} = \hat{\ddot{x}}_{n,n-1} + \gamma * \left(\frac{z_n - \hat{x}_{n,n-1}}{0.5 * \Delta t^2}\right) \quad (6)$$

α, β, γ constants can be experimentally determined in such a way that the α - β - γ filter can estimate the physical state of the system as accurately as possible. β controls how much reactive the filter is

proportional to the first derivative of the measured state and γ for the second derivative of the measured state.

The general algorithm for implementing a Kalman Filter will be divided in 5 steps, although steps 1 and 2 can be seen by just one step. Step 1 will initialize the System State Estimate and the System State Error Covariance $\boldsymbol{x_1}$ $\boldsymbol{and}$ $\boldsymbol{P_1}$. Step 2 will re-initialize the two previous mentioned parameters. $\boldsymbol{x_2}$ $\boldsymbol{and}$ $\boldsymbol{P_2}$. Next, the step 3 will predict the System State and also System State Error Covariance to Measurement Time, $\boldsymbol{x_p = Ax_2}$, $\boldsymbol{P_p = AP_2A^T + Q}$. The step fourth will deal with the computation of the Kalman Gain that can be calculated from the formula $\boldsymbol{K_3 = P_pH^T(HP_pH^T + R)^{-1}}$. The last step will be the calculation of the Estimate System State and System State Error Covariance at Measurement Time with the two formulas: $\boldsymbol{x_3 = x_p + K_3(z_3 - Hx_p)}$, $\boldsymbol{P_3 = P_p - KHP_p}$.

Both the α - β - γ filter and the Kalman filter are established techniques for State Estimation in dynamic systems. They utilize noisy sensor measurements to infer the underlying state of a system. While they share some similarities, there are key differences in their underlying frameworks and implementation complexities.
Similarities can refer to the idea that both filters aim to estimate the state of a system by combining a priori knowledge of the system dynamics with noisy sensor measurements. They operate optimally in linear systems where the state-space model can be represented by linear equations. Both filters are recursive, meaning they update the state estimate at each time step based on the previous estimate and the current measurement.
α - β - γ and Kalman filters, while both used for estimation, differ in their complexity and approach. The α - β - γ filter employs a simpler model, focusing on tracking position, velocity, and acceleration. It relies on manually tuned gains assumed to be constant, making it easier to implement. Kalman filters, on the other hand, utilize a more comprehensive model that can handle various system dynamics. This adaptability comes at the cost of increased complexity. The Kalman filter calculates a gain at each step based on noise characteristics, leading to a more statistically rigorous but intricate implementation. This difference in noise modelling also impacts performance. α - β - γ filters assume constant noise, which can limit their accuracy in highly dynamic or non-linear systems. Kalman filters explicitly model noise covariances, resulting in generally higher accuracy and robustness. In essence, the α - β - γ filter offers a simpler, easier to implement solution for systems with moderate dynamics, while the Kalman filter provides superior performance and adaptability for more complex scenarios, albeit with a steeper learning curve.

3. CONCLUSIONS

This study has explored the application of sensor fusion algorithms, specifically comparing the α - β – γ filter and the Kalman filter, in the context of a small flight trajectory tracking of an UAV.
Our analysis revealed that the α - β – γ filter, while computationally efficient and well-suited for systems with well-defined dynamics, might not be ideal for the dynamic environment of a UAV. Its reliance on constant, pre-defined gains limit its adaptability to changing noise characteristics and complex flight conditions. In contrast, the Kalman filter, with its comprehensive state-space model and adaptive Kalman gain, offers superior performance and robustness.
Therefore, for applications like UAV flight path tracking, where accuracy and robustness are paramount, the Kalman filter emerges as the preferred choice. Its ability to adapt to changing conditions and noise characteristics ensures a more reliable and safe flight for the UAV (Unmanned Aerial Vehicle). However, the increased complexity of the Kalman filter implementation compared to the α - β – γ filter necessitates careful consideration of computational limitations in resource-constrained embedded systems.

On the Admissibility of Fractional Singular Continuous-Time Systems Using Caputo Derivative: An LMI Approach

Kamel BENYETTOU[1] and Djillali BOUAGADA[2]

[1]National $National Higher School of Mathematics, Scientific and Technology Hub of Sidi Abdellah, ACSY Team-Laboratory of Pure and Applied Mathematics (UMAB), P.O. Box 75, Algiers 16093, Algeria.

[2] Abdelhamid Ibn Badis University Mostaganem, Department of Mathematics and Computer Science, ACSY Team-Laboratory of Pure and Applied Mathematics, Faculty SEI-BP 227/118 Mostaganem 27000, Algeria.

Corresponding author email: kamel.benyettou@nhsm.edu.dz [1] and

djillali.bouagada@univ-mosta.dz[2] ,

Abstract

The objective of this work is to explore new extended necessary and sufficient conditions for the asymptotic stability and admissibility of two-dimensional fractional singular continuous-time systems described by the Roesser models, utilizing the Caputo derivative. We propose an LMI (Linear Matrix Inequality) approach to address this problem. The results obtained are compared with existing studies that test these conditions in the context of integer-order derivatives. To demonstrate the applicability and accuracy of the proposed method, several illustrative examples and simulations have been conducted.

Key words*: Fractional systems, Singular systems, Fractional Roesser models, Stability , Admissibility of two dimensional systems, Linear matrix inequality.*

1. INTRODUCTION

Many researchers have been drawn to two-dimensional systems in recent decades. They have attracted the attention of numerous researchers because they may be used for diverse purposes in modern circuit design, digital image or signal processing, biomechanics, physics, medicine and other fields.

Stability analysis on two-dimensional systems has been studied by a number of researchers, including Jury(1973), Sijlak(1975), Kaczorek(2009), Bouagada et al.(2011), Elosmani et al.(2021). The stability analysis of both multidimensional and two-dimensional systems has been a research question for many years. Due to its high robustness analysis and application in engineering fields like circuit theory, digital filtring.

In recent years, Kaczorek and Rogowski have introduced the singular fractional continuous Roesser models and their solutions using fundamental matrix in (2015), where they also demonstrate some of its applications. Furthermore, Marir et al.(2017) have recently investigated the admissibility problem for singular linear continuous-time fractional-order systems with $1 < \alpha \leq 2$.

Building upon this foundational work, we aim to extend our analysis in several key directions. Firstly, we will investigate the impact of varying fractional orders on the stability and performance of the system. Secondly, we plan to explore the use of alternative fractional derivatives, such as the

Riemann-Liouville and Grunwald-Letnikov derivatives, to examine if they offer any advantages or improvements over the Caputo derivative in this context.

Furthermore, we intend to develop more sophisticated LMI-based techniques that can handle higher-dimensional systems and more complex dynamic behaviors. This includes the integration of robust control strategies to enhance system resilience against uncertainties and external disturbances.

Additionally, our research will extend to the examination of time-varying and nonlinear fractional systems, broadening the scope of the current study. We will employ numerical methods and optimization techniques to derive more general solutions applicable to a wider range of systems.

Finally, we will apply our extended methods to practical engineering problems, such as signal processing, control of robotic systems, and biomedical engineering, to validate the theoretical findings and demonstrate real-world relevance. Through these efforts, we aim to contribute significantly to the field of fractional calculus and its applications in control theory and dynamic systems.

2. CONTENT

Let's us consider the 2D singular continuous time system described by the Roesser models

$$\begin{bmatrix} E_{11} & E_{12} \\ E_{21} & E_{22} \end{bmatrix} \begin{bmatrix} D_{t_1}^{\alpha} x^h(t_1,t_2) \\ D_{t_2}^{\beta} x^v(t_1,t_2) \end{bmatrix} = \begin{pmatrix} A_{11} & A_{12} \\ A_{21} & A_{22} \end{pmatrix} \begin{bmatrix} x^h(t_1,t_2) \\ x^v(t_1,t_2) \end{bmatrix} + \ + \begin{bmatrix} B^h \\ B^v \end{bmatrix} u(t_1,t_2)$$

Where $x^h(t_1,t_2) \in R^{n_1}$, $x^v(t_1,t_2) \in R^{n_2}$ are respectively the horizontal and the vertical state vectors, $0 < \alpha \leq 1$ and $0 < \beta \leq 1$, $E \in R^{n \times n}$ is the singular matrix of the system with $0 \leq rank(E) \leq 1$, $u(t_1,t_2) \in R^m$ is the input vector, $B^h \in R^{n_1 \times m}$, $B^v \in R^{n_2 \times m}$, $A_{11} \in R^{n_1 \times n_1}$, $A_{12} \in R^{n_1 \times n_2}$, $A_{21} \in R^{n_2 \times n_1}$, $A_2 \in R^{n_2 \times n_2}$ and $n_1 + n_2 = n$. The boundary conditions are $x^v(t_1,0)$ And $x^h(0,t_2)$.

A novel sufficient and necessary conditions for asymptotic stability and admissibility conditions using the LMI approach.

3. CONCLUSIONS

We have developed the requisite as well as sufficient conditions for the stability and admissibility of 2-D general singular fractional Roesser systems in this paper. A new approach has been suggested that involves the Kronecker product, characteristic polynomial and linear matrix inequality (LMI). In order to show the efficiency and versatility of our approach, we have numerically simulated and illustrated the results using an electrical circuit application. Our method demonstrates promise.

A STATISTICAL STUDY OF DIABETES PREVENTION RESEARCH: INSIGHTS INTO GLUCOMETER-GUIDED BIOMARKER PATTERNS

Ruxandra Ioana CIPU[1,2], Larisa UNGUREANU[1,3], Elena Corina CIPU[1,4]

[1]Centre for Research and Training in Innovative Techniques of Applied Mathematics in Engineering "Traian Lalescu" (CiTi), University Politehnica of Bucharest, Romania
[2] Faculty of Medical Engineering, University Politehnica of Bucharest
[3] Faculty of Energy Engineering, University Politehnica of Bucharest
[4]Department of Applied Mathematics, Faculty of Applied Sciences, University Politehnica of Bucharest

Corresponding author email: larisa.ungureanu@stud.energ.upb.ro

Abstract
This paper focuses on a statistical analysis of data performed on data sets from diabetes prevention research. Starting with aspects on people's health and their correlation with diabetes. Through examination of various health factors such as age, gender, BMI, hypertension, heart disease, and smoking history, alongside key biomarkers like blood glucose and haemoglobin A1C, the study uncovers correlations crucial for early detection and prevention strategies. The use of glucometer technology is being considered to highlight patterns of biomarkers that indicate the onset of diabetes. The device generally comprises a test strip for placing blood, a sensor for detecting the level of glucose in the sample, and an electronic display for presenting the results. Hypothesis testing, correlation analysis, regression analysis, and clustering techniques to examine several factors. Through the analysis of these characteristics, the objective is to identify patterns that could facilitate the classification of diabetes and improve the efficiency of its diagnosis. The knowledge obtained from this investigation has significant ramifications for the prevention and promotion of awareness of diabetes.

Key words*: statistical analysis, hypothesis testing, glucometer, diabetes mellitus, correlation, regression, clustering*

1. INTRODUCTION

This paper describes an exploratory data analysis conducted on datasets from diabetes preventive research. The analysis focuses on aspects pertaining to people's health and their correlation with diabetes. We utilize hypothesis testing, correlation analysis, regression analysis, and clustering techniques to examine several factors. The project explores the use of glucometer technology to reveal biomarker patterns that indicate the beginning of diabetes. The device generally comprises a test strip for blood placement, a sensor for glucose level detection in the sample, and an electronic display for presenting the results. [1]

Through examination of various health factors such as age, gender, BMI, hypertension, heart disease, and smoking history, alongside key biomarkers like blood glucose and haemoglobin A1C, the study uncovers correlations crucial for early detection and prevention strategies. Additionally, the paper explores the impact of BMI on diabetes diagnosis, shedding light on the role of body weight and composition in disease risk assessment. It employs electrochemical reactions to quantify the glucose concentration in the blood sample, yielding a digital reading for the user to understand. Precise blood glucose level forecasting is vital in predicting diabetes and establishing appropriate insulin dosages to regulate metabolism and prevent high or low blood sugar levels. Forecasting provides patients with valuable information to make informed decisions on the timing and dosage of insulin administration, hence minimizing the likelihood of problems.

2. CONTENT

Using statistics, we first highlight the usefulness of glucometer technology with its impact on managing diabetes effectively, by a structured approach: prevalence of diabetes**,** healthcare costs**,** impact of glucometer use (reductions in HbA1c levels and decreased risk of complications with frequent monitoring) patient outcomes (better quality of life, and increased life expectancy), cost-effectiveness, user satisfaction (accuracy, and reliability).

The purpose of statistical hypothesis testing is to decide which of the following hypotheses is true: the null hypothesis or the alternative hypothesis. Testing the alternative hypothesis:

$$H_1 : \theta \neq \theta_0 \qquad (1)$$

There are two types of errors that can occur during hypothesis testing: type I error (2), which is a false positive, rejecting a true null hypothesis and type II error (β), which is a false negative, failing to reject a false null hypothesis. Related to β is the power of the test (3). [2]

$$\alpha = P(reject\ H_0 / H_0\ is\ true) \quad (2)$$

$$1 - \beta = P(reject\ H_0 / H_1\ is\ true) \quad (3)$$

In Figure 1 a histogram compares blood glucose levels in diabetic and non-diabetic groups. A mixed area around 125-160 may suggest future prediabetes for some non-diabetic individuals.

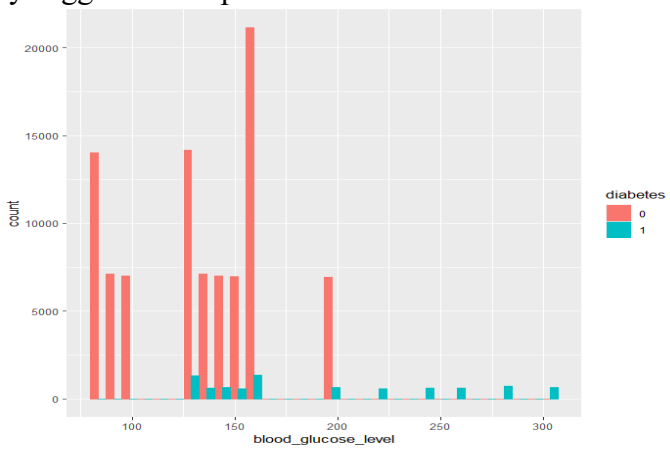

Fig. 1

Furthermore, we study advanced electronic glucometer technology, focusing on sensors and calibration algorithms to improve accuracy and data reliability.

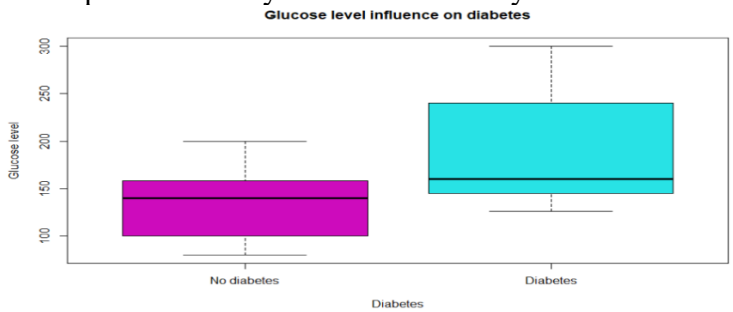

Fig.2

Finally, a data analysis seeks to develop a companion application to glucometers to provide users with useful information about their blood sugar trends and patterns. By combining statistical evidence of glucometer effectiveness with proposed improvements in electrical and electronic aspects, one can make a compelling case for the continued advancement and adoption of glucometer technology in diabetes management. [3]

3. CONCLUSION

Through the analysis of these characteristics, the objective is to identify patterns that could facilitate the classification of diabetes and improve the efficiency of its diagnosis. The findings emphasize the interrelationships among several elements, improving our comprehension of risk factors for diabetes and enabling proactive treatments to prevent its development, thus contributing to the overall effort to combat the diabetes epidemic.

REFERENCES

[1]. Alotaibi MM, Istepanian R, Philip N. A mobile diabetes management and educational system for type-2 diabetics in Saudi Arabia (SAED). Mhealth. 2016 Aug 24;2:33. doi: 10.21037/mhealth.2016.08.01. PMID: 28293606; PMCID: PMC5344130.

[2]. Prodan L., Turdean M.-S., 2018; Jimeno Martin A., 2023

[3]. Jonathan A. Gaev, 80 - Technology in Health Care, Editor(s): Joseph F Dyro, In Biomedical Engineering, Clinical Engineering Handbook, Academic Press, 2004, Pages 342-345, ISBN 9780122265709, https://doi.org/10.1016/B978-012226570-9/50088-0.

INTEGRITYINSIGHTAI: AUTHENTICITY DETECTION APPLICATION BASED ON FACIAL MOVEMENTS USING ARTIFICIAL INTELLIGENCE

Maria-Giulia GHEORGHIU[1,2], Iustinian-Costin TURCULEȚ[1,2], Eduard-Constantin GEORGESCU[1,2], Radu-Marian ORIȚĂ[1,2], Simona Mihaela BIBIC[1,4], Ioana Corina BOGDAN[3,4]

[1]National University of Science and Technology POLITEHNICA Bucharest, 313 Splaiul Independentei, District 6, Bucharest, Romania,
[2]Faculty of Electrical Engineering, Bucharest
[3]Department of Electronics and Computers, Transilvania University of Brasov, Romania
[4]Center for Research and Training in Innovative Techniques of Applied Mathematics in Engineering, 'Traian Lalescu' (CiTi), Bucharest, Romania

Corresponding author email: maria.gheorghiu@stud.electro.upb.ro

Abstract
IntegrityInsightAI is an innovative application designed to detect authenticity and truthfulness based on facial movements, using artificial intelligence (AI) and augmented reality (AR). It uses advanced AI algorithms to analyze micro-expressions and subtle facial movements, identifying patterns associated with a variety of emotions such as astonishment, fright, melancholy, joy. Real-time AR overlays provide visual and interactive feedback on facial analysis, highlighting areas of interest and concern during conversations. The application allows live monitoring of facial movements during interviews or interactions, generating detailed reports with information and probabilities of veracity, and providing customizable alarms and notifications based on detected anomalies. Its uses are varied, from law enforcement, where it assists in interrogations and verifying statements, to human resources, where it improves hiring processes by assessing the honesty of candidates, and social interactions, providing valuable information in negotiations, counseling and therapy. IntegrityInsightAI represents a significant advance in authenticity detection technology, providing a trusted tool for verifying truthfulness in various professional and personal contexts, transforming the way honesty is perceived and evaluated in human interactions.

Key words*: Artificial Intelligence (AI), Augmented Reality (AR), Social Interactions, convolutional neural networks.*

1. INTRODUCTION

In an increasingly interconnected and complex world, authentication and verification of veracity are becoming essential in many areas, from law enforcement and human resources to social interactions and negotiations. Over time, traditional lie detection methods based on behaviors and physiological cues have had their limitations, being often subjective and susceptible to human error. Integrating advanced artificial intelligence (AI) and augmented reality (AR) technologies, the IntegrityInsightAI application positions itself as a revolutionary solution in detecting authenticity based on facial movements. One of the most efficient algorithms that involves artificial intelligence are Convolutional Neural Networks (CNNs), due to their effectiveness in extracting features and identify faces in images for this type of identification. The purpose of this algorithm is to process an image given into a series of representation by increasing the abstraction level and decreasing the detail level.

2. CONTENT

Our application benefits of a large database that covers a large set of questions and answers, which result in a wide spectrum of emotions transposed in the form of a report. This way, one of its main usages would be in communication therapies among people in search of such a need.

IntegrityInsightAI combines artificial intelligence (AI) and augmented reality (AR) to detect authenticity and truthfulness based on facial movements. Using advanced deep learning algorithms, the app can analyze micro-expressions and subtle facial movements to identify patterns associated with sincerity and deception. Augmented reality enhances this analysis through real-time visual overlays, providing users with instant and interactive feedback, highlighting areas of interest and concern during conversations.

To develop the application, we implemented an advanced machine learning algorithm that uses histogram calculation, convolutional neural networks and a database to analyze and interpret facial movements in images. The data required for model training and validation were collected from various sources and were properly processed and labeled to ensure their quality and accuracy.

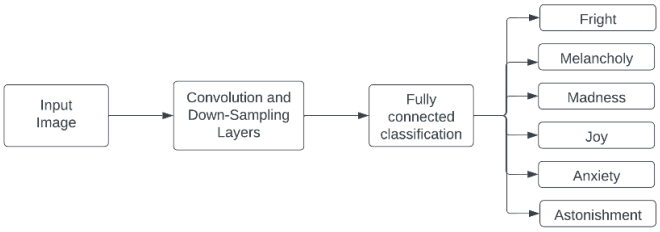

Fig. 1 Emotion Recognition Flow

The application of histograms and the fractal method of counting in the box within the analysis of facial movements allows a more detailed and precise interpretation of the data. Histograms are used to represent frequency distributions of facial movements, making it easier to identify anomalies and subtle variations in expressions. The box-counting method measures the complexity and irregularity of facial movements, providing insight into self-similarity structure and irregular patterns. These mathematical techniques contribute to a robust and nuanced assessment of authenticity, increasing the accuracy and reliability of detection.

IntegrityInsightAI is designed to be used in a wide range of scenarios such as law enforcement, where it can assist in questioning and verification of statements, human resources, where it improves the selection process of candidates by assessing their honesty, and in social interactions, providing support in negotiation, counseling and therapy. The user-friendly interface, compatibility with various devices including smartphones, tablets and AR glasses, and advanced data security through encryption ensure easy and protected use, meeting international privacy standards. By integrating AI and AR with advanced mathematical techniques such as histograms and fractal box counting, as well as using convolutional neural networks, the app represents a significant step forward in truthfulness detection technology, providing a reliable tool for assessing honesty and contributing to creating a safer and more transparent environment. Histograms are resulted by computing image gradient using Sobel filter, calculating gradient magnitude and orientation that are divided into cells. Foreach cell, we create Histogram of Gradients in the end we concatenate block histograms into final feature after normalizing histograms over blocks. The usage of fractals is integrated by the method called Box-Counting that involves the estimation of a geometric object, as well a dataset. Considering human face as a plan object, this tool approximates the outlines of facial elements as borders, that are modifying with every move recorded by the IntegrityInsightAI resulting in possible recognizable emotions.

3. CONCLUSIONS

In conclusion, IntegrityInsightAI represents a cutting-edge technology in truthfulness detection, providing a reliable tool for assessing honesty and creating a safer and more transparent environment. Through the advanced integration of artificial intelligence (AI) and augmented reality (AR), the app manages to accurately analyze micro-expressions and subtle facial movements, identifying patterns associated with sincerity and deception. The use of convolutional neural networks and the application of advanced mathematical techniques, such as histograms and the fractal box-counting method, allow a detailed and accurate interpretation of facial data.

INDOORPATH: INTERACTIVE MAP THAT IMPROVES ACCESSIBILITY AND EFFICIENCY OF ANY BUILDING

Maria-Giulia GHEORGHIU[1,2], Iustinian-Costin TURCULEȚ[1,2], Eduard-Constantin GEORGESCU[1,2], Radu-Marian ORIȚĂ[1,2], Simona Mihaela BIBIC[1,4], Ioana Corina BOGDAN[3,4]

[1]National University of Science and Technology POLITEHNICA Bucharest, 313 Splaiul Independentei, District 6, Bucharest, Romania,

[2]Faculty of Electrical Engineering, Bucharest

[3]Department of Electronics and Computers, Transilvania University of Brasov, Romania

[4]Center for Research and Training in Innovative Techniques of Applied Mathematics in Engineering, 'Traian Lalescu' (CiTi), Bucharest, Romania

Corresponding author email: maria.gheorghiu@stud.electro.upb.ro

Abstract

IndoorPath is an innovative indoor navigation application designed to provide users with accurate and efficient guidance in large and complex buildings. Using advanced location technologies such as the Browser's Geolocation API, Wi-Fi Positioning Systems (WPS), and the Global Positioning System (GPS), IndoorPath enables accurate determination of users' positions in real-time. The application leverages powerful mathematical algorithms, including Dijkstra's algorithm and the Bellman-Ford algorithm, to calculate the most efficient routes within buildings. These algorithms ensure that users receive the quickest and most reliable directions, even in the most intricate layouts. The map is available to users on various platforms such as web browsers and smartphone apps, and can also be used with smart electrical devices such as electrical panels installed inside the building. The ability to access the map from a smartphone or tablet makes it possible to access the map easily from anywhere, making it a more practical tool. By combining these technologies and algorithms, IndoorPath transforms the indoor navigation experience, providing an essential solution for visitors and commuters, reducing the time and stress associated with navigating complex indoor spaces.

Key words*: Dijkstra algorithm; Bellman-Ford algorithm; Geolocation application; Machine learning .*

1. INTRODUCTION

In today's digital age, accurate and efficient navigation is no longer limited to the outdoors. With the increasing complexity and size of modern buildings such as shopping malls, airports, hospitals and office buildings, there is an urgent need for indoor navigation solutions. IndoorPath positions itself as an innovative solution in this context, offering users accurate and real-time guidance inside these complex spaces.

IndoorPath addresses the challenges of indoor navigation, where GPS signals falter, by utilizing advanced technologies like Cellular Network Triangulation, Wi-Fi Positioning Systems (WPS), and IP Addressing for accurate user positioning. Employing mathematical algorithms such as Dijkstra's and Bellman-Ford, the app calculates efficient routes, helping users find classrooms, offices, and facilities quickly, thereby enhancing campus accessibility. Machine learning further optimizes navigation by analyzing historical data and traffic patterns to provide real-time, efficient routes. Accessible via web browsers, smartphone apps, and smart devices, IndoorPath offers a practical and reliable navigation solution within complex indoor environments.

2. CONTENT

Routing algorithms, such as Dijkstra and Bellman-Ford, are used to calculate the most efficient routes between points of interest, thus optimizing the time and effort required to reach the

destination. Mapping and modeling technologies and computer vision algorithms allow the creation and updating of indoor maps in real time.

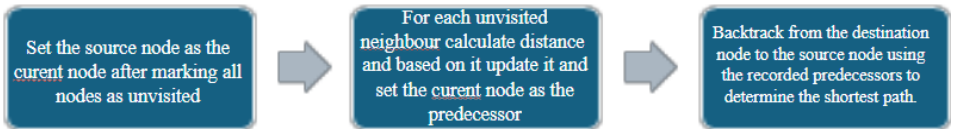

Fig.1 Dijkstra's algorith represented in steps

1. Interface and accessibility

The IndoorPath project aims to enhance accessibility by offering indoor maps on various platforms, including smartphone apps, web browsers, and smart electrical panels installed in buildings. This allows users to plan routes and explore the building from anywhere, making it a practical and indispensable tool for effective indoor navigation. Smart panels provide immediate guidance for those without mobile devices.

Fig.2 IndoorPath application interface

2. Technologies and methodology

- BROWSER GEOLOCATION API: The Browser Geolocation API allows the location of a device to be determined using various methods, including GPS, Wi-Fi, and mobile networks. This technology is used to provide accurate location data when users access the application through a web browser.

- WI-FI POSITIONING SYSTEMS (WPS): WPS uses Wi-Fi signals to determine the position of a device within a building. This method is effective in closed spaces, where GPS signals are poorly accessible. Wi-Fi access points are used to triangulate the exact position of users.

- GLOBAL POSITIONING SYSTEM (GPS): Although GPS is less effective inside buildings, it can be used in combination with other technologies to provide accurate positioning at the edge of buildings or in areas where the signal is strong enough.

3. Offline use

IndoorPath includes a database that stores the previous routes used by users, allowing access to this information in offline mode as well. This functionality ensures users can efficiently navigate complex buildings, even when internet connection is not available. By analyzing the stored routes, the application can provide optimized and personalized directions based on frequently traveled routes, thus improving the navigation experience and reducing search time.

3. CONCLUSIONS

IndoorPath is a comprehensive indoor navigation application that enhances user interaction with complex environments. It combines advanced location technologies with an intuitive interface, providing efficient and accurate orientation, making it standard in inland navigation.

National University of Science and Technology POLITEHNICA Bucharest
Faculty of Materials Science and Engineering

MRI processing techniques - a comparative study

Author:
Mihaela-Cristina STRIMTOREANU
Advisor:
PhD Lecturer Mariana-Mirela STANESCU

Nowadays, image processing is all around us, perhaps often without us even realizing it. Image, as a short definition, is the 2D or 3D representation of an object, a scene, a landscape, a person or any representation of the living world and beyond. Medical images, on the other hand, constitute a set of information of particular importance for doctors, physicians, clinicians and so on.

The role of improved medical imaging in diagnosing and treating patients is very important, requiring continuous advancements for higher accuracy. Good image quality can play an essential role in diagnosing pathologies and guiding surgical procedures. Recent advances have led to the development of various algorithms to enhance structural details and improve quality.

Magnetic Resonance Imaging (MRI) has evolved over the last 30 years from being a technique with great potential to becoming the earliest diagnostic investigation for many clinical problems. While this medical imaging application was initially limited to the neuraxis, it now covers all regions of the body. An expanded knowledge base has provided a better understanding of how it can best be used, either alone or in combination with other techniques, to increase diagnostic certainty.

In this study, we focus on image processing techniques for magnetic resonance imaging (MRI), particularly the Richardson-Lucy (RL) kernel estimation method and deconvolution algorithms, which iteratively refine images to reduce blurring and enhance details. Additionally, we explore Split Bregman (SB) and Constrained Spherical Deconvolution (CSD).

Mathematical Framework with MRI Considerations:

- Richardson-Lucy Deconvolution Algorithm

The RL algorithm iteratively refines the estimate of the original image \(I \) using the following update equation:

$$I_{k+1}(x,y) = I_k(x,y)\left(\frac{B(x,y)}{(I_k * P)(x,y)} * P^*(x,y)\right)$$

where:

- I_k is the current estimate of the image at iteration k,

- B is the observed blurred image,

- P is the point spread function (PSF),

- P^* is the flipped PSF (PSF rotated 180 degrees),

- / denotes element-wise division,

- * denotes the convolution operation.

In MRI, image intensity represents tissue properties. Negative values lack physical meaning. Therefore, the incorporate non-negativity constraint into the RL update step:

$$I_{k+1} = \max\left(0, I_k * \left(\frac{B}{I_k * P}\right) * P^*\right.$$

This ensures all elements in the estimated image remain non-negative, maintaining the physiological relevance of the processed image.

The Richardson-Lucy (RL) deconvolution method offers significant benefits such as improved image clarity by reducing blur and being relatively straightforward to implement. It's particularly suitable for low-noise conditions and doesn't require explicit regularization. However, RL is sensitive to noise, which can lead to noise amplification if not properly regularized. It often requires many iterations to converge and can be computationally expensive, especially for large images. Additionally, in high-noise scenarios, RL may introduce artifacts.

- Split Bregman Algorithm

The choice of regularization term R(I) in the SB algorithm significantly impacts the processed image. For cardiac MRI, we often seek to promote spatial smoothness while preserving sharp edges that delineate anatomical structures. The Total Variation (TV) norm, defined as the sum of the absolute values of image gradients, is well-suited for this purpose:

$$R(I) = \|\nabla I\|_1$$

Here, ∇I denotes the gradient of the image I. The SB algorithm updates become:

$$I_{k+1} = arg\ min_I(\|B - (I * P)\|^2 + \lambda\|\nabla I\|_1 + \beta\|I - U_k\|^2)$$

This formulation incorporates an L1-norm penalty on the image gradient, encouraging smoothness while preserving edges. The parameters λ and β control the trade-off between data fidelity, image smoothness, and the influence of the auxiliary variable, respectively. Solving this minimization problem often involves iterative optimization algorithms.

The Split Bregman (SB) algorithm is effective in handling images with both sharp edges and smooth regions, thanks to its Total Variation (TV) regularization which helps in preserving edges while reducing noise. It has good convergence properties and can often be faster than standard methods. Moreover, the SB algorithm's flexible framework allows it to be adapted to different types of regularization. However, it is more complex to implement due to the need for auxiliary variables and iterative solvers. The method is computationally intensive and requires careful tuning of regularization parameters (λ and β) to avoid over-smoothing or under-smoothing.

- Constrained Spherical Deconvolution (CSD)

Motion artifacts due to heart movement can significantly degrade image quality in cardiac MRI. CSD can be adapted to incorporate motion correction information. By incorporating a motion-compensated version of the PSF (PSF_m), the update formula becomes:

$$I_{k+1} = I_k * \frac{B * \overline{PSF_m}}{|PSF_m|^2 + \eta}$$

Here, PSF_m represents the motion-corrected PSF, often estimated using image registration techniques. This approach leverages the properties of spherical convolutions in the Fourier domain to achieve deconvolution while mitigating motion artifacts. The small constant η is added for numerical stability to prevent division by zero.

Constrained Spherical Deconvolution (CSD) is specifically designed for deconvolution in spherical coordinates, making it ideal for certain MRI applications such as diffusion MRI. It effectively incorporates motion correction, which is particularly beneficial for applications like brain tumor MRI, and can mitigate motion artifacts. CSD is capable of handling directional data, which enhances its suitability for specialized MRI tasks. Nevertheless, it has a complex mathematical framework that can be challenging to implement and requires accurate estimation of the Point Spread Function (PSF) and motion parameters. Furthermore, CSD has a high computational cost, particularly for 3D data, and is sensitive to the quality of the input data and initial estimates.

Performance Evaluation:

Using metrics like peak signal-to-noise ratio (PSNR) and structural similarity index (SSIM), we evaluate these algorithms. PSNR measures signal-to-noise ratio, while SSIM assesses image similarity. These metrics provide insights into algorithm effectiveness. Higher PSNR values indicate better image quality, and higher SSIM values suggest better structural similarity with the reference image.

Simulations show these methods can enhance image quality and detail. Advanced deconvolution techniques significantly improve MRI quality, aiding accurate diagnosis and effective treatment planning.

Conclusion:

The development of advanced image processing algorithms is essential for improving medical imaging quality. Methods like Richardson-Lucy deconvolution, Split Bregman, and Constrained Spherical Deconvolution significantly enhance image clarity and detail, crucial for accurate diagnosis and effective treatment planning, ultimately leading to better patient care. The incorporation of mathematical constraints and optimization techniques ensures that these algorithms produce clinically relevant results, paving the way for future innovations in medical imaging technology.

References

[1] Understanding Digital Image Processing Vipin Tyagi Department of Computer Science and Engineering Jaypee University of Engineering and Technology Raghogarh, Guna (MP), India, 2018

[2] Improved Classification of Blurred Images with Deep-Learning Networks Using Lucy-Richardson-Rosen Algorithm Amudhavel Jayavel, Shivasubramanian Gopinath, Praveen Periyasamy Angamuthu, Francis Gracy Arockiaraj , Andrei Bleahu , Agnes Pristy Ignatius Xavier, Daniel Smith , Molong Han , Ivan Slobozhan, Soon Hock Ng, Tomas Katkus, Aravind Simon John Francis Rajeswary, Rajesh Sharma, Saulius Juodkazis and Vijayakumar Anand, 2024

[3] Multi-tissue constrained spherical deconvolution for improved analysis of multi-shell diffusion MRI data; Ben Jeurissen, Jacques-Donald Tournier, Thijs Dho,
llander, Alan Connelly, Jan Sijbers, 2014

[4] Deconvolution of subcellular protrusion heterogeneity and the underlying actin regulator dynamics from live cell imaging; Chuangqi Wang, Hee June Choi, Sung-Jin Kim, Aesha Desai, Namgyu Lee, Dohoon Kim, Yongho Bae, Kwonmoo Lee, 2018

[5] Motion Deblurring for Light Fields; Donald G. Dansereau, Anders Eriksson and Jurgen Leitner, 2016

[6] Understanding Digital Image Processing; Vipin Tyagi, 2018

[7] Richardson–Lucy Deconvolution as a General Tool for Combining Images with Complementary Strengths; Dr. Maria Ingaramo, Dr. Andrew G. York, Eelco Hoogendoorn, Dr. Marten Postma, Dr. Hari Shroff, Dr. George H. Patterson, 2014

[8] Split Bregman method for Total Variation Denoising by Benjamin Tremoulheac, 2012

BETTI NUMBERS OF POWERS OF PATH IDEALS OF CYCLES

Silviu BĂLĂNESCU[1], Mircea CIMPOEAȘ[1] and Thanh VU[2]

[1]National University of Science and Technology Politehnica of Bucharest,
313 Splaiul Independentei, District 6, Bucharest, Romania

[2]Institute of Mathematics, VAST, 18 Hoang Quoc Viet, Hanoi, Vietnam

Corresponding author email: mircea.cimpoeas@imar.ro

Abstract

We let $J_{n,m} = (x_1 \cdots x_m, x_2 \cdots x_{m+1}, \dots, x_n x_1 \cdots x_{m-1})$ be m-path ideal of a cycle of length n over a polynomial ring $S = K[x_1, \dots, x_n]$. Let $t \geq 1$ be an integer. We show that $J^t_{,m}$ has linear free resolution and we give a precise formula for all its Betti numbers when m = n-1; n-2.

Key words*: Betti numbers, Monomial ideal, Path ideal, Cycle graph, Projective dimension, Regularity*

1. INTRODUCTION

Let $S = K[x_1, \dots, x_n]$ be a standard graded polynomial ring over a field KFor a finitely generated graded S-module M, the i-th Betti number of M, denoted by $\beta_i(M)$ is defined by

$$\beta_i(M) = \dim_K \mathrm{Tor}_i^S(K, M)$$

The Betti numbers of a homogeneous ideal I, among the most important invariants of I, capture many geometric properties of the projective variety defined by I. Given I, computing all of ist Betti numbers is always a challenging but interesting problem. We have very few classes of ideals for which we know all of their Betti numbers. When considering the powers of I, much less is known.

In this work, we not only give formulae for the Betti numbers of powers of some path ideals of cycles but also give a construction of their minimal free resolutions via the mapping cone constructions.

Let us now recall the main object of study in this work. The cycle (graph) of length n, where $n \geq 3$, is the (simple) graph C_n on the vertex set $V(C_n) = \{1,2, \dots, n\}$ and the edge set

$$E(C_n) = \{\{1,2\}, \dots, \{n-1, n\}, \{n, 1\}\}$$

For an integer m with $2 \leq m \leq n$, the m-path ideal of C_n is

$$J_{n,m} = (x_1 \cdots x_m, x_2 \cdots x_{m+1}, \dots, x_n x_1 \cdots x_{m-1})$$

Alilooee and Faridi [1] computed all the Betti numbers of path ideals of cycles. The problem of calculating all the Betti numbers of the powers of general path ideals of cycles is very complicated. In this work, we study the first two non-trivial instances of the problem m=n-1 and m=n-2, and we give precise formulas for Betti numbers of $J^t_{n,m}$.

This presentation is based on our preprint [2].

2. CONTENT

The main results of our paper are the following:

Theorem 1. For all n≥ 2 and t≥1, the ideal $J_{n,n-1}^t$ has linear free resolution and
$$\beta_i\left(J_{n,n-1}^t\right) = \binom{n-1}{i}\binom{n+t-i-1}{t-i}, \text{ for all i}\geq 0.$$

Theorem 2. For all n≥ 3 and t≥1, the ideal $J_{n,n-2}^t$ has linear free resolution and
(1) $pd\left(J_{n,n-2}^t\right) = min\{n-1, 2t\}$, if n is odd,
(2) $pd\left(J_{n,n-2}^t\right) = min\{n-2, 2t\}$, if n is even.

Theorem 3. Let $k \geq 1$ be an integer.
(1) For all $i \geq 0, t \geq 0$ *and* $n = 2k+1$ we have:
$$\boldsymbol{\beta_i\left(J_{n,n-2}^t\right)} = \sum_{\boldsymbol{j=0}}^{\left\lfloor \frac{\boldsymbol{i}}{\boldsymbol{2}} \right\rfloor} \binom{\boldsymbol{n}}{\boldsymbol{i-2j}}\binom{\boldsymbol{n+t-1-i+j}}{\boldsymbol{n-1}} - \sum_{\boldsymbol{j=0}}^{\left\lfloor \frac{\boldsymbol{i-1}}{\boldsymbol{2}} \right\rfloor} \binom{\boldsymbol{n}}{\boldsymbol{i-1-2j}}\binom{\boldsymbol{t+k-1-j}}{\boldsymbol{n-1}}$$
(2) For all $i \geq 0, t \geq 0$ *and* $n = 2k$ we have:
$$\boldsymbol{\beta_i\left(J_{n,n-2}^t\right)} = \sum_{\boldsymbol{j=0}}^{\left\lfloor \frac{\boldsymbol{i}}{\boldsymbol{2}} \right\rfloor} \binom{\boldsymbol{n}}{\boldsymbol{i-2j}}\binom{\boldsymbol{n+t-1-i+j}}{\boldsymbol{n-1}} - \sum_{\boldsymbol{j=0}}^{\left\lfloor \frac{\boldsymbol{i}}{\boldsymbol{2}} \right\rfloor} \binom{\boldsymbol{n}}{\boldsymbol{i-2j}}\binom{\boldsymbol{t+k-1-j}}{\boldsymbol{n-1}}$$

To prove the main results, we establish various Betti splittings involving powers of n-1 and n-2-path ideals of n-cycles. These Betti splittings give rise to recursive equations for the Betti numbers. In the case of the n-1-path ideal, we deduce a formula for the generating function of the Betti numbers. In the case of n-2-path ideal, to prove Theorem 3, we show that both sides satisfy the same set of recurrent relations and agree at the boundary terms.

3. CONCLUSIONS

We proved precise formulas for all the Betti numbers of $J_{n,n-1}^t$ and $J_{n,n-2}^t$, where n≥ 2 and t≥1. This allows us to deduce the projective dimension and the regularity of these ideals.

Bibliography

[1] A. Alilooee and S. Faridi, *Graded Betti numbers of path ideals of cycles and lines*, J. Algebra Appl. 17, no. 1, 1850011, 17pp.

[2] S. Balanescu, M. Cimpoeas, T. Vu, *Betti numbers of powers of path ideals of cycles*, arXiv: 2404.17880 (2024)

SEVERAL INEQUALITIES RELATED TO LINEAR AND BOUNDED OPERATORS

Miruna-Daniela ROȘU[1], Conf. Dr. Nicușor MINCULETE[2]

[1]Transilvania University of Brașov, Faculty of Mathematics and Informatics, Strada Iuliu Maniu 50, Brașov, România

[2]Transilvania University of Brașov, Faculty of Mathematics and Informatics, Strada Iuliu Maniu 50, Brașov, România

Corresponding author email: miruna.rosu@student.unitbv.ro

Abstract

In this paper we started from the central results of the article by Mohammed Al-Dolat and Imad Jaradat, "A refinement of the Cauchy-Schwarz inequality accompanied by new numerical radius upper bounds". The purpose of this paper was to generalize the results obtained by them and to obtain an improvement of those inequalities. We managed to do this by using in the proofs an improvement of the inequality of the means. This led to some better results for inequalities on certain powers of numerical radius of some operators. This aspect is concretely presented based on an example by taking a certain linear and bounded operator for which we determined the values of the terms that appear in the inequality.

Key words*: linear operator; bounded operator; numerical radius; inner product; norm; inequality.*

1. INTRODUCTION

Let H be a complex Hilbert space, with the inner product $\langle\cdot,\cdot\rangle$ and the associated norm $\|\cdot\|$. Let $\mathcal{B}(H)$ denotes the C^*-algebra of all bounded linear operators on the space H.

Lemma 1. (Cauchy-Schwarz Inequality)

$$|\langle x, y\rangle|^2 \leq \|x\|^2 \cdot \|y\|^2 \Leftrightarrow |\langle x, y\rangle| \leq \|x\| \cdot \|y\|, (\forall)\, x, y \in H$$

Three relevant concepts for linear and bounded operators are norm, numerical radius and Crawford number, which are defined below:

$$\|A\| \overset{def}{=} \sup_{\|x\|=1} \|Ax\|.$$
$$\omega(A) \overset{def}{=} \sup_{\|x\|=1} |\langle Ax, x\rangle|.$$
$$c(A) \overset{def}{=} \inf_{\|x\|=1} |\langle Ax, x\rangle|.$$

The next fundamental inequalities immediately follow from the above definitions:

$$\|Ax\| \leq \|A\| \cdot \|x\|, (\forall)\, A \in B(H), (\forall)\, x \in H$$
$$|\langle Ax, x\rangle| \leq \omega(A) \cdot \|x\|^2, (\forall)\, A \in B(H), (\forall)\, x \in H$$
$$|\langle Ax, x\rangle| \geq c(A) \cdot \|x\|^2, (\forall)\, A \in B(H), (\forall)\, x \in H$$
$$\sup_{\|x\|=\|y\|=1} |\langle Ax, y\rangle| = \|A\|, (\forall)\, A \in B(H)$$
$$\|Ax\|^p = \langle Ax, Ax\rangle^{\frac{p}{2}} = \sqrt{\langle A^*Ax, x\rangle}^p = \sqrt{\langle |A|^2 x, x\rangle}^p, (\forall)\, A \in B(H), (\forall)\, x \in H, (\forall)\, p \in \mathbb{R}.$$

Theorem 1. Let $A \in \mathcal{B}(H)$. Then we have the following double inequality: $\omega(A) \leq \|A\| \leq 2\omega(A)$, which also justifies the fact that $\omega(A)$ is an equivalent norm to $\|A\|$.

2. MAIN RESULTS

In this section we will present some important results obtained, which improve the inequalities given by Al-Dolat and Jaradat in their article.

Lemma 2. Let $a, b \in H$, $\alpha \geq 0, p \geq 1$. Then

$$|\langle a,b\rangle|^{2p} \leq \frac{1}{\alpha+1}\|a\|^p\|b\|^p|\langle a,b\rangle|^p + \frac{\alpha}{\alpha+1}\|a\|^{2p}\|b\|^{2p} \leq \|a\|^{2p}\|b\|^{2p}.$$

Lemma 3. (The generalization of the Buzano inequality) Let $a, b, e \in H$, $\|e\| = 1, \alpha \geq 0,\ p \geq 1$. Then

$$|\langle a,e\rangle\langle e,b\rangle|^{2p} \leq \frac{2\alpha+1}{2\alpha+2}\|a\|^{2p}\|b\|^{2p} + \frac{1}{2\alpha+2}\|a\|^p\|b\|^p|\langle a,b\rangle|^p.$$

Theorem 2. Let $A \in \mathcal{B}(H), \alpha \geq 0, p \geq 1$. Then

$$\omega^{4p}(A) \leq \frac{1}{2^p}\left(\frac{2\alpha+1}{2\alpha+2}\||A|^4+|A^*|^4\|^p + \frac{1}{2\alpha+2}\||A|^2+|A^*|^2\|^p\omega^p(A^2)\right) - \frac{2\alpha+1}{2\alpha+2} \cdot \frac{1}{2^p}c^{2p}(|A|^2-|A^*|^2).$$

Theorem 3. Let $A, B \in \mathcal{B}(H), \alpha \geq 0, p \geq 1$. Then

$$\omega^{2p}(B^*A) \leq \frac{1}{2^p}\left(\frac{1}{\alpha+1}\||A|^2+|B|^2\|^p\omega^p(B^*A) + \frac{\alpha}{\alpha+1}\||A|^4+|B|^4\|^p\right) - \frac{\alpha}{\alpha+1} \cdot \frac{1}{2^p}c^{2p}(|A|^2-|B|^2).$$

Theorem 4. Let $A \in \mathcal{B}(H), \alpha \in [0,1], p \geq 1$. Then

$$\omega^{2p}(A) \leq \frac{1}{2^p}\left(\alpha\||A|^2+|A^*|^2\|^p + (1-\alpha)\omega^p(A)\||A|+|A^*|\|^p\right) - \alpha\frac{1}{2^p}c^{2p}(|A|-|A^*|).$$

In the particular case when $p = 1$, we obtain the inequalities of the two authors mentioned above.

3. CONCLUSIONS

Considering the matrix operators $A, B \in \mathcal{B}(\mathbb{C}^2)$, where: $A = \begin{pmatrix}\sqrt{2} & 0\\ 0 & -\sqrt{2}\end{pmatrix}, B = \begin{pmatrix}1 & 0\\ 0 & -1\end{pmatrix}$, we obtain $\||A|^2+|B|^2\| = 3, \||A|^4+|B|^4\| = 5, \omega(B^*A) = \sqrt{2}$ and $c(|A|^2-|B|^2) = 1$.

According to Al-Dolat and Jaradat, the following inequality is true:

$$\omega^2(B^*A) \leq \frac{1}{2\alpha+2}\||A|^2+|B|^2\|\omega(B^*A) + \frac{\alpha}{2\alpha+2}\||A|^4+|B|^4\|.$$

which leads to:

$$\omega^2(B^*A) \leq \frac{1}{2\alpha+2}\cdot 3\sqrt{2} + \frac{\alpha}{2\alpha+2}\cdot 5 \Rightarrow \omega^{2p}(B^*A) \leq \left(\frac{1}{2\alpha+2}\cdot 3\sqrt{2} + \frac{\alpha}{2\alpha+2}\cdot 5\right)^p, \alpha \geq 0.$$

On the other hand, from Theorem 3 we have:

$$\omega^{2p}(B^*A) \leq \frac{1}{2^p}\left(\frac{1}{\alpha+1}\cdot 3^p\cdot\sqrt{2}^p + \frac{\alpha}{\alpha+1}\cdot 5^p\right) - \frac{1}{2^p}\cdot\frac{\alpha}{\alpha+1}, \alpha \geq 0.$$

By analyzing the graphs presented in the following figures, we can observe that for certain values of p, the inequality from Theorem 3 is better than the one's given by Al-Dolat and Jaradat.

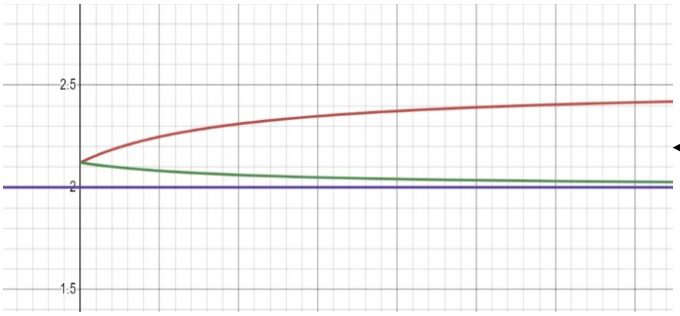

Author: Roșu M., Mathematical Software: Desmos

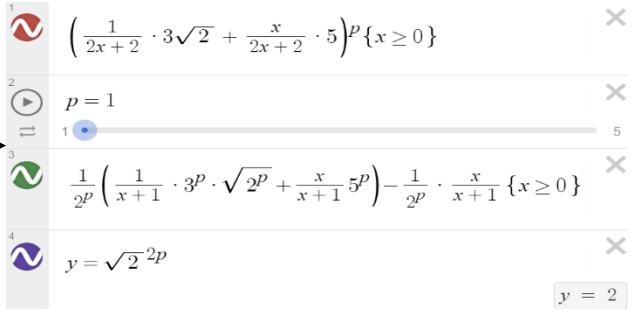

Author: Roșu M., Mathematical Software: Desmos

MARKOV CHAIN APPROACH FOR IOT PLANT WATERING SYSTEM

Alexandru-Laurențiu ZAHARIA[1,2], Alex-Ionuț MARINESCU[1,2], Miruna-Elena TĂLMĂCEL[1,2], Simona Mihaela BIBIC[1,3], Ana-Maria DUMITRESCU[1,2]

[1]National University of Science and Technology POLITEHNICA Bucharest, 313 Splaiul Independentei, District 6, Bucharest, Romania,

[2]Faculty of Electrical Engineering

[3]Center for Research and Training in Innovative Techniques of Applied Mathematics in Engineering, 'Traian Lalescu' (CiTi), Bucharest, Romania

Corresponding author email: miruna.talmacel@stud.electro.upb.ro

Abstract

Unprecedented population growth has led to soaring energy demands, triggering uncontrolled greenhouse gas emissions and consequent ozone layer depletion, altering the global ecosystem. While sensors alone can't solve pollution, they provide crucial data on atmospheric and soil conditions. This information aids in predicting weather changes vital for preserving biosystems, necessitating artificial interventions to prevent agricultural losses. Soil moisture sensors, coupled with pumps, automate watering by detecting soil dryness and adding water until optimal moisture levels are reached, although this solution primarily suits indoor plants. Integrating data from soil moisture, barometric, and temperature sensors enables accurate weather behaviour prediction, optimizing irrigation timing. Predicting climate change relies on Markov chains, stochastic models applied across various domains. Implementing this involves developing software for Arduino or Raspberry Pi to control water pumps based on sensor data. Additionally, an IoT system featuring Arduino Nano 33 IoT and Arduino IoT Cloud facilitates live data visualization, accessible globally via internet-connected devices, enhancing monitoring and intervention capabilities in agriculture and environmental management.

Key words*: climate change, Markov Chain, sensors, Arduino, IoT, real-time irrigation management*

1. INTRODUCTION

Climate change harms ecosystems, biodiversity, and planetary health by causing habitat loss, species decline, and ecosystem degradation, disrupting vital services like pollination and water purification. It also worsens other issues like deforestation and pollution, compounding global crises. Additionally, climate change heightens health risks, increasing heat-related illnesses and food insecurity, and affecting mental health. Addressing these challenges requires holistic strategies, including nature-based solutions, sustainable practices, carbon emission reductions, and fostering research and public awareness.

2. CONTENT

For each plant analyzed by the Arduino circuit, optimal temperature and humidity values, called the "safe zone," are determined to ensure long-term health. Humidity data is collected over weeks and divided into daily intervals, labeled YES if in the safe zone and NO otherwise. Accurate Markov chain predictions depend on these intervals.

Observations over seven days allow weekly predictions. Two scenarios are identified: a pessimistic one with a 33.4% chance of staying in the safe zone, and an optimistic one with a 66.6% chance. Temperature data is also collected to meet plant needs. Data comes from the UK Centre of Ecology and Hydrology for Hollin Hill, covering June 9-15, 2020, and May 20-26, 2018. The seventh day is excluded due to future uncertainties.

The MATLAB program takes as inputs the number of steps k and the probabilities read along lines which sum up to one by column.

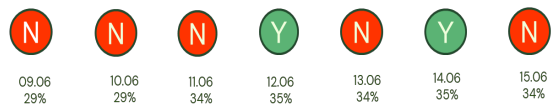

Fig. 1. Pessimistic scenario between 09 and 15 June 2020

Fig. 2. Optimistic scenario between 20 and 26 May 2018

Using the commands [T, D] = eig(P) at line 12, Pk=T*D^k*T1 from line 16 the transition matrix is diagonalized and the last line of code returns the desirable result: the probability distribution vector after k steps: Xk=Pk*X0. The diagonalized form provides a general formula for X_k (the state after k weeks) where k is a constant, not a variable. An optimized version of this code would return a warning message if the two probabilities are too spaced out after enough steps. This distance between values would be customizable by the user. The results for k going for 1 to 5 for the examples mentioned above and the data interpretation are depicted using IoT evaluation, see *Fig. 3* and *Fig. 4*.

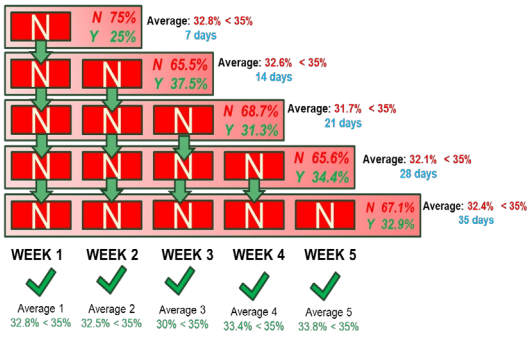

Fig. 3. Weekly prediction data analysis

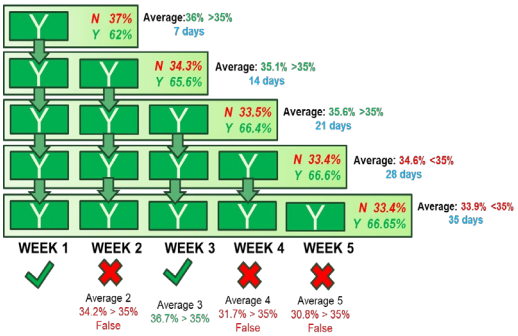

Fig. 4. Weekly prediction data analysis

3. CONCLUSIONS

This project aims to integrate soil moisture and temperature sensors into an autonomous system using IoT technology to provide statistical information on irrigation. Real-time data from sensors is analyzed with a Markov chain-based algorithm to predict future conditions and manage crop needs. Accurate surveillance is crucial for capturing critical stages like droughts and temperature shifts. Focusing on spring wheat from May to July, the project includes a database of plant requirements displayed on an OLED screen. Users can view current data and future estimates, enhancing agricultural efficiency and sustainability by anticipating plant needs and reducing resource use.

DESIGN AND IMPLEMENTATION OF A CABLE-DRIVEN ROBOT CARRYING A PLATFORM FOR OBJECT RECOGNITION AND 3D RECONSTRUCTION

Yassine HAJJEJ[2], Mohamed BOUTAYEB[1], Latifa BOUTAT-BADDAS[1]

[1]CRAN, UMR 7039, Université de Lorraine
[2]IUT de Longwy, 186, Rue de Lorraine,
54400 Cosnes et Romain, France

Corresponding author email: Latifa.baddas@univ-lorraine.fr
Corresponding author email: hajjej.yassine99@gmail.com

Abstract: *This project outlines the design and implementation of a cable-driven robot intended for object recognition and 3D reconstruction. It explores the feasibility of using cable-driven mechanisms in large workspaces where precise movements are necessary. The robot uses a camera system to identify and reconstruct objects using advanced AI algorithms. Cable-driven systems offer several advantages over traditional rigid robots, including high-speed movements, ability to cover large areas, and low cost and maintenance. The robot, utilizing four motors to maneuver a platform via cables, captures images which are processed in real-time to recognize and reconstruct objects within its operating space. These features make the robot adaptable for applications in industries like manufacturing for quality control, logistics for optimized storage solutions, and various research fields requiring detailed 3D modeling. The project combines innovative engineering with practical applications, aiming to transform industrial practices and enhance technological training and development.*

Key words *cable-driven robot, object recognition, 3D reconstruction, artificial intelligence, automation*

1. INTRODUCTION:

Industrial robots have experienced significant growth over the past seven decades. To address challenging, dangerous, manually slow, repetitive, and less precise tasks, their increasingly massive use significantly increases productivity while ensuring very high quality and reliability. Virtually all sectors are affected by this increased robotization, including the automotive, pharmaceutical, metallurgical, and logistics industries, ….

It is important to note that most robotized tasks involve a restricted workspace. Indeed, the majority of industrial robots are rigid articulated-arm robots, whose cost and maintenance increase exponentially when the workspace is large, ranging from a few cubic centimeters for small robots to several tens of cubic meters for the largest ones.
In this project, we will focus on the study and realization of a cable robot. This represents a special class of parallel robots where rigid links are replaced by flexible links due to the use of cables as a means of force transmission. This structure offers several advantages over rigid robots : very high-speed movements, large workspaces (which can reach several tens of cubic meters), the ability to move very heavy loads, as well as low cost and maintenance.

2. PROJECT OBJECTIVES:

The primary goal of this project is to create a cable-driven robot capable of transporting a camera system to capture images necessary for the recognition and 3D reconstruction of objects. By using four motors to wind and unwind cables, the robot's effector can move precisely within a three-dimensional space defined by the four pillars. This robot will be able to locate and recognize objects in its workspace and reconstruct them in 3D using artificial intelligence (AI) algorithms.

3. PROJECT DESCRIPTION :

The platform we aim to implement is represented by the figures below. The goal is to create a cable robot composed of 4 motors attached to 4 pillars. Each motor winds/unwinds a cable where the other end is attached to an effector. This effector carries a camera system for object recognition and 3D reconstruction. Through a winding/unwinding of the cables, the effector can move from point A to point B along a given trajectory. The effector can reach any point (in 3D) within the volume formed by the 4 pillars.
The images captured by the cameras during the effector's movement will be processed by an AI-based algorithm to locate and recognize objects within the workspace and reconstruct them in 3D. This system can also be used to detect and locate defects in very large parts.
The design and development of this platform present multiple scientific and technological challenges. Indeed, the dynamic behavior of the effector is described by complex nonlinear differential equations of large dimension with six degrees of freedom with very strong constraints on cable tensions to avoid their breakage. Moreover, it is important to develop an embedded, real-time system for the AI recognition algorithms.

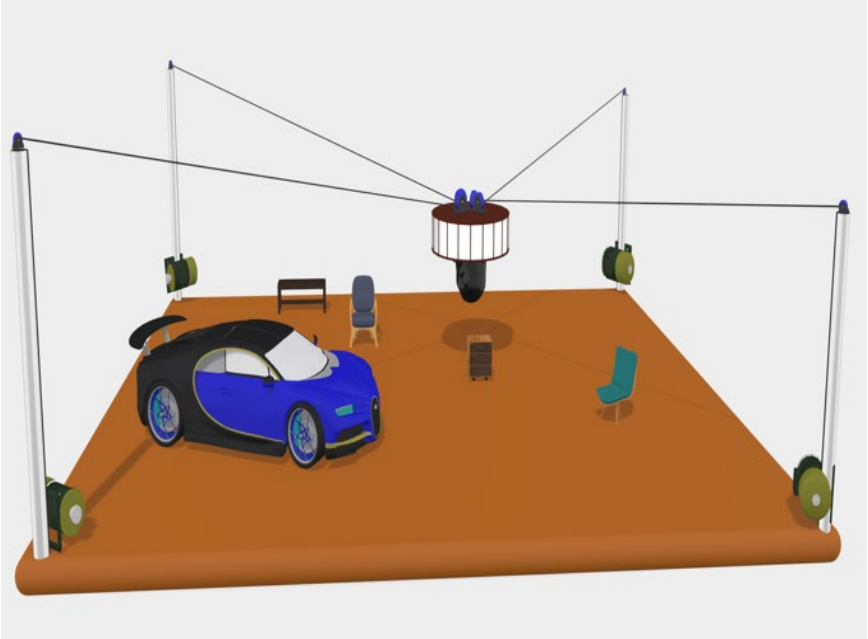

Figure 1: Robot Diagram

4. POTENTIAL APPLICATIONS:

This system can be used in various industrial and commercial fields:

- **Manufacturing Industry:** For detecting and locating defects in large parts, thus improving quality control.
- **Logistics and Warehousing:** For object recognition and handling, optimizing storage and retrieval operations.
- **Research and Development:** For applications requiring precise and detailed 3D reconstruction of objects, such as archaeology or medicine.

5. CONCLUSION:

This multidisciplinary project is an ambitious initiative aimed at developing cutting-edge technology for the recognition and 3D reconstruction of objects. By overcoming complex scientific and technological challenges, we hope to create an innovative and versatile cable-driven robot capable of transforming industrial practices and training a new generation of skilled and innovative engineers.

ON THE STABILITY OF 2D GENERAL ROESSER LYAPUNOV SYSTEMS

Mohammed Amine GHEZZAR[1], Djillali BOUAGADA[2], Kamel BENYETTOU[3], Mohammed CHADLI[4] and Paul VAN DOOREN[5]

[1,3]National Higher School of Mathematics, Scientific and Technology Hub of Sidi Abdellah, ACSY Team-Laboratory of Pure and Applied Mathematics (UMAB), P.O. Box 75, Algiers, Algeria.

[2] Abdelhamid Ibn Badis University Mostaganem, Department of Mathematics and Computer Science, ACSY Team-Laboratory of Pure and Applied Mathematics, Faculty SEI-BP 227/118 Mostaganem 27000, Algeria.

[4] Paris-Saclay University, IBISC Lab. UEVE, 0 rue du Pelvoux, 91020 Evry – Fran

[5] ICTEAM, Universit\'e Catholique de Louvain, Belgium, Av Lemaitre 4, B-1348 Louvain-la-Neuve. Belgium.

Corresponding author email: amine.ghezzar@nhsm.edu.dz[1] , djillali.bouagada@univ-mosta.dz[2] , kamel.benyettou@nhsm.edu.dz [3], mohammed.chadli@univ-evry.fr[4] , paul.vandooren@uclouvain.be[5]

Abstract

The investigation of stability problem for discrete-time and continuous-discrete-time Lyapunov systems in 2D is the main objective of this article. The basic idea is to come up with a number of new criteria capable of guaranteeing that the studied systems are asymptotically stable within the framework of linear matrix inequalities. We have proposed a universal approach based on the flexibility and robustness properties of the LMI method, which allows us solving both discrete and hybrid problems.

Key words*: 2D General Systems, Lyapunov Systems, Roesser System, Stability, LMI's..*

1. INTRODUCTION

The most popular models of two-dimensional linear systems are models introduced by Roesser, Fornasini-Marchecini. They have been generalized for singular 2D models by Kurek and Kaczorek has found many applications in control theory, modern circuit design and digital image processing, iterative learning, control synthesis or repetitive processes, image processing, seismological and geographical data processing, power transmission lines...etc.

The stability test is the most important and fundamental problem for design and analysis of systems. A number of stability test of 2D systems has been studied. Thus internal stability and asymptotic behaviour of 2D linear models were investigated by Valcher and asymptotic stability of 2D linear systems was investigated in servals works in literature.

An LMI approach to checking stability of 2D systems was proposed by Twardy, with generalizations to 2D positive systems by delays in Kaczorek. In sufficient LMI conditions for the internal stability of 2D singular linear systems with respect to acceptability and jump modes were given. Another LMI approach for the stability of the 2D state-space singular models was investigated by Bouagada and Van Dooren.

In the last few years, a new class of 1D and 2D discrete-time and continuous-time Lyapunov linear systems has been introduced. In the 2D Lyapunov systems described by the Roesser model, the independent variables are discrete and/or continuous and propagating in two different directions. Such models appear for example in circuit design, X-ray image enhancement.

In this work, the new general 2D discrete-time singular Lyapunov systems and also the 2D continuous-discrete-time singular Lyapunov systems has been considered. The main purpose of this paper is to present a sufficient conditions for asymptotic stability test in term of linear matrix inequalities (LMI's). An LMI's approach is used to produce highly significant new results on the stability analysis of these processes and to design the control schemes for these models.

2. CONTENT

Let's us consider the 2D singular continuous time system described by the Roesser models

$$\begin{bmatrix} E_{11} & E_{12} \\ E_{21} & E_{22} \end{bmatrix} \begin{bmatrix} \dfrac{\partial x^h(t_1,j)}{\partial t_1} \\ x^v(t_1,j+1) \end{bmatrix} = A_0 \begin{bmatrix} x^h(t_1,j) \\ x^v(t_1,j) \end{bmatrix} + \begin{bmatrix} x^h(t_1,j) \\ x^v(t_1,j) \end{bmatrix} A_1 + \begin{bmatrix} B^h \\ B^v \end{bmatrix} u(t_1,j)$$

Where $x^h(t_1,j) \in R^{n_1}$, $x^v(t_1,j) \in R^{n_2}$ are respectively the horizontal and the vertical state vectors, , $E \in R^{n\times n}$ is the singular matrix of the system with $0 \leq rank(E) \leq 1$, $u(t_1,j) \in R^m$ is the input vector, $B^h \in R^{n_1\times m}$, $B^v \in R^{n_2\times m}$, $A_0 \in R^{n\ \times n}$, $A_1 \in R^{n\ \times n}$. The boundary conditions are $x^v(t_1,0)$
And $x^h(0,t_2)$.

A novel sufficient and necessary conditions for asymptotic stability and admissibility is proposed and solved using the LMI approach.

3. CONCLUSIONS

In this paper, sufficient conditions for 2D general Lyapunov Roesser systems are derived to guarantee asymptotic stability. We have developed new test of stability for 2D discrete and continuous-discrete systems. An LMI approach is then described. In this case all obtained LMI's have at most dimension $2n^2 \times 2n^2$.

Existence of Initial Value Problem for Impulsive Fractional q-Difference Equations in Banach Space

Nadia Allouch and Samira Hamani

Laboratory of Pure and Applied Mathematics
University of Mostaganem
B.P. 227, 27000, Mostaganem, Algeria
Email : nadia.allouch.etu@univ-mosta.dz, hamani_samira@yahoo.fr

Abstract

In this work, we discuss the existence of solutions to the initial value problem for impulsive fractional q-difference equations in Banach space involving the Caputo's fractional q-derivative. Our result is based on Mönch's fixed point theorem combined with the technique of Kuratowski's measure of noncompactness. Finally, an example is given to illustrate the effectiveness of our result.
Key Words and Phrases: Initial value problem; Fractional q-difference equations; Caputo fractional q-derivative; Kuratowski's measure of noncompactness; Mönch's fixed point theorem.

1 Introduction

Fractional q-difference calculus is a fundamental branch in mathematical analysis that generalizes the notions of q-derivation and q-integration to arbitrary orders. Its origins date back to the late 1960s thanks to the contributions of Al-Salam [11] and Agarwal [4], who proposed and developed fractional q-calculus. Since then, much work has appeared on the theory of fractional q-calculus, due to its application in modeling phenomena in many areas of science and engineering. It has attracted wide attention from many scientists; for more information see the references [12, 18, 22, 23].

Moreover, fractional q-difference equations are also essential for modelling a large number of phenomena in a variety of fields, which are currently being studied by many academics in different domains such as technical sciences, engineering, physics and biomathematics. As a result, initial and boundary value problems for fractional q-difference equations have attracted the interest of several researchers, for example; see the works of Abbas *et al.* [1, 2, 3], Ahmed *et al.* [6, 7], Allouch *et al.* [8, 9, 10].

Recently, many authors discussed the existence of solutions to initial value problems for impulsive fractional q-difference equations involving the Caputo's fractional q-derivative, due to its importance and applications in various areas. This has made it a vital and active field of research in modern mathematics and applied sciences; see [5, 17, 21, 24] and the references therein.

This paper deals with the existence of solutions to the initial value problem for impulsive fractional q-difference equations in Banach space involving the Caputo's fractional q-derivative of the following form:

$$\begin{cases} ({}^{C}D_q^{\alpha} y)(t) = f(t, y(t)), \quad t \in J = [0,T],\ t \neq t_i,\ i = \overline{1,n},\ 1 < \alpha \leq 2, \\ \Delta y \mid_{t=ti} = \mathfrak{I}_i(y(t_i^-)), \quad i = \overline{1,n}, \\ \Delta y' \mid_{t=ti} = \overline{\mathfrak{I}}_i(y(t_i^-)), \quad i = \overline{1,n}, \\ y(0) = y_0, \quad y'(0) = y_0^*, \end{cases} \tag{1}$$

where $T > 0$, $q \in (0,1)$, ${}^{C}D_q^{\alpha}$ is the Caputo's fractional q-derivative, and $f : J \times \mathbb{E} \to \mathbb{E}$ is a continuous function, $\mathfrak{I}_i, \overline{\mathfrak{I}}_i : \mathbb{E} \to \mathbb{E}$, $i = \overline{1,n}$ are continuous functions, and $\mathbb{E}$ be a Banach space with norm $\|.\|_{\mathbb{E}}$, $y_0, y_0^* \in \mathbb{R}$, $0 = t_0 < t_1 < \cdots < t_n < t_{n+1} = T < \infty$, $\Delta y \mid_{t=t_i} = y(t^+) - y(t^-)$ and $\Delta y' \mid_{t=t_i} = y'(t^+) - y'(t^-)$, $y(t^+) = \lim_{h \longrightarrow 0^+} y(t_i + h)$ and $y(t^-) = \lim_{h \longrightarrow 0^-} y(t_i + h)$ represent the right and left limits of y at $t = t_i$, $i = \overline{1,n}$.

The paper is organized as follows: First, we introduce some basic concepts including definitions and properties of fractional q-calculus and some properties of the Kuratowski's measure of noncompactness. Next, we prove the existence of solutions to the initial value problem (1) using Mönch's fixed point theorem combined with Kuratowski's measure of noncompactness. Finally, we present an illustrative example.

2 Preliminaries

In this section, we begin by introducing preliminary facts that will be used in the rest of this work.

Now, let $(\mathbb{E}, \|.\|_{\mathbb{E}})$ be a Banach space and $J = [0,T]$ be an interval of $\mathbb{R}$, then we give some functional spaces [15, 19]:

- Consider $C(J, \mathbb{E})$ the Banach space of continuous functions $y : J \to \mathbb{E}$, equipped with the norm
$$\|y\|_{\mathbb{E}} = \sup_{t \in J} |y(t)|.$$
- Consider $L^{\infty}(J, \mathbb{R})$ the Banach space of measurable functions $y : J \to \mathbb{R}$ which are essentially bounded, with the norm
$$\|y\|_{L^{\infty}} = ess \sup_{t \in J} |y(t)| = \inf \{c > 0 \ : \ |y(t)| \leq c \text{ a.e } t \in J\}.$$
- Let $J_0 = [t_0, t_1]$, $J_1 = (t_1, t_2], \cdots, J_i = (t_i, t_{i+1}]$ where $i = \overline{1,n}$, we consider the Banach space
$$\mathbb{PC}(J, \mathbb{E}) = \left\{ y : J \to \mathbb{E} \mid y \in C(J_i, \mathbb{E}), \text{ and } y(t_i^+), y(t_i^-) \text{ exist, with } y(t_i^-) = y(t_i^+),\ i = \overline{1,n} \right\},$$
with the norm
$$\|y\|_{\mathbb{PC}} = \sup_{t \in J} |y(t)|.$$

Next, we review some notations, definitions of fractional q-calculus; for details, see references [12, 18, 22, 23].
For $a \in \mathbb{R}$ and $0 < q < 1$, we set

$$[a]_q = \frac{1-q^a}{1-q}.$$

The q-analogue of the power $(a-b)^{(n)}$ is expressed by

$$(a-b)^{(0)} = 1,\ (a-b)^{(n)} = \prod_{k=0}^{n-1}(a-bq^k),\ a,b \in \mathbb{R},\ n \in \mathbb{N}.$$

In general,

$$(a-b)^{(\alpha)} = a^\alpha \prod_{k=0}^{\infty}\left(\frac{a-bq^k}{a-bq^{k+\alpha}}\right),\ a,b,\alpha \in \mathbb{R}.$$

Note that if $b = 0$, then $a^{(\alpha)} = a^\alpha$.

Definition 2.1. *[18] The q-gamma function is defined by*

$$\Gamma_q(\alpha) = \frac{(1-q)^{(\alpha-1)}}{(1-q)^{\alpha-1}},\ \alpha \in \mathbb{R} - \{0,-1,-2,\ldots\}.$$

Notice that the q-gamma function satisfies $\Gamma_q(\alpha+1) = [\alpha]_q\Gamma_q(\alpha)$.

Definition 2.2. *[18] The q-derivative of order $n \in \mathbb{N}$ of a function $f : J \to \mathbb{R}$, is defined by*

$$(D_q^0 f)(t) = f(t),$$

and

$$(D_q f)(t) = (D_q^1 f)(t) = \frac{f(t)-f(qt)}{(1-q)t},\ t \neq 0,\ (D_q f)(0) = \lim_{t\to 0}(D_q f)(t),$$

$$(D_q^n f)(t) = (D_q^1 D_q^{n-1} f)(t),\ t \in J,\ n \in \{1,2,\ldots\}.$$

Set $J_t := \{tq^n : n \in \mathbb{N}\} \cup \{0\}$.

Definition 2.3. *[18] The q-integral of a function $f : J_t \to \mathbb{R}$, is defined by*

$$(I_q f)(t) = \int_0^t f(s)d_q s = \sum_{n=0}^{\infty} t(1-q)q^n f(tq^n),$$

provided that the series converges.

Notice that $(D_q I_q f)(t) = f(t)$, while if f is continuous at 0, then

$$(I_q D_q f)(t) = f(t) - f(0).$$

Definition 2.4. *[4] The Riemann-Liouville's fractional q-integral of order $\alpha \geq 0$ of a function $f : J \to \mathbb{R}$, is defined by defined by*

$$\begin{cases} \left(I_q^0 f\right)(x) = f(x); & \text{if } \alpha = 0, \\ \left(I_q^\alpha f\right)(x) = \frac{1}{\Gamma_q(\alpha)}\int_a^x (x-qt)^{(\alpha-1)} f(t)d_q t; & \text{if } \alpha > 0. \end{cases}$$

Note that for $\alpha = 1$, we have $(I_q^1 f)(t) = (I_q f)(t)$.

Lemma 2.5. *[22] For $\alpha \in \mathbb{R}_+$ and $\beta \in (-1, +\infty)$, we have*

$$(I_q^\alpha (t-a)^{(\beta)})(t) = \frac{\Gamma_q(\beta+1)}{\Gamma_q(\alpha+\beta+1)}(t-a)^{(\alpha+\beta)}, \ 0 < a < t < T.$$

In particular,

$$(I_q^\alpha 1)(t) = \frac{1}{\Gamma_q(\alpha+1)} t^{(\alpha)}.$$

Definition 2.6. *[23] The Riemann-Liouville's fractional q-derivative of order $\alpha \geq 0$ of a function $f : J \to \mathbb{R}$, is defined by*

$$\left({}^{RL}D_q^\alpha f\right)(x) = \begin{cases} f(x); & \text{if} \quad \alpha = 0, \\ \left(D_q^{[\alpha]} I_q^{[\alpha]-\alpha} f\right)(x); & \text{if} \quad \alpha > 0, \end{cases}$$

where $[\alpha]$ is the integer part of α.

Definition 2.7. *[23] The Caputo's fractional q-derivative of order $\alpha \geq 0$ of a function $f : J \to \mathbb{R}$, is defined by*

$$\left({}^{C}D_q^\alpha f\right)(x) = \begin{cases} f(x); & \text{if} \quad \alpha = 0, \\ \left(I_q^{[\alpha]-\alpha} D_q^{[\alpha]} f\right)(x); & \text{if} \quad \alpha > 0, \end{cases}$$

where $[\alpha]$ is the integer part of α.

Lemma 2.8. *[23] Let $\alpha, \beta \in \mathbb{R}_+$ and let f be a function defined on J. Then the next identities hold:*

(i) $(I_q^\alpha I_q^\beta f)(t) = (I_q^{\alpha+\beta} f)(t)$.

(ii) $({}^{RL}D_q^\alpha I_q^\alpha f)(t) = f(t)$.

Lemma 2.9. *[23] Let $\alpha \in \mathbb{R}_+$ and let f be a function defined on J. Then the following equality holds:*

$$(I_q^\alpha \ {}^{C}D_q^\alpha f)(t) = f(t) - \sum_{k=0}^{[\alpha]-1} \frac{t^k}{\Gamma_q(k+1)} (D_q^k f)(0).$$

In particular, if $\alpha \in (0, 1)$, then

$$(I_q^\alpha \ {}^{C}D_q^\alpha f)(t) = f(t) - f(0).$$

Following that, we introduce the basic concepts and certain properties of the Kuratowski's measure of non-compactness.

Definition 2.10. *[13] Let $\mathbb{E}$ be a Banach space and $\Omega_{\mathbb{E}}$ be the family of bounded subsets of $\mathbb{E}$. The Kuratowski's measure of non-compactness is the map $\mu : \Omega_{\mathbb{E}} \to \mathbb{R}_+$ defined as*

$$\mu(\mathcal{A}) = \inf\{\varepsilon > 0 : \mathcal{A} \subset \cup_{i=1}^m \mathcal{A}_i \text{ and } diam(\mathcal{A}_i) \leq \varepsilon\}; \text{ where } \mathcal{A} \in \Omega_{\mathbb{E}}.$$

Properties 2.11. *[13] The Kuratowski's measure of non-compactness has the following properties:*

(1) $\mu(\mathcal{A}) = 0 \Leftrightarrow \overline{\mathcal{A}}$ *is compact* ($\mathcal{A}$ *is relatively compact).*

(2) $\mu(\mathcal{A}) = \mu(\overline{\mathcal{A}})$.

(3) $\mathcal{A} \subseteq \mathcal{B} \Rightarrow \mu(\mathcal{A}) \leq \mu(\mathcal{B})$.

(4) $\mu(\mathcal{A} + \mathcal{B}) \leq \mu(\mathcal{A}) + \mu(\mathcal{B})$.

(5) $\mu(\gamma\mathcal{A}) = |\gamma|\mu(\mathcal{A}),\ \gamma \in \mathbb{R}$.

(6) $\mu(conv\mathcal{A}) = \mu(\mathcal{A})$.

(7) $\mu(\mathcal{A} + x_0) = \mu(\mathcal{A}),$ *for every* $x_0 \in \mathbb{E}$.

Where $conv\mathcal{A}$ *and* $\overline{\mathcal{A}}$ *denote the convex hull and the closure of the bounded set* $\mathcal{A}$*, respectively.*

Definition 2.12. *[14] A map* $f : J \times \mathbb{E} \to \mathbb{E}$ *is said to be Carathéodory, if*

1. *The map* $t \to f(t, y)$ *is measurable for each* $y \in \mathbb{E}$,
2. *The map* $y \to f(t, y)$ *is continuous for almost each* $t \in J$.

Moreover, for a given set $\mathcal{V}$ of functions $v : J \to \mathbb{E}$ let us denote by

$$\begin{aligned} \mathcal{V}(t) &= \{v(t) : v \in \mathcal{V},\ t \in J, \\ \mathcal{V}(J) &= \{v(t) : v \in \mathcal{V},\ t \in J\}. \end{aligned}$$

Finally, we recall the fixed point theorem of Mönch and an essential lemma.

Theorem 2.13. *[20]* ***(Mönch)***
Let X *be a bounded, closed and convex subset of a Banach space* $\mathbb{E}$ *such that* $0 \in X$*, and let* $\mathcal{H}$ *a continuous mapping of* X *into* X*. If the implication*

$$\mathcal{V} = \overline{conv}\mathcal{H}(\mathcal{V}) \quad or \quad \mathcal{V} = \mathcal{H}(\mathcal{V}) \cup \{0\} \Rightarrow \mu(\mathcal{V}) = 0 \tag{2}$$

holds for every subset $\mathcal{V}$ *of* X*, then* $\mathcal{H}$ *has a fixed point.*

Lemma 2.14. *[16] If* $\mathcal{V} \subset C(J = [0, T], \mathbb{E})$ *is a bounded and equi-continuous set, then*

1. *The function* $t \to \mu(\mathcal{V}(t))$ *is continuous on* J.
2. $\mu\left(\left\{\int_J y(t)dt \ :\ y \in \mathcal{V}\right\}\right) \leq \int_J \mu(\mathcal{V}(t))dt.$

3 Main Result

This section focuses on presenting the result of the existence of solutions to the intial value problem (1).

Let us start by defining what we mean by a solution of the problem (1).

Definition 3.1. *A function $y \in \mathbb{PC}(J,\mathbb{E})$ is said to be a solution of the problem (1) if y satisfies the equation $({}^{C}D_{q}^{\alpha}y)(t) = f(t,y(t))$ on J, and satisfies the following conditions:*

$$\begin{gathered}\Delta y\mid_{t=t_i} = \mathfrak{I}_i(y(t_i^-)), \quad i=\overline{1,n},\\ \Delta y'\mid_{t=t_i} = \overline{\mathfrak{I}}_i(y(t_i^-)), \quad i=\overline{1,n},\\ y(0)=y_0, \quad y'(0)=y_0^*,\end{gathered}$$

To prove our main result for problem (1), we need the following lemma:

Lemma 3.2. *Let $h: J\to\mathbb{E}$ be continuous. Then a function y is a solution for the following impulsive initial value problem:*

$$\begin{cases}({}^{C}D_{q}^{\alpha}y)(t)=h(t), \quad t\in J=[0,T],\ t\neq t_i,\ i=\overline{1,n},\ 1<\alpha\leq 2,\\ \Delta y\mid_{t=t_i}=\mathfrak{I}_i(y(t_i^-)), \quad i=\overline{1,n},\\ \Delta y'\mid_{t=t_i}=\overline{\mathfrak{I}}_i(y(t_i^-)), \quad i=\overline{1,n},\\ y(0)=y_0, \quad y'(0)=y_0^*,\end{cases}$$

Given by

$$y(t)=\begin{cases} y_0+y_0^*t+\int_0^t \frac{(t-qs)^{(\alpha-1)}}{\Gamma_q(\alpha)}h(s)d_qs; & if \quad t\in J_0=[0,t_1];\\ y_0+y_0^*t+\sum_{i=1}^n \mathfrak{I}_i(y(t_i^-))+\sum_{i=1}^n (t-t_i)\overline{\mathfrak{I}}_i(y(t_i^-)) & if \quad t\in J_i=(t_i,t_{i+1}],\\ +\sum_{i=1}^n\int_{t_{i-1}}^{t_i}\frac{(t_i-qs)^{(\alpha-1)}}{\Gamma_q(\alpha)}h(s)d_qs & \quad i=\overline{1,n}.\\ +\sum_{i=1}^n(t-t_i)\int_{t_{i-1}}^{t_i}\frac{(t_i-qs)^{(\alpha-2)}}{\Gamma_q(\alpha-1)}h(s)d_qs+\int_{t_i}^t\frac{(t-qs)^{(\alpha-1)}}{\Gamma_q(\alpha)}h(s)d_qs; & \end{cases}$$

Now, we introduce the following hypotheses:

(H_1) The function $f: J\times\mathbb{E}\to\mathbb{E}$ satisfies the Carathéodory conditions.

(H_2) There exists $p\in L^{\infty}(J,\mathbb{R}_+)$, such that for each $t\in J$ and each $y\in\mathbb{E}$, we have

$$\|f(t,y)\|\leq p(t)\|y\|.$$

(H_3) There exist constants $k,k^*>0$, such that for each $y\in\mathbb{E}$, we have

$$\|\mathfrak{I}_i(y)\|\leq k\|y\| \quad \text{and} \quad \|\overline{\mathfrak{I}}_i(y)\|\leq k^*\|y\|, \quad \text{for} \quad i=\overline{1,n}.$$

(H_4) For each $t\in J$ and each bounded set $\mathcal{A}\subset\mathbb{E}$, we have

$$\mu(f(t,\mathcal{A}))\leq p(t)\mu(\mathcal{A}).$$

(H_5) For each bounded set $\mathcal{A}\subset\mathbb{E}$, we have

$$\mu(\mathfrak{I}_i(\mathcal{A}))\leq k\mu(\mathcal{A}) \quad \text{and} \quad \mu(\overline{\mathfrak{I}}_i(A)))\leq k^*\mu(\mathcal{A}), \quad \text{for} \quad i=\overline{1,n}.$$

Following that, we prove the existence result for the intial value problem (1) by using Mönch's fixed point theorem.

Theorem 3.3. *Assume that the hypotheses (H_1)-(H_2)-(H_3) and (H_4)-(H_5) are satisfied. If*

$$n(k+k^*T)+\|p\|_{L^\infty}\left(\frac{nT^{(\alpha)}}{\Gamma_q(\alpha)}+(n+1)\frac{T^{(\alpha)}}{\Gamma_q(\alpha+1)}\right)<1. \tag{3}$$

Then, the initial value problem (1) has at least one solution on J.

Proof. Firstly, we transform the problem (1) into a fixed point problem and we consider the operator

$$\mathcal{H}:\mathbb{PC}(J,\mathbb{E})\longrightarrow\mathbb{PC}(J,\mathbb{E})$$

Defined by

$$\begin{aligned}(\mathcal{H}y)(t) &= y_0+y_0^*t+\sum_{i=1}^{n}\mathfrak{I}_i(y(t_i^-))+\sum_{i=1}^{n}(t-t_i)\overline{\mathfrak{I}}_i(y(t_i^-))+\sum_{i=1}^{n}\int_{t_{i-1}}^{t_i}\frac{(t_i-qs)^{(\alpha-1)}}{\Gamma_q(\alpha)}f(s,y(s))d_qs\\ &\quad+\sum_{i=1}^{n}(t-t_i)\int_{t_{i-1}}^{t_i}\frac{(t_i-qs)^{(\alpha-2)}}{\Gamma_q(\alpha-1)}f(s,y(s))d_qs+\int_{t_i}^{t}\frac{(t-qs)^{(\alpha-1)}}{\Gamma_q(\alpha)}f(s,y(s))d_qs,\\ &\quad t\in J_i=(t_i,t_{i+1}],\ \ i=\overline{1,n}.\end{aligned}$$

Clearly, the fixed points of the operator $\mathcal{H}$ are solutions of problem (1).
Let $\mathcal{R}>0$, we consider the set

$$\mathcal{D}=\{y\in\mathbb{PC}(J,\mathbb{E})\ :\ \|y\|_{\mathbb{E}}\leq\mathcal{R}\}. \tag{4}$$

Evidently, the subset $\mathcal{D}$ is bounded, closed and convex of $\mathbb{PC}(J,\mathbb{E})$.

Next, we will show that the operator $\mathcal{H}$ satisfies the conditions of Mönch's fixed point theorem. The proof will be presented in steps.
Step 1: *$\mathcal{H}$ is a continuous operator on $\mathbb{PC}(J,\mathbb{E})$.*
Let $\{y_m\}_{m\in\mathbb{N}}$ be a sequence such that $y_m\to y$ in $\mathbb{PC}(J,\mathbb{E})$. Then, for every $t\in J$, we have

$$\begin{aligned}|(\mathcal{H}y_m)(t)-(\mathcal{H}y)(t)| &\leq \sum_{i=1}^{n}\left|\mathfrak{I}_i(y_m(t_i^-))-\mathfrak{I}_i(y(t_i^-))\right|+\sum_{i=1}^{n}(t-t_i)\left|\overline{\mathfrak{I}}_i(y_m(t_i^-))-\overline{\mathfrak{I}}_i(y(t_i^-))\right|\\ &\quad+\sum_{i=1}^{n}\int_{t_{i-1}}^{t_i}\frac{(t_i-qs)^{(\alpha-1)}}{\Gamma_q(\alpha)}\left|f(s,y_m(s))-f(s,y(s))\right|d_qs+\sum_{i=1}^{n}(t-t_i)\\ &\quad\times\int_{t_{i-1}}^{t_i}\frac{(t_i-qs)^{(\alpha-2)}}{\Gamma_q(\alpha-1)}\left|f(s,y_m(s))-f(s,y(s))\right|d_qs+\int_{t_i}^{t}\frac{(t-qs)^{(\alpha-1)}}{\Gamma_q(\alpha)}\\ &\quad\times\left|f(s,y_m(s))-f(s,y(s))\right|d_qs.\end{aligned}$$

Let $\rho>0$ be such that

$$\|y_m\|_{\mathbb{E}}\leq\rho,\ \ \|y\|_{\mathbb{E}}\leq\rho.$$

From the hypothesis (H_2), we get

$$\|f(s,y_m(s))-f(s,y(s))\|_{\mathbb{E}}\leq 2\rho p(s):=\delta(s);\quad \delta(s)\in L^\infty(J,\mathbb{R}_+).$$

Since $\mathfrak{I}_i$, $\overline{\mathfrak{I}}_i$ are continuous functions and f satisfies the Carathéodory conditions, thanks to the Lebesgue's dominated convergence theorem, we find

$$\|\mathcal{H}(y_m) - \mathcal{H}(y)\|_{\mathbb{PC}} \to 0 \quad as \quad m \to \infty.$$

Consequently, $\mathcal{H}$ is a continuous operator on $\mathbb{PC}(J, \mathbb{E})$.
Step 2: *$\mathcal{H}$ maps $\mathcal{D}$ into $\mathcal{D}$.*
Let $y \in \mathcal{D}$ and using hypotheses (H_2)-(H_3), for every $t \in J$, we have

$$\begin{aligned}
|(\mathcal{H}y)(t)| &\leq |y_0| + |y_0^*|t + \sum_{i=1}^{n} \left|\mathfrak{I}_i(y(t_i^-))\right| + \sum_{i=1}^{n}(t-t_i)\left|\overline{\mathfrak{I}}_i(y(t_i^-))\right| + \sum_{i=1}^{n}\int_{t_{i-1}}^{t_i} \frac{(t_i - qs)^{(\alpha-1)}}{\Gamma_q(\alpha)} |f(s, y(s))|\, d_q s \\
&\quad + \sum_{i=1}^{n}(t-t_i)\int_{t_{i-1}}^{t_i} \frac{(t_i - qs)^{(\alpha-2)}}{\Gamma_q(\alpha-1)} |f(s, y(s))|\, d_q s + \int_{t_i}^{t} \frac{(t - qs)^{(\alpha-1)}}{\Gamma_q(\alpha)} |f(s, y(s))|\, d_q s, \\
&\leq |y_0| + |y_0^*|t + \sum_{i=1}^{n} k\|y\| + \sum_{i=1}^{n}(t-t_i)k^*\|y\|_{\mathbb{E}} + \sum_{i=1}^{n}\int_{t_{i-1}}^{t_i} \frac{(t_i - qs)^{(\alpha-1)}}{\Gamma_q(\alpha)} p(s)\|y\|_{\mathbb{E}} d_q s \\
&\quad + \sum_{i=1}^{n}(t-t_i)\int_{t_{i-1}}^{t_i} \frac{(t_i - qs)^{(\alpha-2)}}{\Gamma_q(\alpha-1)} p(s)\|y\|_{\mathbb{E}} d_q s + \int_{t_i}^{t} \frac{(t - qs)^{(\alpha-1)}}{\Gamma_q(\alpha)} p(s)\|y\|_{\mathbb{E}} d_q s.
\end{aligned}$$

By the set (4) and for each $t \in J$, we find

$$\begin{aligned}
\|\mathcal{H}(y)\|_{\mathbb{PC}} &\leq |y_0| + |y_0^*|T + nk\mathcal{R} + nk^*T\mathcal{R} + \frac{n\mathcal{R}T^{(\alpha)}}{\Gamma_q(\alpha+1)}\|p\|_{L^\infty} + \frac{n\mathcal{R}T^{(\alpha)}}{\Gamma_q(\alpha)}\|p\|_{L^\infty} + \frac{\mathcal{R}T^{(\alpha)}}{\Gamma_q(\alpha+1)}\|p\|_{L^\infty}, \\
&\leq \mathcal{R}.
\end{aligned}$$

Consequently,

$$\|\mathcal{H}(y)\|_{\mathbb{PC}} \leq \mathcal{R}.$$

Step 3: *$\mathcal{H}(\mathcal{D})$ is bounded and equi-continuous.*
According to Step 2, it's clear that $\mathcal{H}(\mathcal{D}) \subset \mathbb{PC}(J, \mathbb{E})$ is bounded.
Next, we prove that the equi-continuity of $\mathcal{H}(\mathcal{D})$. Let $y \in \mathcal{D}$ and let $t_1,\ t_2 \in J$ such that $t_1 < t_2$, we have

$$\begin{aligned}
|(\mathcal{H}y)(t_2) - (\mathcal{H}y)(t_1)| &= \Bigg| y_0^* t_2 + \sum_{i=1}^{n}(t_2 - t_i)\overline{\mathfrak{I}}_i(y(t_i^-)) + \sum_{i=1}^{n}(t_2 - t_i)\int_{t_{i-1}}^{t_i} \frac{(t_i - qs)^{(\alpha-2)}}{\Gamma_q(\alpha-1)} f(s, y(s)) d_q s \\
&\quad + \int_{t_i}^{t_2} \frac{(t_2 - qs)^{(\alpha-1)}}{\Gamma_q(\alpha)} f(s, y(s)) d_q s - y_0^* t_1 - \sum_{i=1}^{n}(t_1 - t_i)\overline{\mathfrak{I}}_i(y(t_i^-)) - \sum_{i=1}^{n}(t_1 - t_i) \\
&\quad \times \int_{t_{i-1}}^{t_i} \frac{(t_i - qs)^{(\alpha-2)}}{\Gamma_q(\alpha-1)} f(s, y(s)) d_q s - \int_{t_i}^{t_1} \frac{(t_1 - qs)^{(\alpha-1)}}{\Gamma_q(\alpha)} f(s, y(s)) d_q s \Bigg|, \\
&\leq (t_2 - t_1)|y_0^*| + \sum_{i=1}^{n}(t_2 - t_1)\left|\overline{\mathfrak{I}}_i(y(t_i^-))\right| + \sum_{i=1}^{n}(t_2 - t_1)\int_{t_{i-1}}^{t_i} \frac{(t_i - qs)^{(\alpha-2)}}{\Gamma_q(\alpha-1)} \\
&\quad \times |f(s, y(s))|\, d_q s + \int_{t_i}^{t_1} \frac{\left((t_2 - qs)^{(\alpha-1)} - (t_1 - qs)^{(\alpha-1)}\right)}{\Gamma_q(\alpha)} |f(s, y(s))|\, d_q s \\
&\quad + \int_{t_1}^{t_2} \frac{(t_2 - qs)^{(\alpha-1)}}{\Gamma_q(\alpha)} |f(s, y(s))|\, d_q s.
\end{aligned}$$

Applying the hypothesis (H_2)-(H_3) and by the set (4), we get

$$\begin{aligned}
|(\mathcal{H}z)(t_2)-(\mathcal{H}z)(t_1)| &\leq |y_0^*|(t_2-t_1)+\sum_{i=1}^{n}(t_2-t_1)k^*\|y\|_{\mathbb{E}}+\sum_{i=1}^{n}(t_2-t_1)\int_{t_{i-1}}^{t_i}\frac{(t_i-qs)^{(\alpha-2)}}{\Gamma_q(\alpha-1)}\\
&\quad\times p(s)\|y\|_{\mathbb{E}}d_qs+\int_{t_i}^{t_1}\frac{\left((t_2-qs)^{(\alpha-1)}-(t_1-qs)^{(\alpha-1)}\right)}{\Gamma_q(\alpha)}p(s)\|y\|_{\mathbb{E}}d_qs\\
&\quad+\int_{t_1}^{t_2}\frac{(t_2-qs)^{(\alpha-1)}}{\Gamma_q(\alpha)}p(s)\|y\|_{\mathbb{E}}d_qs,\\
&\leq |y_0^*|(t_2-t_1)+\mathcal{R}k^*\sum_{i=1}^{n}(t_2-t_1)+\mathcal{R}\|p\|_{L^\infty}\sum_{i=1}^{n}(t_2-t_1)\int_{t_{i-1}}^{t_i}\frac{(t_i-qs)^{(\alpha-2)}}{\Gamma_q(\alpha-1)}d_qs\\
&\quad+\mathcal{R}\|p\|_{L^\infty}\int_{t_i}^{t_1}\frac{\left((t_2-qs)^{(\alpha-1)}-(t_1-qs)^{(\alpha-1)}\right)}{\Gamma_q(\alpha)}d_qs+\mathcal{R}\|p\|_{L^\infty}\\
&\quad\times\int_{t_1}^{t_2}\frac{(t_2-qs)^{(\alpha-1)}}{\Gamma_q(\alpha)}d_qs.
\end{aligned}$$

After calculating the integrals, we obtain

$$\begin{aligned}
|(\mathcal{H}z)(t_2)-(\mathcal{H}z)(t_1)| &\leq |y_0^*|(t_2-t_1)+\mathcal{R}k^*\sum_{i=1}^{n}(t_2-t_1)+\frac{\mathcal{R}\|p\|_{L^\infty}}{\Gamma_q(\alpha)}\sum_{i=1}^{n}(t_2-t_1)(t_i-t_{i-1})^{(\alpha-1)}\\
&\quad+\frac{\mathcal{R}\|p\|_{L^\infty}}{\Gamma_q(\alpha+1)}\left((t_2-t_i)^{(\alpha)}-(t_1-t_i)^{(\alpha)}\right).
\end{aligned}$$

As $t_1\to t_2$, the inequality above's right-hand side tends to zero, i.e.

$$|(\mathcal{H}y)(t_2)-(\mathcal{H}y)(t_1)|\to 0 \quad as \quad t_1\to t_2.$$

Consequently, the equi-continuity of $\mathcal{H}(\mathcal{D})$. So, $\mathcal{H}(\mathcal{D})\subset\mathcal{D}$.

Finally, we prove that the implication (2) holds.
Let $\mathcal{V}$ be a subset of $\mathcal{D}$ such that $\mathcal{V}\subset\overline{conv}(\mathcal{H}(\mathcal{V}\cup\{0\})$. Since $\mathcal{V}$ is bounded and equi-continuous, and thus the function $t\to v(t)=\mu(\mathcal{V}(t))$ is continuous on J. Thank to the hypotheses (H_4)-(H_5), Lemma 2.14, and using the properties of the measure μ, then for every $t\in J$, we have

$$\begin{aligned}
v(t) &\leq \mu(\mathcal{H}(\mathcal{V})(t)\cup\{0\}),\\
&\leq \mu(\mathcal{H}(\mathcal{V})(t)),\\
&\leq \sum_{i=1}^{n}k\mu(\mathcal{V}(t))+\sum_{i=1}^{n}k^*(t-t_i)\mu(\mathcal{V}(t))+\sum_{i=1}^{n}\int_{t_{i-1}}^{t_i}\frac{(t_i-qs)^{(\alpha-1)}}{\Gamma_q(\alpha)}p(s)\mu(\mathcal{V}(s))d_qs\\
&\quad+\sum_{i=1}^{n}(t-t_i)\int_{t_{i-1}}^{t_i}\frac{(t_i-qs)^{(\alpha-2)}}{\Gamma_q(\alpha-1)}p(s)\mu(\mathcal{V}(s))d_qs+\int_{t_i}^{t}\frac{(t-qs)^{(\alpha-1)}}{\Gamma_q(\alpha)}p(s)\mu(\mathcal{V}(s))d_qs,\\
&\leq \sum_{i=1}^{n}k\|v\|_{\mathbb{E}}+\sum_{i=1}^{n}k^*(t-t_i)\|v\|_{\mathbb{E}}+\sum_{i=1}^{n}\int_{t_{i-1}}^{t_i}\frac{(t_i-qs)^{(\alpha-1)}}{\Gamma_q(\alpha)}\|p\|_{L^\infty}\|v\|_{\mathbb{E}}d_qs\\
&\quad+\sum_{i=1}^{n}(t-t_i)\int_{t_{i-1}}^{t_i}\frac{(t_i-qs)^{(\alpha-2)}}{\Gamma_q(\alpha-1)}\|p\|_{L^\infty}\|v\|_{\mathbb{E}}d_qs+\int_{t_i}^{t}\frac{(t-qs)^{(\alpha-1)}}{\Gamma_q(\alpha)}\|p\|_{L^\infty}\|v\|_{\mathbb{E}}d_qs.
\end{aligned}$$

Thus, for each $t \in J$, we find

$$\begin{aligned} v(t) &\leq nk\|v\|_{\mathbb{E}} + nk^*T\|v\|_{\mathbb{E}} + \frac{nT^{(\alpha)}}{\Gamma_q(\alpha+1)}\|p\|_{L^\infty}\|v\|_{\mathbb{E}} + \frac{nT^{(\alpha)}}{\Gamma_q(\alpha)}\|p\|_{L^\infty}\|v\|_{\mathbb{E}} \\ &\quad + \frac{T^{(\alpha)}}{\Gamma_q(\alpha+1)}\|p\|_{L^\infty}\|v\|_{\mathbb{E}}, \\ &\leq \|v\|_{\mathbb{E}}\left(n(k+k^*T) + \|p\|_{L^\infty}\left(\frac{nT^{(\alpha)}}{\Gamma_q(\alpha)} + (n+1)\frac{T^{(\alpha)}}{\Gamma_q(\alpha+1)}\right)\right). \end{aligned}$$

This implies that,

$$\|v\|_{\mathbb{E}}\left[1 - \left(n(k+k^*T) + \|p\|_{L^\infty}\left(\frac{nT^{(\alpha)}}{\Gamma_q(\alpha)} + (n+1)\frac{T^{(\alpha)}}{\Gamma_q(\alpha+1)}\right)\right)\right] \leq 0.$$

According to the condition (3), we obtain $\|v\|_{\mathbb{E}} = 0$, i.e. $v(t) = 0$ for every $t \in J$. So, $\mathcal{V}(t)$ is relatively compact in $\mathbb{E}$. In light of the theorem of Ascoli-Arzela, $\mathcal{V}$ is relatively compact in $\mathcal{D}$. Thanks to Theorem 2.13, we deduce that the operator $\mathcal{H}$ has a fixed point which represents a solution to the initial value problem (1). □

4 An Example

Let

$$\mathbb{E} = l^1 = \left\{(y_1, y_2, \cdots, y_n, \cdots) \ : \ \sum_{n=1}^{\infty} y_n < \infty\right\},$$

be our Banach space with the norm

$$\|y\|_{\mathbb{E}} = \sum_{n=1}^{\infty} |y_n|.$$

Following that, we examine the following initial value problem for impulsive fractional q-difference equations :

$$\begin{cases} ({}^{C}D_{\frac{3}{4}}^{\frac{3}{2}} y_n)(t) = \frac{\cos(y_n(t))}{\ln(5t+9)}, \ t \in J = [0,1], \ t \neq \frac{1}{2}, \ 1 < \alpha \leq 2, \\ \Delta y_n \mid_{t=\frac{1}{2}} = \frac{\sin(y_n(\frac{1}{2}^-))}{9}, \\ \Delta y_n' \mid_{t=\frac{1}{2}} = \frac{\cos(y_n(\frac{1}{2}^-))}{9}, \\ y_n(0) = 0, \quad y_n'(0) = 0. \end{cases} \tag{5}$$

where $\alpha = \frac{3}{2}$, $q = \frac{3}{4}$, $y_0 = y_0^* = 0$, $T = 1$, $n = 1$, and

$$f_n(t,y) = \frac{\cos(y_n)}{\ln(5t+9)}; \quad (t,y) \in J \times \mathbb{R}.$$

$$\mathfrak{I}_i(y) = \frac{\sin(y_n)}{9} \quad \textit{and} \quad \overline{\mathfrak{I}}_i(y) = \frac{\cos(y_n)}{9}; \quad y \in \mathbb{R}.$$

with

$$y = (y_1, y_2, \ldots, y_n, \ldots) \quad and \quad f = (f_1, f_2, \ldots, f_n, \ldots)$$

.

It is evident that the hypotheses (H_1)-(H_2) and (H_3) are satisfied, where

$$p(t) = \frac{1}{\ln(5t+9)}, \quad k = \frac{1}{9} \quad and \quad k^* = \frac{1}{9}.$$

Next, we will verify that the condition (3) holds with $n = 1$ and $T = 1$. In fact,

$$\begin{aligned} n(k + k^*T) + \|p\|_{L^\infty} \left(\frac{nT^{(\alpha)})}{\Gamma_q(\alpha)} + (n+1)\frac{T^{(\alpha)}}{\Gamma_q(\alpha+1)} \right) &= \left(\frac{1}{9} + \frac{1}{9}\right) + \frac{1}{ln(9)} \left(\frac{1}{\Gamma_{\frac{3}{4}}(\frac{3}{2})} + \frac{2}{\Gamma_{\frac{3}{4}}(\frac{5}{2})} \right) \\ &= 0.5423 < 1. \end{aligned}$$

Consequently, according to Theorem 3.3, the initial value problem (5) has at least one solution on $[0, 1]$.

5 Conclusion

In this contribution, we presented the existence result of solutions to the initial value problem for impulsive fractional q-difference equations in Banach space involving the Caputo's fractional q-derivative, by applying the fixed point theorem of Mönch's combined with Kuratowski's measure of noncompactness technique. To support our result, we have provide an illustrative example.

References

[1] S. Abbas, A. Bashir, M. Benchohra and S. Abdelkrim, *Fractional Difference, Differential Equations, and Inclusions: Analysis and Stability*, Morgan Kaufmann, (2024).

[2] S. Abbas, M. Benchohra, J. Henderson, *Existence and oscillation for coupled fractional q-difference systems*, Fract. Calc. Appl., **12** (1), (2021), 143-155.

[3] S. Abbas, M. Benchohra, N. Laledj and Y. Zhou, *Exictence and Ulam stability for implicit fractional q-difference equation*, Adv. Differ. Equ., **2019** (480), (2019), 1-12.

[4] R. Agarwal, *Certain fractional q-integrals and q-derivatives*, Proc. Camb. Philos. Soc., **66**, (1969).

[5] B. Ahmad, A. Alsaedi, S.K. Ntouyas, J. Tariboon and Faris Alzahrani, *Nonlocal boundary value problems for impulsive fractional q_k-difference equations*, Adv. Differ. Equ., **2016** (124), (2016), 1–26.

[6] B. Ahmad, *Boundary value problem for nonlinear third order q-difference equations*, Electron. J. Differ. Equ., **2011** (94), (2011), 1-7.

[7] B. Ahmad, S. K. Ntouyas and I. K. Purnaras, *Existence results for nonlocal boundary value problems of nonlinear fractional q-difference equations*, Adv. Differ. Equ., **2011** (140), (2012), 1-15.

[8] N. Allouch and S. Hamani, *Boundary Value Problem for Fractional q-Difference Equations in Banach Space*, Rocky Mountain J. Math., **53** (4), (2023), 1001-1010.

[9] N. Allouch, S.Hamani and J.R. Graef, *Boundary value problem for fractional q-difference equations with integral condition in Banach space*, Fractal Fract., **6** (94), (2022), 1-11.

[10] N. Allouch, S. Hamani and J. Henderson, *Boundary Value Problem for Fractional q-Difference Equations, Nonlinear Dynamics and Systems Theory*, **24** (2), (2024), 111-122.

[11] W. Al-Salam, *Some fractional q-integrals and q-derivatives*, Proc. Edinb. Math. Soc., **15** (2), (1966-1967), 135-140.

[12] M. H. Annaby and Z. S. Mansour, *q-Fractional Calculus and Equations*, Lecture Notes in Mathematics, **2056**, Springer, Heidelberg, (2012).

[13] J. Banaś and K. Goebel, *Measure of Noncompactness in Banach Spaces*, Institute of Mathematics Polish Academy of Sciences, (1979).

[14] R.F. Curtain and A.J. Pritchard, *Functional Analysis in Modern Applied Mathematics*, Academic Press INC., London, **Vol.132**, (1977).

[15] I. Fonseca, G. Leoni, *Modern Methods in the Calculus of Variations: L^p Spaces*, Springer Monographs in Mathematics, (2007).

[16] D. Guo, V. Lakshmikantham and X. Liu, *Nonlinear Integral Equations in Abstract Spaces, Mathematics and its Applications*, Springer US, **Vol.373**, (1996).

[17] M. Jiang, R. Huang, *Existence and stability results for impulsive fractional q-difference equation*, J. Appl. Math. Phys., **8** (7), (2020), 1413-1423.

[18] V. Kac and P. Cheung, Quantum calculus, Springer, New York, (2002).

[19] A.A. Kilbas, H.M. Srivastava and J.J. Trujillo, *Theory and Applications of Fractional Differential Equations*, North-Holland Mathematics Studies, Elsevier B.V., Amsterdam The Netherlands, **Vol.204**, (2006).

[20] H. Mönch, *Boundary Value Problem for Nonlinear Ordinary Differential Equations of Second Order in Banach Spaces*, Nonlinear Analysis, Theory, Methods & Applications, **4(5)**, (1980), 985–999.

[21] T. Nuntigrangjana, S. Putjuso, S.K. Ntouyas and J. Tariboon, *Impulsive quantum (p, q)-difference equations*, Adv. Differ. Equ., **2020** (98), (2020), 1-20.

[22] P. M. Rajkovic, S. D. Marinkovic and M. S. Stankovic, *Fractional integrals and derivatives in q-calculus*, Appl. Anal. Discrete Math., **1**, (2007), 311-323.

[23] P. M. Rajkovic, S. D. Marinkovic and M. S. Stankovic, *On q-analogues of Caputo derivative and Mittag-Leffler function*, Fract. Calc. Appl. Anal., **10** (4), (2007), 359-373.

[24] J. Tariboom, S.K. Ntouvas and R. Agarwal, *New concepts of fractional quantum calculus and applications to impulsive fractional q-difference equations*, Adv. Differ. Equ., **2015** (18), (2020), 1-19.

CONVEX FUNCTIONS AND APPLICATIONS

Natalia FĂRCAȘ[1]

[1]National College Vasile Lucaciu, 2 Culturii, Baia Mare, România

Corresponding author email: nathaliafarcas@gmail.com

Abstract

The study of the properties of convex functions in all aspects has proven to be extremely useful in important chapters of mathematics. The knowledge in this field is far too vast to be known by most students, and therefore, we considered it necessary to present in this paper a synthesis of results that students can invoke when solving problems where they recognize the existence of a convex function and refer to classical results. The aim of the paper is to investigate the theoretical aspects of concavity and convexity, to highlight their importance, and to identify problems where the notions of concavity and convexity are key to the solution. These notions are treated using both elementary methods and techniques of differential calculs. Besides a theoretical summary of theorem and examples of inequalities for convex functions, we have exemplified their use in several olympiad problems.

Key words*: concavity, convexity, applications*

1.INTRODUCTION

Concavity and convexity of functions provide us with a wide range of information about the properties of the investigated problem, representing an important chapter in mathematics due to its relevance in detecting innovative solutions for various types of problems. The first part of the study lay the basic properties, some definitions, proofs of theorems and some examples of convex functions, the theoretical foundations of these notions, which will be used in the last part of the study, dedicated to applications.

2. CONTENT

2.1. Theoretical summary

Definition 2.1.1. A function $f: I \to \square$, define on an interval $I \subseteq \square$, is said to be *convex* if for each two points $x_1, x_2 \in I$ and each two nonnegative real numbers λ_1, λ_2 satisfying $\lambda_1 + \lambda_2 = 1$, the following inequality is valid

$$f\left(\lambda_1 x_1 + \lambda_2 x_2\right) \le \lambda_1 f(x_1) + \lambda_2 f(x_2).$$

The function f is *concave* if the function $-f$ is convex, i.e., if the opposite inequality

$$f\left(\lambda_1 x_1 + \lambda_2 x_2\right) \ge \lambda_1 f(x_1) + \lambda_2 f(x_2)$$

always holds. If, in the previous inequalities (assuming $x_1 \neq x_2$), the equality takes place only in the case when $\lambda_1 = 0$ or $\lambda_2 = 0$, then the function f is said to be *strictly convex* (resp. *strictly concave*).

Observation 2.1.2. Geometrically, this say that the chord connecting the points $\left(x_1, f(x_1)\right)$ and $\left(x_2, f(x_2)\right)$ lies always above or on the curve *f*. Analogously, f is concave if the line segment always lies below or on the curve.

2.2. Famous algebraic inequalities that are proven using convex functions

Theorem 2.2.1. (*AM-GM Inequality*) Let $n \in \mathbb{N}, n \geq 2,$ and $x_1, x_2, ..., x_n > 0$. Then

$$\frac{x_1 + x_2 + ... + x_n}{n} \geq \sqrt[n]{x_1 x_2 \cdot ... \cdot x_n}.$$

2.3. Problems proposed in various competition or olympiads that are solved using convexity

Problem 2.3.1. Solve the equation

$$2^{\lg x} + 8 = (x-8)^{\frac{1}{\lg 2}}.$$

National Mathematics Olympiad, Romania, 2001

3. CONCLUSIONS

Convexity is a simple and natural notion which can be traced back to Archimedes. Convexity has a generalization for the case of multiple variables, a case used in some optimization problems and in control theory. For this reason, the convex function has been extended to Banach spaces and even beyond. Although convexity may seem like a simple concept, it is actually quite a complicated matter for those who have not studied mathematical analysis sufficiently. This study is intended to help students acquire more knowledge on convex and concave functions of single variables. The theory of convex functions is part of the general subject of convexity, which has a great impact on our everyday life through its numerous applications in industry, business, medicine, art, etc.

REFERENCES

[1] Gh. Rotariu, C*onvex functions: beyond the curriculum*, Dorohoi, 2015.
[2] A. Wayne Roberts, D. E. Varberg, C*onvex functions,* Academic Press New York And London 1973
[3] Gh. Boroica, V. Pop, N. Muşuroaia, F. Bojor, C. Heuberger, M*atematica de excelenţă pentru concursuri, olimpiade şi centre de excelenţă, Clasa a XI-a, Volumul II, Analiză Matematică*, Editura Paralela 45, 2014
[4] C. P. Niculescu, L. E. Person, *Convex functions and their applications* (*a contemporany approach*), Springer Science+Business Media, Inc., 2006
[5] A. Engel, *Problem-solving strategies*, Springer-Verlag New York, Inc., 1998
[6] T. Andreescu, B. Enescu, *Mathematical olympiad treasures*, Springer Science+Business Media, LLC, 2011
[7] P. Kwasi Sarpong, A. Owusu-Hemeng, J. Ackora-Prah3*, Applications of convex function and concave functions*, Dama International Journal Of Researchers (DIJR), 2018
[8] Rădulescu V, T.Rădulescu : *Problems in real analysis: advanced calculus on the real axis*, Springer, New York, 2009
[9] V. Nicula, *Analiză matematică pentru clasa a XI-a, teorie, exerciţii şi probleme*, Editura Teora, 1999
[10] *Inegalități*, Școala Virtuală A Tânărului Matematician, Http://Math.Ournet.Md
[11] F. Popovici, *Asupra inegalităţii lui Jensen*, Recreaţii Matematice, Nr. 1/2009
[12] D. Sorlecu (Vadana), *Convex functions with applications in variational calculus*, Bacău, 2015

THE SUM OF THE POWERS OF THE DISTANCES FROM A POINT TO THE VERTICES OF AN EQUILATERAL TRIANGLE

Nicolae MUȘUROIA

National College Gheorghe Șincai, 25 Gheorghe Șincai, Baia Mare, România

Corresponding author email: musuroianicolae@yahoo.com

Abstract

In this paper we will use complex numbers and the calculation of the powers of the distances from a point to the vertices of an equilateral triangle. We will analyze the following situations: the point is on the circle circumscribed to the equilateral triangle; the point is on the circle inscribed in the equilateral triangle; the point is on a concentric circle with the circle circumscribed circle to the equilateral triangle. In the end we will present four problems regarding this theme, one of these being proposed for the 2024 OJM (County Math Olympiad), tenth grade.

Key words: *geometry, geometry problems, complex numbers.*

1. INTRODUCTION

Let $A=\{A_1, A_2, \cdots, A_n\}$ be a finite set of points in plane or space (generally, in problems, they are the vertices of a plane polygon or polyhedron). For $\alpha > 0$ the function is considered: $f_\alpha : D \to \square$, $f_\alpha(M) = MA_1^\alpha + MA_2^\alpha + \cdots + MA_n^\alpha$, where $M \in D$, D being a fixed set from the plane or space (for example $D = \square^2$, $D = \square^3$, D is a line, D is a circle or a disk).

The problems we deal with refer to the set of values of the function f_α, to the determination of the values $\alpha \in \square$ for which f_α is constant on D.

In order to solve these problems, we have three approaches.

1) With the help of plane analytical geometry; 2) using vector calculus (especially for geometry in space problems); 3) using geometry in the complex plane.

In this paper, most of the problems addressed are presented in the complex plane.

2. CONTENT

Theorem 1. (page 75, [2])

If M is a variable point on the circumscribed circle of equilateral triangle ABC and $f_\alpha(M) = MA^\alpha + MB^\alpha + MC^\alpha$ is constant, then $\alpha \in \{0, 2, 4\}$

Proposition 1. (page 75, [2])

If M is a point on the circumscribed circle of the equilateral triangle ABC, then

$$MA^2 + MB^2 + MC^2 = 6R^2.$$

Proposition 2. (page 75, [2])

If M is a point on the circumscribed circle of the equilateral triangle ABC, then

$$MA^4 + MB^4 + MC^4 = 18R^4.$$

Theorem 2. If M is a point on the circle inscribed in the equilateral triangle ABC and $MA^\alpha + MB^\alpha + MC^\alpha = \text{constant}$, then α verifies the equation $\left(2\sqrt{7}\right)^\alpha - 2\left(\sqrt{3}\right)^\alpha - 3^\alpha + 1 = 0$.

Note: We find that $x = 0, x = 2$ and $x = 4$ verify equation (2). The demonstration is not elementary.

Proposition 3. If M is a point on the inscribed circle in the equilateral triangle ABC, then

$$MA^2 + MB^2 + MC^2 = 3\left(r^2 + R^2\right)$$

where r is the radius of the inscribed circle, and R is the radius of the circumscribed circle of the triangle ABC.

Proposition 4. If the point M is located on the circle inscribed in the equilateral triangle ABC then: $MA^4 + MB^4 + MC^4 = 3R^4 + 12R^2r^2 + 3r^4$.

We will generalize the results from the previous sentences.

Theorem 3. Consider the concentric circles $C(O, R_1)$, $C(O, R_2)$. If the equilateral triangle ABC is inscribed in the circle $C(O, R_1)$, then for any point M on the circle $C(O, R_2)$ we have:

$$(1)\quad MA^2 + MB^2 + MC^2 = 3\left(R_1^2 + R_2^2\right)$$

$$(2)\quad MA^4 + MB^4 + MC^4 = 3R_1^4 + 12R_1^2R_2^2 + 3R_2^4.$$

Note: For $R_1 = R_2 = R$, from (1) we obtain the result from Proposition 1, and from (2) the result from Proposition 2; for $R_1 = R, R_2 = r$, from (1) we obtain the result of Proposition 3, and from (2), we obtain the result of Proposition 4.

3. CONCLUSIONS

The results of Proposition 1 and Proposition 2 are known and represent the jewels of classic geometry. We extended these formulas for the case in which the point M is on a concentric circle with the circle circumscribed circle to the equilateral triangle. The use of complex numbers simplified the calculus a lot.

REFERENCES

[1] D. Andrica, C. Varga, D. Văcărețu, *Teme de geometrie*, Editura Promedia-Plus, Cluj Napoca, 1997.

[2] N. Bișboacă, *Teme complementare de geometrie*, Editura Paralela 45, 1999.

[3] I. Caius, *Asupra unei teoreme a lui Lagrange și extinderea ei*, G.M. 2/1987.

[4] N. Mușuroia, *Problema 2*, clasa a X-a, OJM 2024.

[5] N. Mușuroia, Gh. Boroica, V. Pop, D. Heuberger, F. Bojor, *Matematica de excelență, pentru concursuri, olimpiade și centre de excelență*, clasa a X-a, Editura Paralela 45.

[6] Gh. Țițeica, *Probleme de geometrie*, Ediția VI, Editura Tehnică, București, 1961.

[7] Colecția revistei *Gazeta Matematică*, seria B.

STUDY OF THE EIGENVALUES OF STURM-LIOUVILLE PROBLEMS UNDER PERTURBATIONS

Octavia-Maria HAPENCIUC[1], Prof. Univ.Dr. Marin MARIN[2]

[1]Transilvania University of Brasov, Bulevardul Eroilor 29, Brasov, Romania

[2]Transilvania University of Brasov, Bulevardul Eroilor 29, Brasov, Romania

Corresponding author email: codrinamaria09@gmail.com

Abstract

This research paper aims to investigate how the eigenvalues of Sturm-Liouville problems behave when the differential equation or coefficients are subjected to perturbations. Also, part of this paper is dedicated to analyse the changes in eigenvalues, when we modify the boundary conditions and the stability of the solutions regarding boundary conditions perturbations. Specifically, the study seeks to examine the continuity of eigenvalues concerning these perturbations.
In order to do so, we applied two fundamental methods for this study: operator theory and complex function theory. These methods are used either independently or in combination to gain a comprehensive understanding of the behaviour of solutions for the Sturm-Liouville problems studied.
The research involves theoretical analysis, numerical simulations using Python and MATLAB programming languages, and potential development of new mathematical techniques to characterize the behaviour of eigenvalues.

Key words*: eigenvalues, eigenfunctions, perturbations, potential function, differential equations.*

1. INTRODUCTION

We consider the Sturm-Liouville problem for the function $x(t)$ defined on the interval $[a, b]$, given by the differential equation:

$$(p(t)x')' + \big(q(t) + \lambda r(t)\big)x = 0 \tag{1}$$

where $p(t)$, $q(t)$, and $r(t)$ are known functions, and λ is the associated eigenvalue. Originally, the problem is accompanied by boundary conditions of the form:

$$\begin{aligned} \alpha_1 x(a) + \beta_1 x'(a) &= 0 \\ \alpha_2 x(b) + \beta_2 x'(b) &= 0 \end{aligned} \tag{2}$$

The methods used for studying these problems include:

1. **Operator Theory**: Using linear operators L defined by:

$$L[x] = -\frac{d}{dt}\left(p(t)\frac{d}{dt}x\right) + q(t)y \tag{3}$$

   with the domain defined by functions satisfying the boundary conditions.

2. **Complex Function Theory**: Analysing the functions and eigenvalues through techniques from complex function theory, such as using entire functions proprieties and well known theorems to investigate the behaviour of solutions and eigenvalues.

2. CONTENT

Starting from the results of P. Kosowski, we generalize these results for Sturm–Liouville problems of the form given by relations (1) and (2).

We consider the set

$$D = \{x \in L^2[a,b]: x, x' \text{ continuous and } x'' \in L^2[a,b], \\ \alpha_1 x(a) + \beta_1 x'(a) = 0, \alpha_2 x(b) + \beta_2 x'(b) = 0\}.$$

For $x \in D$, we consider the operators

$$\begin{cases} Lx = -x'' + q(t)x, \\ \tilde{L}x = -x'' + \tilde{q}(t)x, \end{cases} \tag{4}$$

where q and $\tilde{q}$ are in $C[a,b]$.

Let λ_k be the k-th eigenvalue of the first problem and $\tilde{\lambda}_k$ be the k-th eigenvalue of the second problem $k = 1,2,3, \ldots$.

Then the following theorem holds.

Theorem 2. *If* $||q - \tilde{q}||_\infty = \sup_{t\in[a,b]}|q(t) - \tilde{q}(t)| \leq \varepsilon$ *then* $\left|\lambda_k - \tilde{\lambda}_k\right| \leq \varepsilon$ *for all* $k = 1,2 \ldots$.

Corollary 1. *Suppose that the function* q *in the unperturbed problem in (4) depends on a parameter* p *with a Lipschitz constant* $C > 0$*, such that* $|q(t,s) - q(t,p)| \leq C|s - p|$*,* $t \in [a,b]$*,* $s, p \in \mathbb{R}$*. Then each* λ_k *depends continuously on* p *with the same Lipschitz constant.*

To simplify the discussion, it helps to assume that L is a positive operator, which, according to the Courant-Fischer-Poincare theorem, is equivalent to having a smallest eigenvalue $\lambda_1 > 0$. Let's denote by F the bounded symmetric operator $Fx = (q - \tilde{q})x$ defined for $x \in L_r^2(a,b)$. We start with a simple lemma, which gives us an estimate of the operator norm for the relative error.

Lemma 5. *Under the assumption above, the following inequality holds for each* $k = 1,2,3, \ldots$*:*

$$\left|\frac{\tilde{\lambda}_k - \lambda_k}{\lambda_k}\right| \leq \| L^{-1} \| \cdot \| F \|. \tag{5}$$

Theorem 3. *Under the assumption above, the following inequality holds for each* $k = 1,2,3, \ldots$*:*

$$\left|\frac{\tilde{\lambda}_k - \lambda_k}{\lambda_k}\right| < \rho(L^{-1}F), \tag{6}$$

where ρ *represents the spectral radius.*

3. CONCLUSIONS

By analysing the results presented above, we conclude that the best boundary for the estimated error of eigenvalues is given when we use the spectral radius of the operator $L^{-1}F$. This also gives us an open question, regarding if there is an even better boundary and how can we find it. The articles that we have studied give no improvement to this matter, but this is a future perspective that we would like to analyse.

Also, from numerical computations using MATLAB and Python, and by graphically representing the solutions of some practical and physical phenomena, we acquire that the theory that has been developed so far is applicable in various situations.

In this study, we also have sections dedicated to perturbations in boundary conditions, using both separated and coupled boundary conditions in order to get a better perspective on the subject. The theory here has been exemplified with practical applications.

The sections dedicated to continuous dependence of eigenvalues and continuous differentiability of eigenvalues give us insights of the stability of the problem when perturbing the coefficient functions.

A MILP MODEL THAT OPTIMISES THE SCHEDULING OF SHIFT PERSONNEL WORKING A 12-HOUR DAY/NIGHT SHIFT

Radu-Adrian MIHAI[1]

[1]National University of Science and Technology Politehnica of Bucharest, 313 Splaiul Independentei, District 6, Bucharest, Romania

Corresponding author email: mihai.raduadrian@gmail.com

Abstract

We present a MILP (mixed-integer linear programming) model that optimizes the scheduling of shift personnel working a 12-hour day/night shift. The objective of the model is to maximize the "satisfaction" of the personnel regarding the program, while maintaining the required operating conditions (e.g.: legal time off; minimum necessary personnel). Furthermore, using the resulting monthly scheduling, a more in-depth model can be described for day-by-day operations in order to indicate specific tasks during the shift, thus ensuring the optimal use of available personnel while maintaining an equitable repartition between the employees, all while meeting the operational requirements of the specific time interval.

Key words*: Mixed-Integer Linear Programming; Shift schedule; Air traffic management.*

1. INTRODUCTION

The model is separated in two parts, monthly optimization, and daily optimization.

Both the monthly and daily schedule optimization models use the standard MILP form, similar to the models presented in [1]:

$$\begin{aligned} \min_{\boldsymbol{x}} \quad & \boldsymbol{c}^t \cdot \boldsymbol{x} \\ \text{s.t.} \quad & \boldsymbol{A} \cdot \boldsymbol{x} \leq \boldsymbol{b} \\ & \boldsymbol{x} \in \{0,1\}^n \end{aligned}$$

Where $\boldsymbol{A} \in \mathbb{R}^{m \times n}$, $\boldsymbol{b} \in \mathbb{R}^m$, $\boldsymbol{c} \in \mathbb{R}^n$.

To utilize a standardized format for all the months of the year, each month will be represented as having 42 days, where the first day is a Monday. The days that are artificially added will be replaced with the corresponding days from the previous and following month, thus also ensuring a continuity between consecutive months. Furthermore, to represent the two shift options (day/night), each day will be divided in two 12-hour half-days. This results in each month having 84 half-days.

In the case of the monthly optimization, the goal is to assure the daily minimum required workforce when providing days off, while in the case of the daily optimization problem the objective is to maximize break times by merging tasks when the workload is low in order to assure that the personnel maintains maximum performance when the workload nears its capacity, in high intensity, high stress conditions. This is done according to an hourly demand prediction. To utilize a standardized format $\boldsymbol{x} \in \{0,1\}^{5 \cdot 6 \cdot n_e}$, where 5 represents the number of operational positions, 6 represents the number of time intervals and n_e represents the number of employees.

Both models are inspired by other research in shift schedule [2] or resource allocation [3].

2. CONTENT

2.1. Monthly optimization

2.1.1. Decision vector and cost vector

Considering the 84 half-day month, each element of the decision vector corresponding to a working half-day will be equal to 1, while the half-day that will not be worked will be assigned as equal to 0. For the MILP to take into consideration all the available employees, the decision vector will be $\boldsymbol{x} \in \{0,1\}^{84n_t}$, where n_t represents the total number of employees.
The cost vector has the same dimensions as the decision vector, $\boldsymbol{c} \in \mathbb{R}^{84n_t}$. To indicate a certain employee's preference for his set shift, the shift's working half-day elements will be equal to -2 and the non-working ones equal to 1. As an example, the cost could be $\boldsymbol{c} = (-2,1,1,-2,1,1,1,1,\dots)$.

2.1.2. Constraints
The linear constraint matrix can be divided in two matrixes:

$$\boldsymbol{A} = (\boldsymbol{A}_1, \boldsymbol{A}_2, \boldsymbol{A}_e)^t, \ \boldsymbol{b} = (\boldsymbol{b}_1, \boldsymbol{b}_2, \boldsymbol{b}_e)^t,$$

where $\boldsymbol{A}_1 \cdot \boldsymbol{x} \leq \boldsymbol{b}_1$ represents the condition that after working a 12-hour shift, a minimum 24-hour rest time is required before being scheduled again, $\boldsymbol{A}_2 \cdot \boldsymbol{x} \leq \boldsymbol{b}_2$ represents the condition that at least 3 persons need to be scheduled for day shift while at least 2 for night shift and $\boldsymbol{A}_E \cdot \boldsymbol{x} \leq \boldsymbol{b}_e$ represents the condition that assures specific days off, and where $\boldsymbol{A}_1 \in \mathbb{R}^{82n_t \times 84n_t}$, $\boldsymbol{A}_0 \in \mathbb{R}^{82\times 84}$, $\boldsymbol{b}_1 \in \mathbb{R}^{84\cdot n_t}$, $\boldsymbol{A}_2 \in \mathbb{R}^{84\times 84n_t}$, $\boldsymbol{b}_2 \in \mathbb{R}^{84\cdot n_t}$, $\boldsymbol{A}_e \in \mathbb{R}^{n_e \times 84n_t}$ and $\boldsymbol{b}_e \in \mathbb{R}^{n_e}$.
Here, $\boldsymbol{A}_e$ is the zero matrix when no vacation leave is scheduled and has the elements corresponding to desired paid leave days equal to 1, while $\boldsymbol{b}_e$ is a null vector. In this way, considering that the decision variables are binary, the equality constraints are included in the inequality constraints matrix $\boldsymbol{A}$.

2.2. Daily optimization

The daily optimization model uses the results of the monthly optimization as input to determine the number of employees working in a certain day. The model is similar in form to the monthly optimization one, but with different conditions imposing the constraints. The cost function in this case is $\boldsymbol{c} = (0,0,0,0,-1,0,0,0,0,-1,0,0,\dots)$, where the position of -1 is the operational position representing the "break" time.

3. CONCLUSIONS

The models are successful at arranging the available workforce in order to assure operational and legal requirements. In the cases when the monthly model is constrained by many vacation leaves, it finds unintuitive solutions that are not biased for or against any other employee. When no solution exists, the models are unfeasible.

Bibliography

[1] J. Bailey, Integrated days off and shift personnel scheduling. Computers & Industrial Engineering, 9(4), 395–404 (1985)
[2] S. Al-Yakoob, H. Sherali. Mixed-integer programming models for an employee scheduling problem with multiple shifts and work locations. Annals OR. 155. 119-142. (2007)
[3] J. Meyers, D. Morrison. Math Department Schedule Optimization. UW-L Journal of Undergraduate Research (2016)

Mathematical Modeling of Immune Dynamics in Chronic Myeloid Leukemia Therapy: Unraveling Allergic Reactions and T Cell Subset Modulation by Imatinib

Rawan ABDULLAH[1], Irina BADRALEXI[2], Laurance FAKIH[1] Andrei HALANAY[1]

[1] Department of Mathematics and Informatics, University Politehnica of Bucharest, 313 Splaiul Independentei, District 6, Bucharest, Romania

[2]Department of Mathematical Methods and Models, University Politehnica of Bucharest

Corresponding author email: rawan.b.abdullah@gmail.com

Abstract

This mathematical model explores the complex dynamics of the immune system during Chronic Myeloid Leukemia (CML) treatment with imatinib. It aims to shed light on the allergic reactions triggered by imatinib, particularly focusing on its effects on T helper (Th) cells and Treg cells. By integrating cellular interactions, drug pharmacokinetics, and immune responses, the model reveals the mechanisms behind the predominance of Th2 cells over Th1 and Treg cells, leading to allergic reactions. Utilizing a system of coupled delay differential equations, we investigate the interactions between healthy and leukemic cells, the impact of imatinib on T cell dynamics, and the development of allergic responses during CML therapy.

Key words*: Chronic Myeloid Leukemia, Imatinib Therapy, Mathematical Modeling, Immune System Dynamics, T Cell Subset Modulation, Allergic Reactions, Pharmacokinetics, Cellular Interactions, Th1, Th2, Treg Cells, Stem-like, Mature Cell Populations, Time Delays, Differential Equations, Pharmacodynamics.*

1. INTRODUCTION

Chronic Myeloid Leukemia (CML) presents unique treatment challenges, particularly with imatinib, a tyrosine kinase inhibitor effective in targeting leukemic cells. Imatinib's impact on the immune system introduces complex dynamics that require detailed examination. This model addresses these complexities by incorporating various cell populations, including stem-like and mature healthy and leukemic cells, as well as distinct T cell subsets.

The model explores the differentiation of naive T cells into effector states, considering positive growth and suppressive signals with time delays to reflect cellular processes. It also highlights how leukemic cells influence the evolution of CD8+ cytotoxic T-cells.

Th2 cells stimulate the production of IgE, while Th1 cells promote the production of IgG. Consequently, a transition from a Th2-dominated memory state to a Th1-dominated memory state indicates successful chemotherapy without the occurrence of allergic reactions. Induced regulatory T cells (Treg) play a crucial role in allergic reactions by releasing cytokines like IL-10 and TGF-β, capable of suppressing both Th1 and Th2 immune responses. Their differentiation from naive T cells follows a similar process as observed in other subsets.

A procedure known as drug desensitization assists patients in tolerating medications that previously triggered hypersensitive reactions. As reported in the literature, by employing a gradual desensitization approach, all

patients successfully tolerated a daily dose of 400 mg of imatinib, and the dosage of prednisolone was. This was one of the reasons that stimulated our research .

2. THE MATHEMATICAL MODEL

The model includes descriptions of healthy and leukemic cell behaviors, encompassing processes like self-renewal, differentiation, and mortality due to interactions with cytotoxic T-cells. Additionally, equations represent the dynamics of antigen-presenting cells (APCs), naive and mature T cell subsets (including CD4+ Th1, Th2, and Treg cells), as well as naive and mature CD8+ T cells. These equations reflect interactions such as activation by antigens, differentiation, and immune regulation. Furthermore, the model incorporates equations for imatinib pharmacokinetics, capturing drug dynamics within the body. Together, these components provide a comprehensive framework for simulating the complex cellular interactions involved in CML therapy.

Some equilibriq are calculated and their stability is studied both analytically and numerically. Near one equilibrium point, unstable, Th2 cells outnumber Th1 cells and both healthy and leukemic cell concentrations decline. A second equilibrium point shows a positive evolution with diminishing leukemic cells despite instability. A third equilibrium point demonstrates positive evolution with decreasing leukemic cells and rapid growth in Th1 cells, despite persistent allergic reactions due to high Th2 cell concentrations. A fourth equilibrium point exhibits favorable progressions, with diminishing leukemic cells and absence of allergic reactions, attributable to Th1 cell dominance over Th2 cells.

3. CONCLUSIONS

By using delayed-differential equations, the model captures the timing of biological processes and offers detailed insights into immune system behavior, including cell activation and responses. The model ensures positivity of solutions and conducts a local stability analysis for four equilibrium points that correspond to different patient outcomes.

Further research aims to explore parameter scenarios to better understand the correlation between drug concentration and allergic reaction onset, with implications for pharmacology and clinical medicine.

FOURIER SERIES FOR FUNCTIONS WITH COMPLEX VALUES. APPLICATIONS

Ruxandra-Mihaela CEAUȘU[1,2], Alexandru-Valentin AVRAM[1,2]
Romeo BERCIA[1,3]

[1]National University of Science and Technology POLITEHNICA Bucharest,
313 Splaiul Independentei, Bucharest, Romania

[2]Faculty of Applied Sciences, POLITEHNICA Bucharest
[3]Department of Applied Mathematics, Faculty of Applied Sciences, POLITEHNICA of Bucharest
Corresponding author email: ruxandra.ceausu@stud.fsa.upb.ro

Abstract
Fourier series are fundamental in mathematics for representing functions through simpler sine and cosine terms. This paper focuses on utilizing complex Fourier series to approximate complex-valued functions whose graphs are curves (parametrically defined). Therefore, a MATLAB program was developed. A Python script using the OpenCV2 library for precise extraction of curve points' coordinates from a picture was elaborated. As an application, another MATLAB program was created; it is capable of generating words by leveraging a custom contour library for letters. This demonstrates the practical application of Fourier series in digital image processing, pattern recognition, and typography.
Key words*: Fourier series, complex valued functions, numerical approximation, MATLAB, Python.*

1. INTRODUCTION

Fourier series are a fundamental tool in mathematics for analysing and representing periodic functions. By decomposing a complex waveform into a sum of simpler sine and cosine functions, Fourier series allow for a deeper understanding and manipulation of signals. This paper delves into the theoretical framework and practical implications of applying Fourier series to functions with complex values. These applications are crucial in fields such as signal processing, electrical engineering, and applied mathematics, where they provide powerful methods for analysing and reconstructing complex signals and waveforms.

2. CONTENT

The first focus is on the general form of Fourier series. In that scope, let us consider a continuous function, $f:[0,1]\to\mathbb{R}$, with $f(0)=f(1)$, or a continuous function $f:\mathbb{R}\to\mathbb{R}$ that has a period of T=1. The expansion of such a function into a Fourier series is:

$$f(t)=\frac{a_0}{2}+\sum_{n=1}^{\infty}(a_n\cos(2\pi nt)+b_n\sin(2\pi nt)),\ \forall\, t\in[0,1] \quad (1)$$

The a_n and b_n coefficients are defined:

$$a_n=2\int_0^1 f(t)\cos(2\pi nt)\,dt,\ \text{n}\geq 0 \quad (2)$$

$$b_n=2\int_0^1 f(t)\sin(2\pi nt)\,dt,\ \text{n}\geq 1 \quad (3)$$

Now, to get to the complex form of the Fourier series, we begin from Euler's formulas in order to rewrite the cosine and the sine: $\cos\theta=\frac{e^{i\theta}+e^{-i\theta}}{2}$, $\sin\theta=\frac{e^{i\theta}-e^{-i\theta}}{2i}$. By replacing them into (1):

$$f(t)=\frac{a_0}{2}+\sum_{n=1}^{\infty}\left(a_n\frac{e^{2\pi int}+e^{-2\pi int}}{2}+b_n\frac{e^{2\pi int}-e^{-2\pi int}}{2i}\right)$$

$$f(t)=\frac{a_0}{2}+\sum_{n=1}^{\infty}\left(\frac{a_n-ib_n}{2}e^{2\pi int}\right)+\sum_{n=1}^{\infty}\left(\frac{a_n+ib_n}{2}e^{-2\pi int}\right)$$

The following notations will be used so that we may reduce the Fourier series to its complex form: $c_0=\frac{a_0}{2}$, $c_n=\frac{a_n-ib_n}{2}$, $c_{-n}=\frac{a_n+ib_n}{2}$, $n\geq 1$:

$$f(t)=\sum_{-\infty}^{\infty}c_n e^{2\pi int} \quad (4)$$

Because the function that was considered has real values, each c_{-n} coefficient will equal to the conjugate of c_n, respectively: $c_{-n}=\overline{c_n}$ (5)

Let us now consider a function $f:[0,1]\to\mathbb{C}$, with its expansion into a complex Fourier series:

$$f(t)=\sum_{-\infty}^{\infty}c_n e^{2\pi int}=\ldots+c_{-2}e^{-2\cdot 2\pi it}+c_{-1}e^{-1\cdot 2\pi it}+c_0e^{0\cdot 2\pi it}+c_1e^{1\cdot 2\pi it}+c_2e^{2\cdot 2\pi it}+\ldots \quad (6)$$

Determining the c_n coefficients remains of importance now. We start by integrating the function on the [0,1] interval: $\int_0^1 f(t)dt=\int_0^1(\ldots+c_{-2}e^{-2\cdot 2\pi it}+c_{-1}e^{-1\cdot 2\pi it}+c_0e^{0\cdot 2\pi it}+c_1e^{1\cdot 2\pi it}+c_2e^{2\cdot 2\pi it}+\cdots)dt$

This represents the integral of an infinite sum and we switch the integral with the sum, obtaining:

$$\int_0^1 f(t)dt=\ldots+\int_0^1 c_{-1}e^{-1\cdot 2\pi it}dt+\int_0^1 c_0e^{0\cdot 2\pi it}dt+\int_0^1 c_1e^{1\cdot 2\pi it}dt+\int_0^1 c_2e^{2\cdot 2\pi it}dt+\ldots$$

Due to the exponentials, each of these separate integrals equals to zero, but one: the integral with the c_0 term, that actually equals to c_0.

To continue the process of determining the coefficients, we now integrate the function multiplied by $e^{-n\cdot 2\pi it}$ and we use the same procedure to switch the integral with the infinite sum:

$$\int_0^1 f(t)e^{-n\cdot 2\pi it}dt=\ldots+\int_0^1 c_{-1}e^{-(n+1)\cdot 2\pi it}dt+\int_0^1 c_0e^{-n\cdot 2\pi it}dt+\int_0^1 c_1e^{(1-n)\cdot 2\pi it}dt+\cdots+\int_0^1 c_ne^{0\cdot 2\pi it}dt+\ldots$$

For the same reason as before, all of the integrals that resulted equal to zero, but the one with the c_n term, which brings us to the conclusion that: $c_n=\int_0^1 f(t)e^{-2\pi int}dt$ (7)

Unlike the previous case, the c_{-n} coefficients won't necessarily equal to the conjugate of c_n, since the function has now complex values. Additionally, this function can be written using the following form:

$$f(t)=u+iv \quad (8)$$

The graphical representation is a curve in the complex plane and it has a parametric form:

$$\begin{cases}x=u(t)\\y=v(t)\end{cases},t\in[0,1] \quad (9)$$

Two aspects need to be taken into consideration when referring to the numerical approximation are:

1. the number N of terms considered from the Fourier series: $f(t)\approx\sum_{-N}^{N}c_ne^{2\pi int}$
2. the numerical approximation of the c_n coefficients: $c_n=\int_0^1 f(t)e^{-2\pi int}dt$

Knowing the values of the function in some points that belong to its domain, we can approximate the integral using quadrature formulas: $\int_0^1 g(t)dt\approx\sum_{k=0}^{M}\omega_k\,g(t_k)$ (10)

In our program, we have considered the trapezoidal rule for uniform division, for which MATLAB uses the *trapz* procedure. As an application, we started with a Python script to identify the points in (x,y) coordinates corresponding to a given image; we then used the acquired data to approximate the curve in a MATLAB script using Fourier series for complex valued functions.

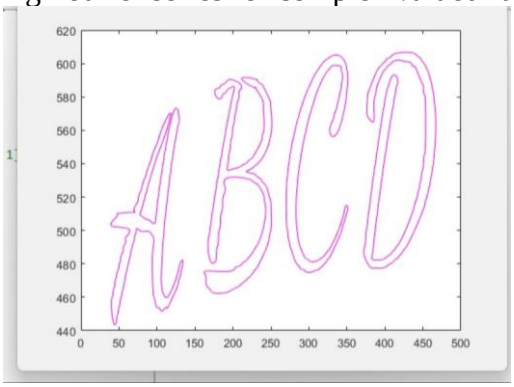

Approximating different letters' contour by using the Fourier series for complex valued functions

3. CONCLUSIONS

Fourier series are fundamental in mathematics, used to represent complex periodic functions through sine and cosine terms. We explored their theoretical underpinnings, detailing their formulation for both real and complex-valued functions. Numerical aspects such as selecting the number of terms for approximation and employing integration methods ensure precise coefficient computation.

REFERENCES

[1] V. Serov – *Fourier Series, Fourier Transform and Their Applications to Mathematical Physics*, Springer Verlag, 2017

[2] Karan Asher - *Fourier series And Fourier Transform*, IOSR Journal of Mathematics (IOSR-JM), Volume 4, Issue 6 (Jan. - Feb. 2013), pp 73-76

HILBERT DEPTH OF SOME CLASSES OF MONOMIAL IDEALS

Silviu BĂLĂNESCU[1] and Mircea CIMPOEAȘ[1]

[1]National University of Science and Technology Politehnica Bucharest,
313 Splaiul Independentei, District 6, Bucharest, Romania

Corresponding author email: silviu.balanescu@stud.fsa.upb.ro

Abstract

We study the Stanley depth and the Hilbert depth for I and S=I, where $I \subset S = K[x_1, \dots, x_n]$ *is the intersection of monomial prime ideals with disjoint sets of variables.*

Key words*: Depth, Stanley depth, Hilbert depth, Monomial ideal,Squarefree ideal*

1. INTRODUCTION

Let $S = K[x_1, \dots, x_n]$ be a standard graded polynomial ring over a field KFor a finitely generated graded S-module M, the Hilbert series of M is defined by

$$H_M(t) = \sum_{j \geq 0} \dim_K(M_j) t^j$$

The Hilbert depth is $hdepth(M) = max\{r : (1-t)^r H_M(t) \text{ is positive}\}$, see [3].

Let $I \subset J \subset S$ be some monomial ideals. A Stanley decomposition of J/I is a decomposition

$$\mathcal{D}: J/I = \bigoplus_{i=1}^{r} u_i K[Z_i],$$

where u_i are monomials and $Z_i \subset \{x_1, \dots, x_n\}$ for all i. The Stanley depth of $\mathcal{D}$ is the minimal cardinality of some Z_i. The Stanley depth of J/I is

$$sdepth(J/I) = max\{sdepth(\mathcal{D}) : \mathcal{D} \text{ a Stanley decomposition of } J/I\}.$$

It is well known that hdepth(J/I) gives upper bounds for both depth(J/I) and sdepth(J/I).

Let $I \subset J \subset S$ be two squarefree monomial ideals. For all $0 \leq j \leq n$, we let
$\alpha_j(J/I) :=$ the number of squarefree monomials u in S such that $u \in J \setminus I$ and $\deg(u) = j$. Let

$$\beta_k^q(J/I) = \sum_{j=0}^{k} (-1)^{k-j} \binom{q-j}{k-j} \alpha_j(J/I) \text{ for all } 0 \leq k \leq q \leq n$$

In [1] we proved the following result.

Theorem. hdepth(J/I)=$max\{q : \beta_k^q(J/I) \geq 0 \text{ for all } 0 \leq k \leq n\}$.

Our aim is to compute the Hilbert depth for several classes of squarefree monomial ideal, using this formula.

We tackle the case of the ideal $I = (x_1, x_2, \dots, x_n) \cap (x_{n+1}, \dots, x_{n+m}) \subset S = K[x_1, x_2, \dots, x_{n+m}]$ and a certain generalization of I.

The presentation is based on the preprint [2].

2. CONTENT

Let n and m be two positive integers. We let $S = K[x_1, x_2, \dots, x_{n+m}]$ and we consider the squarefree monomial ideal $I = (x_1, x_2, \dots, x_n) \cap (x_{n+1}, \dots, x_{n+m}) \subset S$. With these notations, we have that:

Theorem 1. $sdepth(S/I) \leq hdepth(S/I) \leq n + m + \frac{1}{2} - \sqrt{2mn + \frac{1}{4}}$.

Theorem 2. $\left\lceil \frac{n}{2} \right\rceil + \left\lceil \frac{m}{2} \right\rceil \leq sdepth(I) \leq hdepth(I) = \left\lfloor \frac{n+m+2}{2} \right\rfloor$.

Let $n_1, n_2, \dots, n_r$ be some positive integers, $N = n_1 + \cdots + n_r \ and \ S \coloneqq K[x_1, \dots, x_N]$. We consider the ideal $I \coloneqq (x_1, \dots, x_{n_1}) \cap (x_{n_1+1}, \dots, x_{n_1+n_2}) \cap \cdots \cap (x_{n_1+\cdots+n_{r-1}+1}, \dots, x_N) \subset S$. With these notation, we have the following (partial) generalization of Theorem 2:

Theorem 3. $\left\lceil \frac{n_1}{2} \right\rceil + \cdots + \left\lceil \frac{n_r}{2} \right\rceil \leq sdepth(I) \leq hdepth(I) \leq \left\lfloor \frac{n_1+\cdots+n_r+r}{2} \right\rfloor$.

Based on our computer experiments, we believe that the last inequality is in fact an equality.

3. CONCLUSIONS

We compute the Hilbert depth of a monomial ideal $I = (x_1, x_2, \dots, x_n) \cap (x_{n+1}, \dots, x_{n+m}) \subset S = K[x_1, \dots, x_{n+m}]$, which is the intersection of two prime monomial ideals with distinct sets of variables and we give an upper bound for the Hilbert depth of S/I.
Also, we obtained some partial generalization of these results for an arbitrary intersection of monomial prime ideals in distinct sets of variables.

Bibliography

[1] S. Balanescu, M. Cimpoeas, C. Krattenthaller, *On the Hilbert depth of monomial ideals*, arXiv:2306.09450 (2024).

[2] S. Balanescu, M. Cimpoeas, *On the Hilbert depth of certain monomial ideals and applications*, arXiv:2306.11015 (2024).

[3] J. Uliczka, *Remarks on Hilbert series of graded modules over polynomial rings*, Manuscripta math. **132** (2010), 159--168.

Mathematical and physical aspects of the solution to the initial value problem in the thermodiffusion in solid body with applications in mechanical engineering

Prof. Ph Dr Dr Sci. Math. Eng Jerzy August Piotr Gawinecki,
Prof. Ph Dr Dr Eng Stanisław Kachel*,
Prof. Ph Dr Dr Eng Adam Kozakiewicz

Military University of Technology
(MUT) Warsaw, Poland
Faculty of Mechatronics, Armament and Aerospace

Abstract

Under an influence exerted by the action of external loads, heating of the body and the diffusion of the matter into solid body will arise in this body a displacement field $\boldsymbol{u}(\boldsymbol{x},t)$, the temperature $T(\boldsymbol{x},t)$, and the chemical potential field $P(\boldsymbol{x},t)$.

The relations which these functions fullfield at a space point $x \in \mathbb{R}^3$ and the time $t \in \mathbb{R}_+ \cup \{0\}$ are called the Equation of thermodiffusion and described the phenomenon of thermodiffusion in solid body. The phenomenon of thermodiffusion appearing in some materials, which are used in mechanical engineering, specialy in materials used in aviation, not only in the civil aviation but air force as well.

The aim of this paper is to consider the system of partial differential operators which governs linear thermodiffusion in elastic solids.

Basing on the derived matrix of fundamental solutions to this system of equations, explicit formulae for the solution to the Cauchy problem for this system of equations were presented.

*Dean of the Faculty of Mechatronics, Armament and Aerospace
Military University of Technology, Warsaw, Poland
e-mail: stanislaw.kachel@wat.edu.pl

For the obtained solution, its mechanical and mathematical aspects and properties have been analyzed for the considered thermodiffusion medium.

Introduction

These are a lot of examples conected with the penetration the liquid and gases into solid body.

These causes generated the deformation of the body, its expanding and contraction.

So for example hydrogen penetrating under the pressure into the steal produce its significant deformation.

The thin plate, in which penetrating the hydrogen, flexure itself, the thin plate suffer twist.

Also loaded with consequences is influence the heating of the body in the diffusing process.

From some experiments we have has change the distribution of humidity in the porous medium under the influence of changing of the temperature field.

In order to acceleration the process of the separating the gas from the metal one can apply the heating of the body, such that the proces like carburizing or decarburization of the steal to come after the presence of the changeable field of the temperature.

Such the phenomena taking part in some materials, which are used in mechanical engineering.

Specially in materials in aviation not only in the civil aviation but air force, as well.

So, there exist the necessary to creation the theory including correlation beetwen the diffusing process – which is described by the chemical potential, termical process with is described by the temperatue field and the deformation of the body described by the displacement and state of stress.

Such a theory described above is so called the thermodiffusion in solid body.

REMARKABLE INEQUALITIES AND OPERATIONAL RESEARCH APLICABILITY

Stefan CHIVULESCU[1,2], Stefan-Gabriel MINA[1,2]
Cosmin Dănuț BARBU[3], Elena Corina CIPU[1,3]

[1]Centre for Research and Training in Innovative Techniques of Applied Mathematics in Engineering "Traian Lalescu" (CiTi), Bucharest, Romania

[2]National University of Science and Technology Politehnica of Bucharest (UNSTPB), Power Engineering Faculty,

[5]Department of Applied Mathematics, Faculty of Applied Sciences, University Politehnica of Bucharest

Corresponding author email: stefan.chivulescu04@gmail.com

Abstract

Our presentation explores how mathematical inequalities significantly impact various engineering and scientific fields, highlighting both their practical and theoretical importance. We begin by discussing the foundational role of inequalities in mathematics and then showcase their real-world applications through the work of three influential mathematicians: Jakob Bernoulli, Hermann Minkowski, and Titu Andreescu.
Bernoulli's inequality, essential in mathematical analysis, helps solve complex engineering problems. Minkowski's inequality, crucial in physics and geometry, is widely used in signal processing and coding theory. Andreescu's variations of the Cauchy-Bunyakovsky-Schwarz inequality are vital for optimization tasks.
Our research applies Andreescu's inequality to an optimization problem aimed at minimizing budget losses in a nuclear power plant's Safety, Maintenance, and Operations departments. By dynamically adjusting budget allocations based on a mathematical model, we demonstrate improved plant performance.

Key words: *mathematical inequalities; Bernoulli's inequality; Minkowski's inequality; optimization; resource allocation; efficiency graph.*

1.INTRODUCTION

Inequalities in mathematics serve as powerful tools, revealing connections between quantities and guiding us towards solving complex problems. From defining limits to optimizing resource allocations, their significance cannot be overstated. In this presentation, we'll explore how inequalities form the backbone of modern mathematical analysis and contribute to real-world solutions.

2.CONTENT

2.1. Fundamental inequalities

This chapter explores fundamental inequalities in mathematics that serve as essential tools in problem-solving. From mean inequalities to exponential and trigonometric inequalities like:

$$\arctan x \leq x;\ e^x \geq x + 1 \tag{1}$$

These relationships are foundational in various mathematical contexts, providing insights and facilitating solutions to a wide range of problems.

2.2. Jakob Bernoulli's Influence and Hermann Minkowski's Contributions

Jakob Bernoulli's inequality, inspired by his investigations into interest and probability, showcases his significant impact on mathematical analysis. This inequality offers a valuable framework for establishing boundaries and addressing intricate equations, playing a vital role in engineering computations and modelling endeavours.
Hermann Minkowski's groundbreaking research in the geometry of numbers and spaces led to the formulation of a fundamental inequality. known as the Minkowski inequality. It describes important

relationships that have far-reaching applications in fields such as physics and geometry. Its versatility makes it extremely useful, particularly in signal processing and coding theory, where it offers powerful solutions and insights.

2.3.Titu Andreescu's Inequality. Optimization Problem

Titu Andreescu, known for his extensive work in international mathematics competitions, has developed inequalities particularly useful in the field of optimization. His innovative adaptation of the Cauchy-Bunyakovsky-Schwarz inequality provides a robust methodology for resource allocation within economic models.

In this chapter, we focus on applying Titu Andreescu's inequality to minimize budget losses in a nuclear power plant.
By dynamically adjusting budget fractions based on a derived mathematical model, represented in our efficiency graph, we enhance overall plant performance.
This practical example underscores the powerful impact of mathematical inequalities in solving real-world challenges.

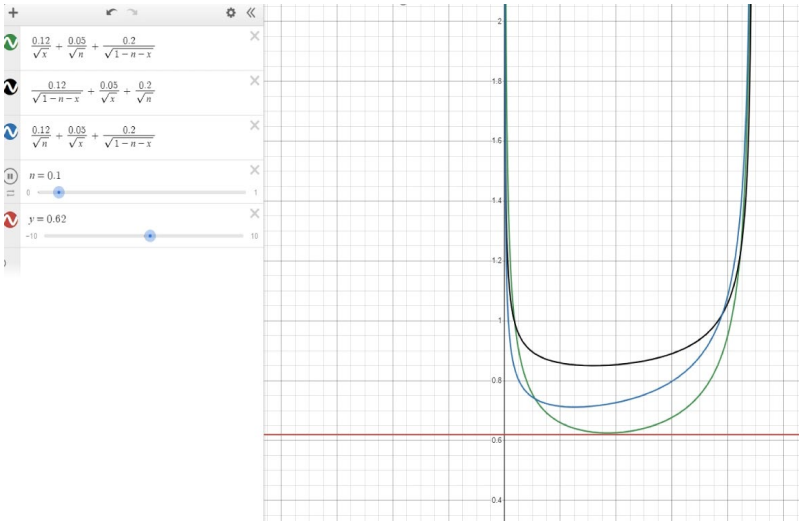

Figure 1. Graphical representation of the Titu Andreescu Inequality, applied to optimize budget allocation across three departments in a nuclear power plant

3.CONCLUSIONS

We managed to create a presentation that shows the work of three most brilliant minds whose research have put bases on what we study today. With their unique applicability's, these inequalities show how much we use them in various fields and, furthermore, how we can evolve our studies through them. Also, we think that people can evolve by understanding conceptual thoughts on various ideas, such as minimum salvage and maximum output, all of them being limited by inequalities.

REFERENCES

- discoverwalks.com:*10 outstanding facts about Jakob Bernoulli*
- ccdfocsani.ro:*Inegalitati matematice optional liceu*
- wikipedia. org*: Titu Andreescu*
- wikipedia.org:*Cauchy Schwarz inequality*
- pro-didactica.ro:*forum Titu Andreescu*
- math.stackexchange.com:*proof-by-induction-of-bernoullis-inequality*
- math.stackexchange.com:*where-does-one-even-need-bernoullis-inequality*
- wikipedia.org:*Methods of computing square roots*
- Yu Miao - *Several variants of via Titu Andreescu type and Popoviciu type inequalities*
- Gregory Mankiw – *Principles of economics*
- *K. Kedlaya. A < B (A is less than B). based on notes for the Math Olympiad Program (MOP) Version 1.0, last revised August 2, 1999*
- wikipedia.org:*Inegalitatea lui Minkowski*

The impact of mathophobia on the STEM community

Firstname: VALERIA, Lastname: CIRLAN

STEFAN CEL MARE University, University Street no. 13
720229 Suceava, Romania

Corresponding author email: Valeria Cirlan_valeria.sutu@student.usv.ro

Abstract

It seems that although the number and variety of jobs in STEM have increased, the number of women who choose to work in these fields is decreasing. In this sense, we set out to find which are the causes regarding girl's lack of interest in the STEM field. A number of N=194 secondary school students (52.1% girls and 47.9% boys), from rural (74.7%) and urban areas (25.3%), from Suceava county, answered to our questionnaire, 4 respondents were eliminated for duplicate answers. As expected, our results confirmed that there is a significant positively correlation between self-esteem and math and school performance. In agreement with our predecessor's studies, the hypothesis that math performance correlates significantly positively with school performance was confirmed. Contrary to previous studies, our research showed that there are no gender differences between math and school performance. Moreover, we identified that there are differences regarding self-esteem, math performance and school performance, depending on the environment of origin. The results obtained motivate us to seek and develop counselling programs for students, parents and teachers, in order to prevent and reduce the mathophobia of secondary school students, by increasing self-esteem, strengthening motivation, reducing gender stereotypes and promoting a mentality of growth.

Key words*: math anxiety (mathophobia), self-esteem, motivation, STEM, math performance, school performance*

1. INTRODUCTION

The results of the PISA tests from the last 5 years highlight the inability of Romanian students education (and not only) to use and apply the assimilated theoretical notions in practical problems. Mathematics in the current school context is closely related to a phenomenon of anxiety. We want to know if a student's math difficulties are associated with cognitive or affective difficulties. In this sense, (Van Nieuwenhoven et al., 2019) analysed the theoretical framework of memory, which are the origins of numeracy, we will decipher the impact of the student's affective sphere in the development of difficulties related to understanding mathematics and we will highlight which disorders and difficulties are characteristic of mathematics. Finally, we will learn that anxiety is one of the causes of some of the students' difficulties in mathematics. We will become aware of the influence that family, school and surroundings have on the student's behaviour and career choice at the right time.

(Widlund et al., 2020) demonstrated that math performance has a positive influence on school performance and self-esteem correlates positively with STEM educational and career aspirations among both girls and boys (Widlund et al., 2020). Thus, students with high performance in mathematics have embraced careers in the field of biology, law or business. Other researchers, such as (Lazarides & Lauermann, 2019) concluded that in the case of girls with skills and performance in mathematics, the probability of them choosing a career in the human sphere was quite low.

2. CONTENT

As a professor of mathematics, considering that Mathematics is an exam discipline and the low results of these evaluations, I proposed to evaluate the possible causes that led to this situation and to identify solutions / ways to improve it and to help students better overcome such periods.

The objectives of my research are to identify possible correlations that I intuit after analysing some studies on this subject: to check if there are correlations between self-esteem and school

performance of students, if gender differences and the environment of origin influences the level of self-esteem, school performance and students' mathematical abilities.
We processed the answers obtained through the questionnaire with the help of the JAMOVI statistical analysis program. In order to verify the initial hypotheses, we used descriptive analysis to highlight the sample (age, gender and environment), correlations to test the hypotheses established between the variables and independent samples t-test to conclude whether there were gender and environmental differences in self-esteem, math skills and school performance.
Although previous studies (Lazarides & Lauermann, 2019) demonstrated that boys have greater inclinations than girls towards mathematics, my study did not confirm this hypothesis. Girls and boys recorded the same average M=39.9. Also, (Perez-Felkner et al., 2017) showed that boys have a higher self-esteem than girls and tend to constantly self-evaluate in relation to their mathematical abilities, while girls have a tendency to underestimate and reject the idea of careers in the field of mathematics and exact sciences in general. Probably due to the small number of subjects, our study did not record these differences either.
Another factor that influences this students's aversive attitude towards mathematics is the factor, which corresponds to the conceptions that the student has acquired and developed regarding mathematics in the family for the most of the time. Indeed, many students create a view of mathematics that negatively influences their involvement in learning it, in the sense that, even before they have begun to assimilate a mathematical concept, some students perceive it as inaccessible for them and no longer submit effort to understand and assimilate it (Van Nieuwenhoven et al., 2019).
More recent studies (Anaya et al., 2022) show us that although the number and range of jobs in STEM have increased, the number of women who choose to work in these fields has not increased, on the contrary, it is decreasing. In this sense, other researchers (Perez-Felkner et al., 2017) reinforce the idea that girls' self-esteem regarding mathematics is lower than that of boys, which explains girls' lack of interest in the STEM field.
However, we need to take a look at how mathematical knowledge is transmitted. Thus, the researchers addressed the theoretical framework of memory, what are the origins of calculation, what disturbances and difficulties are characteristic of mathematical learning and whether anxiety is one of the sure causes of the difficulties encountered by students in understanding mathematics. In 2007, the Center for Research and Innovation in Education published an article "Understanding the brain: the birth of a science" which is actually a scientific research that takes place over a period of twenty years and aims to guide towards an improvement of educational policies and practices, putting first of all the role that the brain plays in the creation and development of computation in the human being.

3. CONCLUSIONS

We further decline to the opinion expressed by Perez-Felkner et al. which says that boys have a higher self-esteem than girls and tend to constantly self-evaluate in relation to their mathematical abilities, while girls have a tendency to underestimate and reject the idea of a career in the field STEM. However, there is worrisome because contemporary statistics show that there are gender discrimination regarding the remuneration of women in STEM field. The causes of this reality would be the girls' beliefs and convictions regarding their low mathematical abilities. The solution would be to improve girls' beliefs about their mathematical abilities, which would have significant effects in choosing a career in the field of science, which underlines the need for the mandatory presence of a school counsellor in school, introducing one hour of career counselling per week into the curriculum. Teachers must take into account that the world is constantly changing, that education must also keep pace with the tide of change and adapt the way of teaching and assessment to the needs of the student today. Thus, together, parents and teachers, we will create a better, more capable, more educated world, and the current students - the future society, will be able to keep up with the changes that await them.

Differential equations with elementary approaches and solutions in high-school mathematical contests

Vladimir CERBU[1], Nicolai GĂITAN[2]

[1]Military National College "Ștefan cel Mare", Câmpulung Moldovenesc, Suceava, Romania
[2]Military Technical Academy "Ferdinand I", București, Romania

cerbuvlad@yahoo.com, nicolai.gaitan261@gmail.com

Abstract: *Authored by an active high school teacher and one of his former students, this paper presents a compilation of problems composed for high-school mathematical contests over several years. Solutions illustrate that certain differential equations can be solved using concepts of differentiable and continuous functions, with the aid of important theorems from one-variable real analysis. Notably, some problems have multiple solutions, showcasing the versatility of approaches. Divided into sections for 11th and 12th grades, the paper incorporates integrals for the latter, aligning with*

the Romanian high school curriculum. Despite the complexity, solutions emphasize elementary principles, fostering a deeper understanding of mathematics among secondary education students.

***Key words**: Darboux property, Differential Equations, Problem Solving, Mathematical Contest, Real Analysis*

1. INTRODUCTION

The required knowledge for the discussed problems stays in the area of basic one variable real analysis, concerning well-known theorems and properties like Lagrange mean value theorem, Rolle's Theorem, Fundamental Theorem of Calculus, Intermediate value property/theorem.

2. CONTENT

The first section titled "Problems for 11 graders" discusses two main problems which occurred in the final stages of the Romanian National Mathematical Olympiad (2012, 2015). The statements of the problems are:

Statement 1.1: *Find all differentiable functions* $f:[0,\infty)\to[0,\infty)$ *with* $f(0)=0$ *and*

$$f'(x^2)=f(x),\forall x\in[0,\infty).$$

Statement 1.2: *Find all real differentiable functions f which satisfies simultaneous the following:*

i) $x\in\mathbb{Z}\Rightarrow f'(x)=0$

ii) $f'(x)=0, x\in\mathbb{R}\Rightarrow f(x)=0$ (2)

The second sections, "Problems for 12 graders" which examines the problems addressing the students in the last year of high-school are the following and, as main difference, there is observed the presence of the explicit notion of anti-derivative/primitive:

Statement 2.1: *Find all real bijective functions such that* $f\in\int(f\circ f)(x)dx$.

Statement 2.2: *Find all real functions f which satisfy*

$$\big(xf(x)-2F(x)\big)(F(x)-x^2)=0,\forall x\in\mathbb{R}$$

, where F is a primitive of the initial function f.

Statement 2.3: *Find all* $f:[0,\infty)\to\mathbb{R}$ *which respects simultaneous the next properties:*

i) f is an increasing function

ii) f admits a primitive F with F(0)=0 and $F(x+y)\le F(x)+F(y),\forall x,y\in\mathbb{R}$.

Statement 2.4: *Let n be a non-zero natural number. Find all functions* $f:[0,\infty)\to\mathbb{R}$ *, which are n times differentiable, with the n-th derivative lower-bounded and* $\int_x^{x+1}f(t)dt=\int_0^x f(t)dt, \forall x\ge 0$.

The paper presents in detail the right way of approaching the problems and their solutions, among with their alternatives where is the case.

The bibliography involved in the work of the current material is: [1] Probleme alese de matematică pentru pregătirea Olimpiadei Naționale – *Mihai Piticari, Ovidiu Avădanei, Dragoș Crișan* – for the problem 2.4 , [2] Colecția Gazeta Matematică – for the problems 1.1, 1.2, 2.3, [3] *www.cnlr.ro* – the webpage of the contest for problems 2.1, 2.2.

3. CONCLUSION

In conclusion, the compilation of problems presented in this paper serves as a valuable resource for students preparing for mathematical contests in Romania. Furthermore, it offers significant insights for those with a deeper interest or understanding of the standard curriculum, as it provides diverse perspectives on problem-solving approaches. The inclusion of problems with varying levels of difficulty facilitates an authentic learning experience, fostering the assimilation of key concepts and the development of problem-solving heuristics. Overall, this paper contributes to enhancing the mathematical proficiency and critical thinking skills of secondary education students, thereby enriching their educational journey.